The Dissertation Committee for Phu Trong Nguyen certifies that this is the approved version of the following dissertation:

A STUDY OF SHEAR BEHAVIOR OF REINFORCED CONCRETE DEEP BEAMS

Committe:

James O. Jirsa, Supervisor

Oguzhan Bayrak

Wassim Ghannoum

David Fowler

Stelios Kyriakides

A STUDY OF SHEAR BEHAVIOR OF REINFORCED CONCRETE DEEP BEAMS

by

Phu Trong Nguyen, B. E.; M. Computational M. E.

Dissertation

Presented to the Faculty of Graduate School of

The University of Texas at Austin

in Partial Fulfillment

of the Requirements

for the Degree of

Doctor of Philosophy

The University of Texas at Austin

December 2013

Dedication

To all my loving, my wife, Hanh Thai and our kids, Thang Minh Nguyen and Bao Ngoc Nguyen

Acknowledgements

First of all, I would like to thank US Government and VietNam Education Foundation (VEF), an organization of US Government for all great work and financial support they have done in my first two years of studying Doctoral degree at University of Texas at Austin.

I would like to thank staffs of Ferguson Structural Engineering Laboratory and my laboratory-mates for making an excellent friendly international atmosphere.

I would like to express the deepest appreciation and gratitude to my advisor, Dr. Jirsa, who has the attitude and the substance of a genius: he continually and convincingly conveyed a spirit of adventure in regard to research and scholarship, and an excitement in regarding to teaching. This dissertation would not have been possible without his excellent guidance, endless caring, and unconditional patience. I also would like to thank my committee members: Professor Bayrak, Professor Wood, Professor Ghannoum, and Professor Kyriakides, who were so patient with me. I would like to offer my special thanks to Professor Fowler, who was willing to participate in my committee at the last moment.

I would like to express my deepest appreciation to my parents, who were always supporting and encouraging me with endless love.

Finally, I would like to express the deepest appreciation to my wife, Hanh Thai, and our kids, Thang Minh Nguyen and Bao Ngoc Nguyen. As a husband I owe my wife I should always stand by her to share harsh of life, protect from bad, and bring happiness. As a father I owe my kids I should give all my time to them to care, teach, and play. Although very so much suffering I brought they were always there encouraging, cheering me up and stood by me through the good times and bad.

Abstract

A Study of Shear Behavior of Reinforced Concrete Deep Beams

Phu Trong Nguyen, Ph.D

The University of Texas at Austin, 2013

Supervisor: James O. Jirsa

Reinforced concrete deep beams are vital structural members serving as load transferring elements. The behavior of reinforced concrete deep beams is complex. Nonlinear distribution of strain and stress must be considered. Prior to 1999, ACI 318 Codes included an empirical design equation for reinforced concrete deep beams. Since 2002, the strut and tie model and nonlinear analysis have been required. However, both methods have disadvantages of complexity or lack of transparency.

The objective of this study is to produce a simple, reliable design equation for reinforced concrete deep beams. A nonlinear finite element program, ATENA, was used for analyzing and predicting the behavior of concrete and reinforced concrete structures. First, applicability of ATENA was verified by developing the computer models of simply supported and two span continuous deep beams based on Birrcher's tests of simply supported deep beams. Tests by Rogowsky and Macgregor and by Ashour are the basis for the models of continuous two span deep beams. Those tests were selected because the researchers reported adequate details of the experimental program and on specimen behavior.

Then a series of simply supported and two span continuous deep beam models were developed based on the details and geometry of Birrcher's beams. The computer models were used to investigate the following parameters: the compressive strength of concrete, shear span to depth ratios, longitudinal reinforcement ratios, web reinforcement, effect of member depth, and loading conditions.

Finally, a proposed design equation for shear strength of reinforced concrete deep beams was derived based on the observed the behavior of reinforced concrete deep beam tests, the results of the analytical study, and a plastic truss model. The proposed equations were in good agreement with test values and provide an alternate approach to current design procedures for deep beams.

Table of Contents

List of Tables

List of Figures

Chapter 1 Introduction

1.1 Overview

A deep beam is defined in the ACI Code 318-11 Section 11.7.1 as members with l_n, which is clear span, not exceeding four times the overall member depth or regions of beams with concentrated loads within twice the member depth from the support that are loaded on one face and supported on the opposite face so that compression struts can develop between the loads and supports. The shear behavior of deep beam is considerable different from that of slender beams that exceed the limits noted above. The assumptions of plane sections in analysis of normal beams can no longer be used for deep beams. The behavior of deep beams is dominated by shear deformation, thus in design of deep beam one needs a design procedure based on mechanisms of failure of deep beams. In practice, one typically encounters deep beams when designing transfer girders in tall buildings, pile supported foundation, or bent caps in bridges. Prior to 1999, ACI Code 318 included a design equation for designing reinforced concrete deep beams, but since 2002, the strut and tie model and nonlinear analysis have been specified. The strut and tie model is a powerful tool for designing reinforced concrete structures, but it is a multiple-step, complex procedure. Using Strut-and-Tie models requires some structural design and analysis experience. For nonlinear analysis, one needs a computer and a nonlinear program. In addition, designers need some finite element method knowledge, basic theory for algorithm, and an understanding of the primary variables. It is the reason that many practical designers are not confident using either procedure.

In this study, the behavior of reinforced concrete deep beams will be investigated by using a database of reinforced concrete deep beams, compiled by Brown and Birrcher et al. consisting of the test results of 905 deep beam specimens and a nonlinear finite element program, named ATENA. ATENA is a program specifically designed for concrete and reinforced concrete structures and includes algorithms for concrete cracking, crushing, and reinforcement yielding. So far, most investigations of the behavior of reinforced concrete deep beam were laboratory experimental tests. And the

behavior of deep beams was analyzed using observed test results particularly, ultimate load and crack patterns. But the internal distributions of stresses and strains of concrete and reinforcement in deep beam tests could not be observed. First, ATENA was used to set up models of deep beams from the database. Then ATENA was used to model and analyze simple supported reinforced concrete deep beams and continuous deep beams to investigate the effects of different parameters: compressive concrete strength, loading conditions, shear span to depth ratios, depth of section, shear and flexural reinforcement, and loading plates.

The objective of this study is to investigate analytically the behavior of reinforced concrete deep beams and to produce simple, reliable design equations for reinforced concrete deep beams, especially continuous deep beams.

1.2 Objectives and scope of the research

The general objective of this study is study the response of simply supported and continuous deep beams through the analyses considering the following variables:

1. Compressive strength of concrete.
2. Shear span-to-depth ratio.
3. Web reinforcement in both directions.
4. Loading conditions: concentrated or distributed loads.
5. Depth of section.
6. Manner of load application through steel plates or concrete columns.

Using the results of the analytical study and the database, a procedure for design of deep beams is proposed to give designers a simple, transparent procedure as an alternative to strut-and-tie model or nonlinear analysis procedures.

1.3 Organization

This dissertation consists of 7 chapters.

A review of different Codes for designing of reinforced concrete deep beams and previous works from other researchers are addressed in Chapter 2. A brief review of the

behavior of reinforced concrete deep beam and different Code provisions are provided. Experimental results from previous investigators are discussed and then gaps in literature are addressed.

Chapter 3 describes the database of reinforced concrete deep beams and criteria for filtering the database.

Chapter 4 presents a brief review of the ATENA program. Then finite element models of simply supported and continuous deep beams reported in literature for verifying applicability of ATENA are provided. Comparisons between experimental test results and results using ATENA are presented.

Chapter 5 provides series of computer models for analytical investigation of the behavior of simply supported and continuous deep beams. Computer models consist of series for investigating parameters: concrete strength, shear span-to-depth ratio, longitudinal and web reinforcement, and loading conditions.

Chapter 6 the behavior of reinforced concrete deep beams is discussed based on results of finite element models. A proposed design equation for shear strength of deep beam is addressed. Also, a summary of comparison between experimental test results and the proposed design equation is provided.

In Chapter 7 conclusions and future recommendations are summarized.

Chapter 2 Review of Literature

2.1 Overview

In this Chapter, an overview of the behavior of reinforced concrete deep beams is provided. A review of different Code provisions for designing deep beams is discussed. Also, a discussion of previous research on deep beams is presented.

2.2 Behavior of reinforced concrete deep beam

Analyses of deep beams were based on the theory of elasticity for homogeneous material. Leonhardt and Walther demonstrated that cracking followed the principal tension stress trajectories. Unfortunately, the classical theory of elasticity did not adequately describe the redistribution of stress and strain of deep beam after cracks occurred. Based on experimental measurements, they found that the stresses at sections near supports exceeded theoretical stresses and that theoretical stresses were larger than measured stresses at sections near the center of the span.

The difference between a deep beam and a shallow beam can be based on the contribution of either beam action or tied arch action. As experiments show, a shallow member is one in which beam action is predominant and failure occurs shortly after inclined cracking develops unless web reinforcement is provided. On the other hand, a deep beam may develop considerable reserve shear capacity due to arch action after the formation of inclined cracks.

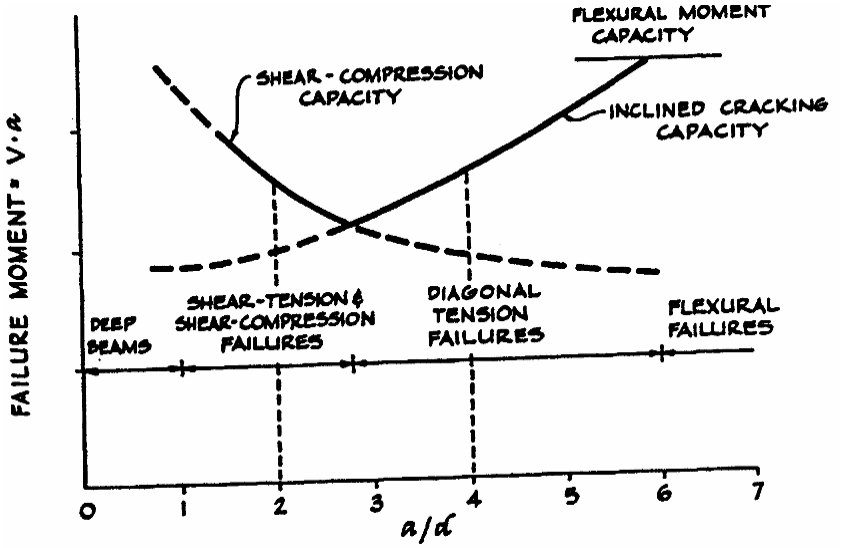

Figure 2.1 Variation in shear capacity with a/d for rectangular beams (Bresler)

It is observed from deep beam tests that there are some modes of failures that vary with shear span-to-depth ratio. Figure 2.1 summarizes the modes of failure as a function of the a/d ratio. The a/d ratio is defined as shear span (the distance from the center of loading to the center of support) divided by the effective depth. For shear span-to-depth ratios from 1 to 2.5 shear-tension failure and shear-compression failure are prevalent (Fig. 2.2).

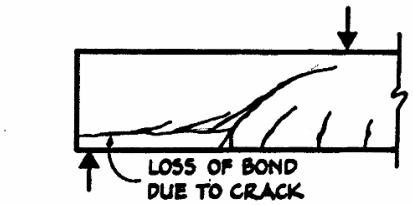

A- SHEAR-TENSION FAILURE

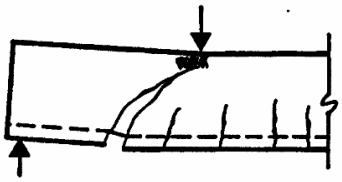

B- SHEAR-COMPRESSION FAILURE

a/d = 1 TO 2.5

Figure 2.2 Modes of failure of deep beams with a/d from 1 to 2.5 (Bresler)

For shear span-to-depth ratios from 0 to 1 modes of failure include (1) anchorage failure of the tension reinforcement, usually combined with splitting along the anchored longitudinal bars; (2) bearing failure or crushing at the reactions; (3) flexure failure either of the steel reinforcement due to yielding or fracture, or of the crown of the arch when the concrete crushes; (4) tension failure of the arch-rib by cracking over the support; or (5) crushing within the web of beam along the inclined cracks.

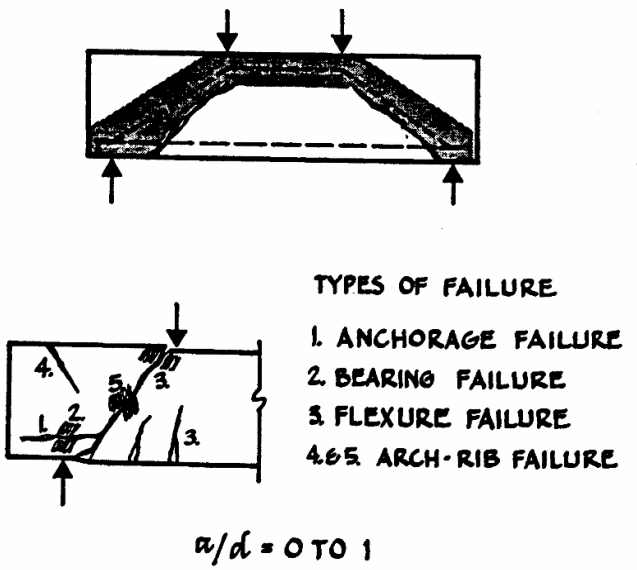

Figure 2.3 Modes of failure modes of deep beams with a/d from 0 to 1 (Bresler)

There are some important factors that affect the behavior and strength of reinforced concrete deep beams. The shear strength of reinforced concrete deep beams with shear span-to-depth ratio, a/d, less than 2.5, was observed to vary inversely with shear span-to-depth ratio. The type of shear reinforcement also affects the shear strength of deep beams. In practice shear reinforcement may consist of vertical reinforcement perpendicular to the longitudinal axis of the beam, and/or horizontal reinforcement, parallel to the longitudinal axis of the beam. It has been shown that when the shear span-to-depth ratio decreases, inclined cracks become more vertical, and vertical shear reinforcement becomes less effective while horizontal shear reinforcement becomes more effective. The tension steel ratio and the concrete strength also affect the behavior and strength of deep beams. It was observed that load applied directly on the compression flange resulted in higher strength than when load was applied on the tension flange.

2.3 Code provisions for deep beams

2.3.1 ACI Building Code 318

The deep beams shear provisions of ACI Code 318 prior to 2002 applied to top-loaded simple or continuous deep beams having a shear span-to-effective depth ratio less than 2.5 or a clear span-to- effective depth ratio less than 5. In the 2002 Code, the range of application was changed to a shear span-to-effective depth ratio less than 2 or a clear span-to-effective depth ratio less than 4.

2.3.1.1 Simply supported deep beams

Before ACI 318-02 was published, the shear strength of simply supported deep beams was based on the geometry of the beam. For uniformly distributed loading, the critical section was taken at $0.15l_0$ from the face of the support; for a concentrated load, it was taken as half way between the load and the face of the support. The shear reinforcement required at the critical section was used throughout the clear span, l_o.

The design is based on:

$$V_u < \Phi V_n \tag{2.1}$$

$$V_n = V_c + V_s \tag{2.2}$$

where,

l_o is the clear span of the beam

V_u is the design shear force at the critical section

V_n is the normal shear strength

Φ is the capacity reduction factor for shear

V_c is the shear strength provided by concrete

V_s is the shear strength provided by reinforcement

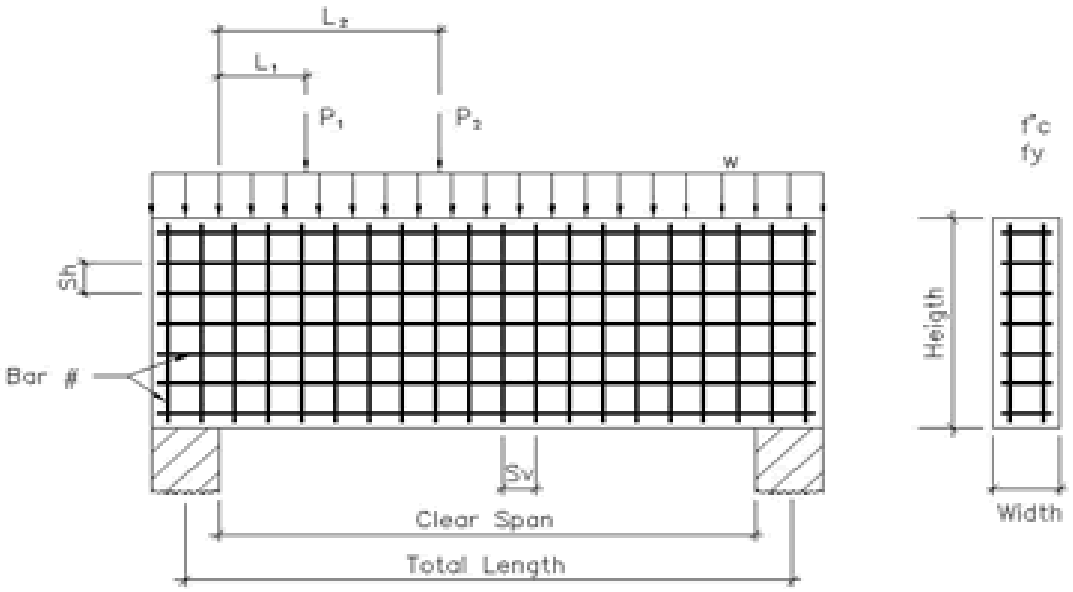

Figure 2.4 Simply supported deep beam

According to ACI Code 318-99 Section 11.8.4 the nominal shear strength V_n for deep flexural members can not exceed the following:

$$V_n = 8\sqrt{f'_c}\, b_w d \qquad \text{for } l_n/\text{d} < 2 \qquad (2.3)$$

$$V_n < \frac{2}{3}(10 + l_n d)\sqrt{f'_c}\, b_w d \qquad \text{for } 2 \le l_n/\text{d} < 5 \qquad (2.4)$$

where,

f'_c is the concrete cylinder compressive strength

b_w is the beam width

d is the effective depth of the beam

The shear strength provided by concrete V_c is calculated by from:

$$V_c = (3.5 - 2.5\frac{M_u}{V_u d})(1.9\sqrt{f'_c} + 2500\rho_w \frac{V_u d}{M_u})b_w d \qquad (2.5)$$

where,

M_u is the factored bending moment occurring simultaneously with V_u at the critical section

ρ_w is the ratio of longitudinal tension reinforcement area to the area of the concrete section.

The term $(1.9\sqrt{f'_c} + 2500\rho_w \frac{V_u d}{M_u})b_w d$ of Eq. (2.5) represents the concrete contribution to shear strength for normal beams. The first term on the right-hand side is a multiplier to allow for strength increase in deep beams, and that term should follow:

$$(3.5 - 2.5M_u/V_u d) < 2.5$$

but the concrete contribution is limited as follows:

$$V_c < 6\sqrt{f'_c} b_w d$$

In the case where factored shear force V_u exceeds shear strength ΦV_c, shear reinforcement must be provided to carry the excess shear. The contribution V_s of shear reinforcement is given by:

$$\frac{V_s}{f_y d} = \frac{A_v}{s_v}\left[\frac{1 + l_0/d}{12}\right] + \frac{A_h}{s_h}\left[\frac{11 - l_0/d}{12}\right] \qquad (2.6)$$

where,

A_v is the area of vertical shear reinforcement within a spacing s_v, but not less than $0.0015 b_w s_v$.

A_h is the area of horizontal shear reinforcement within a spacing s_v, but not less than $0.0015 b_w s_h$.

f_y is the yield strength of web steel

s_v is the spacing of the vertical reinforcement but not exceeding d/5 nor 18 in.

s_h is the spacing of the horizontal reinforcement but not exceeding d/3 nor 18 in.

2.3.1.2 Continuous deep beams

The design of continuous deep flexural members for shear, unlike those for simply supported ones, are not based on the design of shear force at the critical section. Instead, the shear design at any section is based on the shear force at that section.

The design equation is based on:

$$V_u < \Phi V_n \qquad (2.1)$$

$$V_n = V_c + V_s \quad (2.2)$$

For continuous deep flexural members, the concrete nominal shear strength V_c is taken as the smaller value by following:

$$V_c = 3.5\sqrt{f'_c}\,b_w d \quad (2.3)$$

$$V_c = (1.9\sqrt{f'_c} + 2500\rho_w \frac{V_u d}{M_u})b_w d \quad (2.4)$$

where,

M_u is the factored bending moment occurring simultaneously with V_u at the section under consideration.

The values of V_c expressed by Eqs. 2.3 and 2.4 for simply-supported deep beams were applied to continuous beams as were the requirements for area and spacing of horizontal and vertical shear reinforcement. Methods that satisfied equilibrium and strength requirements were permitted but without explanation.

ACI Code 318-02 required that deep beams be designed using nonlinear analysis or by strut-and-tie models.

The nominal shear strength of deep beam was limited to:

$$V_n \leq 10\sqrt{f'_c}b_w d$$

$$V_s \leq 8\sqrt{f'_c}b_w d$$

There were no provisions for calculating V_c and V_s. There was a disagreement regarding the contribution of vertical web and horizontal web reinforcements. The design equation in previous Codes for shear reinforcement was based on equal contribution of both vertical and horizontal web reinforcements. But MacGregor[1983] and Crist[1971] observed that vertical web reinforcement was more effective than horizontal web reinforcement in a deep beam. The reason for removing the equation of the concrete shear strength V_c was that the previous design equation did not reflect the true mechanism of failure and had serious discontinuities as the span-to-depth ratio was varied.

However, there were minimum requirements for web reinforcement that reflected the assertion that vertical reinforcement was more important than horizontal reinforcement.

The required minimum area of tensile reinforcement A_s was:

$$A_s = \frac{3\sqrt{f'_c}}{f_y} b_w d$$

and not less than $200 b_w d / f_y$.

The area of vertical shear reinforcement, A_v, could not be less than $0.0025 b_w s_v$, and s_v could not exceed the smaller of d/5 and 12 in.

The area of horizontal shear reinforcement, A_{vh}, could not be less than $0.0015 b_w s_{vh}$, and s_{vh} could not exceed the smaller of d/5 and 12 in.

2.3.2 Canadian Code CSA A23.3 (2004)

The shear provisions of the Canadian Code apply to those parts of the structural member in which:

(a) The distance from the point of zero shear to the face of the support is less than 2d; or

(b) A load causing more than 50% of the shear at a support is located at less than 2d from the face of the support.

The shear design for deep beams is based on the strut-and-tie model. The strength of the compression strut should be calculated based on:

$$C \leq \Phi_c A_{cs} f_{cu} \qquad (2.7)$$

where,

A_{cs} is the area of the compression strut defined by clause 11.5.2.2

$$f_{cu} = \frac{f'_c}{0.8 + 170\varepsilon_1} \leq 0.85 f'_c \qquad (2.8)$$

$$\varepsilon_1 = \varepsilon_s + (\varepsilon_s + 0.002)\cot^2 \theta_s \qquad (2.9)$$

where,

θ_s is the smallest angle between the compression strut and the adjoining tension ties and

ε_s is the tensile strain in the tension tie inclined at θ_s to the compression strut.

For regions of the compression strut not crossed by a tension tie, the limit for compression strength of the strut is $0.85f'_c$. The expression is based on the assumption that the principal compression strain in the direction of the strut is equal to 0.002 (which corresponds to the peak in the stress-strain curve).

The strength of the tension tie is based on:

$$T_{calc} \leq \Phi_s A_{st} f_y \tag{2.10}$$

where,

A_{st} is the area of the tension tie

f_y is the yield strength of the tensile reinforcement.

The strength of node regions is based on the types of node:

$0.85\Phi_c f'_c$ in the node regions bounded by compression struts and bearing areas, CCC nodes

$0.75\Phi_c f'_c$ in the node regions anchoring an tension tie in only one direction, CCT nodes

$0.65\Phi_c f'_c$ in the node regions anchoring a tension tie in more than one direction, CTT nodes

No design equations were provided for shear strength of simply supported and continuous deep beams. Instead, the design of flexural deep members was based on the strut-and-tie model.

2.3.3 CEB-FIB Model Code (1990)

Analysis of deep beams in Fig. 2.5 is based on one of the following three methods:

(a) A linear analysis based on the theory of elasticity, which is valid for serviceability and ultimate limit states, ULS. The analysis for the ULS requires detailing

of the reinforcement to withstand the resultant tensile forces in the concrete and to satisfy equilibrium conditions.

(b) A statically admissible stress fields in accordance with the lower bound theorem of limit analysis, for example strut-and-tie model. For the structure and its loads an equivalent truss may investigated consisting of: concrete struts and arches as compressive elements, steel ties formed by the reinforcement as tensile elements, and node regions where strut elements and tie element intersect.

(c) A non-linear analysis takes into account the non-linear stress and strain relations of materials. The non-linear analysis involves numerical methods for two-dimensional plane structures. The analysis will give results for serviceability as well as for the ultimate limit states.

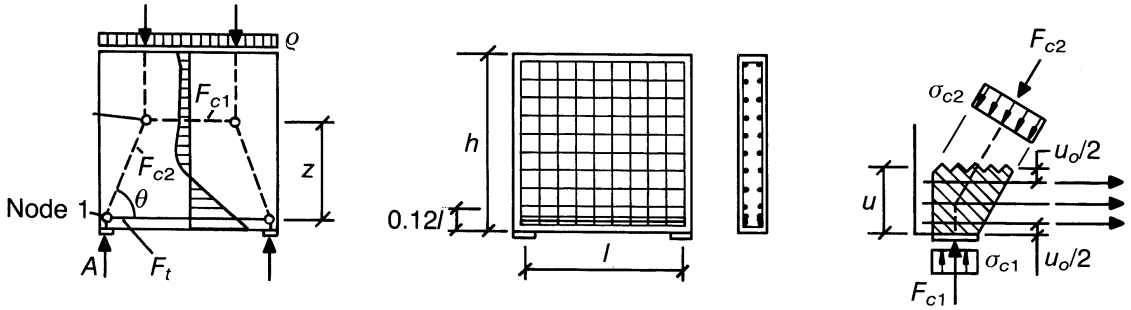

Figure 2.5 Strut-and-tie model, reinforcement and idealized support node for a deep beam (CEB 1990)

It is considered that a deep beam can be defined by discontinuity regions (Fig 2.6) and designed by using a strut-and-tie model. For a strut-and-tie model, the resistance of a structure is based on an arrangement of compression fields: struts, tie and nodes. The compatibility of deformations should be considered by orientating the models using the force systems determined from linear elastic analyses of uncracked members and connections.

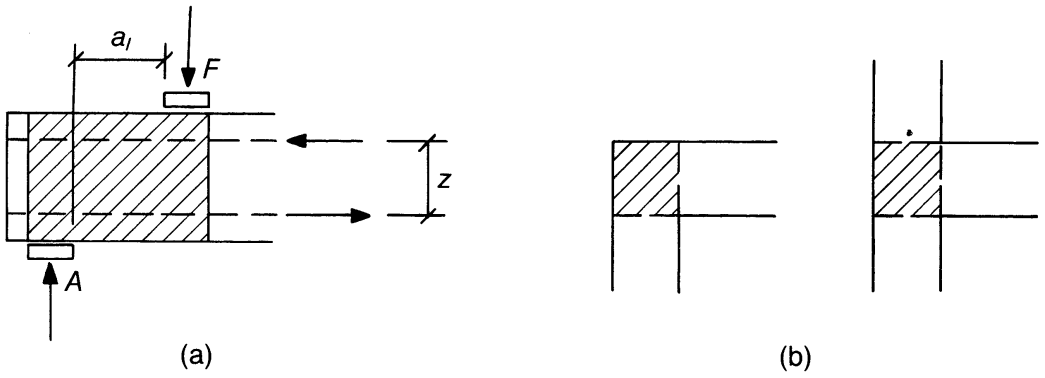

Figure 2.6 D-regions (a) near a concentrated load; (b) geometrical discontinuity (CEB 1990)

2.4 Experimental Research

2.4.1 Leonhardt and Walther (1961)

From 1961 to 1963 an experimental investigation of the shear behavior of reinforced concrete deep beams was conducted by Leonhardt and Walther. The authors found that while elastic solutions provide good agreement with behavior of uncracked beams, the distribution and values of stresses measured after cracking differed significantly from the theoretical elastic stresses. In addition, it was found that the actual stresses in the tensile reinforcement were much smaller than values calculated from classical elastic theory. They also observed strut action, as in a truss with inclined concrete compression members and horizontal steel tension members, that developed after inclined cracks occurred.

In particular, it was observed that the stresses in tensile flexural reinforcement were almost constant across the clear span of deep beams. It meant that the steel acted as a tension tie with approximately constant force from one end of the beam to the other. Therefore, it was recommended that tensile flexural reinforcement should not be cutoff before reaching the supports.

An interesting result from Leonhardt and Walther's investigation was that for beams loaded on top and supported on the bottom, vertical or inclined web reinforcement

had no contribution. They concluded that for deep beams with span-to-depth ratio, L/d, less than 2, one should not speak of shear and shear reinforcement. Such beams always fail because the concrete crushed near the bearing where the principal compression stresses became critical and represented the upper limit of the carrying capacity, if the tie bars were well anchored and distributed.

2.4.2 De Paive and Siess (1965)

De Paiva and Siess conducted an investigation consisting of nineteen simply supported deep beams. The objectives of the investigation were shear strength and behavior of some moderately deep reinforced concrete beams. The investigation focused on the following major factors: the amount of tension reinforcement, the concrete strength, the amount of web reinforcement, and span-to-depth ratios. The beams were loaded at the third points, with span-to-depth ratios, a/d, ranging from 0.67 to 1.33. These beams had different arrangements of web reinforcement, no web reinforcement, and vertical or inclined web reinforcement. It was observed from the load- deflection curves that the behavior of deep beams contained two major stages, first, the elastic behavior of the beams up to yielding of the tension reinforcement, and, second, inelastic behavior after yielding and up to failure. The beams exhibited tied arch action after inclined cracks developed. It was found that after inclined cracks formed, the strain in tensile flexural reinforcement was almost constant along the clear span of the beam, and the concrete strain was concentrated near the mid-span over the ends of the inclined cracks. De Paiva and Siess also found that web reinforcement had no effect on the ultimate strength of beams failing in either flexure or shear. Although the objectives of the investigation were the behavior and shear strength of deep beams, 15 out of 19 of the specimens failed in flexure or flexure-shear. The size of specimens was unrealistically small compared to beams in a typical structure.

2.4.3 Kong et al. (1972)

Kong et al. conducted numerous tests of deep beams. Parameters considered in their study were span-to-depth ratios, l/d; shear span-to-depth ratios, a/d; vertical and horizontal web reinforcement ratios; effect of inclined web reinforcement; weight of concrete and size; and position of web openings. Thirty-five deep beams were tested with span-to-depth ratios varying from 1 to 3 and shear span-to-depth ratios varying from 0.23 to 0.7. The arrangement of web reinforcement varied from light to heavy vertical web reinforcement. It was found that the contribution of web reinforcement depended on the length-to-depth ratios and shear span-to-depth ratios. For small values of l/d and a/d ratios, only horizontal web reinforcement placed close to the bottom of the beam had an effect on the shear strength of deep beams. On the other hand, for larger l/d and a/d ratios, vertical web reinforcement contributed more than to the shear strength the horizontal web reinforcement. A semi-empirical equation for shear capacity was developed:

$$V_u = C_1(1 - 0.35\frac{x}{h}) f_{ti} bh + C_2 \Sigma A_s \frac{y}{h} \sin^2 \beta \qquad (2.11)$$

where,

C_1 is a coefficient equal to 1.4 for normal weight concrete and 1.0 for lightweight concrete,

C_2 is a coefficient equal to 130 MPa for plain round bars and 300 MPa for deformed bars,

f_{ti} is the split cylinder tensile strength of the concrete.

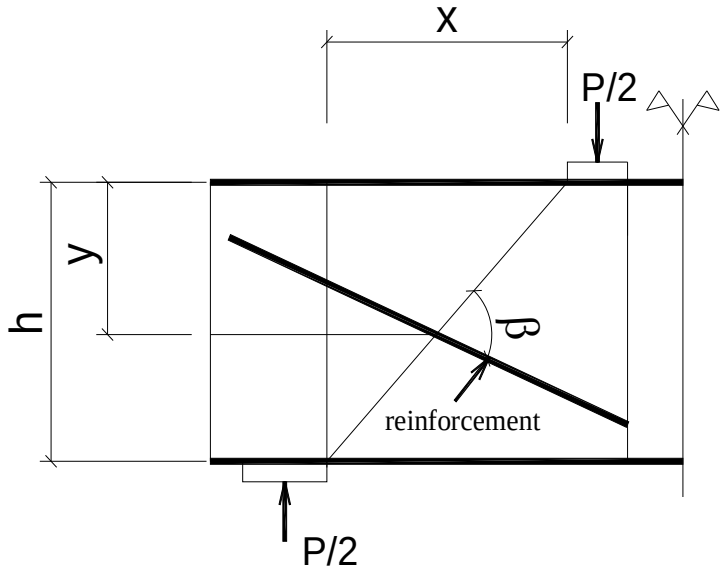

Figure 2.7 Kong's symbol definitions

The first term on the right-hand side of the equation is the contribution of concrete to the shear strength of deep beams. The second term on the right-hand side of the equation relates to the shear carried by the reinforcement. Eq. (2.11) was applied to shear span-to-depth ratios of 0.23 to 0.7.

2.4.4 Smith and Vantsiotis (1982)

In their study, Smith and Vantsiotis carried out an investigation of fifty-two reinforced concrete deep beams, which were loaded by two equal symmetrically placed point loads. The objectives of the investigation were to study the effect of vertical and horizontal web reinforcement and shear span-to-effective depth ratios on inclined cracking shear, ultimate shear strength, mid-span deflection, tension reinforcement strain, and crack width. The beams, in Fig 2.8, were divided into four series A, B, C, and D shear span-to-depth ratios a/d of 0.77, 1.01, 1.34, and 2.01, respectively. The web reinforcement varied from 0 to 0.91% for horizontal reinforcement and from 0 to 1.25% for vertical reinforcement. Concrete strength ranged from 16 to 23 MPa.

All fifty-two beams in this study exhibited shear failure. The web reinforcement had no effect on modes of failure. The formation of a tied-arch system was observed with

the tension reinforcement acting as a tie bar and portions of the beam outside the inclined cracks acting as compression struts after the inclined cracks occurred. Although web reinforcement did not change the modes of failure significantly, it reduced the level of damage and the crack width of beams at failure. It was also observed that inclined cracking occurred at about 40-50% of the ultimate load with/or without web reinforcement. Inclined cracks propagated to a distance equal to 20% of the total depth from the top side of the beams. Finally, beams failed by concrete crushing in either the reduced compression region at the head of inclined crack and the region adjacent to the loading block, or by fracture of the concrete along the inclined crack. The amount of web reinforcement also had no effect on the cracking load. The contribution of web reinforcement to ultimate shear strength was less than the limit value of $4\sqrt{f'_c}b_w d$. The contribution of vertical web reinforcement was greater than the horizontal web reinforcement, especially when shear span-to-depth ratios increased. However, it seems that the effectiveness of vertical web reinforcement diminished when the shear span-to-depth ratio was less than 1.0.

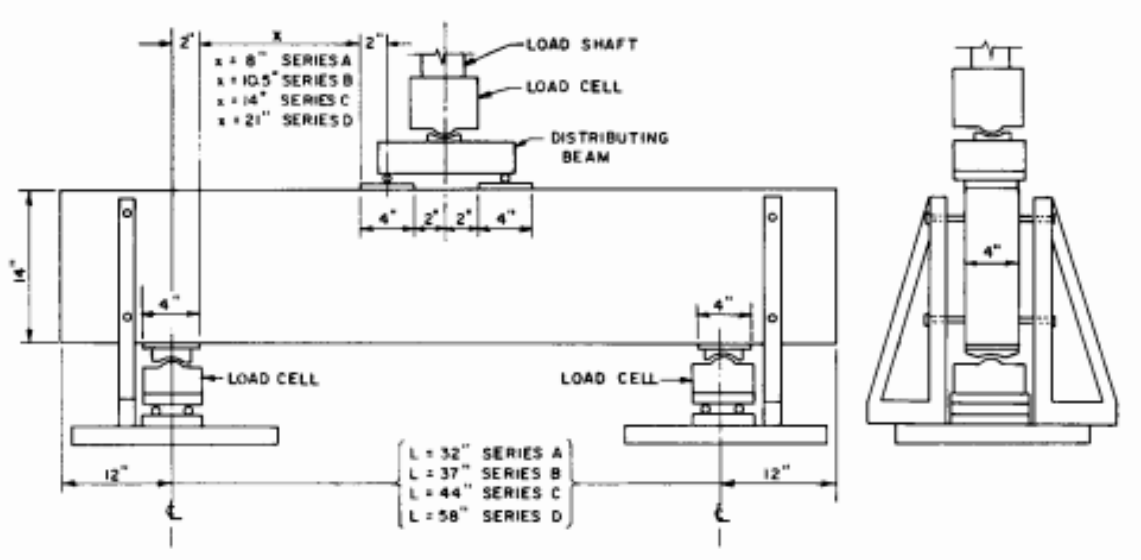

Figure 2.8 Loading and supporting conditions for test beams (Smith and Vantsiotis)

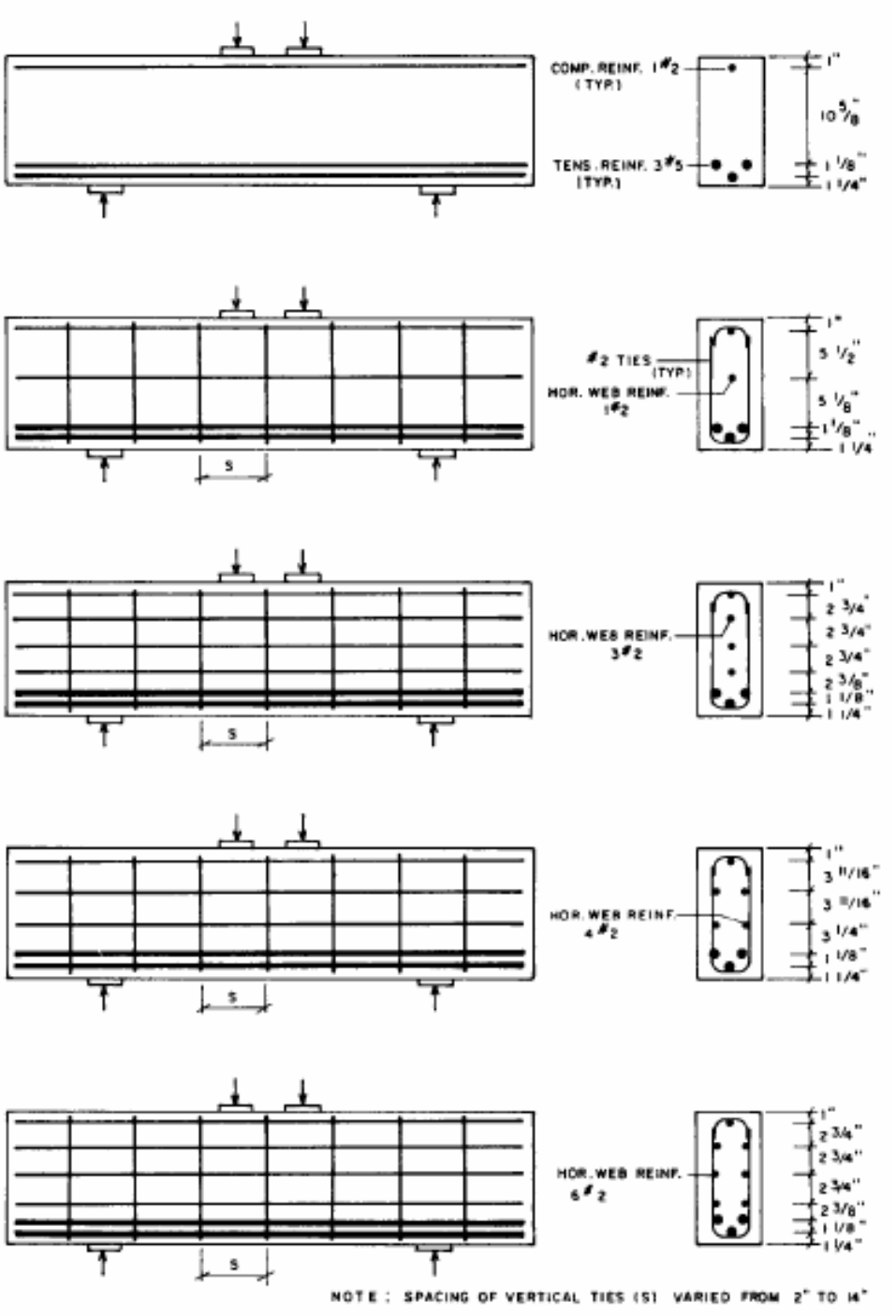

Figure 2.9 Detail of deep beams of Smith and Vantsiotis's investigation

2.4.5 Birrcher (2006)

In 2006, Bircher conducted an intensive full scale investigation of thirty-seven reinforced concrete deep beams with the following cross-sectional dimensions: 21”x23”, 21”x42”, 21”x44”, 21”x75”, and 36”x48”as shown in Figs. 2.10 to 2.14. Details of the specimens are provided in Table 2.1. These beams are some of largest reinforced concrete deep beams reported in literature. These specimens were unsymmetrically loaded with shear span-to-depth ratios, a/d, of 1.2, 1.85, and 2.5. The objectives of this experimental study were to investigate the effect of web reinforcement, effect of member depth, effect of singular nodes triaxially confined by concrete on the strength and serviceability of deep beams and to develop a simple strut and tie model design methodology for deep beams.

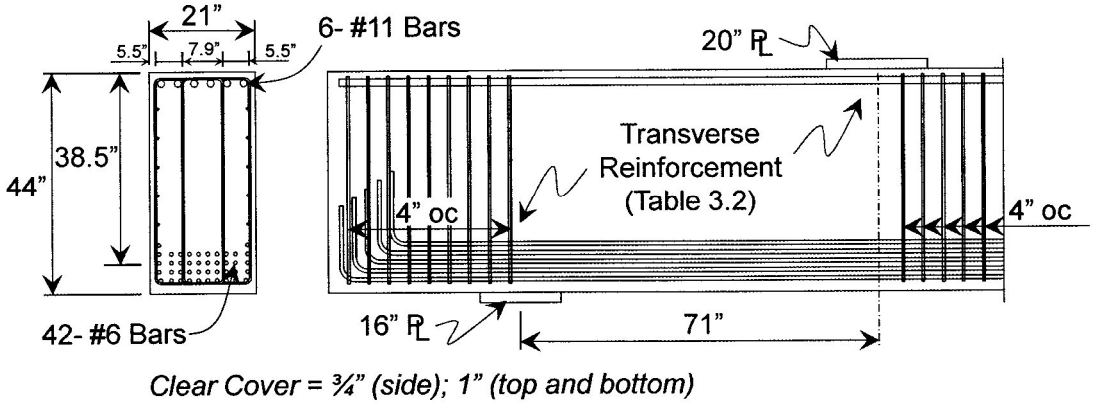

Figure 2.10 Detailing deep beams of series I (Birrcher 2006)

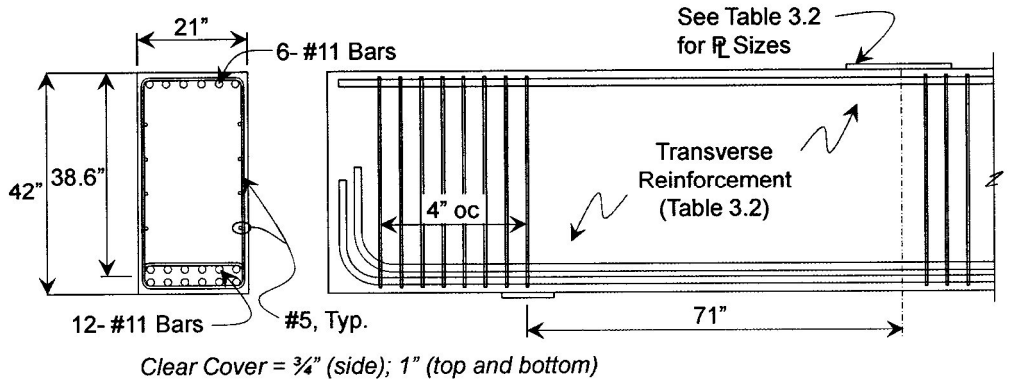

Figure 2.11 Detailing deep beams of series II (Birrcher 2006)

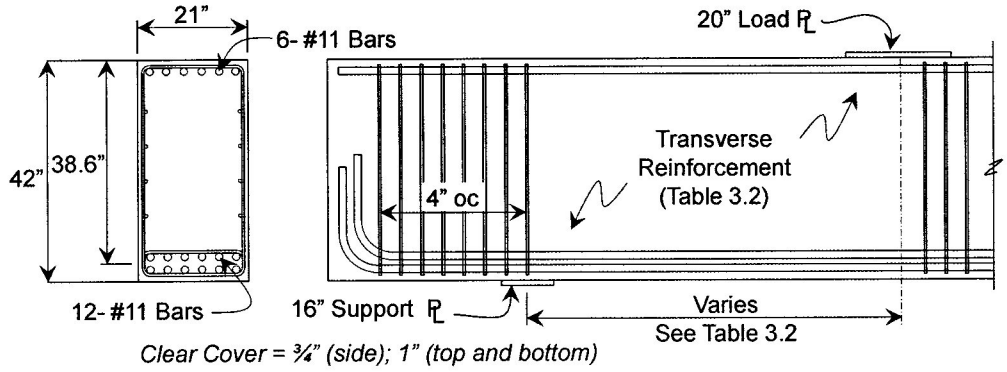

Figure 2.12 Detailing deep beams of series III (Birrcher 2006)

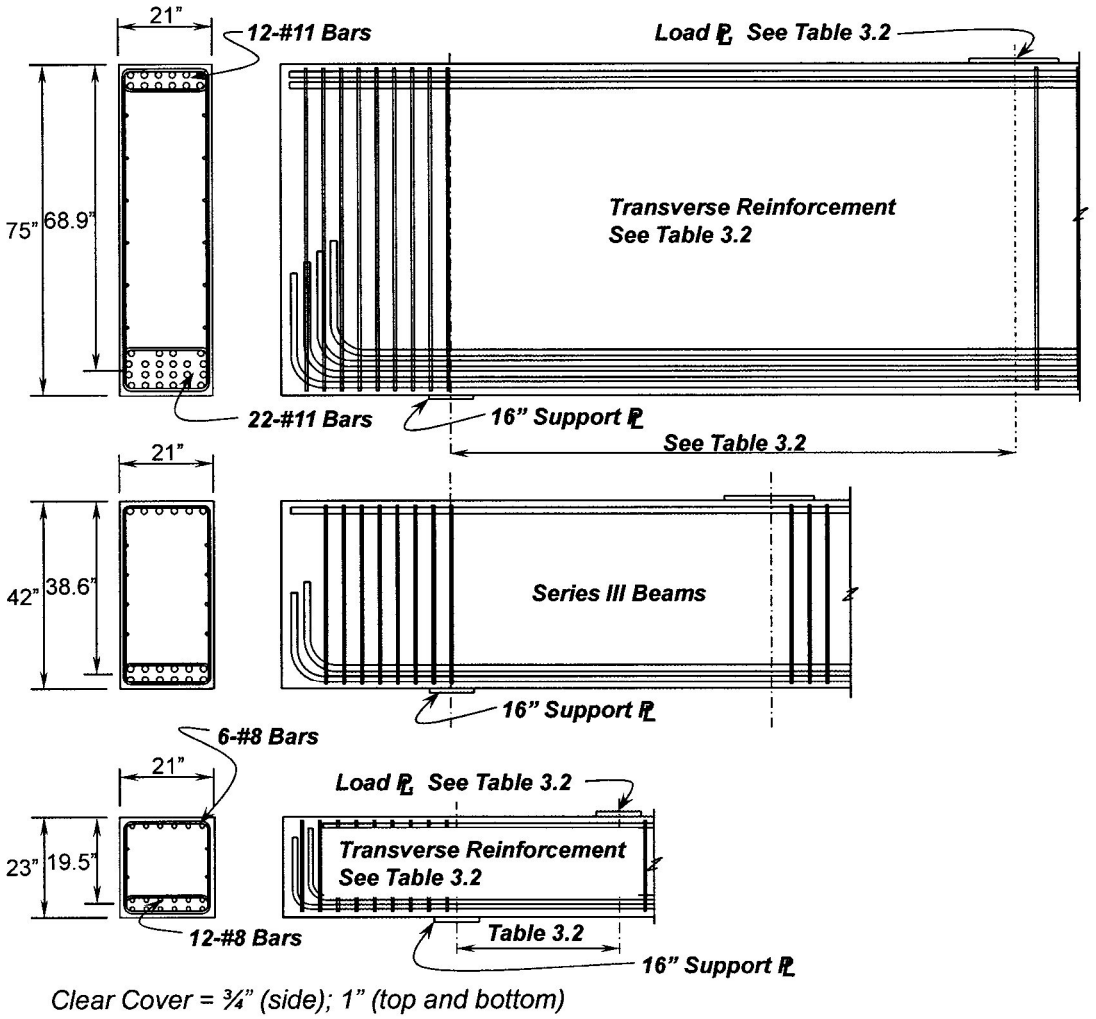

Figure 2.13 Detailing deep beams of series III, and IV (Birrcher 2006)

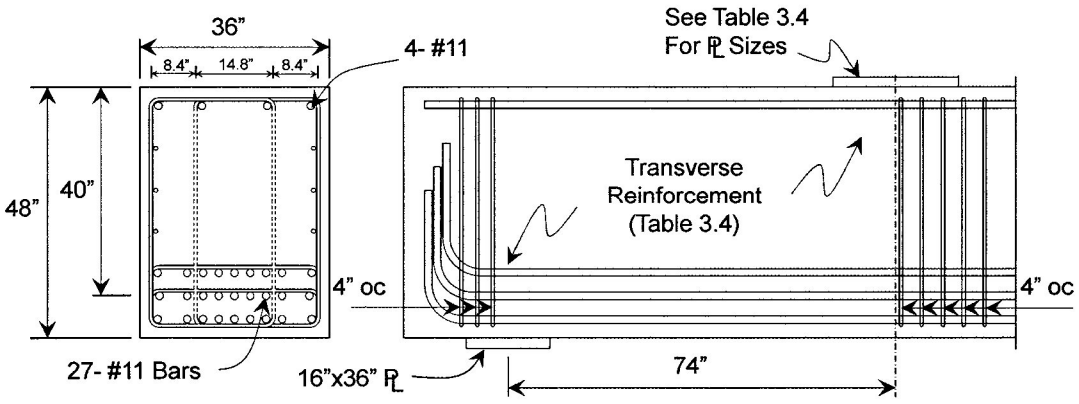

Figure 2.14 Detailing deep beams of series M (Birrcher 2006)

Table 2.1 Detailing dimensions of Birrcher's deep beams

Testing Series	b in.	d in.	Support Plate†	Load Plate†	No. of Stirrup Legs	ρ_v*	ρ_h*	a/d ratio
Series I Dist. of Stirrups across Web	21	38.5	16"x21"	20"x21"	2	0.003	0.003	1.84
					4			
					2	0.002	0.002	
					4			
Series II Triaxially Confined Nodal Regions	21	38.6	10"x21"	20"x21"	2	0.003	0.003	1.84
			10"x21"	10"x7"				
			10"x21"	36"x21"				
			5"x7"	36"x21"				
			5"x7"	36"x21"		0.002	0.002	
			10"x21"	10"x7"				
			10"x21"	10"x21"				
			5"x21"	20"x21"				
Series III Minimum Web Reinforcement	21	38.6	16"x21"	20"x21"	-	0.000	0.000	1.84
								2.47
					2	0.002	0.002	1.84
						0.0025	0.0015	
						0.003	0.003	
						0.001	0.001	
						0.003	0.003	
						0.002	0.002	
						0.002	0.002	1.20
						0.003	0.003	
						0.002	0.002	2.49
						0.003	0.003	
Series IV Depth Effect	21	68.9	16"x21"	29"x21"	2	0.002	0.002	1.85
						0.003	0.003	
				24"x21"		0.002	0.002	2.50
						0.002	0.002	1.20
		19.5		16.5"x21"		0.003	0.003	1.85
						0.002	0.002	
				15.5"x21"		0.002	0.002	2.50
				18"x21"		0.002	0.002	1.20
Series M Multiple Purpose	36	40	16"x36"	24"x36"	4	0.003	0.003	1.85
				8"x12"		0.003	0.003	
				24"x36"		0.009	0.003	
				24"x36"		0.002	0.002	
				24"x36"	2	0.003	0.003	

Birrcher's experimental study provided important information regarding the behavior of full-scale reinforced concrete deep beams. It has been shown that in

discontinuity regions, dimensions also affect on the shear behavior of elements. Even though the purpose of the study was other than to develop a design equation for deep beams, the experimental full-scale tests of deep beams provided the results of tested deep beams that are close to the behavior of real elements. This is also the reason that Birrcher's tests were selected as the original models from which to build computer models for using in ATENA for investigating the behavior of reinforced concrete deep beams. Computer models using ATENA will be presented in detail in Chapters 4 and 5.

2.4.6 Rogowsky and MacGregor (1983)

In 1983 Rogowsky and MacGregor conducted an extensive study of the behavior of both simply supported and continuous deep beams in Fig. 2.15. Six simple span and seventeen two span continuous deep beams with shear span-to-depth ratios ranging from 1 to 2.5 were tested. The effect of various arrangements and amounts of web reinforcement on deep beam behavior was investigated.

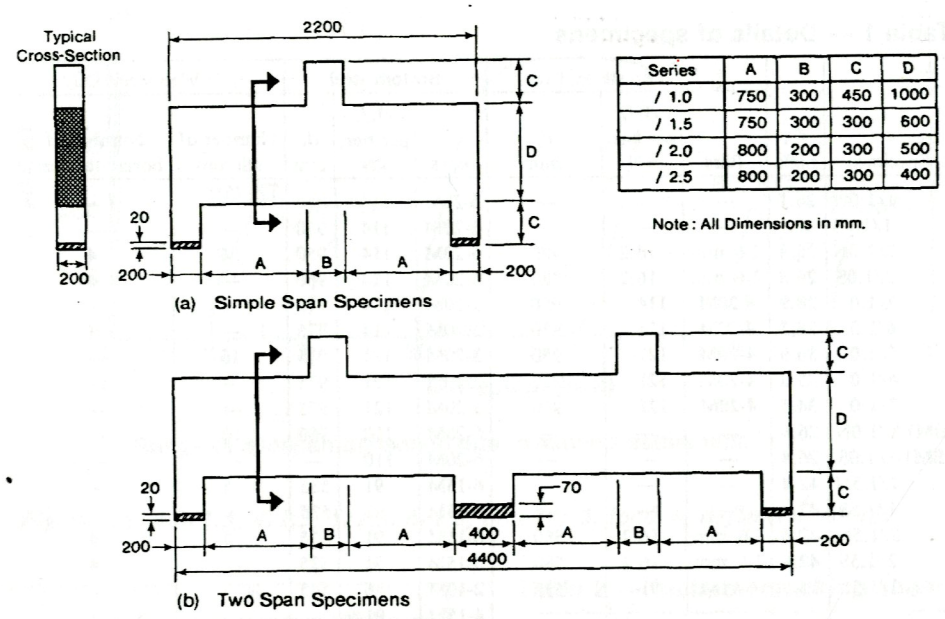

Figure 2.15 Overall dimensions of specimens (Rogowsky and MacGregor 1983)

Different from other investigations, the beams were cast monolithically with columns. The beams supported by columns and the load were applied through columns. The objective of this study was to develop design procedures for continuous deep beams.

The authors observed truss behavior or tied arch behavior after inclined cracks occurred. They also found that the plastic truss model gave good predictions of behavior of reinforced concrete deep beams. A plastic truss model is a model idealizes the beam as a pin jointed truss with concrete acting as compression members and steel acting as tension members. Some different modes of plastic truss were illustrated in Figure 2.16.
The basic assumptions for the plastic truss model are:

(1) Equilibrium must be satisfied,

(2) The concrete only resist compression and has an effective compressive strength $f^*_c = \nu f'_c$, where $\nu < 1.0$,

(3) The steel is required to resist all tensile forces and is represented by an elastic-perfectly plastic stress-strain relationship.

(4) Failure of the truss occurs when it forms a mechanism due to either a concrete compression member crushing, or a steel tension member yielding.

The arrangement of elements in a plastic truss had a large influence on the calculated capacity, especially for continuous deep beams where several different plastic truss models can be formulated. The authors concluded that the appropriate plastic truss was the strongest one which fits within, and is compatible with the geometry of the beam.

Results of tested beams were compared with the design equation in ACI Code 318. The design equation in the ACI Code agreed well with the measured simply supported deep beam capacity. However, the design equation in the ACI Code was not conservative for the continuous deep beams tested. This is not surprising since the ACI design equation for deep beams was based on test results of simply supported deep beams. It was concluded that the design equation in the ACI Code was not based on a true mechanical model of the behavior.

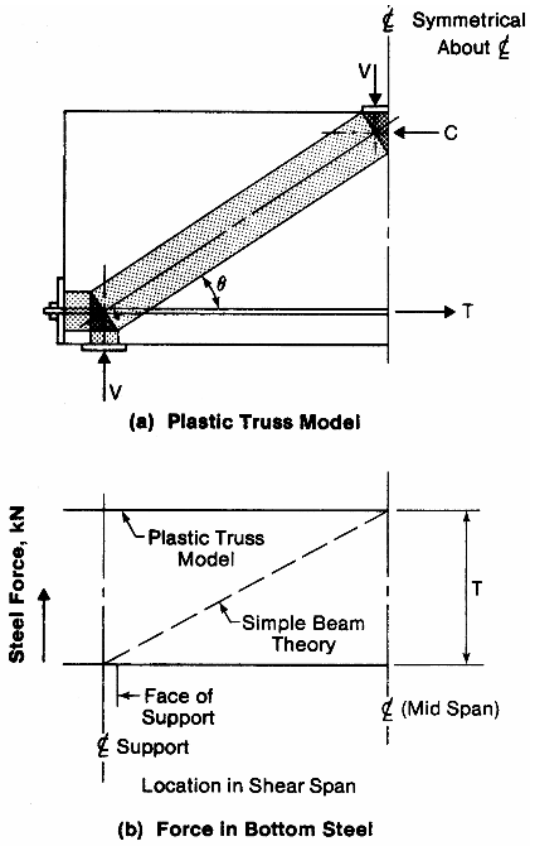

Figure 2.16a Plastic truss model for beam without web reinforcement (Rogowsky and MacGregor 1983)

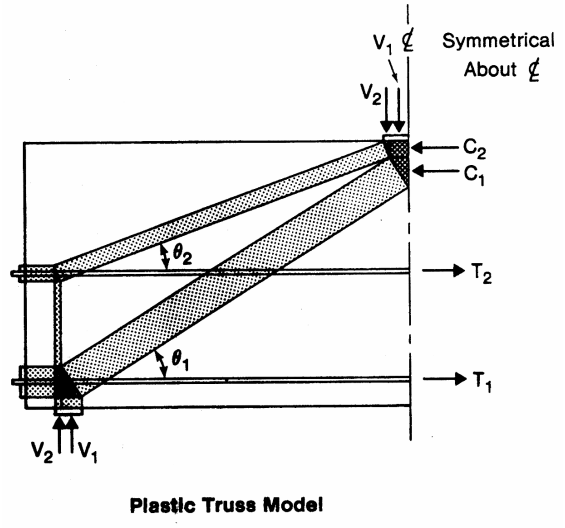

Figure 2.16b Plastic truss model for beam with horizontal web reinforcement (Rogowsky and MacGregor 1983)

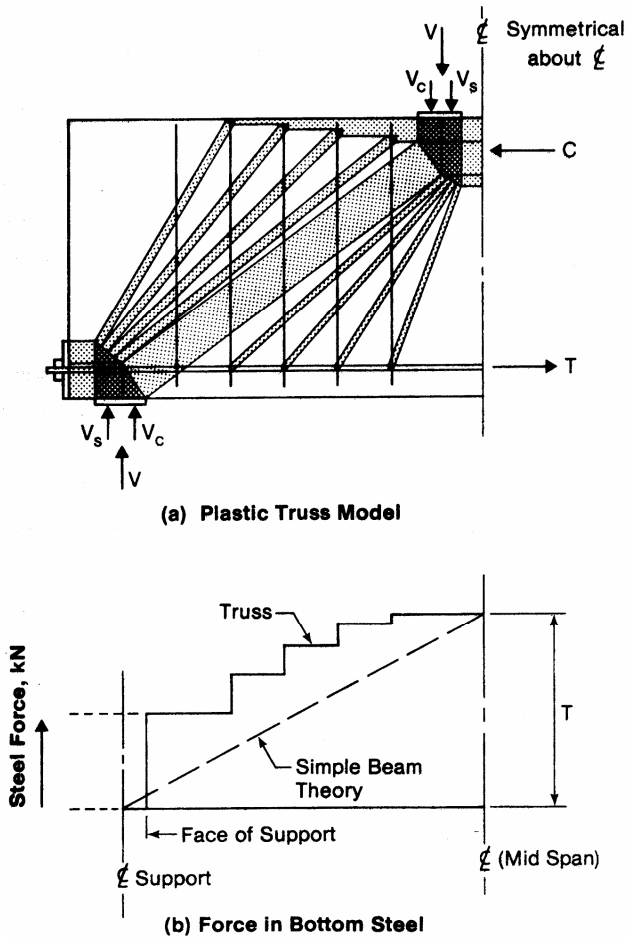

Figure 2.16c Plastic truss model for beam with stirrups (Rogowsky and MacGregor 1983)

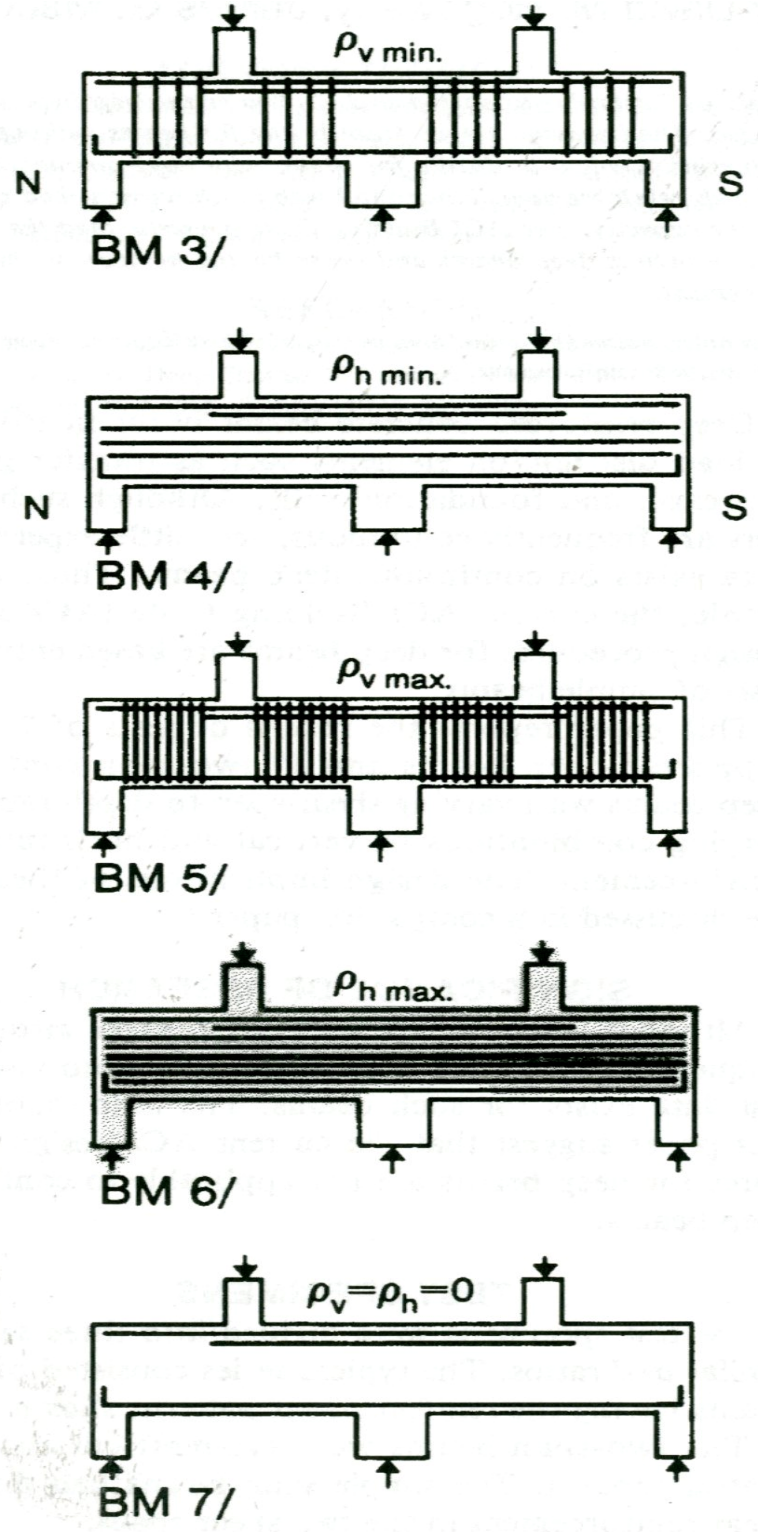

Figure 2.17 Typical test series (Rogowsky and MacGregor 1983)

Prior to the investigation of Rogowsky et al. there were very few tests of continuous reinforced concrete deep beams. The experimental work carried out by Rogowsky et al. made a vital contribution to the understanding of the behavior of continuous deep beams.

2.4.7 Subedi (1997)

Subedi conducted an investigation of both simply supported and two-span continuous deep beams. The author tested thirteen simply supported and four continuous deep beams. The two-span continuous deep beams shown in Fig. 2.18 had overall dimension from 50x400x500 mm to 75x600x1680 mm (width x depth x length) and span-to-depth ratios from 1.25 to 2.8 and shear span-to-depth ratios from 0.29 to 1.28. Web reinforcement consisted of 6 mm steel bars at a spacing of 100 mm from c-c for all beams.

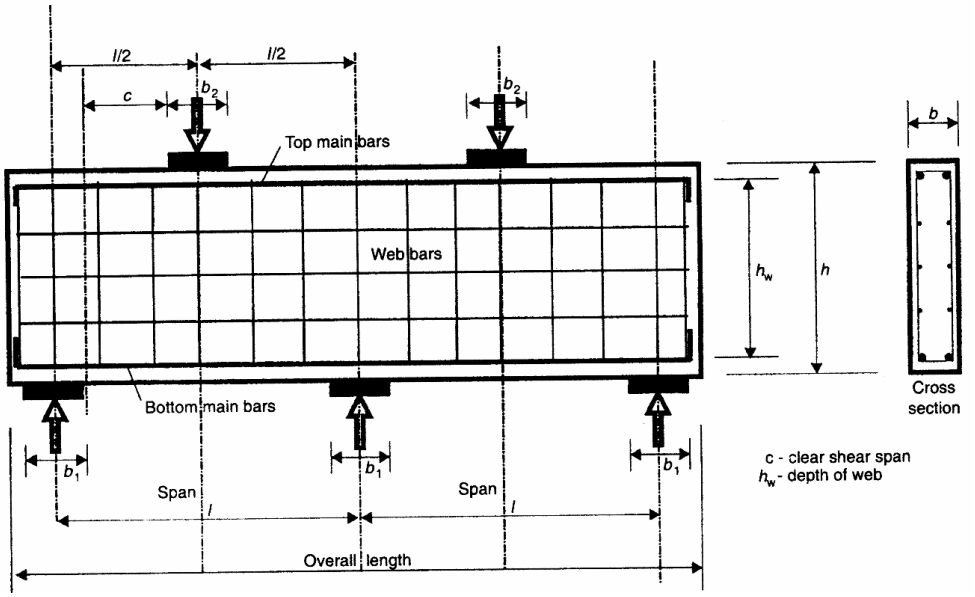

Figure 2.18 A typical two span continuous deep beam (Subedi)

The objective was to describe the structural behavior of two-span continuous deep beams. It was observed that there were three modes of failure (a) an unsymmetrical parallel inclined crack mechanism, (b) a symmetrical inclined crack mechanism, and (c) a bearing failure under loading regions (Figs. 2.19 and 2.20). In the unsymmetrical mode of

failure two major parallel inclined cracks formed between the edges of the loading plates and the supports. Beams failed by the formation of three crushing and one spalling zones at the ends of the major cracks. In the symmetrical inclined cracking mechanism, the beams failed when two major symmetrical diagonal splitting cracks formed. These inclined cracks radiated from the edges of the bearing plates at the central support to the edges of the top loading plates together with the formation of four crushing zones at the ends of the cracks. The bearing failure under loading plates or above the support was caused by concentrated stresses on small bearing areas. This mode of failure should be prevented because it led to premature failure before the full capacity of a beam in flexure or in shear was exploited. From the two failure mechanisms, the author derived two models for calculating the strength of two-span continuous deep beam.

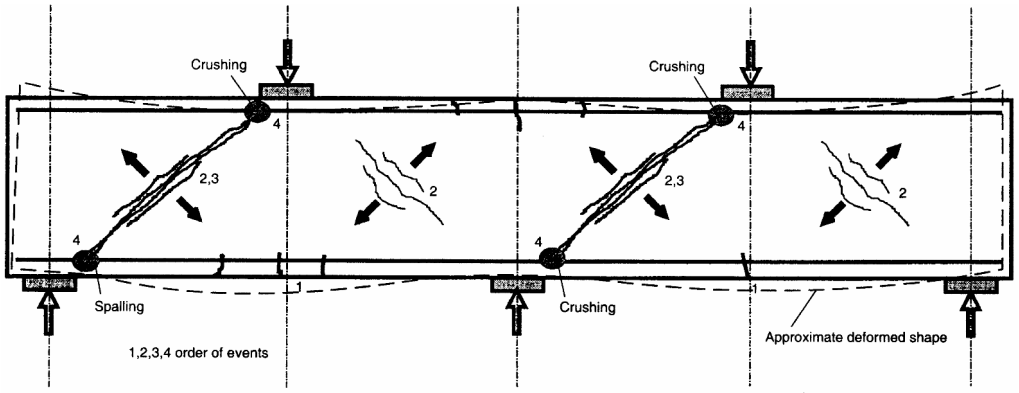

Figure 2.19 Mechanism at failure, unsymmetrical parallel cracks mechanism (Subedi)

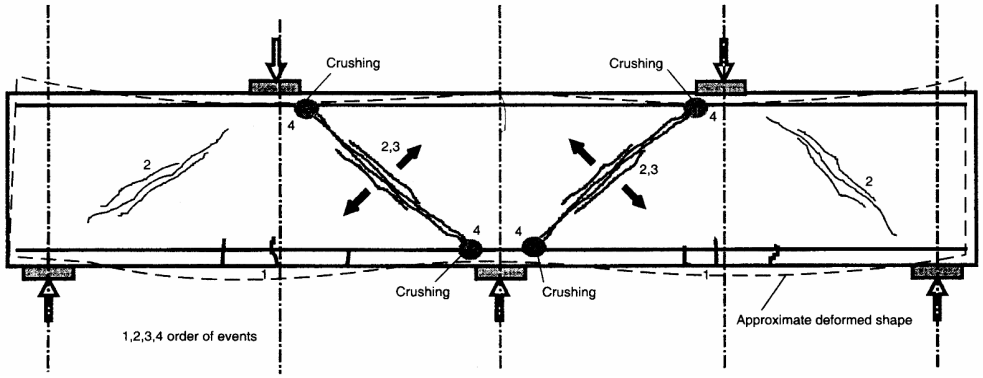

Figure 2.20 Mechanism at failure, symmetrical inclined crack mechanism (Subedi)

2.4.8 Ashour (1997)

At the same time of Subedi's work on continuous deep beams, Ashour conducted an experimental investigation of eight reinforced concrete continuous deep beams (Fig 2.21a and b). The main factors included were shear span-to-depth ratio, amount and type of web reinforcement, and ratio of tensile longitudinal reinforcement. The test results were compared with ACI Building Code 318-1989 and CIRIA Guide 2.

The eight beams were separated into two series with two different shear span-to-depth ratios. For series I, the depth was 24.6 in. to give a clear shear span-to-depth ratio of 0.8 and for series II the depth was 16.7 in. to give a clear shear span-to-depth ratio of 1.18.

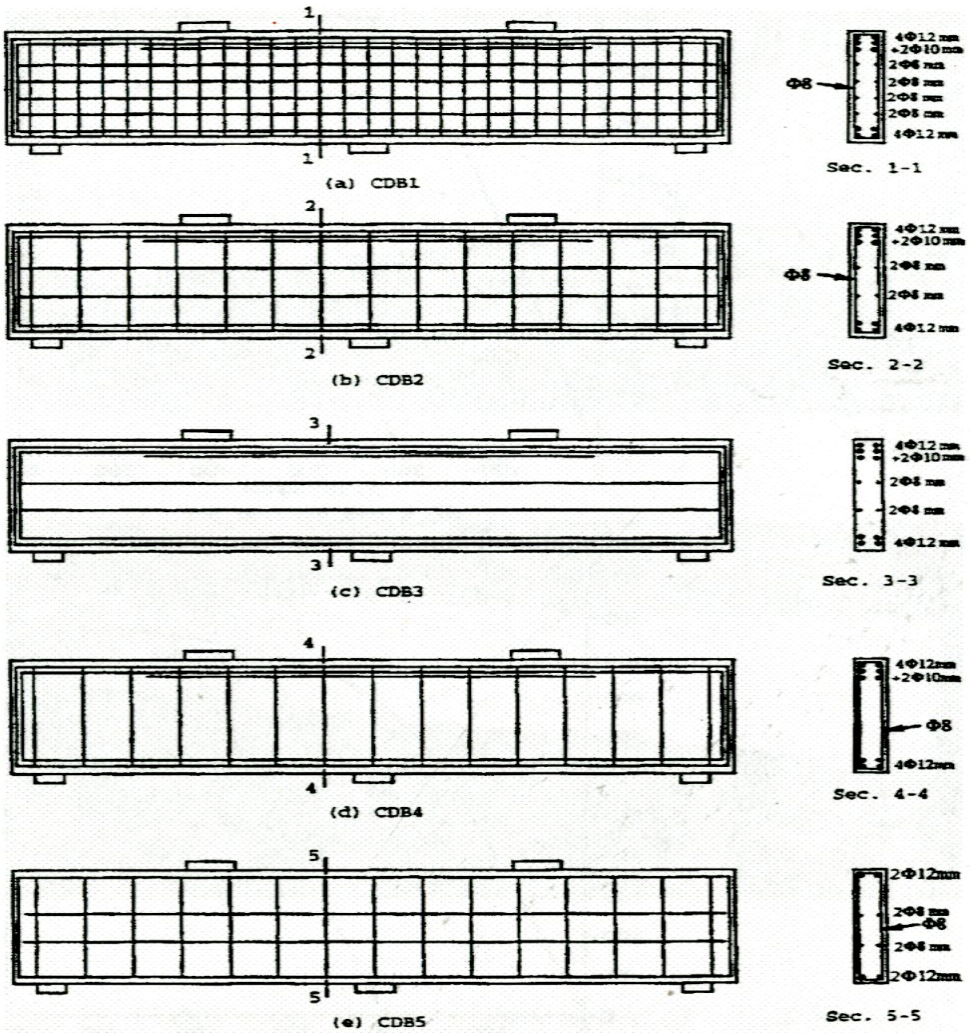

Figure 2.21a Details of specimen reinforcement (Ashour 1997)

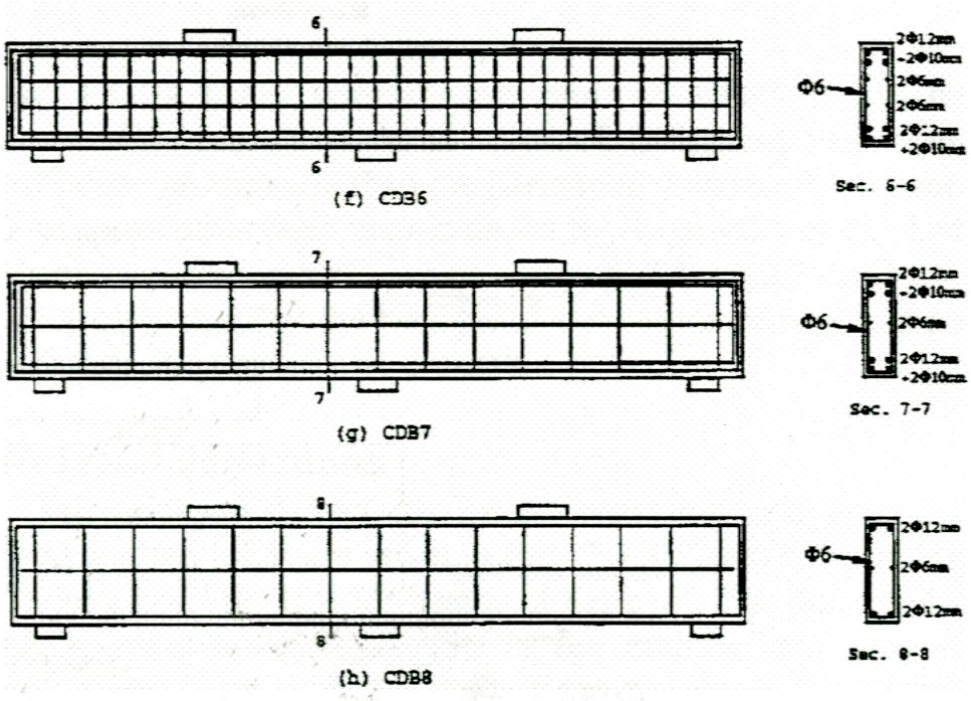

Figure 2.21b Details of specimen reinforcement (Ashour 1997)

It was observed that the shear strength of continuous deep beam was affected by the type of web reinforcement. The author reported that the vertical web reinforcement was more effective than the horizontal web reinforcement. The beams developed a truss or tied arch action after major inclined cracks formed.

2.5 Analytical Research

2.5.1 Crist (1971)

Based on test results Crist derived equations for the static shear strength of deep beams. These semi-rational design equations were the basis for the ACI Code design recommendations for deep beams. The equations were based on the premise that:

Total shear capacity = shear capacity of the concrete + shear capacity of the web reinforcement.

$V_u = V_c + V_s$

The contribution of concrete to the shear capacity, V_c, is:

$$V_c = \left[3.5 - \frac{4}{3}\left(\frac{M}{V}\right)\frac{l}{d}\right]\left[1.9\sqrt{f'_c} + 2500\left(\frac{M}{V}\right)\rho_w d\right]b_w d$$

The term $\left[1.9\sqrt{f'_c} + 2500\left(\frac{M}{V}\right)\rho_w d\right]b_w d$ in the right-hand side of the equation is the inclined cracking load of a normal beam while the term $\left[3.5 - \frac{4}{3}\left(\frac{M}{V}\right)\frac{l}{d}\right]$ of the equation represents the reserve shear capacity of deep beams after the inclined crack formed.

The contribution of web reinforcement was based on shear friction along the inclined crack. The shear friction analogy gives:

$S = F_{DT} \tan\phi$

where,

F_{DT} is the normal force on the inclined crack

$\tan\phi$ is the apparent coefficient of friction

S is the shear along the crack

The vertical component of the shear along the inclined crack is:

$V_s = S \sin\theta$

The normal force F_{DT} is the tensile force in the web reinforcement which results from crack opening as slip occurs.

By assuming that the stirrups yield at the ultimate load:

$F_v = A_v f_y$

and

$$F_{DT} = \Sigma\left(F_{DT}\right)_i = \Sigma F_{vi} \sin(\alpha_i + \theta)$$

where,

θ is the angle between inclined crack plane and longitudinal axis of the beam

α_i is the angle between web reinforcement and longitudinal axis of the beam

and therefore

$$V_s = \Sigma F_{vi} \sin(\alpha_i + \theta) \tan\Phi \sin\theta$$

Using a lower bound to the crack inclination data for uniformly loaded deep beams gives

$$\cos^2\theta = \frac{1}{12}\left(1+\frac{l_n}{d}\right)$$

By substituting $\cos^2\theta$ into the equation of V_s:

$$V_s = f_y d \tan\phi\left[\frac{A_v}{s}\frac{1}{12}\left(1+\frac{l_n}{d}\right)+\frac{A_{vh}}{s_h}\frac{1}{12}\left(11-\frac{l_n}{d}\right)\right]$$

2.5.2 Schlaich, Schafer, and Jennewein

A truss model was developed in 1899 by Ritter. The truss model was refined and expanded by Leonhardt, Rusch, Kupfer, and others. However, a truss model can not account for static or geometric discontinuities such as point loads or frame corners, corbels, deep beams, and other openings. In 1987, Schlaich, Schafer, and Jennewein systematically proposed strut-and-tie models that could be applied systematically to all parts of any concrete structure. In general, the strut-and-tie models could be used for both the ultimate limit state and serviceability in the cracked state.

In using the strut-and-tie model procedure the structure is divided into its B-regions and D-regions (Fig.2.22). B-regions are regions of a structure, in which the Bernoulli hypothesis of plane strain distribution is valid, and D-regions are the other regions and details of a structure where the strain distribution is significantly non-linear (Fig. 2.23). B-regions could be designed by standard truss model or standard methods and B-regions analysis provides the boundary forces for the D-regions.

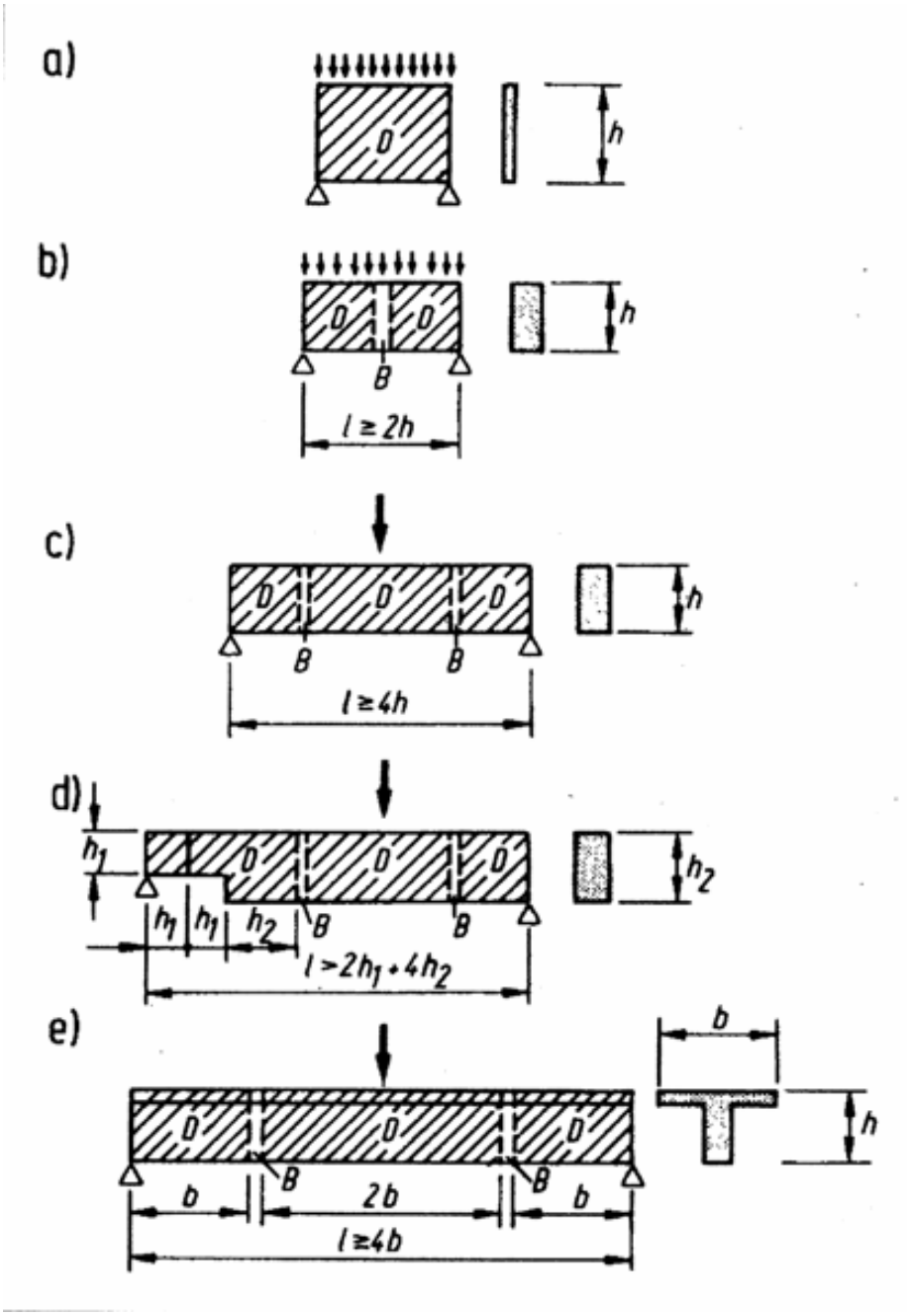

Figure 2.22 The identification of B- and D-regions (Schlaich et al. 1987)

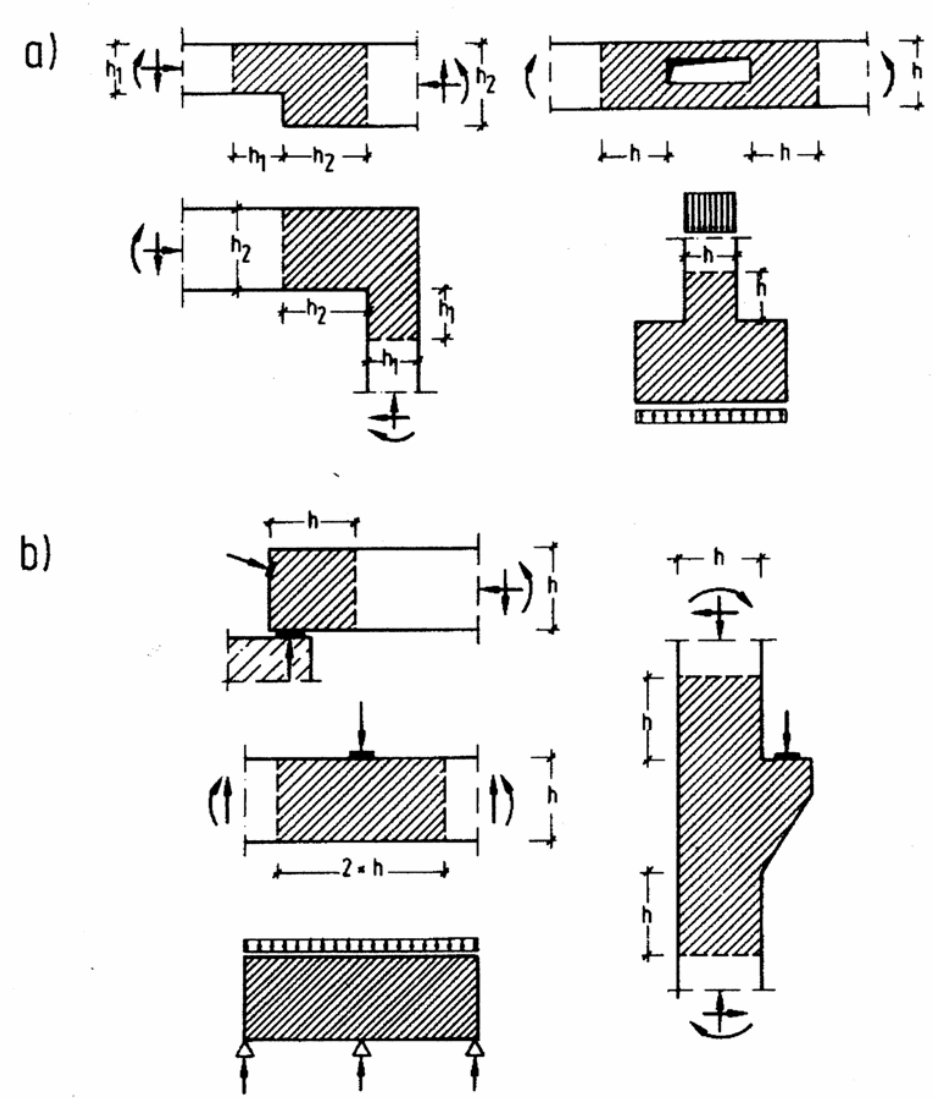

Figure 2.23 D-regions with nonlinear strain distribution (Schlaich et al. 1987)

For designing D-regions, a strut-and-tie model is developed and the internal forces of the strut-and-tie model are calculated based on equilibrium conditions. Dimensions of struts, ties, and nodes are calculated based on the strength conditions. The strut-and-tie model is a powerful and complex procedure. It can be used for designing some parts or all of a structure. Strut-and-tie models are developed for specified D-regions and load cases. However, there are always questions that arise about whether the correct model has been selected. Based on the load path method the authors induced a criterion for choosing a

correct model. The load path method is one way to sketch how load runs internal structure between loads and supports. “The load paths begin and end at the center of gravity of the corresponding stress diagrams and have there the direction of the applied loads or reactions. They tend to take the shortest possible streamlined way in between” Schlaich et al. (Toward a Consistent Design of Structural Concrete 1987). The best model is the one where loads use a path that requires the lowest forces and deformations. Since reinforced ties are much more deformable than concrete struts, the model with the least and shortest ties is the best one. The criterion may be formulated as follows:

$$\Sigma F_i l_i \varepsilon_{mi} = Minimum$$

where,

F_i is force in strut or tie i

l_i is length of member i

ε_{mi} is mean strain of member i

There are basically three types of struts and ties: concrete struts in compression; concrete ties in tension without reinforcement; and ties with reinforcement in tension.

There are four types of nodes depending on the combination of struts and ties such as CCC-node, CCT- node, CTT-node, and TTT-node (Fig. 2.24).

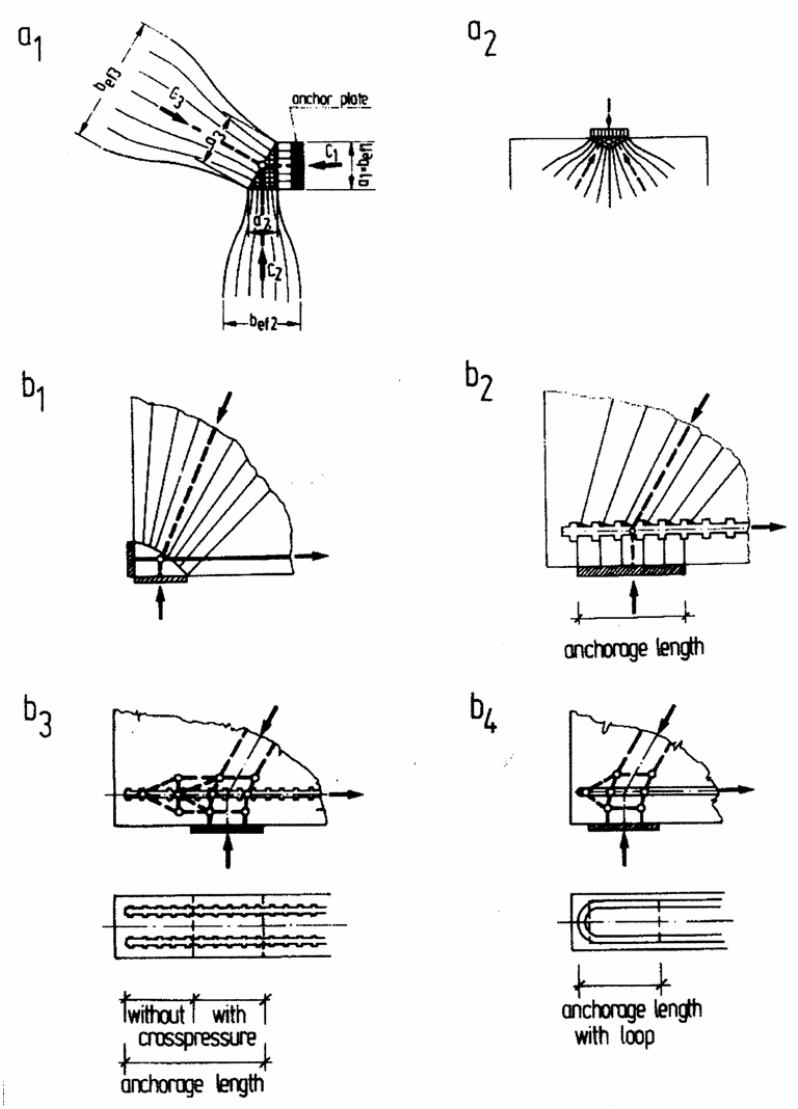

Figure 2.24a Examples of the basic types of nodes: (a) CCC-nodes; (b) CCT-nodes (Schlaich et al. 1987)

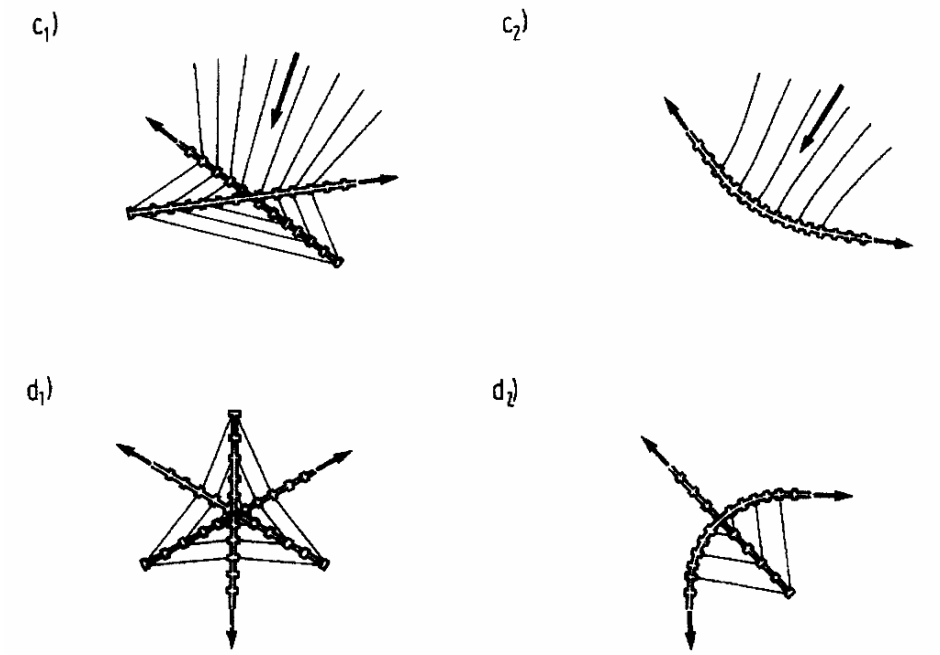

Figure 2.24b Examples of the basic types of nodes: (c) CTT-nodes; (d) TTT-nodes (Schlaich et al. 1987)

The failure criterion of concrete struts and nodes is given by:

$$f^*_{cd} \leq \beta f_{cd}$$

where,

β is the parameter which represents a multi-axial state of stress and is influenced by disturbances from cracks and reinforcement in struts and node regions.

$$f_{cd} = \frac{0.85 f'_c}{\gamma_c}$$

where,

$\gamma_c = 1.5$ is the partial safety factor for the concrete in compression

0.85 accounts for sustained loading

A strut-and-tie model is a powerful and versatile procedure, but it is also a complex, multistep, and laborious approach. It could be used to design a part or all of a structure, and one can check both strength and serviceability limit states with the same one model.

However, an application of a strut-and-tie model, in practice, requires knowledge of structural analysis and experience of structural behavior. It is a reason why many engineers hesitate using the strut-and-tie model procedure for design. A simple design equation for shear strength of deep beams would provide an alternative to the strut and tie approach and would serve as a check on the results of more complex design approaches and equations.

2.5.3 Mau and Hsu (1987-1989)

Mau and Hsu proposed a theoretical model for prediction of shear strength of simply supported deep beams. Using the three equilibrium equations from the truss model, the authors derived a formula for calculating shear strength of simply-supported deep beams. The formula consists of four important factors that influence the shear strength of deep beams: vertical web reinforcement, horizontal web reinforcement, concrete strength, and shear span-to-depth ratio.

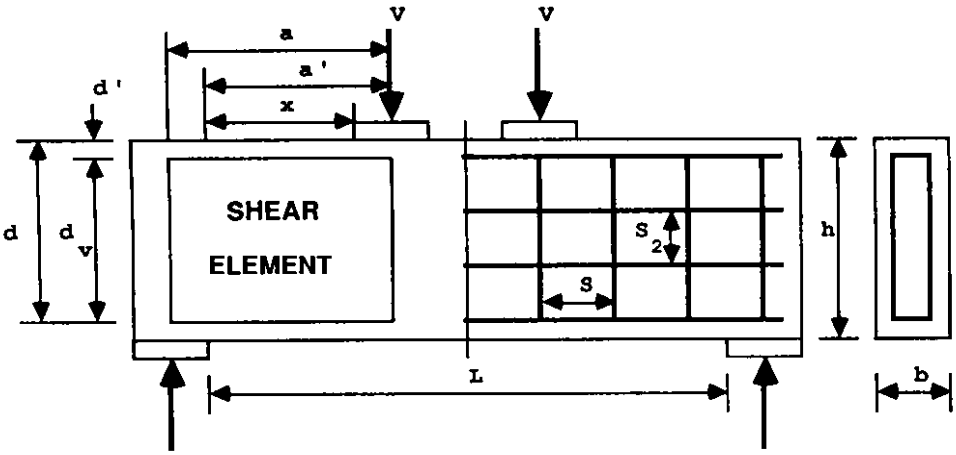

Figure 2.25 Definition of sketch (Hsu et al. 1989)

By introducing the concept of an effective transverse compression in the web of a deep beam (Fig. 2.26), the authors considered that the shear strength of deep beams may be calculated from the shear capacity of a shear element (Fig. 2.25). It was assumed that stresses in this element, a shear stress ν and a compressive stress p, are uniform. The effective compressive stress p is proportional to the shear stress ν:

$$p = K\nu$$

The value of the proportional constant K depends on the shear span-to-depth ratios, a/h, as follows:

$$K = \frac{2d_v}{h} \qquad \text{for } 0 < a/h \le 0.5$$

$$K = \frac{d_v}{h}\left[\frac{h}{a}\left(\frac{4}{3} - \frac{2}{3}\frac{a}{h}\right)\right] \qquad \text{for } 0.5 < a/h \le 2$$

$$K = 0 \qquad \text{for } a/h > 2$$

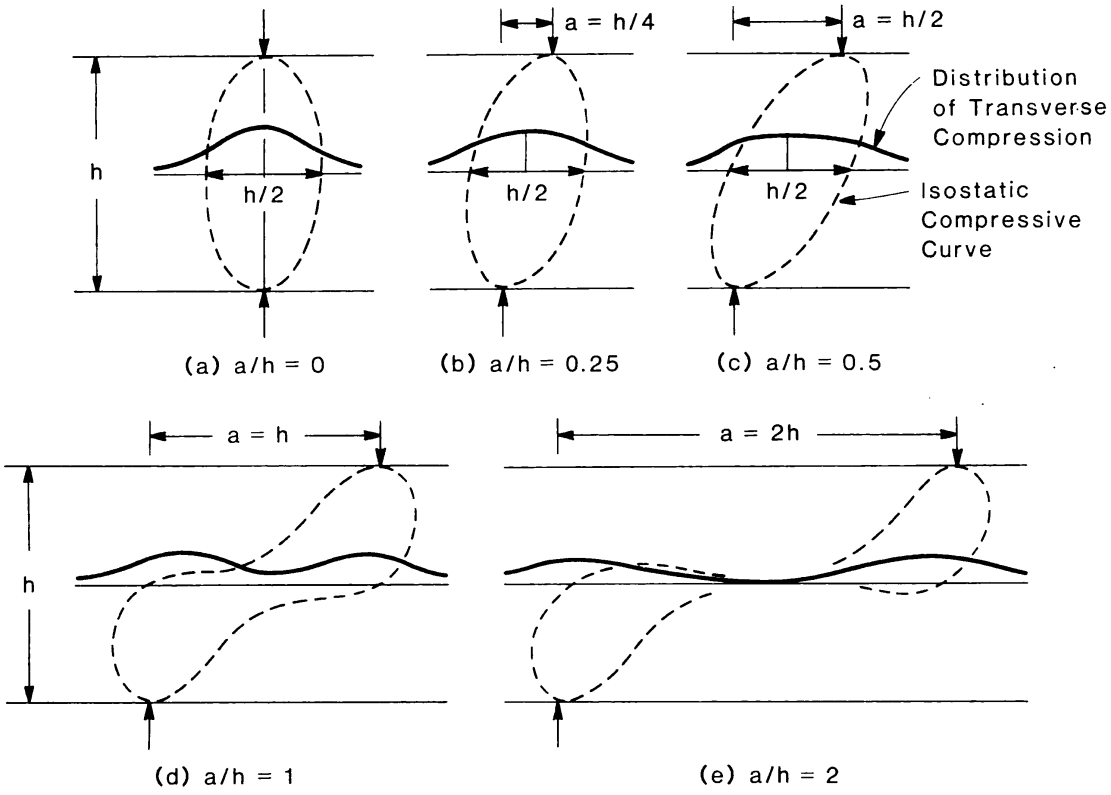

Figure 2.26 Distribution of transverse compressive stresses for various shear spans (Hsu et al. 1987)

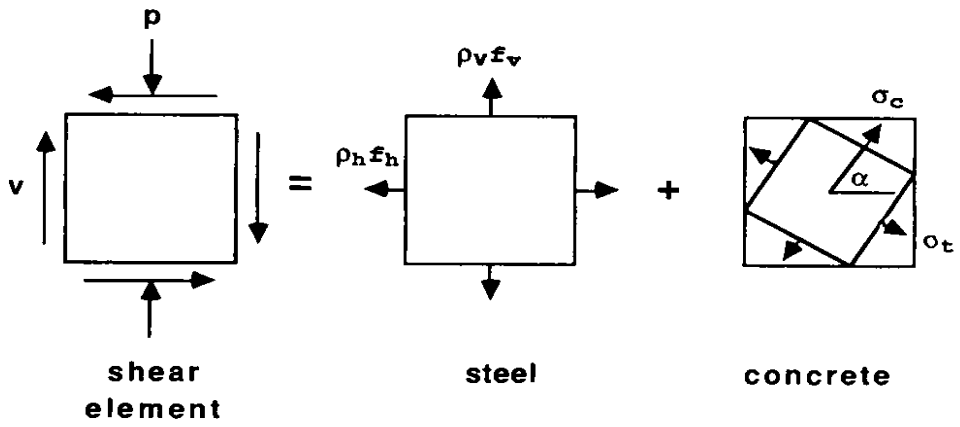

Figure 2.27 Stresses in the shear element (Hsu et al. 1989)

By transforming the concrete principal stresses and considering the equilibrium condition of the shear element, Mau and Hsu derived the formula for shear strength of a shear element and a deep beam:

$$\frac{v}{f'_c} = \frac{1}{2}\left[K(\omega_h + C) + \sqrt{K^2(\omega_h + C)^2 + 4(\omega_h + C)(\omega_v + C)} \right]$$

where,

$$C = \frac{\sigma_t}{f'_c}$$

$$\omega_h = \frac{\rho_h f_y}{f'_c}$$

$$\omega_v = \frac{\rho_v f_y}{f'_c}$$

This formula was compared to and calibrated using the results of 64 deep beam tests reported in the literature. The authors derived the following non-dimensional formula for predicting shear strength of deep beam as follows:

$$\frac{v}{f'_c} = \frac{1}{2}\left[K(\omega_h + 0.03) + \sqrt{K^2(\omega_h + 0.03)^2 + 4(\omega_h + 0.03)(\omega_v + 0.03)} \right] \le 0.3$$

with limiting values of $0 \le \omega_h \le 0.26$ and $0 \le \omega_v \le 0.12$.

As expected, this formula was in good agreement with the 64 tested beams. The disadvantage of Mau and Hsu's formula come from the assumptions of the distribution of

stress and strain in the shear element. These assumptions are invalid for discontinuity regions such as deep beams, corbel.

2.6 Needs for further research

Many other deep beam investigations reported in the literature. They were not included in the discussion of this literature review since they had results and conclusions were similar to those discussed in this chapter.

The literature review illustrated the need for further investigation:

(1) Current code provisions have no simple design equation for shear strength of reinforced concrete deep beams. The semi-empirical design equations have been removed from almost all current code provisions because they were not based on a true failure of mechanism of a deep beam.

(2) Almost all experimental investigations were carried out with dimensions that are small compared to a real structure. There were many simply supported deep beam studies, but very few tests of continuous deep beams.

(3) There is disagreement about the contribution of web reinforcement, particularly horizontal web reinforcement.

(4) Investigations of behavior of reinforced concrete deep beams are based on observations of crack patterns and deflections. There are no investigations of internal redistributions of stress and strain of deep beams after cracks form particularly after inclined major cracks occur.

(5) There are no studies of the influence of loading conditions on the behavior of deep beams. In the past, some investigators tested simply supported deep beams with loading plates and other investigators tested deep beams with columns cast monolithically.

(6) There is no simple design equation for shear strength of reinforced concrete deep beams, reflecting the true mechanism of failure. Currently, a strut-and-tie model procedure is used to design a discontinuity region, especially deep beams. Unfortunately, a strut-and-tie model, which is a multi-step, complex method, requires laborious

calculations. Designers need a simple, reliable, and transparent design equation for the shear strength of deep beams.

Chapter 3 Shear Database

3.1 Overview

In this chapter a deep beam database is introduced. The database consists of two parts: simply supported and continuous deep beams. The database of simply supported deep beams was compiled originally by Brown et al. (2006). The database of two span continuous deep beams has been added as part of the current study. The filtering criteria for selecting tests included in the database for use in this study is introduced.

3.2 Database of simply supported deep beams

Starting in the 1950's, there are numerous investigations on the shear strength of reinforced concrete deep beams (Clark 1951; Moody et al. 1954; Leonhardt and Walther 1962; Mathey and Wastein 1963; De Paiva and Siess 1965; Kani 1967; Crist 1971; Kong 1972; Smith and Vantsiotis 1982; Kotsovos 1984; Rogowsky et al. 1986; Mau and Hsu 1989; ASCE-ACI Committee 445 1998; Shin et al. 1999; Ashour 1997; Subedi 1997; Brown et al. 2006; Birrcher 2008). Since concrete is a non-isotropic material and has complex properties and unpredictable behavior, the information in the database varies widely. Different investigators had a different purposes in mind for their research and conducted limited and, sometimes, arbitrary tests. Thus a fundamental theory explaining the mechanism of shear failure of deep beams is still missing. To develop a mechanism of failure for deep beams, a database of data from deep beams is needed.

In 2006 a database of 905 reinforced concrete deep beam shear tests was originally compiled by Brown. The total includes 37 tests conducted at the University of Texas by Birrcher 2006 within Project 5253. Because the database of deep beams was compiled from technical literature reported over the last fifty years, there is wide variation in the data reported. Some tests may not be suitable for making comparisons and developing design recommendations. As a result, criteria for filtering the collected data are needed. The database was filtered in two stages. In the first stage, test results were removed due to a lack of sufficient details and non-shear modes of failure. The

criteria included minimum compressive strength of concrete material, details of the support and loading conditions, and the mode of failure (specimens failing in flexural and anchorage were not included). The resulting database is called the filtered database. In the second stage, additional tests were eliminated based on a minimum overall height and width of cross section. The resulting database is called the evaluation database.

Table 3.1 Filtering of the database of deep beams (a/d ≤ 2.5)

Collection Database		**905 Tests**
Stage 1 filtering	incomplete plate size information	-284 tests
	stub column failure	-3 tests
	$f'_c < 2000$ psi	-4 tests
Filtered Database		**614 tests**
Stage 2 filtering	$b_w < 4.5$ in.	-222
	$b_w d < 100$ in^2.	-73
	$d < 12$ in.	-13
Evaluation Database		**306 tests**

3.2.1 Filtered Database

A large number of tests in the collection database (284) did not have verifiable dimensions of bearing plates. The dimensions of bearing plates may affect the mode of failure and are needed for analysis of specimens. Hence, it was determined that only the specimens with detailed dimensions of bearing plates would be analyzed.

Of the remaining tests, specimens that had failure other than shear failure and that had concrete compressive strength less than 2000 psi were eliminated from the collection database. The filtered database contains data of 614 tests.

3.2.2 Evaluation Database

In the second stage of filtering, specimens that have dimensions of cross section that were not considered representative of typical members used in buildings or bridges were removed. A deep beam exhibits nonlinear and complex behavior that is influenced

by the dimensions of the cross section. As the dimensions of a cross section increase, the behavior of a deep beam will be more nonlinear and complex.

Beam with a width of less than 4.5 in., a shear area of less than 100 in^2., and an effective depth of 12 in were excluded. The remaining database contains 306 specimens and is called the evaluation database. Birrcher also developed an evaluation database that contained 186 tests because he eliminated a number of tests with small percentages of longitudinal flexural reinforcement.

3.3 Database of two span continuous deep beams

Reinforced concrete deep beams are commonly used as load distribution elements such as transfer girders, pile caps, tanks, folded plates, and foundation walls. Although such elements are frequently continuous, very few experimental investigations have been conducted on continuous deep beams. In fact, prior to 1999, ACI Code 318 provisions for shear in reinforced concrete deep beams were based entirely on procedures for simply supported deep beams. A database of reinforced concrete continuous deep beams was based on experimental investigations reported by Rogowsky et al., Asin, Ashour, and Subedi.

The database of continuous deep beams consists of seventeen two span continuous deep beams from Rogowsky's research, sixteen continuous deep beams from Asin's study, fourty-four continuous deep beams from Ashour's investigation, and four deep beams from Subedi's work.

Table 3.2 Number experimental investigations of continuous deep beams

Investigator	**Number of tests**
Rogowsky et al. (1983)	16 tests
Asin (1999)	12 tests
Ashour (1997)	08 tests
Subedi (1997)	04 tests
Yang et al. (2007)	36 tests
Total number	**76 tests**

Rogowsky et al.'s experimental investigation is especially important in understanding the behavior of reinforced concrete continuous deep beams. Experimental work on continuous deep beams has not received adequate attention from investigators around the world. Although most experimental tests of continuous deep beams were conducted between 1970s - 2000s, the specimens had unrealistic, cross section dimensions. The criteria applied to simply supported deep beams also apply to continuous deep beams. Four specimens in Subedi's investigation were removed because the width of tested beams was less than 4.5 in. The evaluation database for two-span continuous beams after filtering contains 72 specimens.

3.4 Computer modeling of beams tested

The behavior of reinforced concrete deep beams is often characterized by observing: the load or shear force first cracking occurs, when the major inclined crack occurs, ultimate load and deflection. The shear behavior of reinforced concrete structure after cracking is so complex and unpredictable and results in considerable scatter of test results, even though tests were carried out under the same conditions and the same dimensions. Curiosity about the behavior after cracking, redistribution of stress and strain after cracks occur has receives an attention from investigators around the world. Some attempts have been done to define the internal response of deep beams. Most investigators used strain gages on reinforcement to get such information. Others used finite element procedures to get the distribution of stress and strain of deep beams after cracks occurring. Unfortunately, the information regarding the distribution of stress and strain in deep beams has been insufficient to solve the problem.

In this study, a database of computer-models was developed. The database consists of two parts: the first is a verification database of deep beam and the second is a full scale database of computer-models of deep beams. In the verification database, computer-models duplicated real tests reported by Birrcher, Smith and Vantsiotis, and Rogowsly and MacGregor were used to verify the applicability of the ATENA program

for simulating deep beam shear behavior. In the full scale database, the computer-model-tests were based on dimensions of the specimens tested by Birrcher.

The full scale database contains subsets of computer-model-tests to investigate following problems:

(1) the influence of concrete strength on the shear strength of reinforced concrete deep beams. In this subset different values of concrete strength, f'_c, from 3000 psi to 6000 psi, were used

(2) the influence of longitudinal reinforcements on shear strength of deep beams. Different areas of longitudinal reinforcement between requirements of minimum and maximum code requirement for longitudinal reinforcement, were used

(3) the influence of shear span-to-depth ratios, a/d, on the shear strength of deep beams. Different values of a/d, from 1.0 to 2.5, were investigated

(4) the contribution of web reinforcement (vertical, only horizontal, or both vertical and horizontal) on the shear strength of deep beams.

(5) the influence of loading conditions on the shear strength of deep beams. The behavior and ultimate load of deep beams with different loading conditions were compared. Loading conditions investigated included single loading point, two loading points, uniformly distributed loading. Loads or reactions applied through bearing plates or monolithic columns were considered.

(6) the influence of size effect on the shear strength of deep beams. Deep beams with different height, from 23 in. to 75 in., were studied.

Chapter 4 Computer Model for Behavior of Reinforced Concrete Deep Beams

4.1 Overview

The ATENA program used in this study will be described. Computer models developed to replicate experimental tests of Smith and Vantsiotis, Birrcher, and Rogowsky and MacGregor will be discussed. The models were applied to simply supported and continuous deep beams for simulating the behavior of deep beams. The results of the computer models were calibrated used experimental test results.

4.2 ATENA Program

An introduction of ATENA program is provided in Appendix A. More details of background theory and manual documentation will be found in [9].

Computer models of reinforced concrete deep beams were developed as follows:

1. Material properties will be defined first.
    - Properties of concrete named as SBETA material were defined by inputting the value of cube concrete strength (based on f'_c) that was provided in the literature for each test or selected for modeling. Then ATENA will calculate automatically other parameters of concrete such as: elastic modulus, Poisson ratio, tensile strength, and cylinder concrete strength, f'_c. The behavior of concrete will be defined based on tensile and compressive laws for SBETA material.

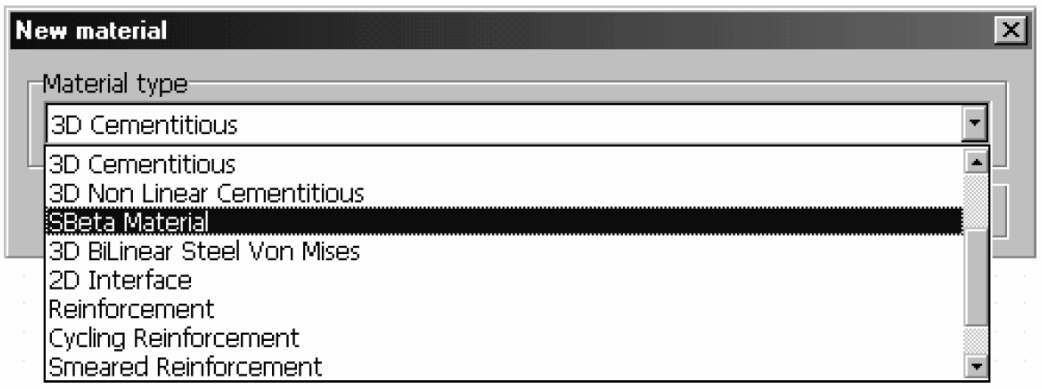

Figure 4.1 Selection of SBETA material model for concrete beam

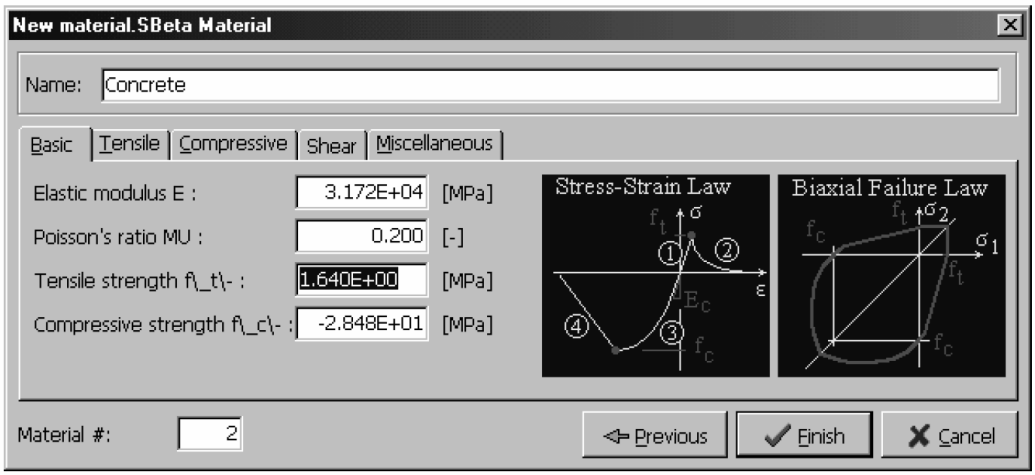

Figure 4.2 The dialog window for the definition of basic properties for SBETA material

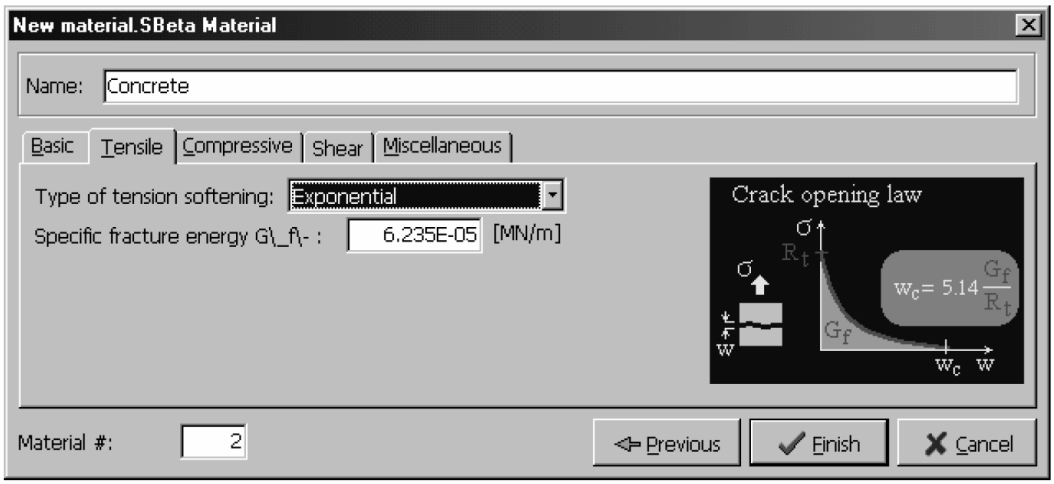

Figure 4.3 The dialog window for the tensile properties for SBETA material

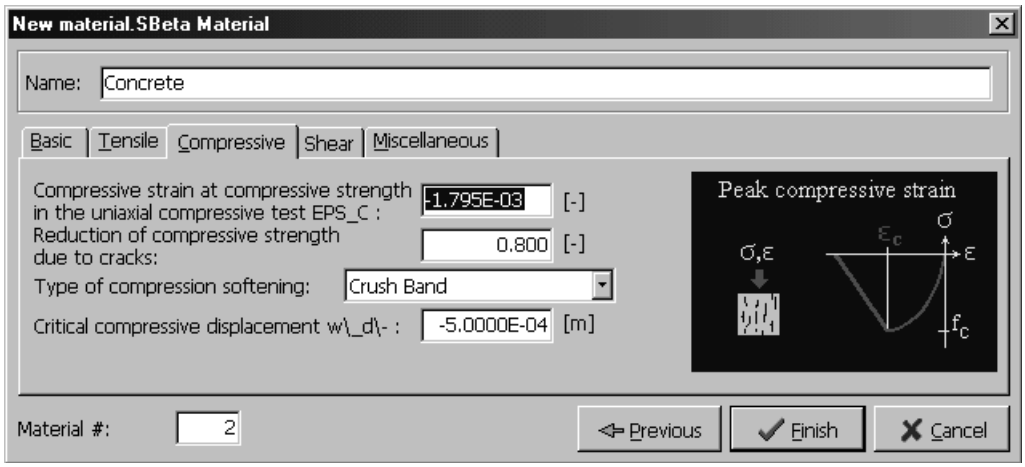

Figure 4.4 The dialog window for the compressive properties of SBETA material

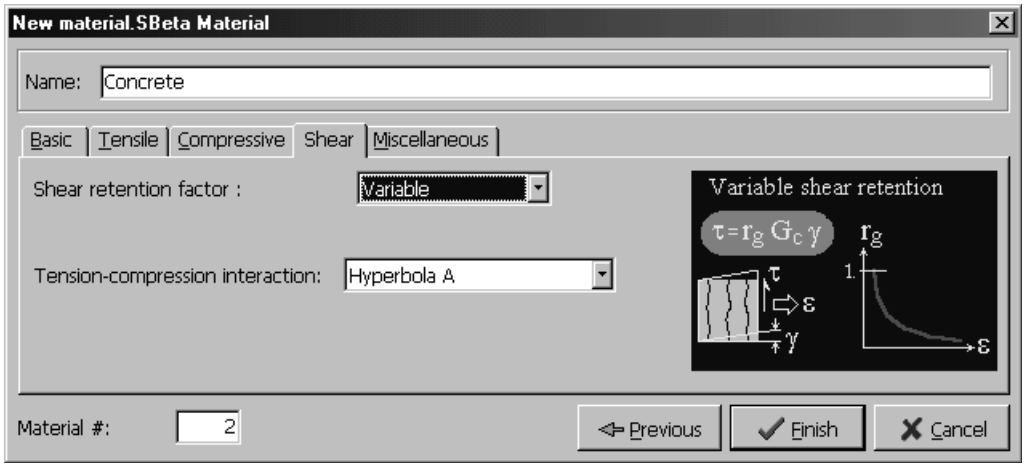

Figure 4.5 The dialog window for the shear properties of SBETA material

- Reinforcement used in computer models was defined as perfectly elastic-plastic material with two input parameters: elastic modulus, E and yield strength, f_y.

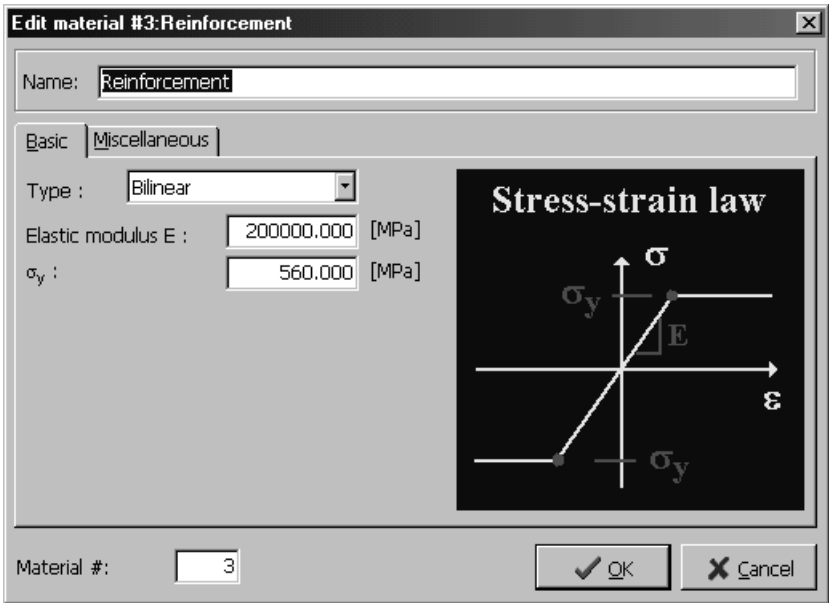

Figure 4.6 The dialog window for the definition of reinforcement material parameters

- Loading and bearing plates were defined as plane stress elastic isotropic material with two input parameters: elastic modulus, E and Poisson ratio.

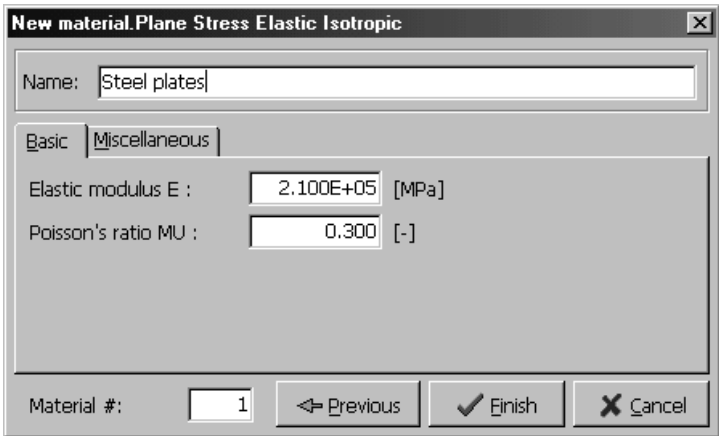

Figure 4.7 The dialog for the definition of material properties for the steel plates

2. Geometry of deep beams will be defined by inputting coordinate points that define the beam. Finally, the coordinates of macro elements which are of different material will be defined (such as the loading plates).

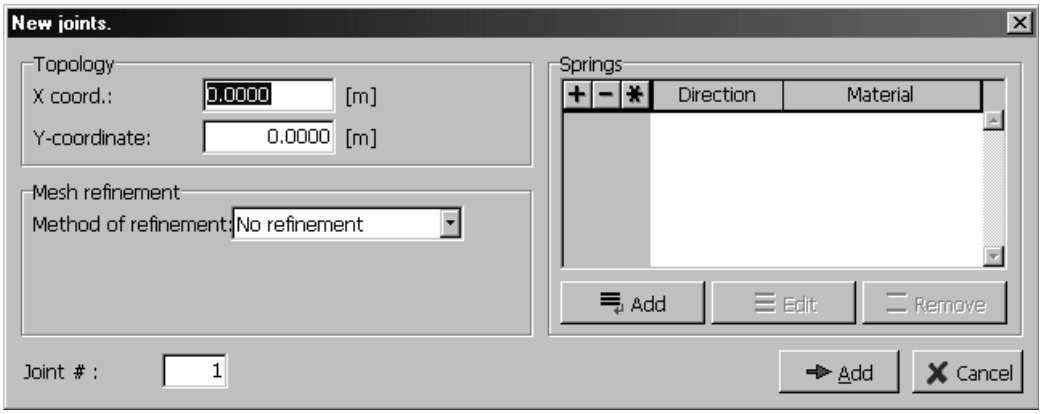

Figure 4.8 The dialog for the specifying the coordinates

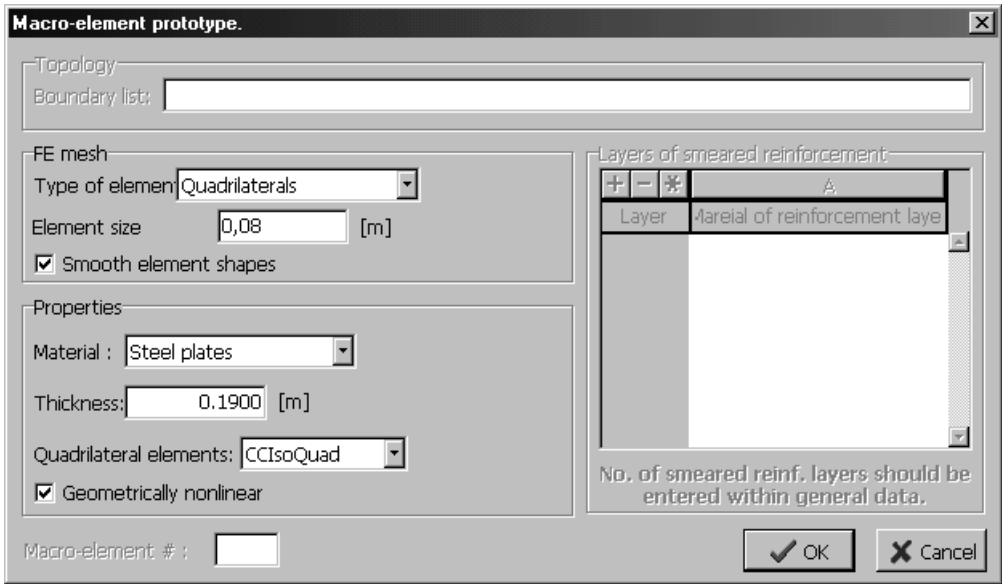

Figure 4.9 This dialog is used for the defining of macro-element prototype

3. Load and constraints will be assigned as load cases. Different load cases are defined in ATENA: force, body force, prescribed deformation, temperature, shrinkage.

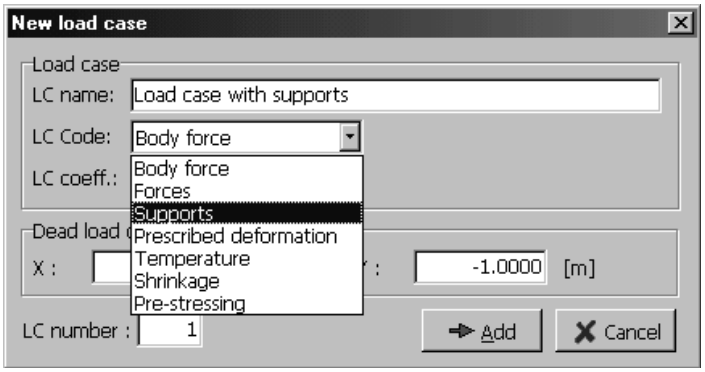

Figure 4.10 This dialog is used for the definition of load cases

4. After size of element is selected by user, ATENA will determine mesh size automatically. Although ATENA includes an algorithm that reduces effect of element size on results, the final output may still be affected by element size. The user can modify the size of element based on observations of output. For this study, adjustments in element size were made in to improve the results of the analysis.

Detail of computer models for analyses of reinforced concrete deep beams will be introduced in Chapter 5 for each computer model series.

4.3 Verification computer models

Applicability of ATENA will be verified by developing computer models duplicating tested beams from database. Tested beams selected from database are Rogowsky and MacGregor's tests, Smith and Vantsiotis's tests, and Birrcher's tests. Deep beams of Rogowsky and MacGregor had a major contribution to understand the behavior of continuous deep beams. Smith and Vantsiotis's tests are typical small unreal deep beams reported in literature. Tests of Birrcher are one of the largest tested deep beams reported in literature.

4.3.1 Computer models of Rogowsky's tests

Rogowsky et al. conducted an experimental study that included both simply supported and continuous reinforced concrete deep beams. Computer models that

simulate Rogowsky's tests were built and the computer simulation results were compared with observed test results. Parameters used consist of crack pattern, ultimate load, deflection, and strain of longitudinal tension steel bars.

Detailed information of Rogowsky's tests is provided in the Table 4.1 and Figs. 4.11 and 4.12

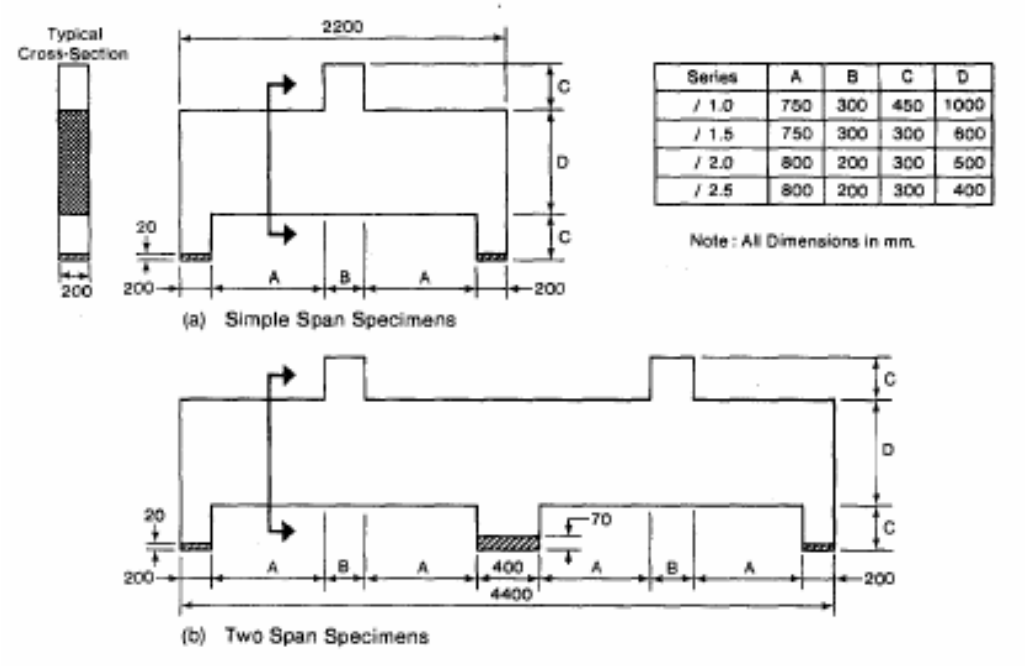

Series	A	B	C	D
/ 1.0	750	300	450	1000
/ 1.5	750	300	300	600
/ 2.0	800	200	300	500
/ 2.5	800	200	300	400

Note : All Dimensions in mm.

Figure 4.11 Overall dimensions of specimens (Rogowsky, et al.)

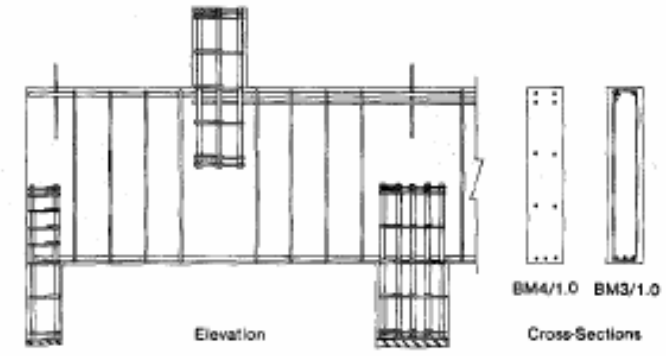

Figure 4.12 Typical reinforcement details of specimens (Rogowsky, et al.)

Table 4.1 Details of Specimens (Rogowsky, et al.)

Specimen	f'_c, MPa	Top steel			Bottom steel			Web steel*	
		Bars	$A_s f_y$ per bar, kN	d, mm	Bars	$A_s f_y$ per bar, kN	d, mm	Number of stirrups	Number of horizontal bars
1/1.0N	26.1	—	—	—	6-20M	114	950	4	—
1/1.0S	26.1	—	—	—	6-20M	114	950	—	—
2/1.0N	26.8	2-6 mm	16.2	980	6-20M	114	950	4	4
2/1.0S	26.8	2-6 mm	16.2	980	6-20M	114	950	—	4
3/1.0	28.9	4-20M	114	950	3-20M	114	975	4	—
4/1.0	28.5	4-20M	114	950	3-20M	114	975	—	4
5/1.0	36.9	4-20M	121	950	3-20M	121	975	16	—
6/1.0	35.8	4-20M	121	950	3-20M	121	975	—	12
7/1.0	34.5	4-20M	121	950	3-20M	121	975	—	—
BM1A/1.0N	26.4	—	—	—	6-20M	110	950	10	—
BM1A/1.0S	26.4	—	—	—	6-20M	110	—	—	—
1/1.5N	42.4	—	—	—	6-15M	91	535	5	—
1/1.5S	42.4	—	—	—	6-15M	91	535	—	—
2/1.5N	42.4	2-6 mm	16.2	580	6-15M	91	535	5	4
2/1.5S	42.4	2-6 mm	16.2	580	6-15M	91	535	—	4
3/1.5	14.5	6-15M	91	535	2-10M	46	545	5	—
					4-15M	91			
4/1.5	32.5	6-15M	91	535	2-10M	46	545	—	4
					4-15M	91			
5/1.5	39.6	6-15M	91	535	2-10M	48	545	16	—
					4-15M	91			
6/1.5	45.0	6-15M	91	535	2-10M	48	545	—	12
					4-15M	91			
7/1.5	30.4	6-15M	91	535	2-10M	46	545	—	—
					4-15M	91			
8/1.5	37.2	6-15M	91	535	2-10M	46	545	5	4
					4-15M	91			
1/2.0N	43.2	—		—	4-15M	91	455	4	—
1/2.0S	43.2	—		—	4-15M	91	455	—	—
2/2.0N	43.2	2-6 mm	16.2	480	4-15M	91	455	4	4
2/2.0S	43.2	2-6 mm	16.2	480	4-15M	91	455	—	4
3/2.0	42.5	4-15M	91	445	4-15M	91	445	4	—
		2-10M	48		2-10M	48			
4/2.0	38.3	4-15M	91	445	4-15M	91	445	—	4
		2-10M	46		2-10M	46			
5/2.0	41.1	4-15M	91	445	4-15M	91	445	16	—
		2-10M	48		2-10M	48			
6/2.0	37.4	4-15M	91	445	4-15M	91	445	—	12
		2-10M	46		2-10M	46			
7/2.0	46.8	4-15M	91	445	4-15M	91	445	—	—
		2-10M	48		2-10M	48			
5/2.5	34.0	4-15M	91	355	4-15M	91	355	16	—

4.3.1.1 Computer models of simply supported deep beams

Simply supported deep beam with a/d 1.0

A computer model of simply supported deep beam with a/d = 1.0 was developed to replicate Rogowsky's simply supported deep beam with the same a/d = 1.0 and with minimum vertical web reinforcement and 6 longitudinal steel bars with a diameter of 19.5 mm. The dimensions of the beam tested and the computer model are shown in Fig. 4.13.

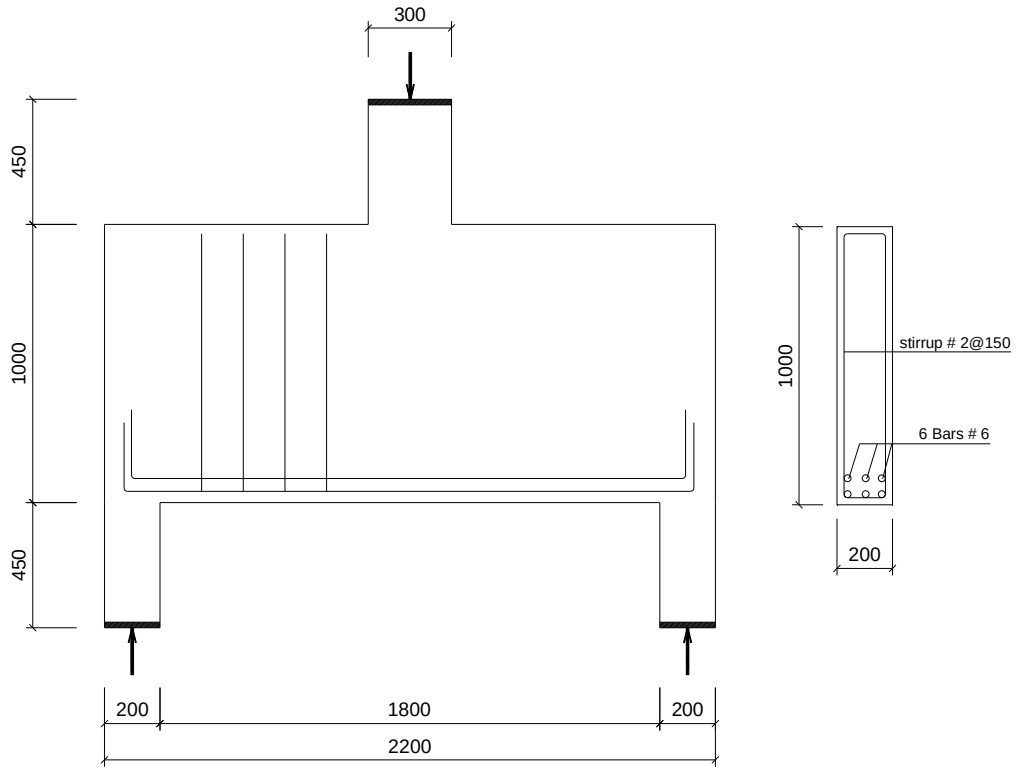

Figure 4.13 Details of beam BM 1/1.0 (Rogowsky, et al.)

In the study, each beam was tested twice (T1 and T2). After one shear span was tested to failure, it was reinforced with external stirrups so that the other shear span could be tested.

The crack pattern at failure in the first test (T1) and the strains in the longitudinal reinforcements at two stages in the first test are shown in Fig. 4.14. In Table 4.2 the measured strains in the longitudinal reinforcement in both test (T1 and T2) are compared to strains obtained from the computer models. The shear forces at inclined cracking forming and failure are provided in the Table 4.3.

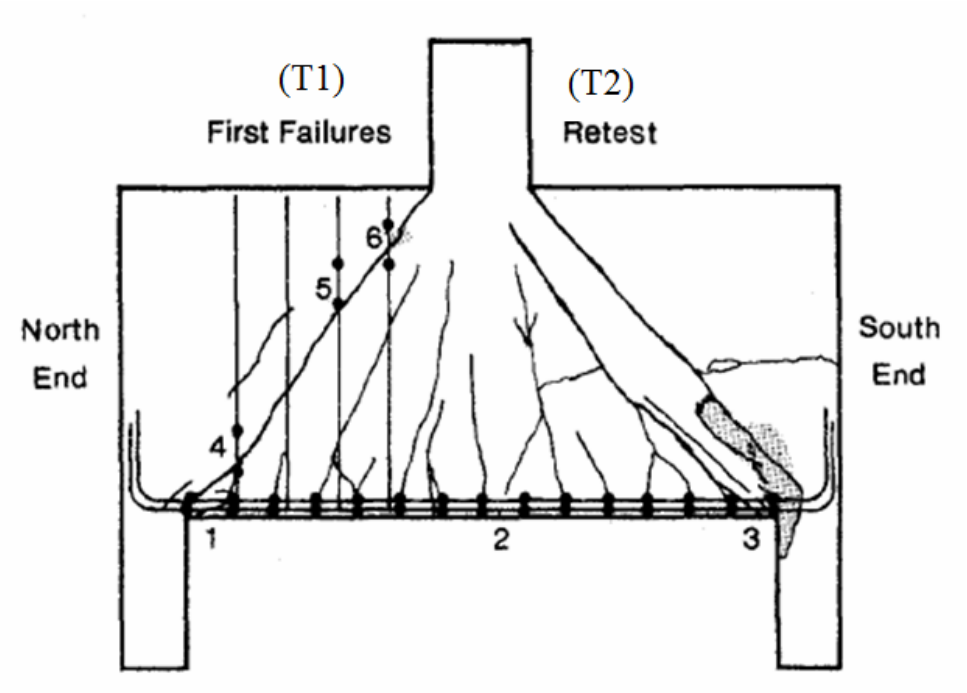

(a) Crack pattern at failure and strain gage locations

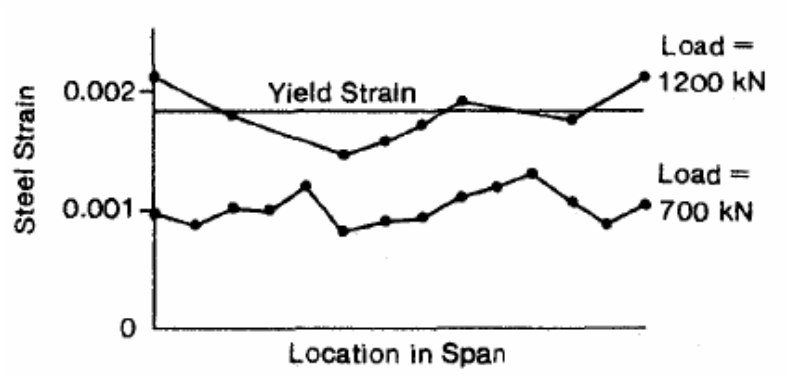

(b) Strains in longitudinal reinforcements

Figure 4.14 Crack pattern at failure and strains in longitudinal reinforcements

Table 4.2 Strains in longitudinal reinforcement at failure

Beam	North end(1)	Mid span(2)	South end(3)
BM 1/1.0 T1	0.0021	0.002	N/A
BM 1/1.0 T2	N/A	0.002	0.0022
Computer model without web rein.	0.00159	0.0016	0.00159
Computer model with web rein.	0.0015	0.001883	0.0015

Table 4.3 Inclined cracking shear and shear at failure of beam BM 1/1.0 and computer model of beam BM 1/1.0

Beam	Type of web reinforcement	N shear span kN	Inclined cracking shears kN	S Shear span kN
BM 1/1.0 T1	vertical	602*	350	-
Bm 1/1.0 T2	None	-	350	699*
Computer model	vertical	540	450	540
	None	500	450	500

(*): Failure occurred in this span.

For beam BM 1/1.0, two different computer models were developed. One beam had no web reinforcement (Fig. 4.15) and the second one had four stirrups 6 mm. at a spacing of 150 mm. c-c. (Fig. 4.16). The details of two computer models were shown in the Fig. 4.15 and Fig. 4.16.

The computer models had the following characteristics:

(1) The concrete beam modeled by using a CCQ10SBeta element and a rectangular mesh. Concrete properties were defined by: compressive strength, tensile strength, and shear stress characteristics of cracked concrete. Compressive strength and tensile strength was calculated based on the value of cube compressive strength of concrete. In ATENA, there are different models for tensile failure, but exponential tension softening and a rotated smear crack model were chosen based on comparisons between the results of the computer model and the experimental observation.

(2) Reinforcement was modeled as a bilinear material with yield strength equal to the measured yield strength of reinforcement in the test beam. Perfect bond between reinforcement and around concrete was assumed.

(3) Bearing and loading plates were modeled by using plane stress elastic isotropic material. The dimensions of the bearing and loading plates were based on the reported dimensions of plates used in the test beam.

(4) Support and load consisted of a perfect pin constraint and roller constraints at other locations.

(5) Loading was modeled as a concentrated load on the loading plate or uniformly distributed load on the loading plate and depended on the loading conditions of the test beam. Increments of loading were chosen from 3% to 5% of the ultimate load applied to the test beam.

(6) Load and deflection of the computer model were measured at the loading and bearing plates and at mid-span on the bottom of the beam.

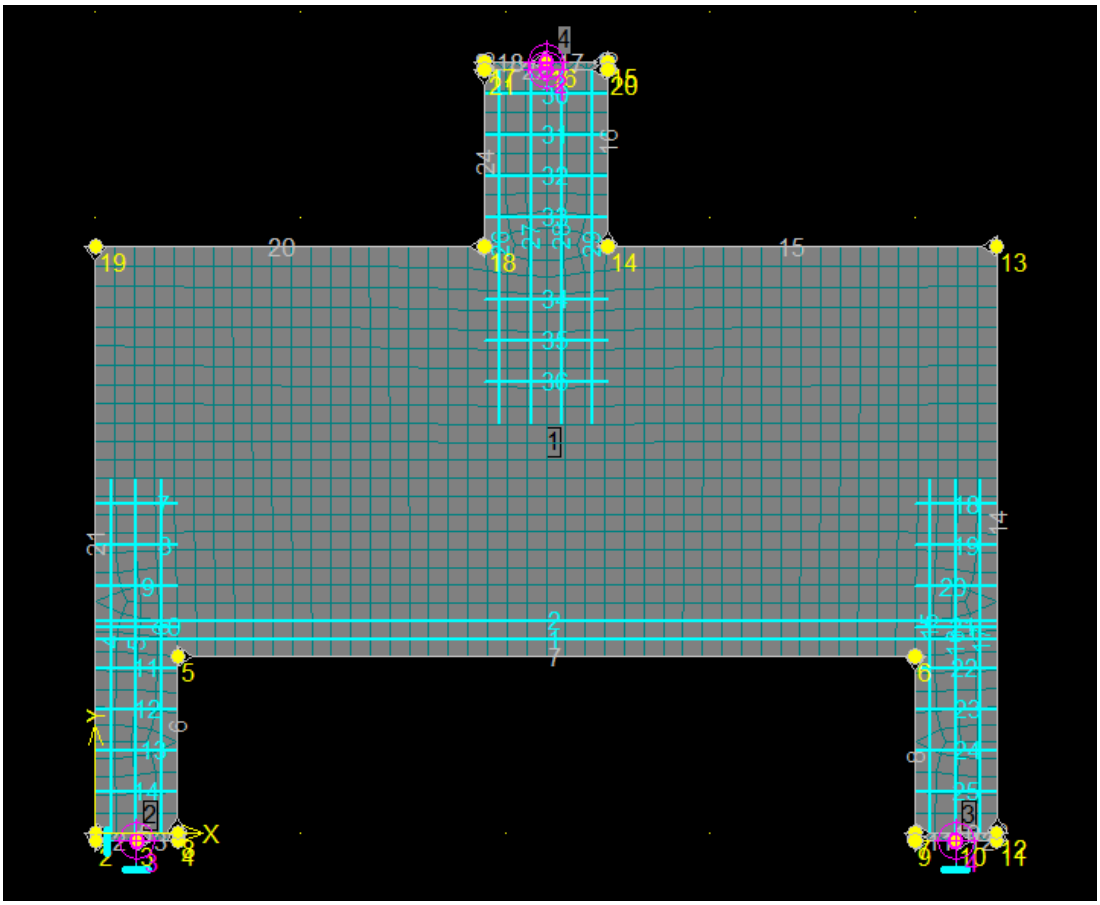

Figure 4.15 Details of constraints of the beam BM 1/1.0 model without web reinforcement

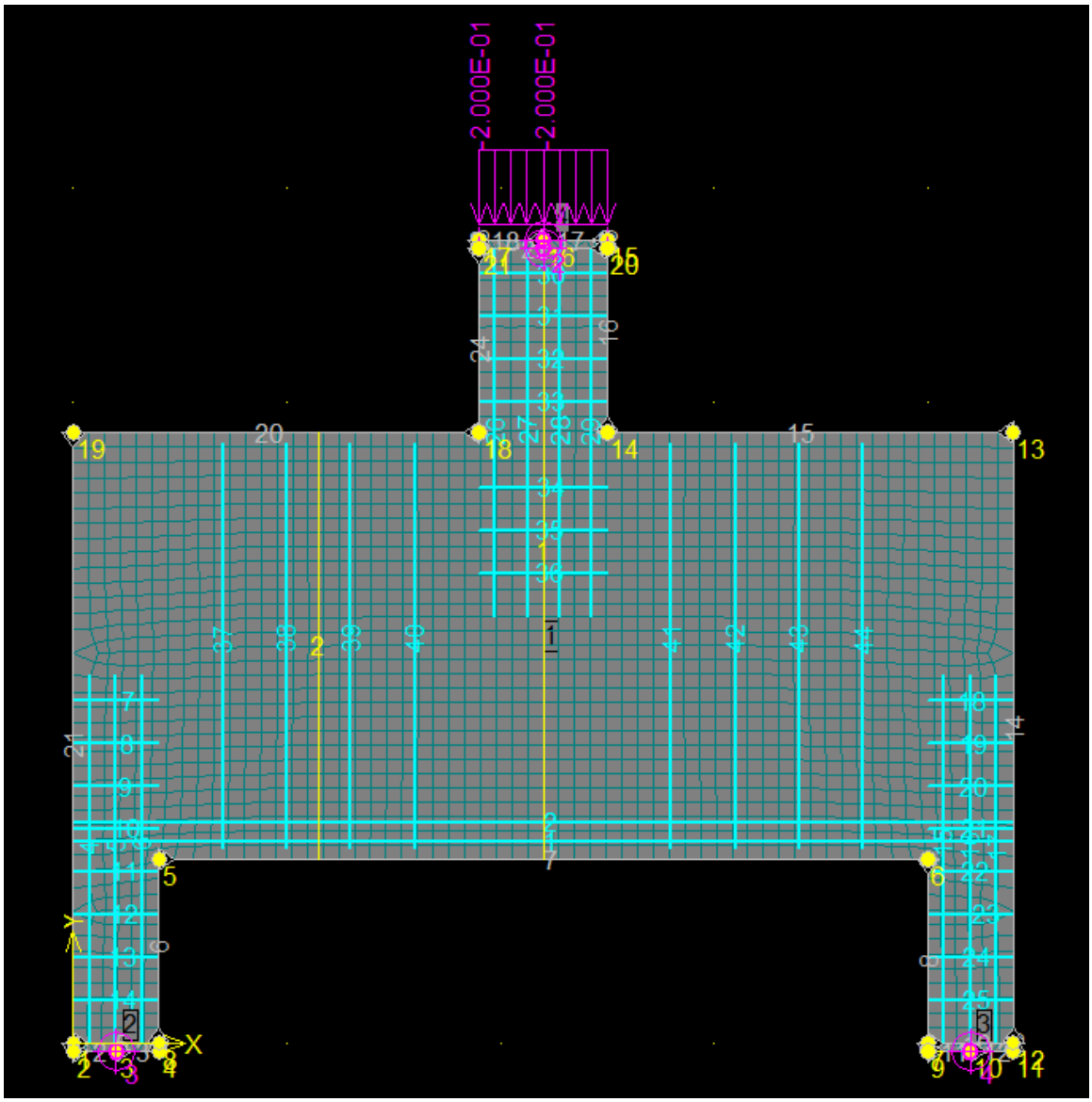

Figure 4.16 Details of beam BM 1/1.0 model with web reinforcement

The crack pattern at failure and strains in longitudinal reinforcements at failure using the two computer models are shown in Figs. 4.17 - 4.21. Figures from 4.22 to 4.24 provide a comparison of inclined cracking shear and ultimate shear of test beam BM 1/1.0 and computer models of beam BM 1/1.0.

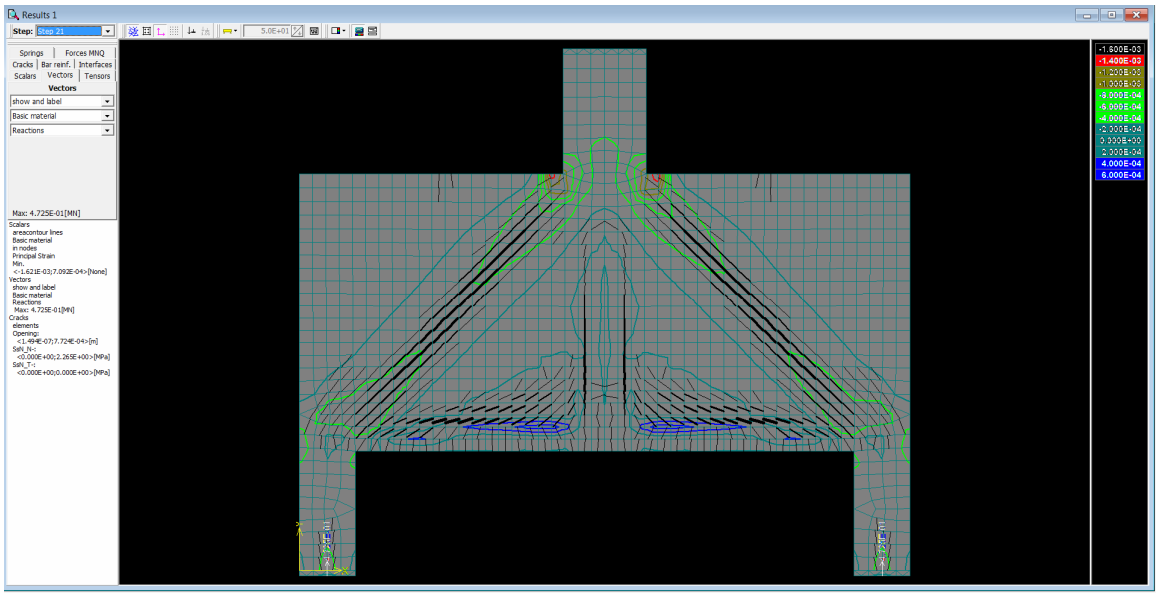

Figure 4.17 Crack pattern at failure of beam BM 1/1.0 model without web reinforcement

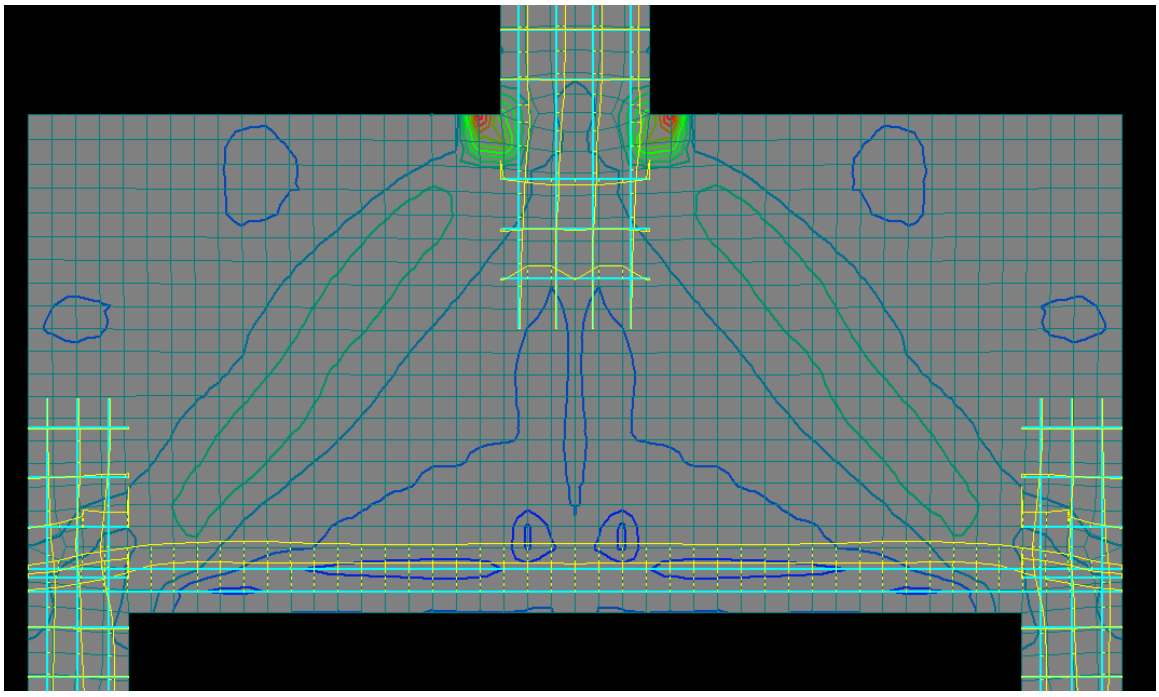

Figure 4.18 Computed strains in longitudinal reinforcements at right before failure of beam BM 1/1.0 model without web reinforcement

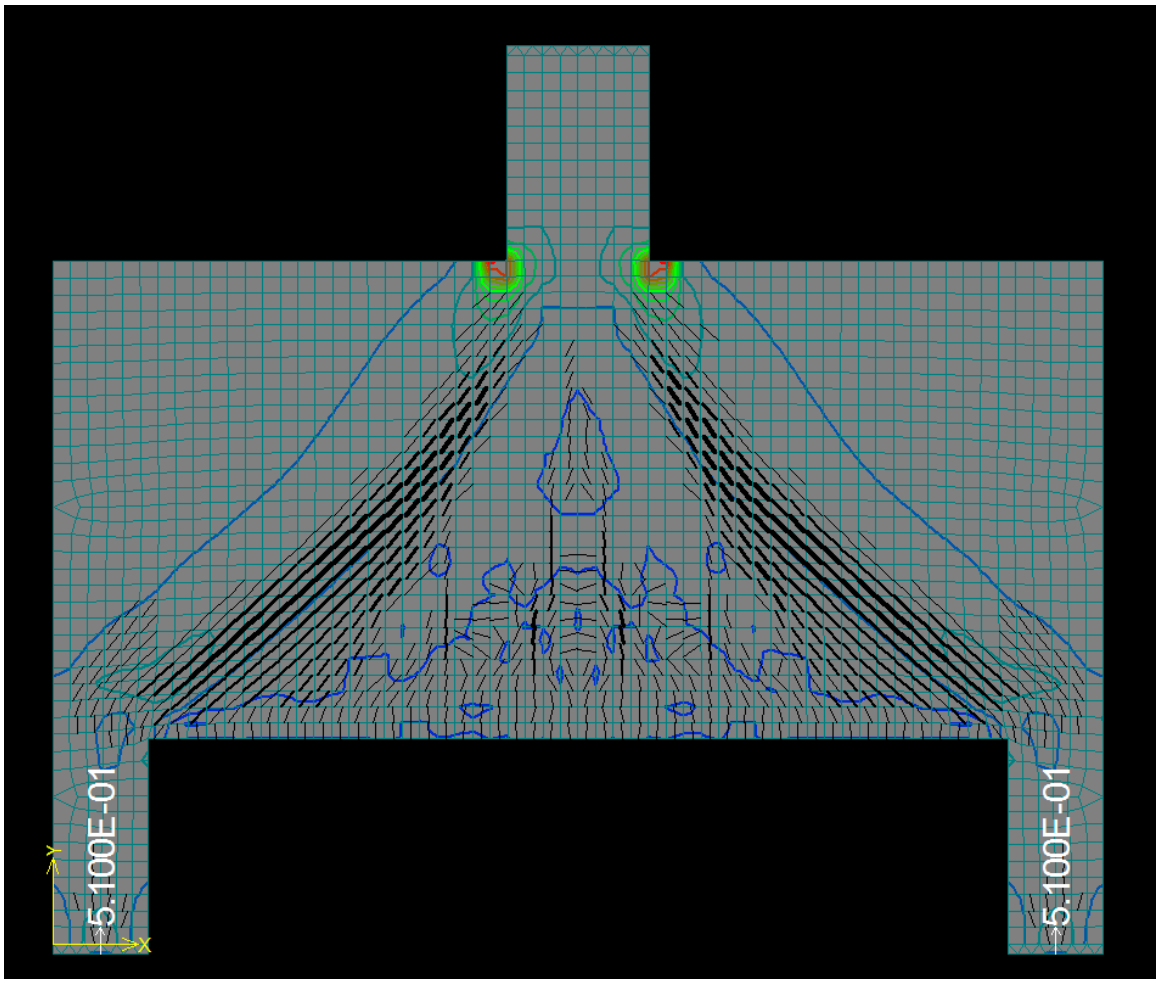

Figure 4.19 Crack pattern right before failure of beam BM 1/1.0 model with web reinforcement

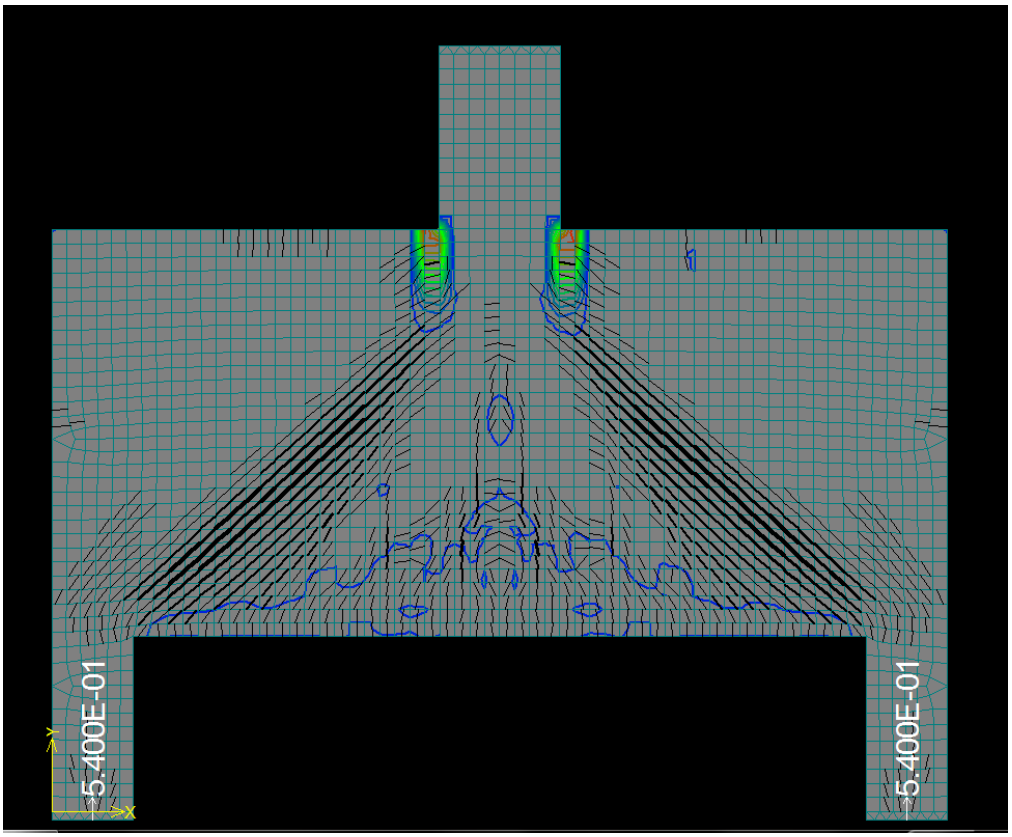

Figure 4.20 Crack pattern at failure of computer model of beam BM 1/1.0 model with web reinforcement

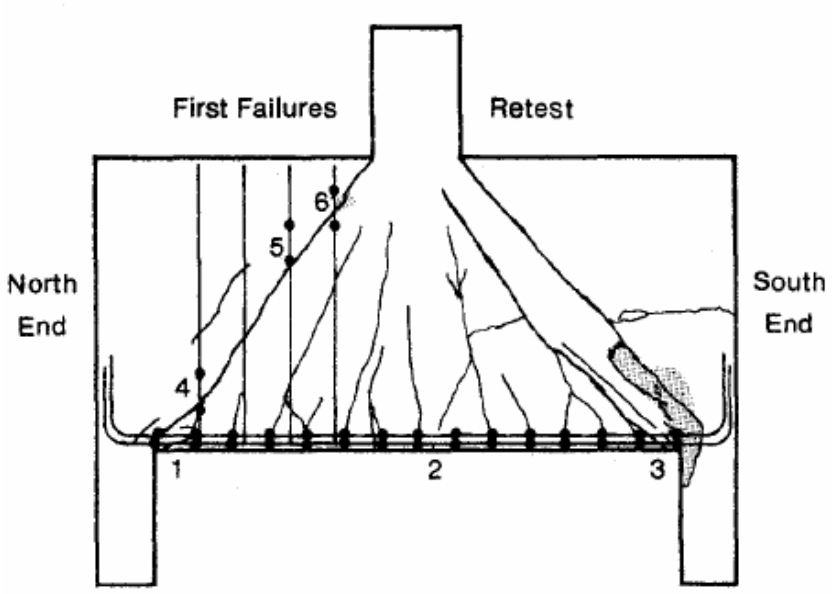

Crack pattern at failure of beam BM 1/1.0

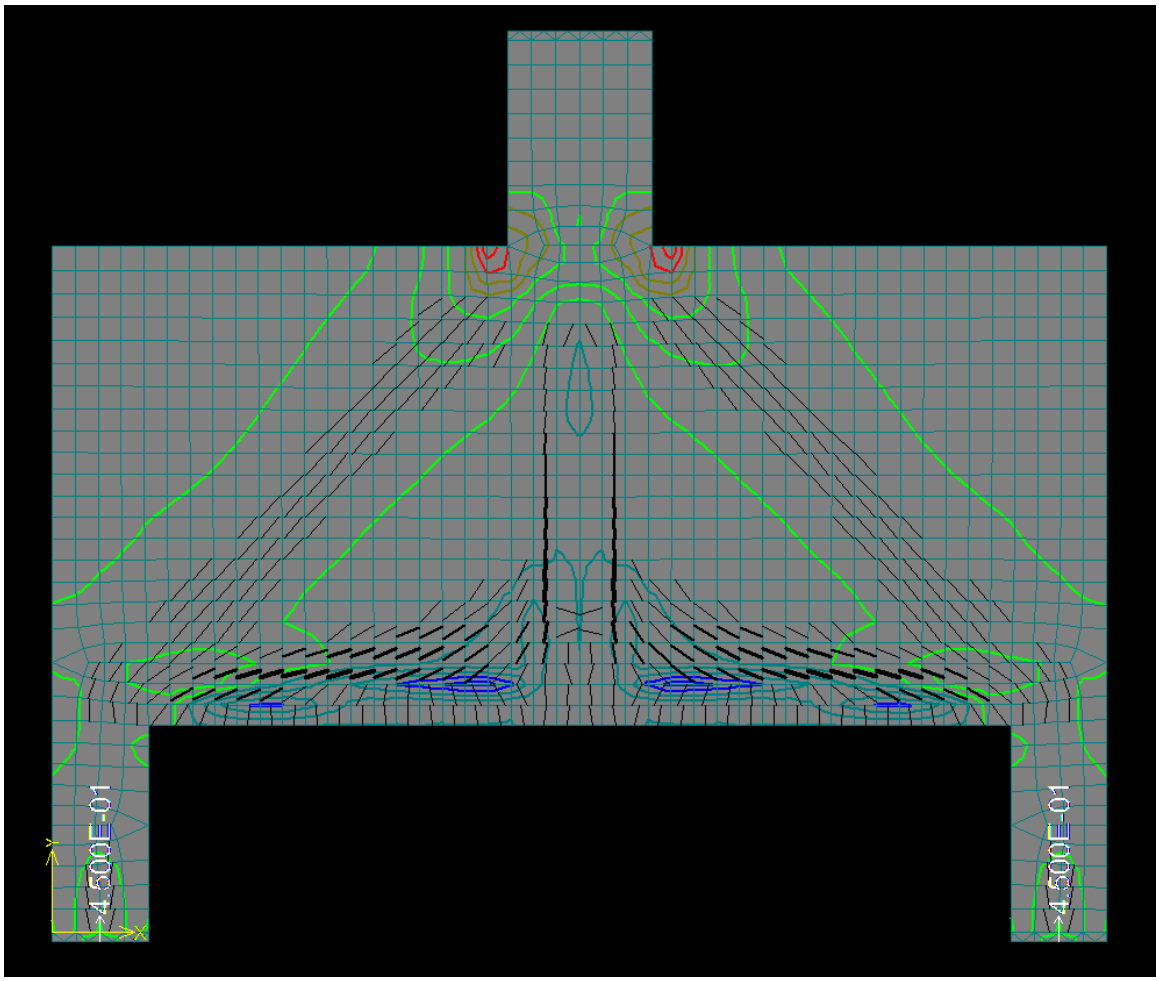

Figure 4.21 Applied shear at inclined cracking of model of beam BM 1/1.0 without web reinforcement

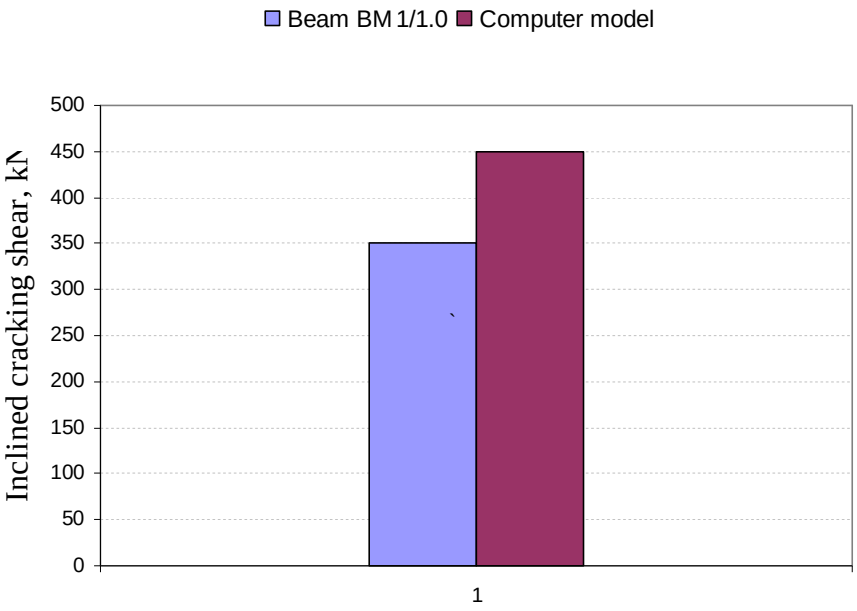

Figure 4.22 Comparison of inclined cracking shears between beam BM 1/1.0 and its computer model

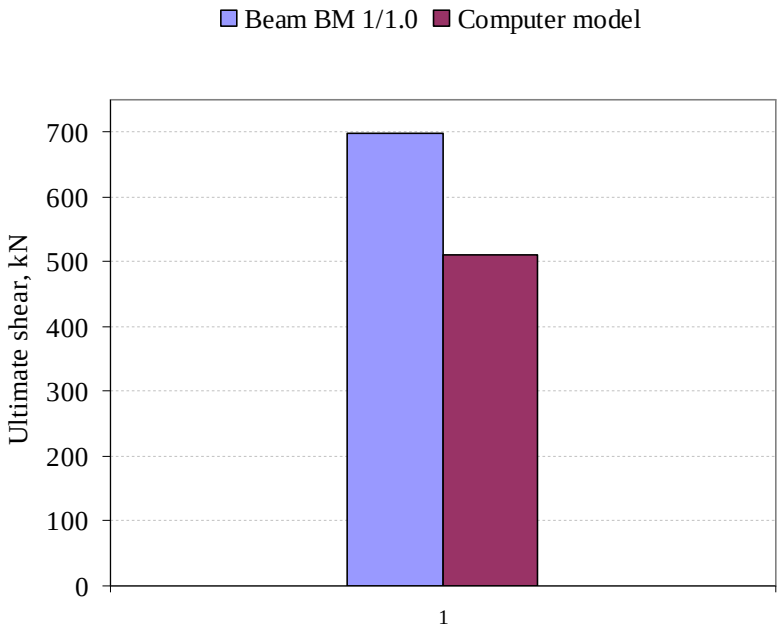

Figure 4.23 Comparison of ultimate shear for beam BM 1/1.0 without web reinforcement and its computer model

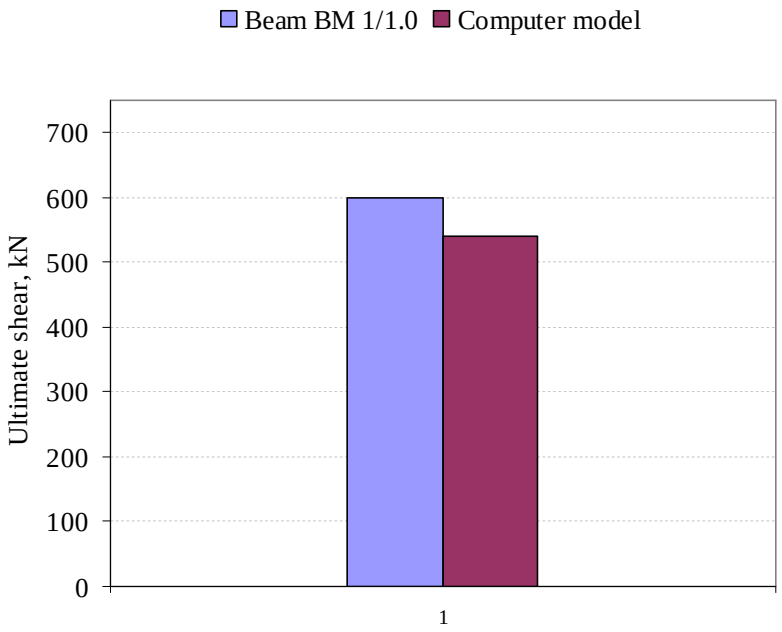

Figure 4.24 Comparison of ultimate shear for beam BM 1/1.0 with web reinforcement and its computer model

It was observed that the computer model captured the general crack pattern at failure. However, there are differences in details of crack pattern at failure. In the test beam, there were some inclined cracks converging toward the loading column and one major inclined crack. The companion computer model showed a band of parallel cracks extending from the face of the support column to the loading column. In ATENA, concrete is modeled as an isotropic material, but concrete materials are a non-isotropic. The cracks in beam formed at the weakest interfaces between mortar - mortar and mortar-aggregate. The test data indicate a lower strength for the beam with web reinforcement. The computer model gave lower values than the test but the beam with web reinforcement had a higher strength. The computer model captured the ultimate shear quite accurately. The difference between tested shear capacity and computer shear capacity is 10%. However, the inclined cracking shear from computer model is 43% higher than that of tested beam.

4.3.1.2 Computer models of continuous deep beams

(a) Continuous deep beam with vertical web reinforcement

The details of a tested continuous deep beam are shown in Fig. 4.25.

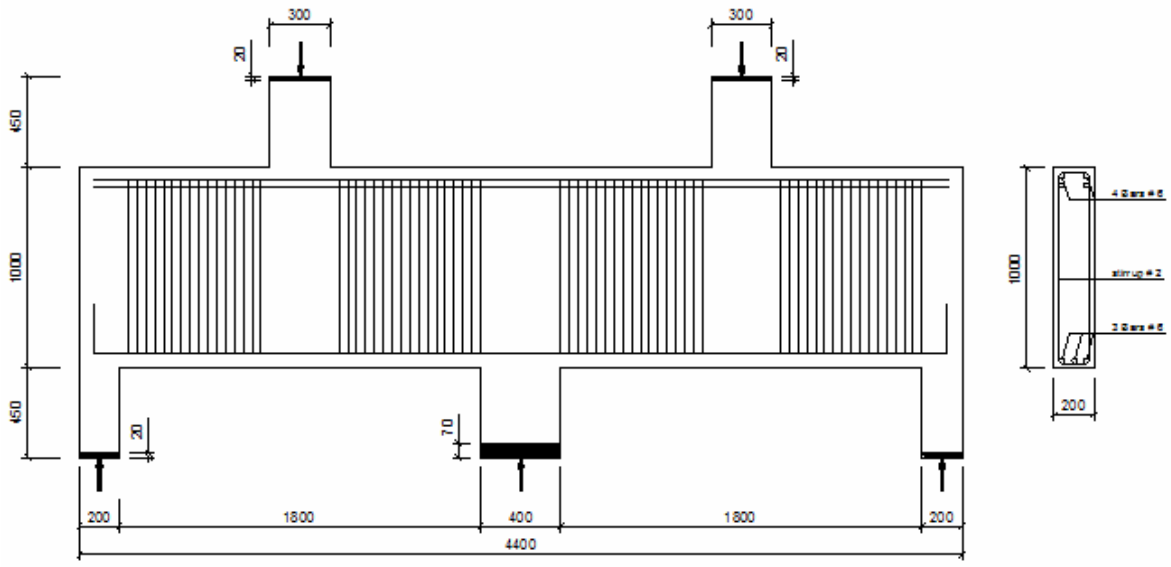

Figure 4.25 Details of continuous deep beam (Rogowsky, et al.)

The details of computer model of beam BM 5/1.0 are shown in Fig. 4.26

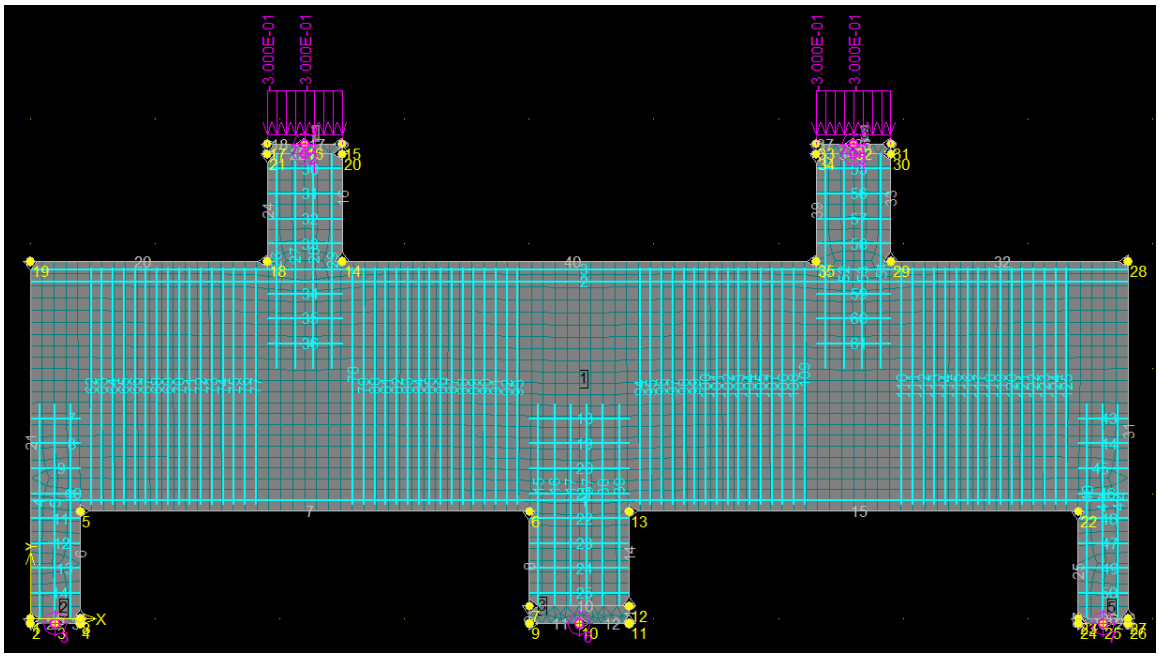

Figure 4.26 Details of computer model of beam BM 5/1.0

In Figures 4.27 to 4.30, the behavior of computer model of beam BM 5/1.0 is shown.

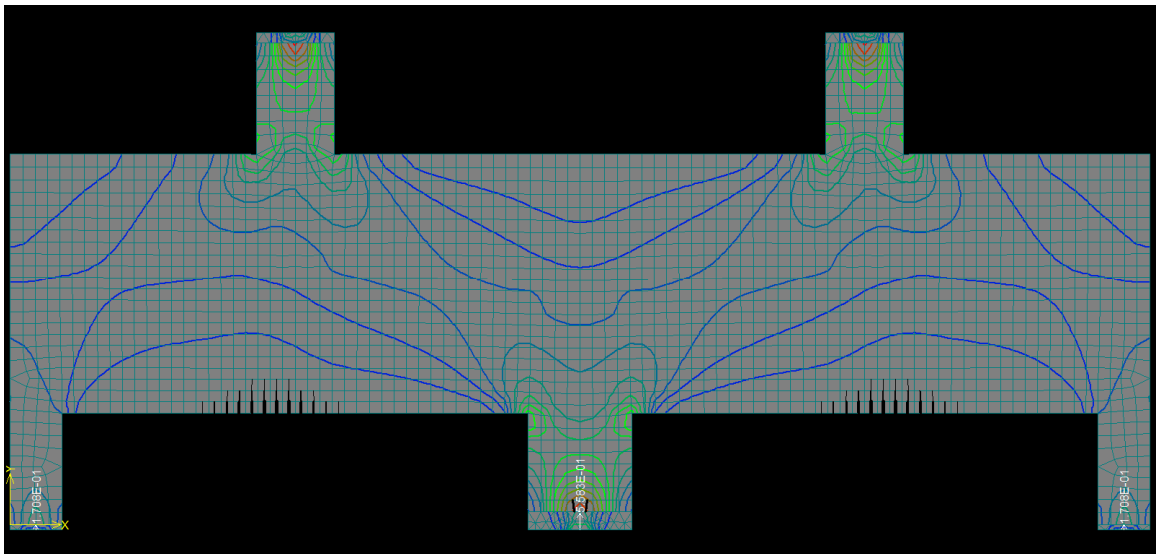

Figure 4.27 Contour line of principal compression strain and crack pattern of computer model of beam BM 5/1.0 at 32% of ultimate shear

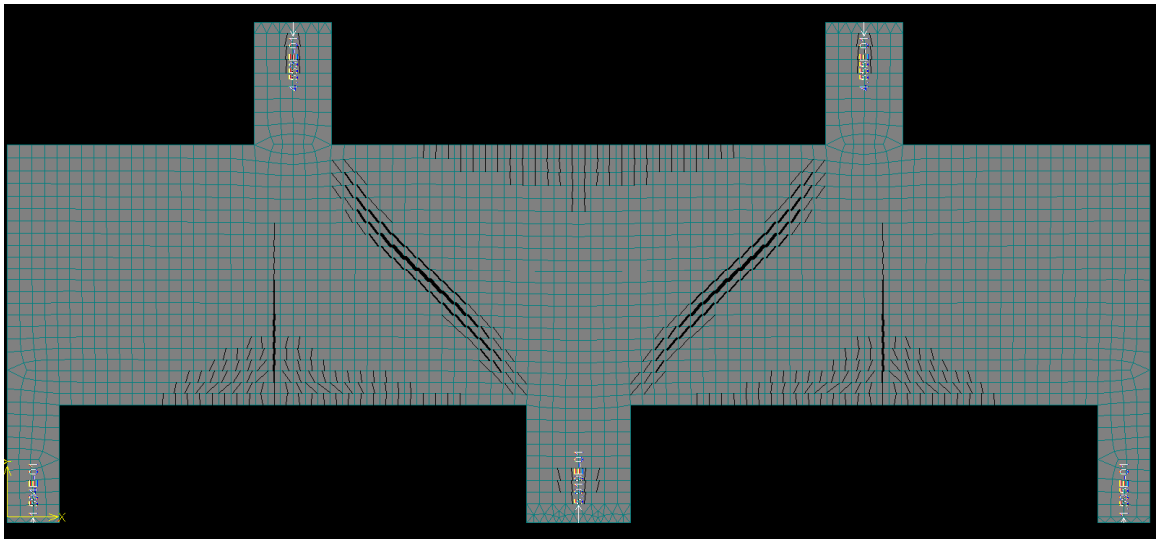

Figure 4.28 Crack pattern of computer model of beam BM 5/1.0 at 33% of ultimate shear

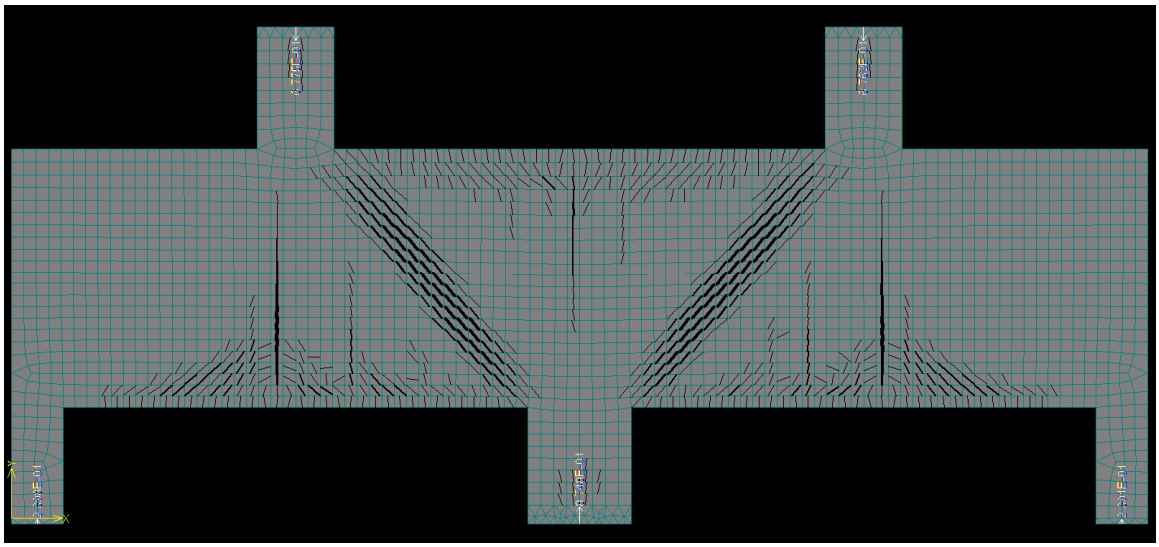

Figure 4.29 Crack pattern of computer model of beam BM 5/1.0 at 50% of ultimate shear

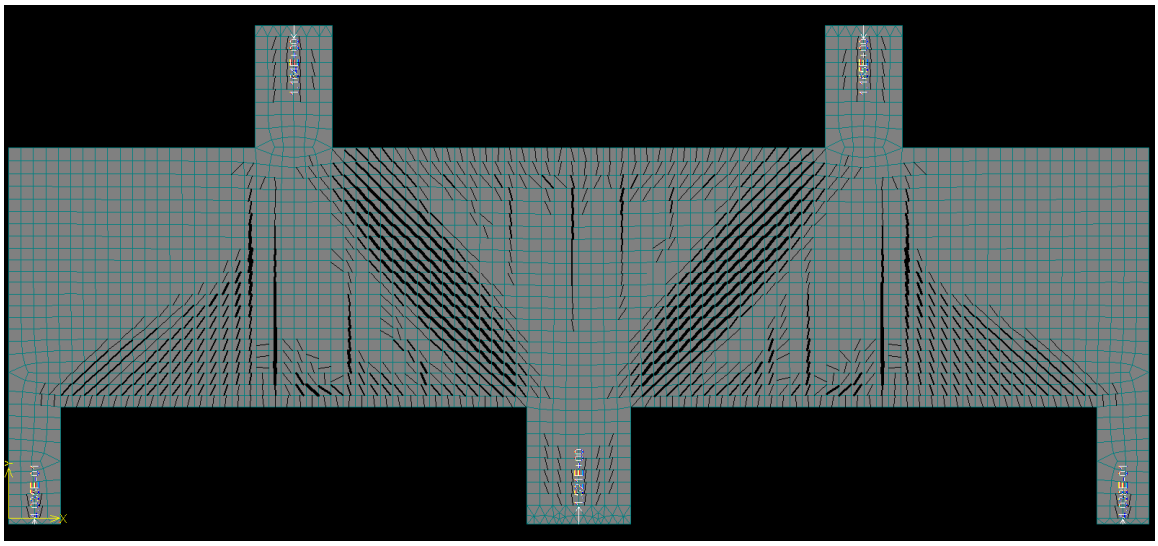

Figure 4.30 Crack pattern of computer model of beam BM 5/1.0 at 85% of ultimate shear

The observed crack pattern at failure and strains measured in longitudinal reinforcements are shown in Figs. 4.31 and 4.32.

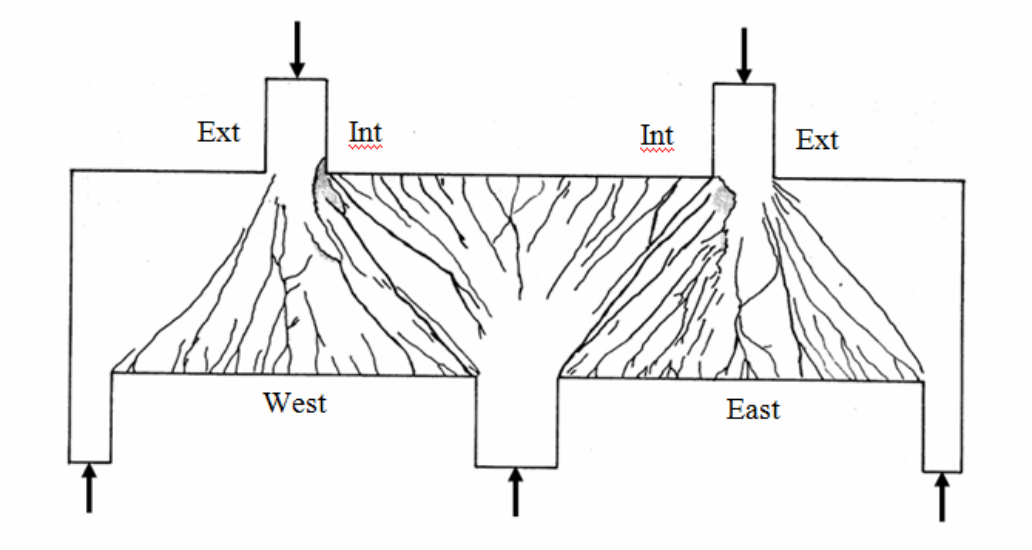

Figure 4.31 Crack pattern at failure of beam BM 5/1.0

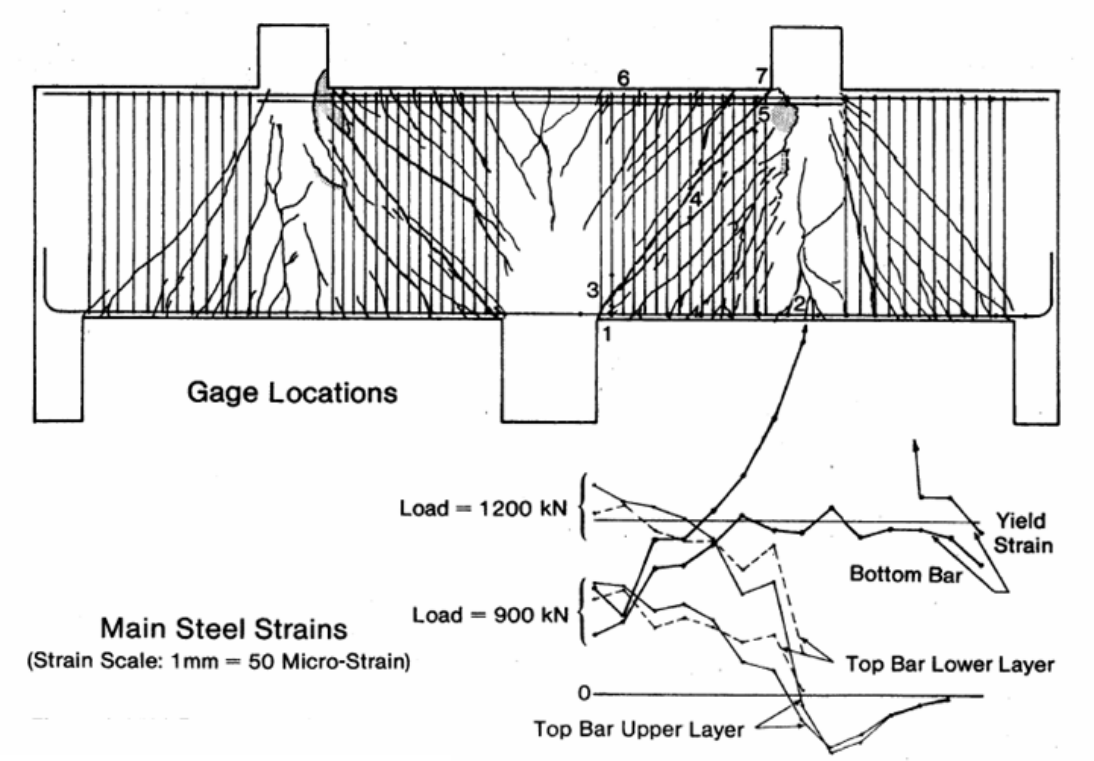

Figure 4.32 Strains in longitudinal reinforcement and gage locations for the test beam

The crack pattern at failure and strains in longitudinal reinforcements for the computer model of beam BM 5/1.0 are provided in Figs. 4.33 and 4.34.

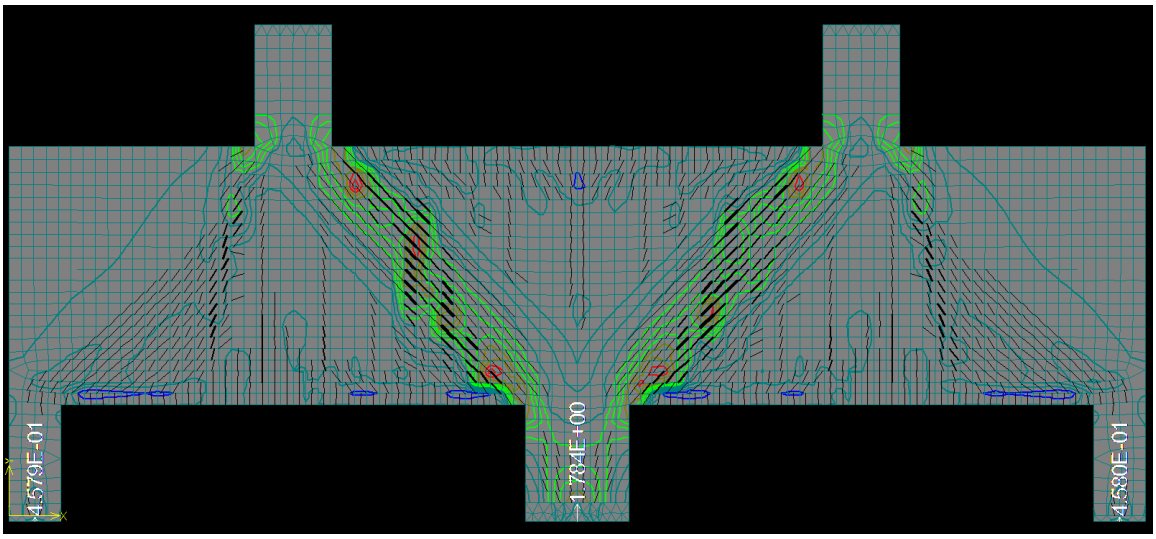

Figure 4.33 Crack pattern at failure of computer model of beam BM 5/1.0

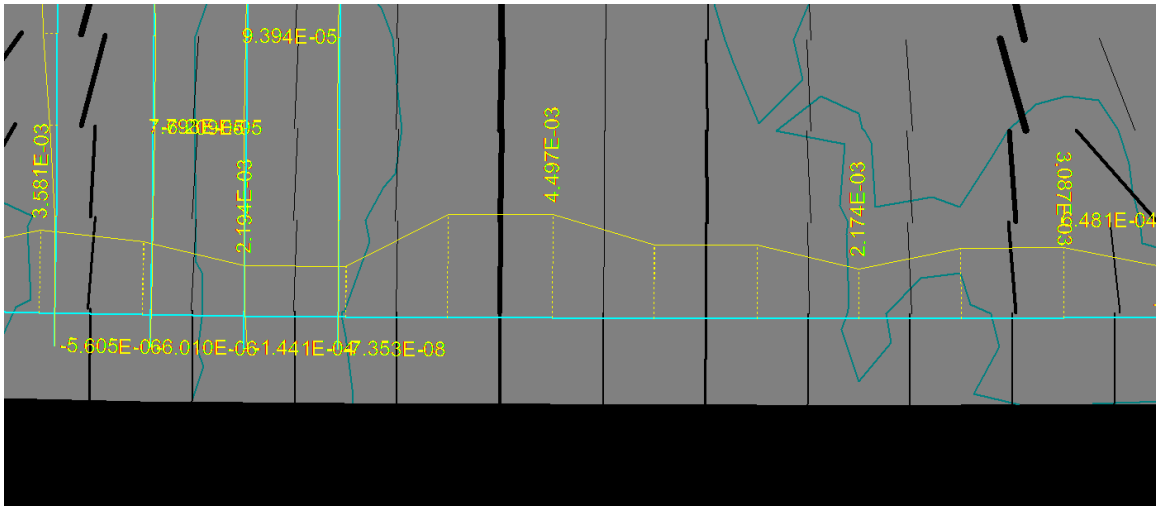

Figure 4.34a Strains in longitudinal reinforcement in interior east shear span at peak load of computer model of beam BM 5/1.0

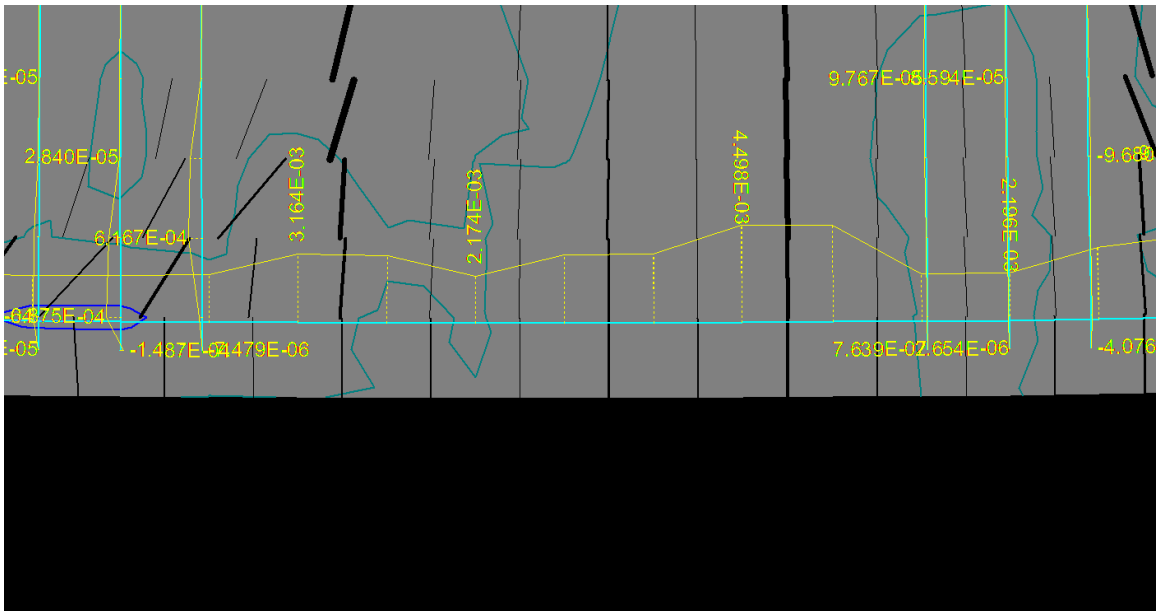

Figure 4.34b Strains in longitudinal reinforcement in east span at peak load of computer model of beam BM 5/1.0

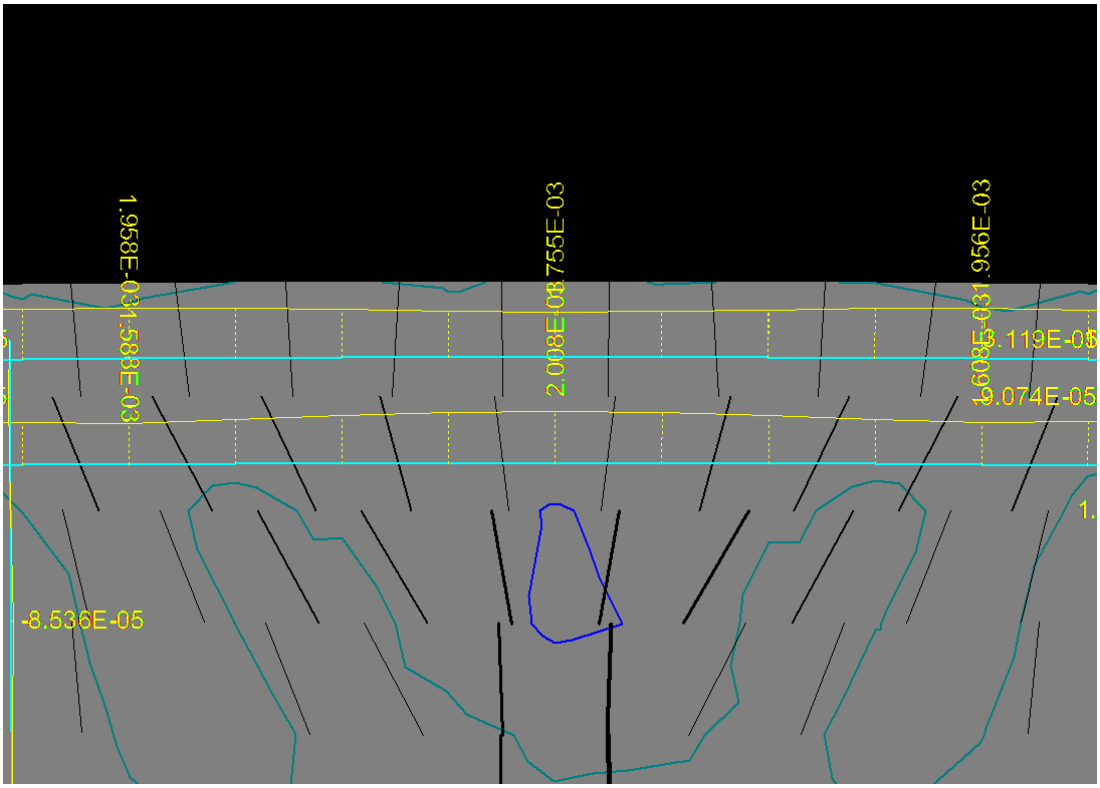

Figure 4.34c Strains in longitudinal reinforcement above middle support at peak load of model beam BM 5/1.0

The values of shear at inclined crack formation and at failure of the beam BM 5/1.0 and those of computer model of the beam BM 5/1.0 are shown in Tables 4.4 and 4.5.

Table 4.4 Shear at failure of beam BM 5/1.0

Beam	Type of web reinforcement	W. exterior shear span kN	W. interior Shear span kN	E. interior Shear span kN	E exterior Shear span kN
BM 5/1.0 T1	vertical	413	875*	866	405
Computer model	vertical	458	892	892	458

(*): Failure occurred in this span.

Table 4.5 Inclined cracking shear

Beam	Type of web reinforcement	W. exterior shear span kN	W. interior Shear span kN	E. interior Shear span kN	E. exterior Shear span kN
BM 5/1.0	vertical	-	460	410	-
Computer model	vertical	-	409	409	-

Results of inclined cracking shear and ultimate shear between beam BM 5/1.0 and computer model of beam BM 5/1.0 are shown in Tables 4.4 and 4.5.

Table 4.6 Strains in longitudinal reinforcement

Beam	Type of web reinforcement	Exterior w. end shear span	Mid shear span	Interior w. end shear span
BM 5/1.0	Bottom	0.0023	0.002	0.0015
Model	Bottom	0.00101	0.001979	0.001388

The comparison of load-deflection curves between beam BM 5/1.0 and that of companion computer model is shown in Figs. 4.35 and 4.36. Table 4.7 shows the comparison of maximum load and deflection at maximum load between beam BM 5/1.0 and its computer model.

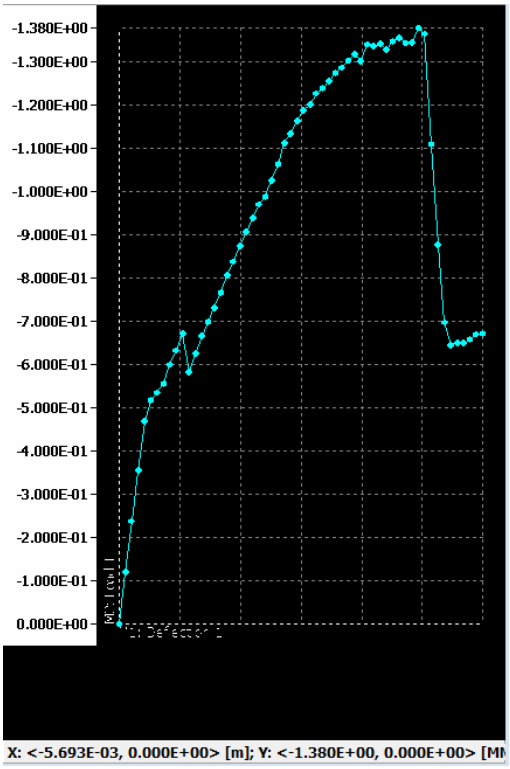

Figure 4.35 Load-deflection curve of computer model of beam 5/1.0 of Rogowsky and MacGregor's tests

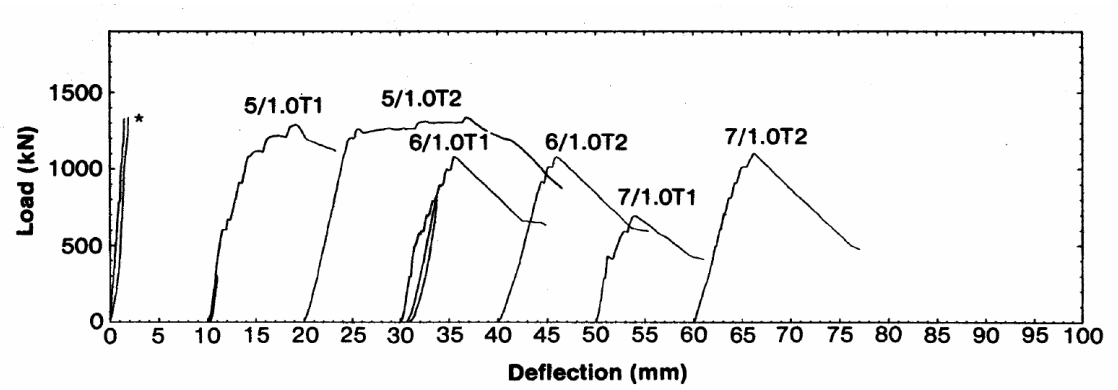

Figure 4.36 Load-deflection curve of beam 5/1.0 of Rogowsky and MacGregor's tests

Table 4.7 Comparison of maximum load and deflection at maximum load between beam BM 5/1.0 and its computer model

Beam	Maximum load, kN	Deflection, mm
Beam BM 5/1.0	1300	8
Computer model	1380	5.7

(b) Continuous deep beam with horizontal web reinforcement

The details of beam BM 6/1.0 are shown in Fig. 4.37.

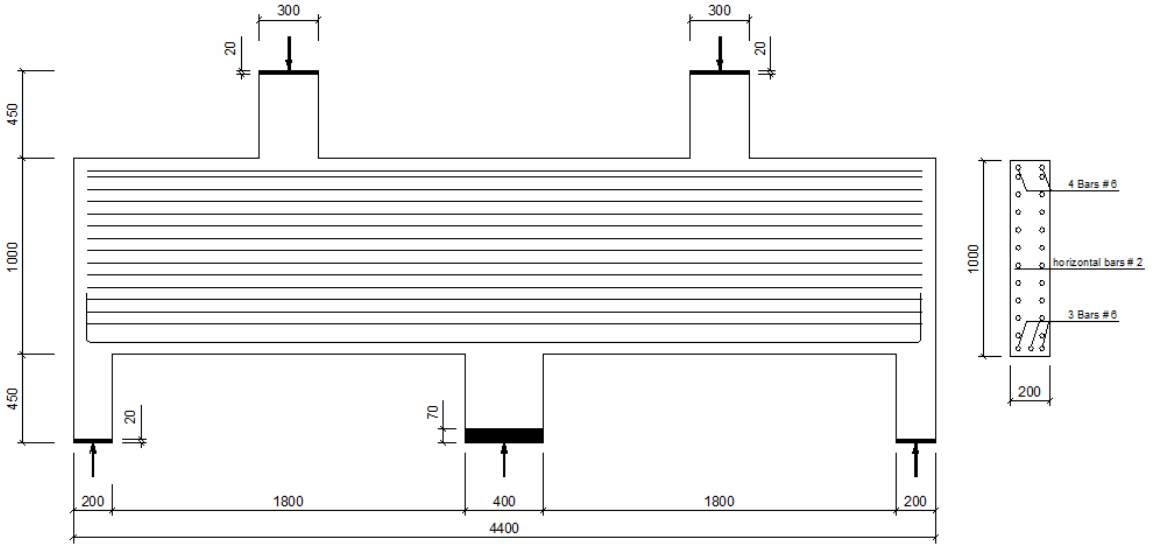

Figure 4.37 Details of beam BM 6/1.0 (Rogowsky et al)

The crack pattern at failure and strains in longitudinal reinforcement of beam BM 6/1.0 are shown in Figs. 4.38 and 4.39.

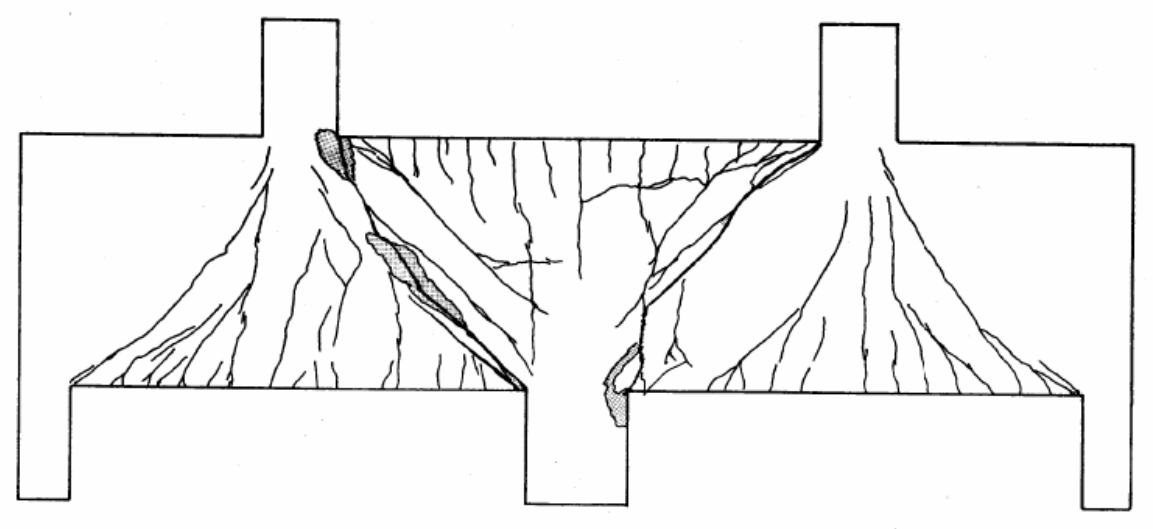

Figure 4.38 Crack pattern at failure of beam BM 6/1.0

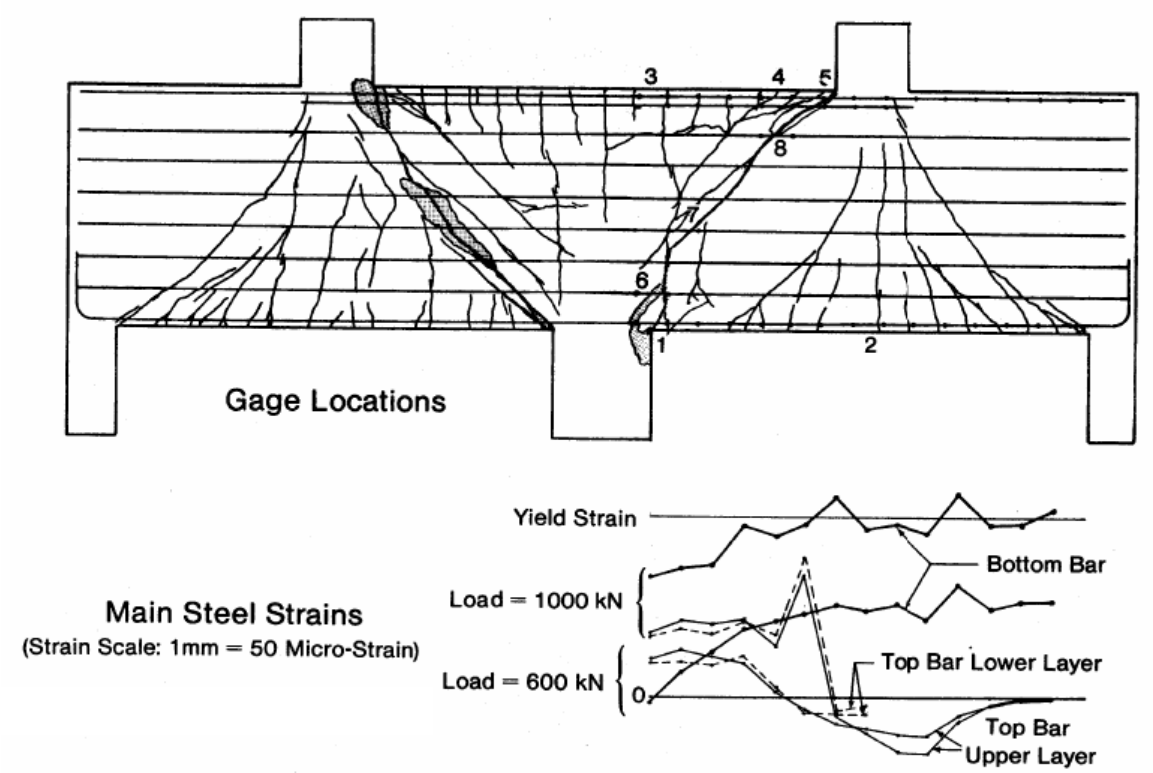

Figure 4.39 Strains in longitudinal reinforcement and gage locations

The crack pattern and strains in longitudinal reinforcement of the computer model of beam BM 6/1.0 are shown in the Figs. 4.40 and Table 4.8.

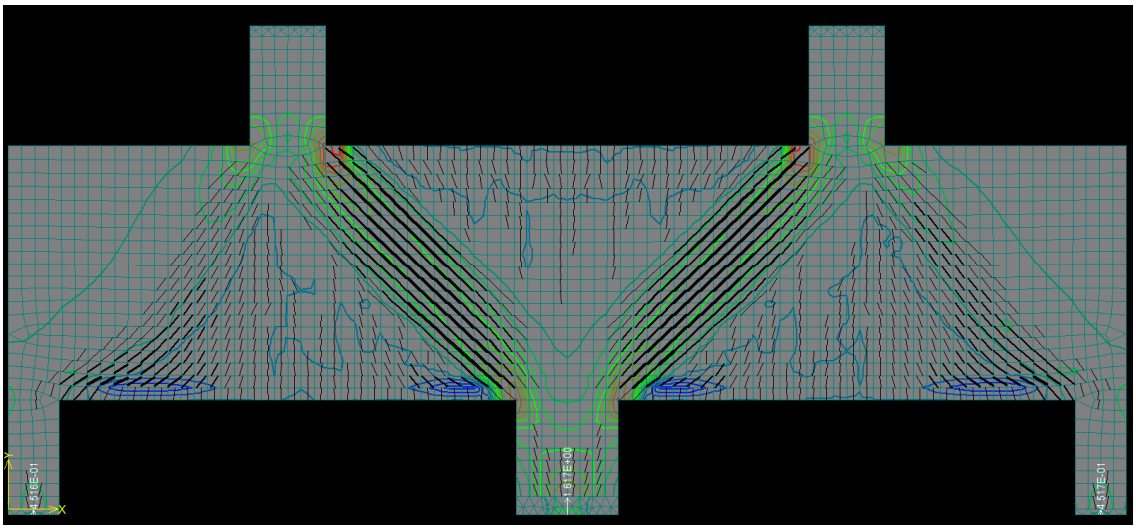

Figure 4.40 Crack pattern at failure of computer model of beam BM 6/1.0

Table 4.8 Strains in longitudinal reinforcement

Beam	Type of web reinforcement	Exterior w. end shear span	Mid shear span	Interior w. end shear span
BM 6/1.0	Bottom	0.0013	0.0022	0.0021
Model	Bottom	0.002801	0.002426	0.001592

The values of shear at failure of beam BM 6/1.0 and those of computer model of the beam BM 6/1.0 were shown in Tables 4.9.

Table 4.9 Shear at failure of beam BM 6/1.0

Beam	Type of web reinforcement	N exterior shear span kN	N interior Shear span kN	S interior Shear span kN	S exterior Shear span kN
BM 6/1.0 T1	horizontal	461	646	635*	448
Computer model	horizontal	451	809	809	451

(*): Failure occurred in this span.

The comparison of inclined cracking shear and ultimate load between beam BM 6/1.0 and computer model of the beam BM 6/1.0 were shown in Figs. 4.41 and 4.42.

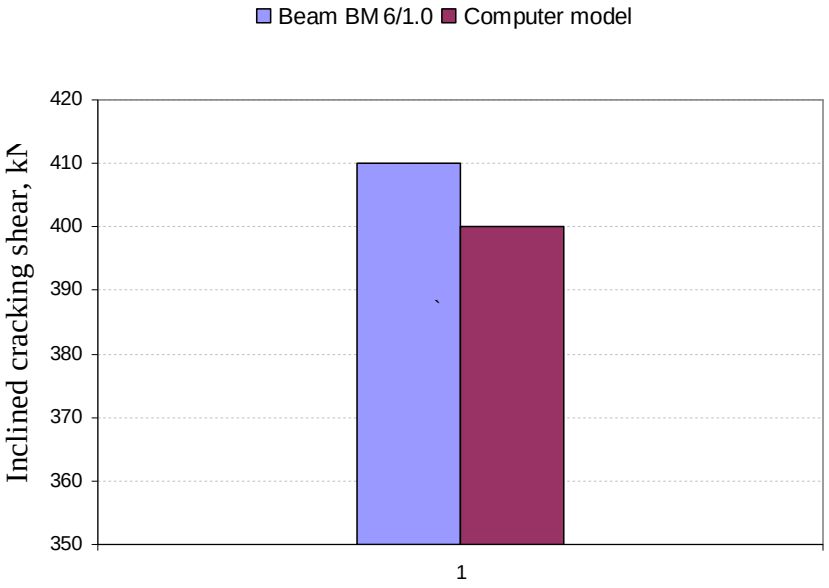

Figure 4.41 Comparison of value of inclined cracking shear between beam BM 6/1.0 and computer model of beam BM 6/1.0

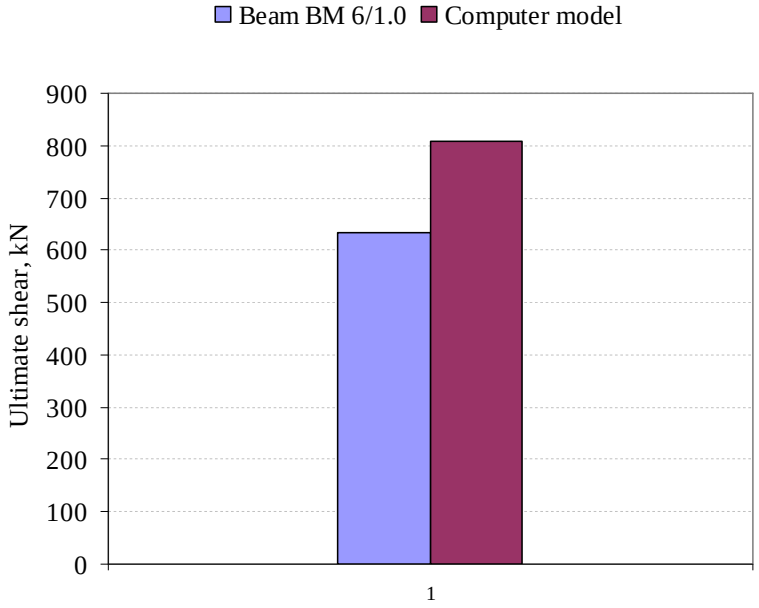

Figure 4.42 Comparison of value of ultimate load between beam BM 6/1.0 and computer model of beam BM 6/1.0

From the comparison of tested results between the real beams and their counterpart computer models, it was observed that the ATENA program captured the behavior of reinforced concrete deep beams. The results of the computer models were close to the crack patterns, values of inclined cracking shears, and values of ultimate shear of the beams tested. The results of the computer model of the continuous deep beam with vertical web reinforcements gave better results.

4.3.2 Computer model of Smith and Vantsiotis's tests

Smith and Vantsiotis conducted experimental research on 52 reinforced concrete deep beams under two equal symmetrically placed point loads. The loading and supporting conditions of test beams were shown in Fig. 4.43. This study consisted of four series (A, B, C, and D) of deep beams with four different ratios of shear span to effective depth, a/d, (0.77, 1.01, 1.34, and 2.01).

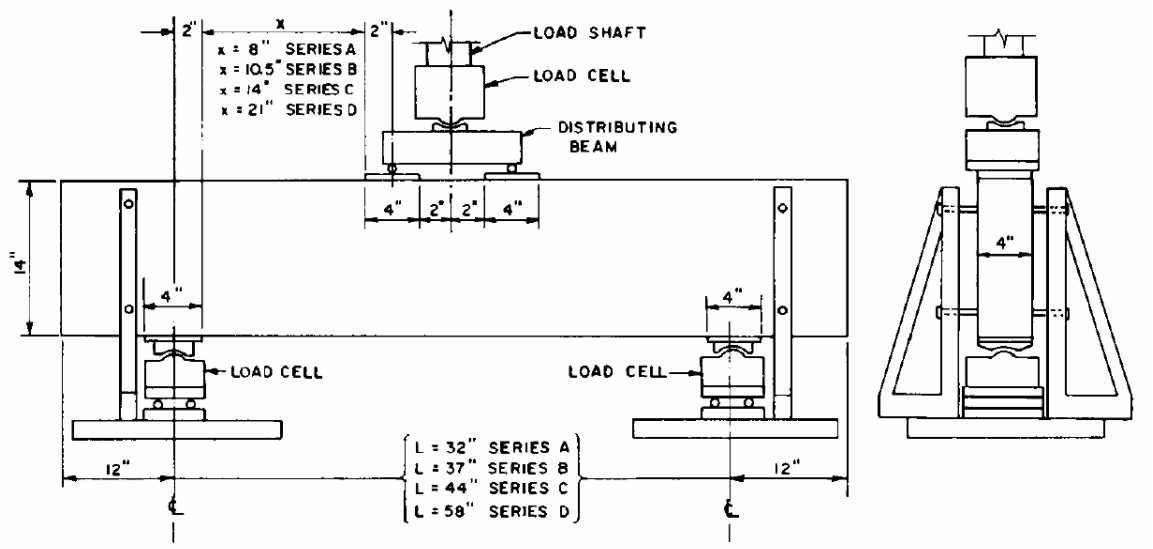

Figure 4.43 Details of loading and supporting conditions of Smith and Vantsiotis's tests

For verifying the applicability of the ATENA program, four tested beams were selected from this study: two beams without web reinforcement and two beams with web reinforcement. Two beams without web reinforcement chosen were beam 0A0-44 and

beam 0C0-50. The two beams with web reinforcement selected were beam 2A1-38 and beam 2C1-17. The details of beams are shown in Figs. 4.44 and 4.45.

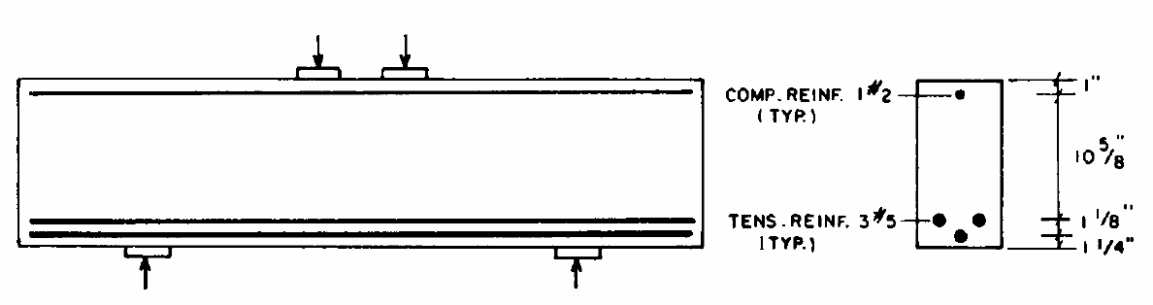

Figure 4.44 Details of beams without web reinforcement

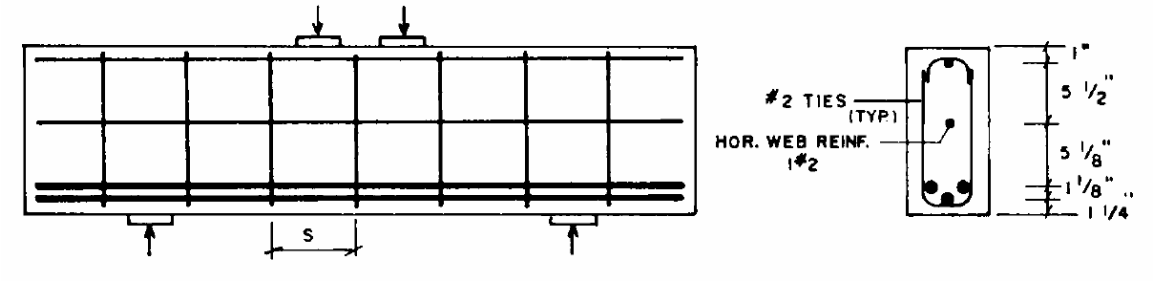

Figure 4.45 Details of beams with web reinforcement selected for simulating

(a) Computer model of beams without web reinforcement

The beam 0A0-44, a/d = 0.77, was modeled as follows:

(1) Geometric dimensions:

- Beam 0A0-44: length of 56 in., height of 14 in., and thickness of 4 in.
- Loading and bearing plates: 4x4x1 in.

(2) Constraint conditions:

- One constraint was a perfect pin and the other a perfect roller.

(3) Loading conditions:

- Two point loads were applied at middle of two loading plates. The increment of load was 20 kips.

(4) Materials:

- Concrete model was CCQ10SBeta: f'_c = 2.97 ksi

- Plates were modeled as plane stress elastic isotropic material
- Reinforcement used as an elastic-perfectly plastic material model: f_y = 62.5 ksi.

(5) Finite element analysis

- Mesh type: rectangular mesh for reinforced concrete beam.

The details of computer model of the beam 0A0-44 are shown in Fig 4.46.

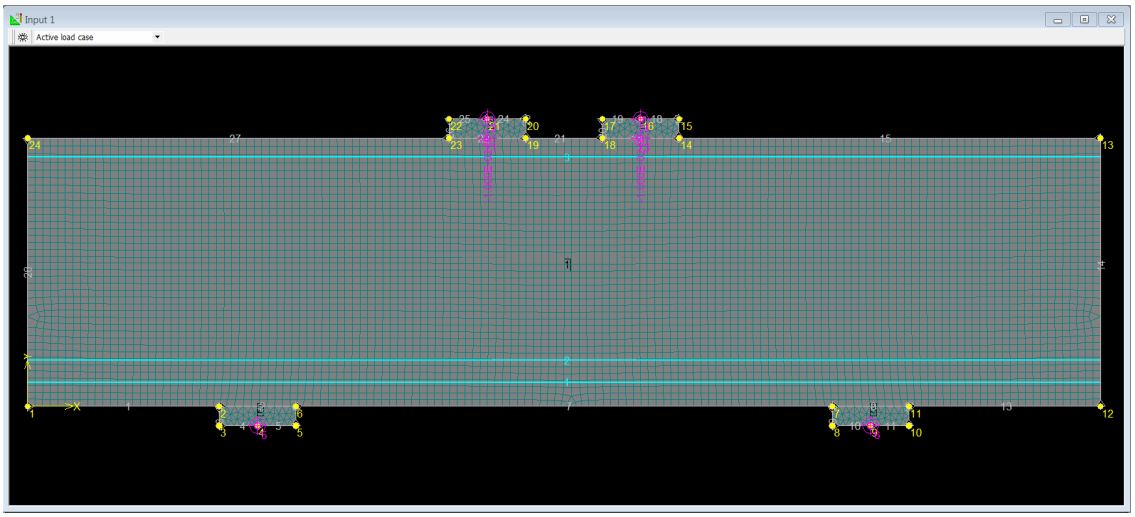

Figure 4.46 Details of the computer model of the beam 0A0-44 of Smith and Vantsiotis's tests

The crack pattern at failure of test beam 0A0-44 and computer model are shown in Fig. 4.47 and 4.48.

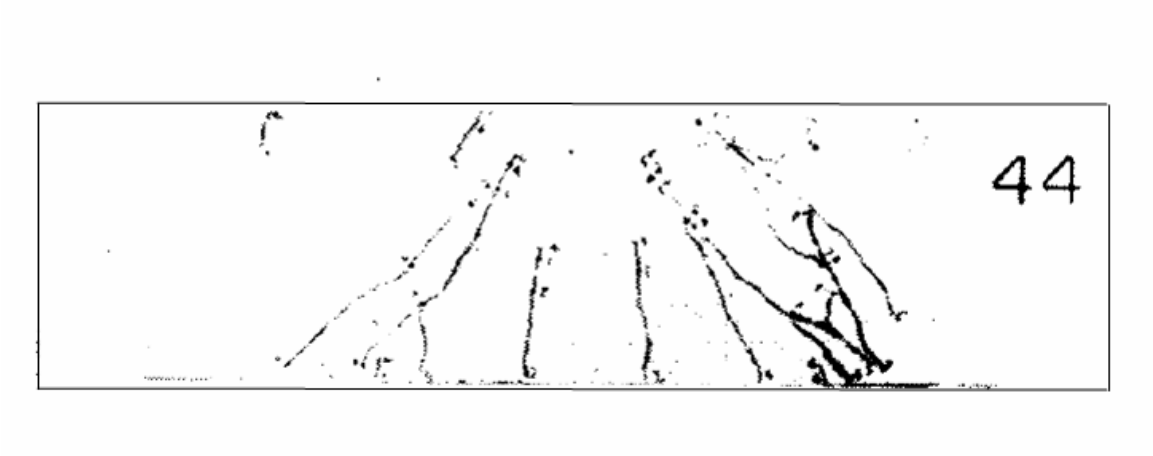

Figure 4.47 Crack pattern of the beam 0A0-44 of Smith and Vantsiotis's tests

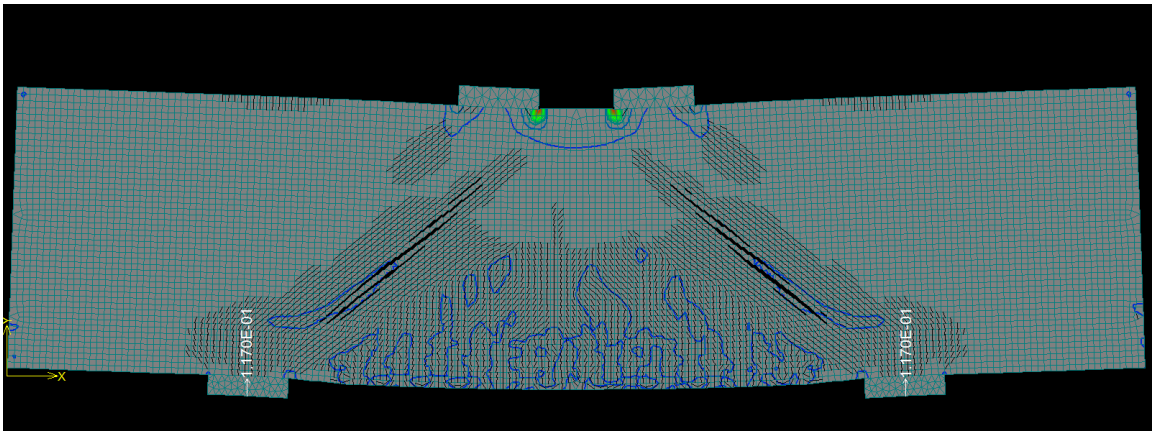

Figure 4.48 Crack pattern at failure of the computer model of the beam 0A0-44 of Smith and Vantsiotis's tests

The comparison of the inclined cracking shear and ultimate load between beam 0A0-44 and the companion computer model are shown in Table 4.10 and Figs. 4.49 and 4.50.

Table 4.10 Shear forces of beam 0A0-44 and those of its computer model

Beam	Inclined cracking shear, kN	Ultimate shear, kN
0A0-44	74	140
Computer model	60	117

The strains in longitudinal reinforcement in computer model of beam 0A0 - 44 are shown in Fig. 4.51.

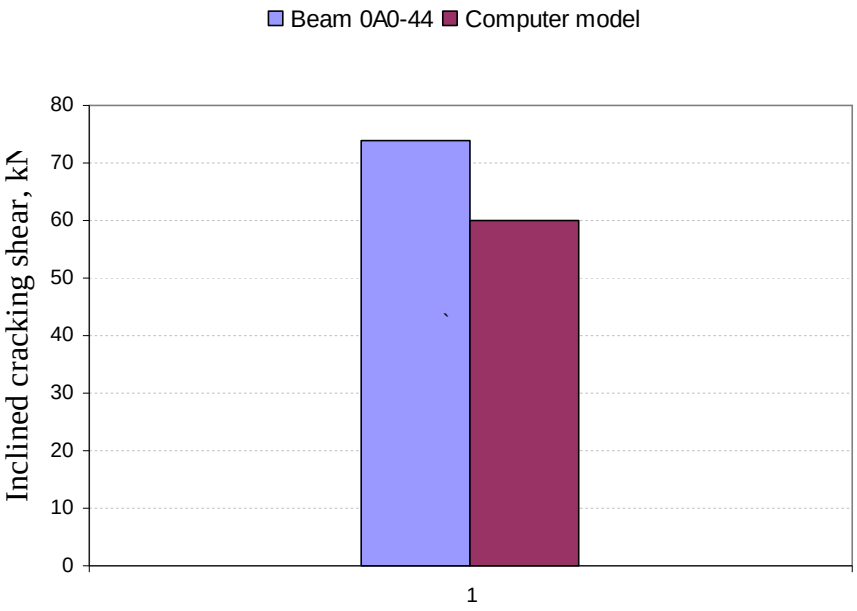

Figure 4.49 Inclined cracking shear of the beam 0A0-44 and the companion computer model

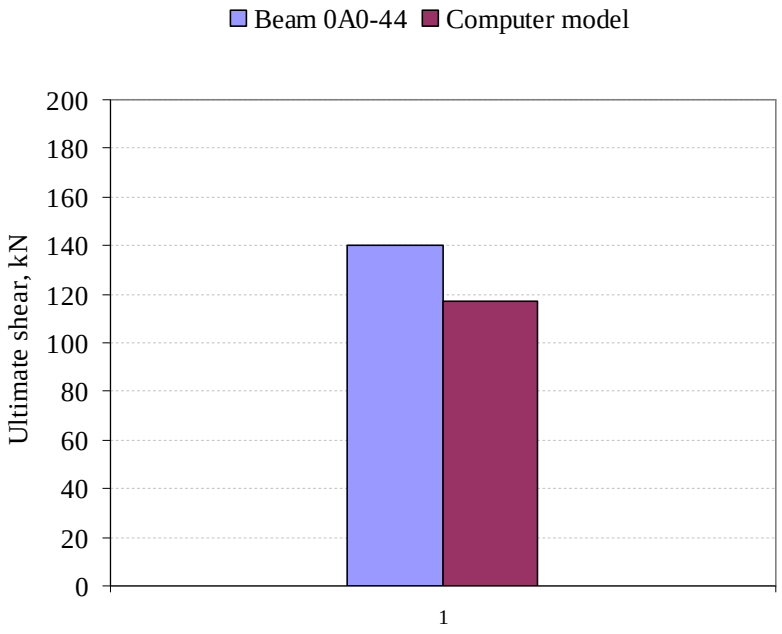

Figure 4.50 Ultimate load of the beam 0A0-44 and the companion computer model

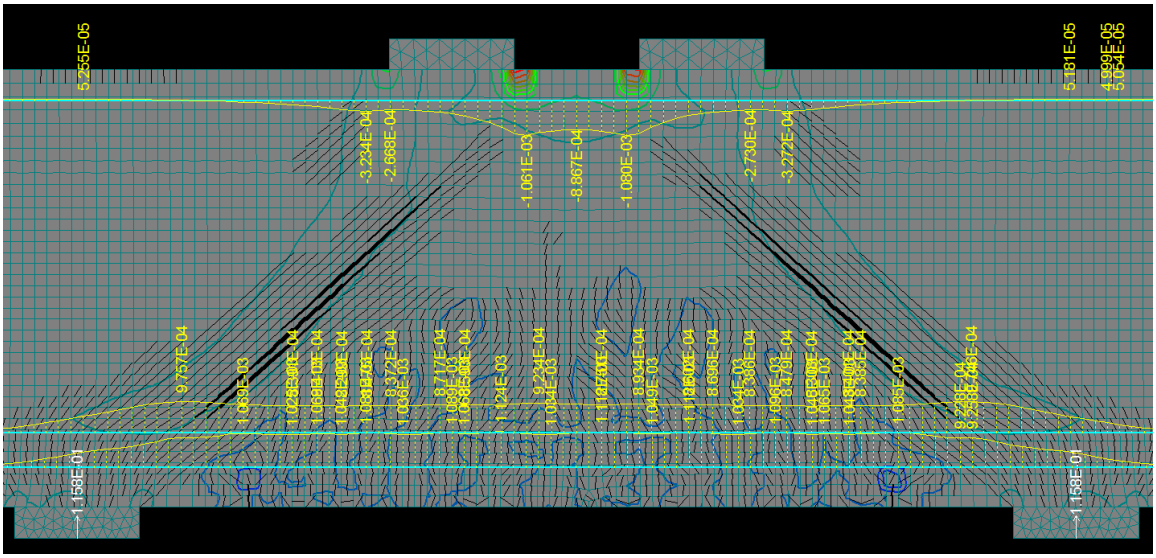

Figure 4.51 Strains in longitudinal reinforcements at failure of the computer model of the beam 0A0-44 of Smith and Vantsiotis's tests

The beam 0C0-50, a/d = 1.34, was modeled as follows:

(1) Geometric dimensions:

- Beam 0C0-50: length of 68 in., height of 14 in., and thickness of 4 in.
- Loading and bearing plates: 4x4x1 in.

(2) Constraint conditions:

- One constraint was a perfect pin and the other a perfect roller.

(3) Loading conditions:

- Two point loads were applied at middle of two loading plates. The increment of load was 20 kips.

(4) Materials:

- Concrete model was CCQ10SBeta: f'_c = 3 ksi.
- Plates were modeled as plane stress elastic isotropic material
- Reinforcement used as an elastic-perfectly plastic material model: f_y = 62.5 ksi.

(5) Finite element analysis

- Mesh type: rectangular mesh for reinforced concrete beam.

The behavior of the computer model of the beam 0C0-50 is shown in Figs. 4.52 to 4.55. Table 4.11 and Fig. 4.56 show the comparison of inclined cracking shear and ultimate shear between beam 0C0 - 50 and companion computer model.

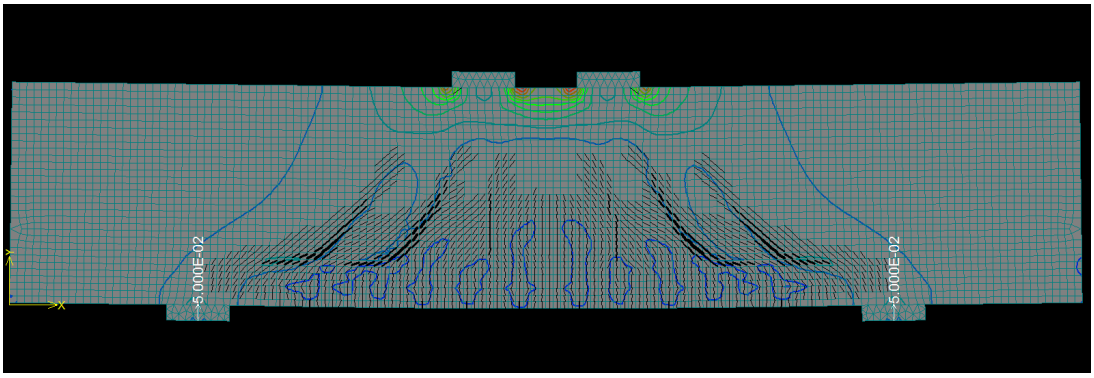

Figure 4.52 Inclined cracking shear of the computer model of the beam 0C0-50 of Smith and Vantsiotis's tests

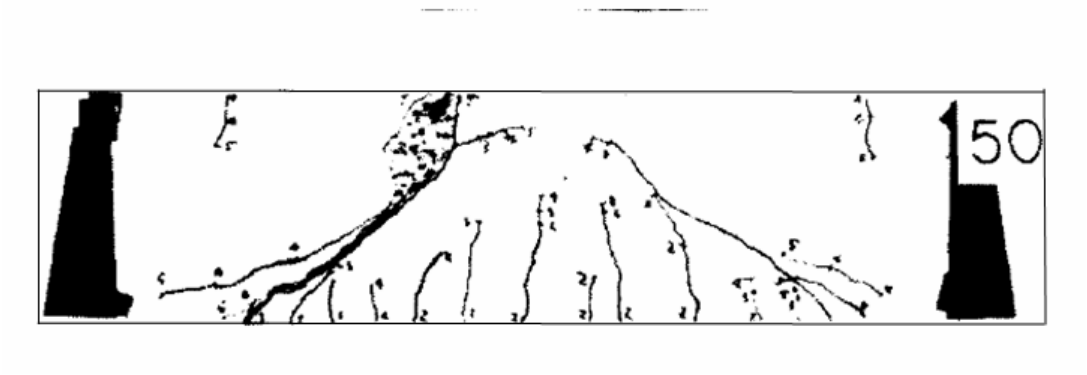

Figure 4.53 Crack pattern at failure of the beam 0C0-50 of Smith and Vantsiotis

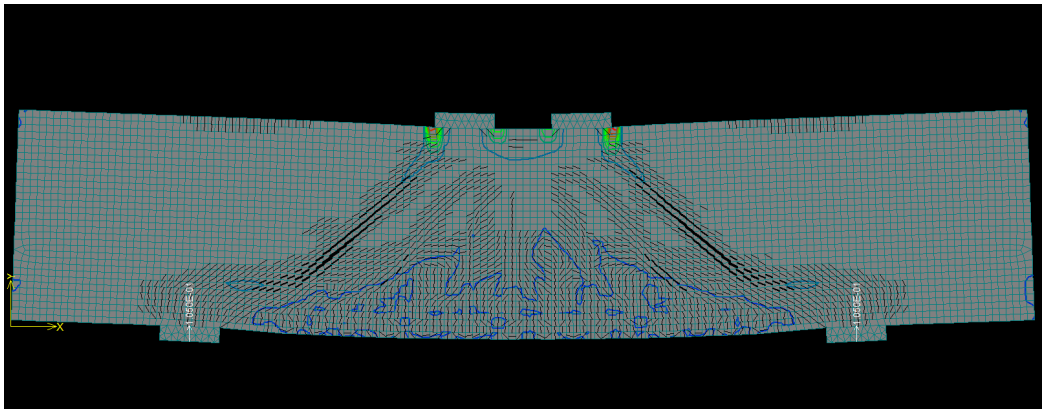

Figure 4.54 Crack pattern at failure of the computer model of the beam 0C0-50 of Smith and Vantsiotis

Table 4.11 Shear forces of beam 0A0-44 and those of its computer model

Beam	Inclined cracking shear, kN	Ultimate shear, kN
0C0-50	49.45	116
Computer model	50	105

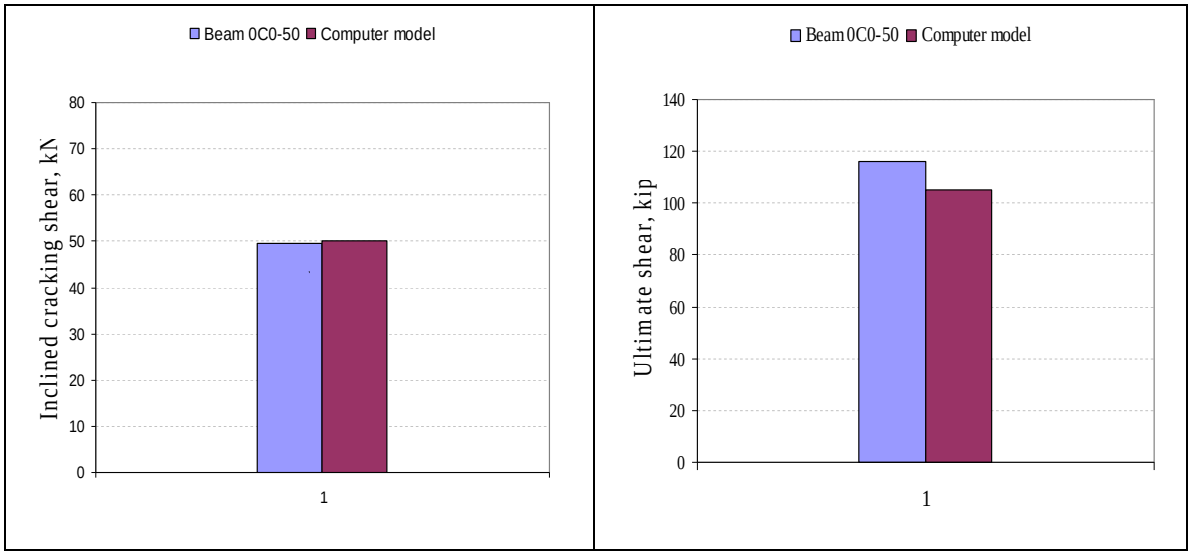

Figure 4.55 Comparison of test results of the beam 0C0-50 and the companion computer model

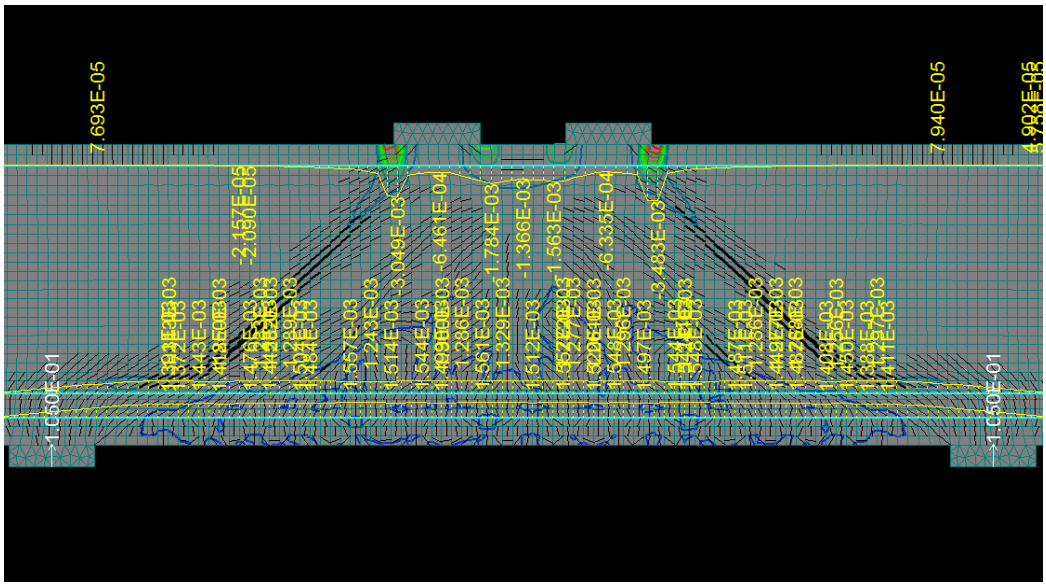

Figure 4.56 Strains in longitudinal reinforcements of the computer model of the beam 0C0-50

The behavior of the beam 0C0-50 was captured closely by the companion computer model. The computed crack pattern at failure compares well with that of test beam 0C0-50. The inclined cracking shear and ultimate load were also captured well. The difference between the inclined cracking shears of beam 0C0-50 and that of the computer model is 2%, and the difference between the ultimate load of the beam 0C0-50 and that of the companion computer model is 8.7%.

(b) Computer model of beams with web reinforcement

The beam 2A1-38, a/d = 0.77, was modeled as follows:

(1) Geometric dimensions:

- Beam 0A0-44: length of 56 in., height of 14 in., and thickness of 4 in.
- Loading and bearing plates: 4x4x1 in.

(2) Constraint conditions:

- One constraint was a perfect pin and the other a perfect roller.

(3) Loading conditions:

- Two point loads were applied at middle of two loading plates. The increment of load was 20 kips.

(4) Materials:

- Concrete model was CCQ10SBeta: f'_c = 3.145 ksi
- Plates were modeled as plane stress elastic isotropic material
- Reinforcement used as an elastic-perfectly plastic material model: f_y = 62.5 ksi

(5) Finite element analysis:

- Mesh type: rectangular mesh for reinforced concrete beam.

The crack pattern at failure of the beam 2A1-38 is shown in Fig. 4.57. It was observed that at failure some parallel inclined cracks occurred between the bearing plate and the loading plate. There was one major inclined crack forming from middle of bearing plate up to outside edge of loading plate. The mode of failure was shear compression leading to compression failure at the outside edge region of loading plate.

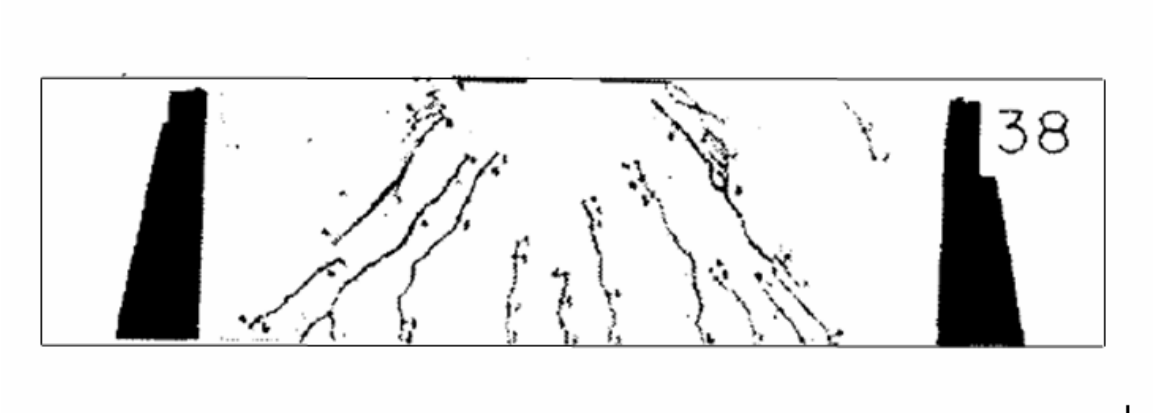

Figure 4.57 Crack pattern at failure of the beam 2A1-38 of Smith and Vantsiotis

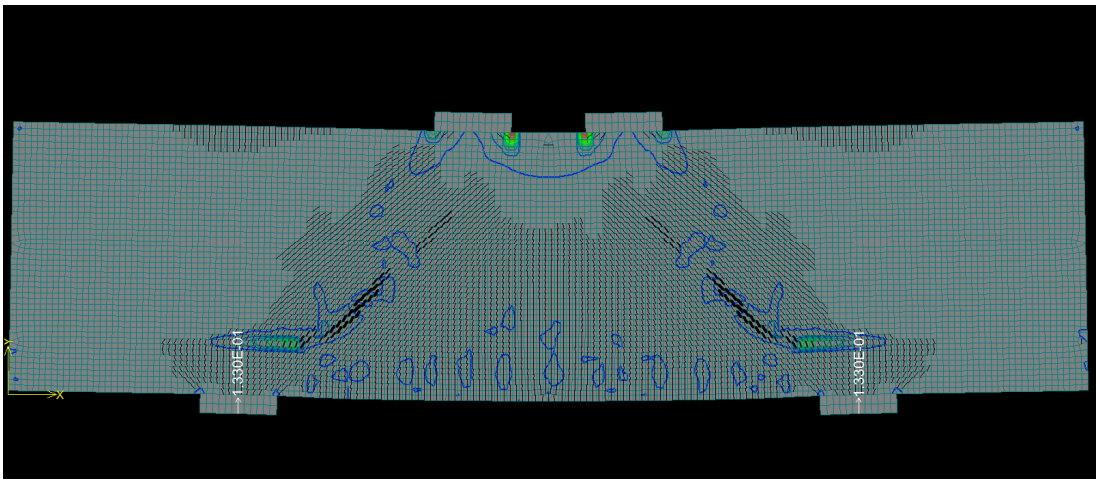

Figure 4.58 Crack pattern at failure of the computer model of the beam 2A1-38 of Smith and Vantsiotis's tests

For this beam, the crack pattern of the computer model did not match that of the companion test beam. There was only one major inclined crack forming at failure. The major inclined crack extend from above the inside edge of bearing plate up to inside edge of loading plate.

However, the inclined cracking shear was captured by the computer model. The inclined crack formed around the middle of the shear span and then extended to the bearing plate and loading plate. The value of inclined cracking shear of the computer model is close to that of the beam 2A1-38. The inclined crack is shown in Fig. 4.58.

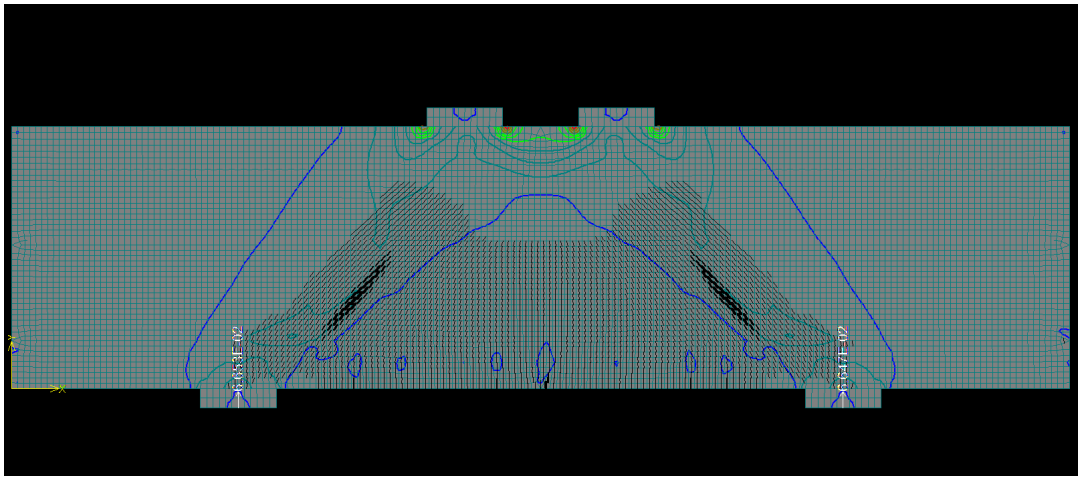

Figure 4.59 Formation of the inclined crack of the computer model of the beam 2A1-38 of Smith and Vantsiotis's tests

Table 4.12 Shear forces of beam 2A1-38 and those of its computer model

Beam	Inclined cracking shear, kN	Ultimate shear, kN
0C0-50	71	174.5
Computer model	65	133

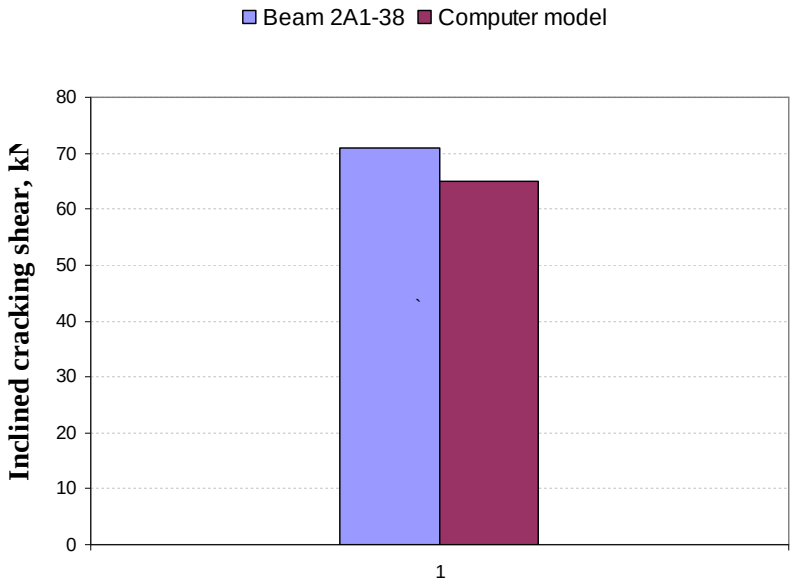

Figure 4.60 The inclined cracking shear of beam 2A1-38 and its companion computer model

The beam 2C1-17, a/d = 1.34, was modeled as follows:

(1) Geometric dimensions:

- Beam 0A0-44: length of 68 in., height of 14 in., and thickness of 4 in.
- Loading and bearing plates: 4x4x1 in.

(2) Constraint conditions:

- One constraint was a perfect pin and the other a perfect roller.

(3) Loading conditions:

- Two point loads were applied at middle of two loading plates. The increment of load was 20 kips.

(4) Materials:

- Concrete model was CCQ10SBeta: f'_c = 2.88 ksi
- Plates were modeled as plane stress elastic isotropic material
- Reinforcement used as an elastic-perfectly plastic material model: f_y = 62.5 ksi.

(5) Finite element analysis:

- Mesh type: rectangular mesh for reinforced concrete beam.

The crack pattern at failure of the beam 2C1-17 and its companion computer model are shown in Fig. 4.61 and 4.62. There was one major inclined crack forming from the inside edge of bearing plate up the outside edge of loading plate. The failure mode of the beam was also shear compression. The compression failure occurred at the outside edge of the loading plate. It was observed that the computer model of the beam 2C1-17 captured the crack pattern at failure.

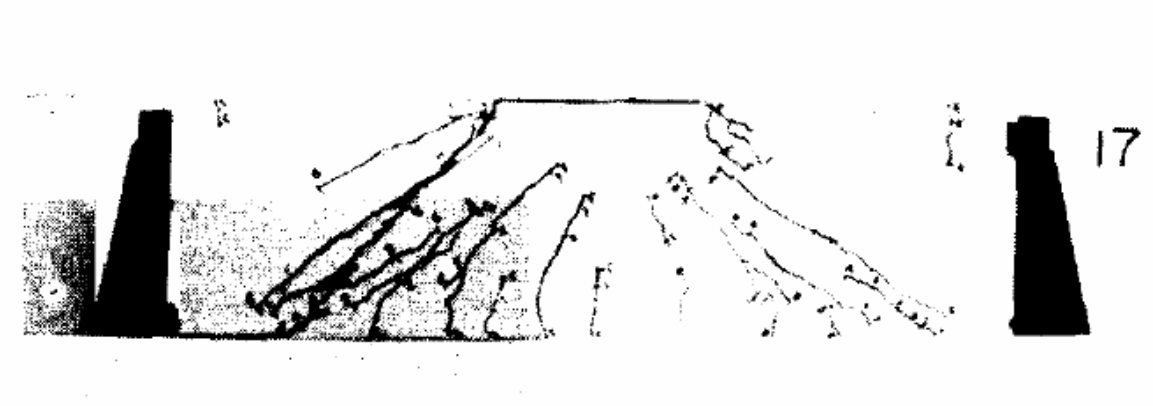

Figure 4.61 Crack pattern at failure of the beam 2C1-17 of Smith and Vantsiotis's tests

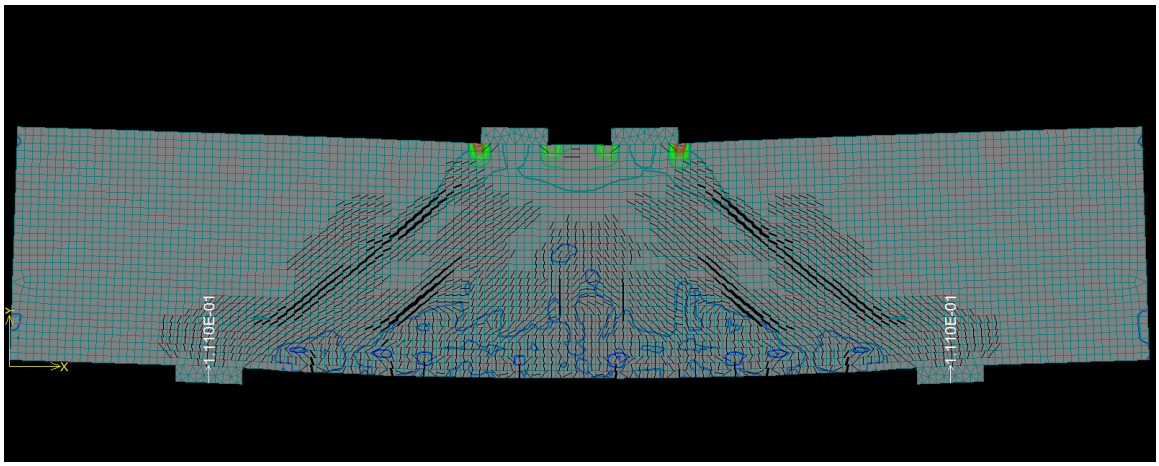

Figure 4.62 Crack pattern at failure of the computer model of the beam 2C1-17 of Smith and Vantsiotis's tests

The computer model of the beam 2C1-17 also captured the inclined cracking shear. The formation of the inclined crack is shown in the Fig. 4.63. The comparison of inclined cracking shear and ultimate shear between 2C1-17 and computer model is shown in Table 4.12.

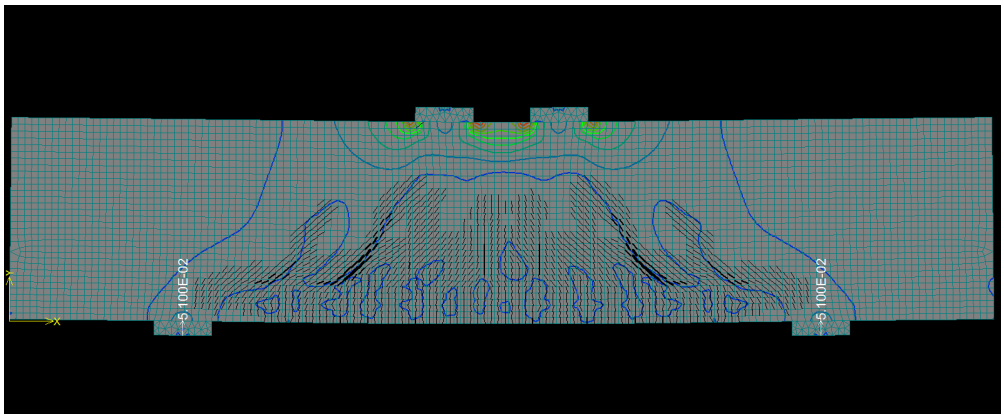

Figure 4.63 Formation of the inclined crack of the computer model of the beam 2C1-17 of Smith and Vantsiotis's tests

Table 4.13 Shear forces of beam 2C1-17 and those of its computer model

Beam	Inclined cracking shear, kN	Ultimate shear, kN
0C0-50	51	124
Computer model	51	111

4.3.3 Computer model of Birrcher's tests

(a) Computer model of the beam IV 2175-1.85-03

The details of dimensions of cross section and reinforcement of series IV of Birrcher's tests are shown in Fig. 4.64.

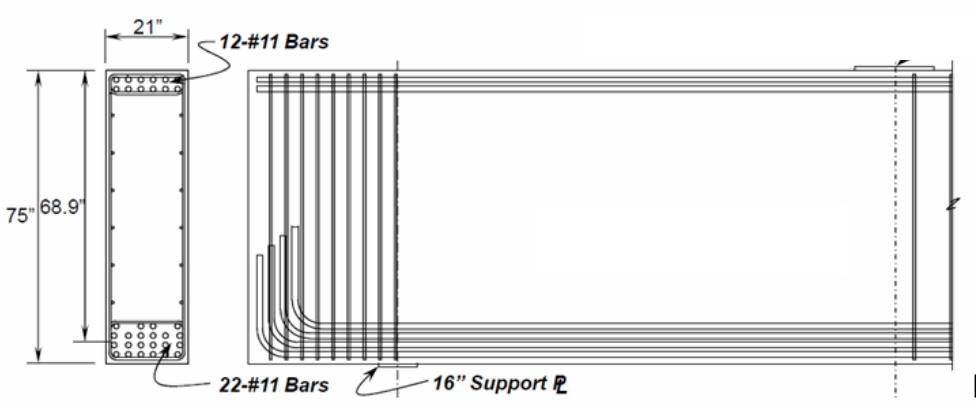

Figure 4.64 Details of cross section and reinforcements of the series IV of Birrcher's tests

All beams of series IV have dimensions of 255x75x21 in. The length was defined from center-to-center of support plates. Each beam has an extended length of 45 in from center of support plate.

For the beam IV 2175-1.85-03, the dimensions of the support plates were 16x21x3 in. (length x width x thickness) and the dimensions of loading plate were 29x21x4 in. (length x width x thickness).

The computer model of the beam IV 2175-1.85-03 was developed based on the real dimensions of the beam IV 2175-1.85-03. The details of the computer model of the beam IV are shown in Fig. 4.65.

The beam IV 2175-1.85-03, a/d = 1.85, was modeled as follows:

(1) Geometric dimensions:

- Beam IV 2175-1.85-03: length of 255 in., height of 75 in., and thickness of 21 in.
- Loading plate: 29x21x4 in.
- Support plates: 16x21x3 in.

(2) Constraint conditions:

- One constraint was a perfect pin and the other a perfect roller.

(3) Loading conditions:

- Single point load were applied at middle of loading plate. The increment of load was 20 kips.

(4) Materials:

- Concrete model was CCQ10SBeta: f'_c = 4.93 ksi.
- Plates were modeled as plane stress elastic isotropic material.
- Reinforcement used as an elastic-perfectly plastic material model: f_y = 68 ksi.

(5) Finite element analysis:

- Mesh type: rectangular mesh for reinforced concrete beam.

Analysis of the computer model was carried out in load increment of 20 kips. The concentrated load was applied at center of the loading plate (Fig.4.65).

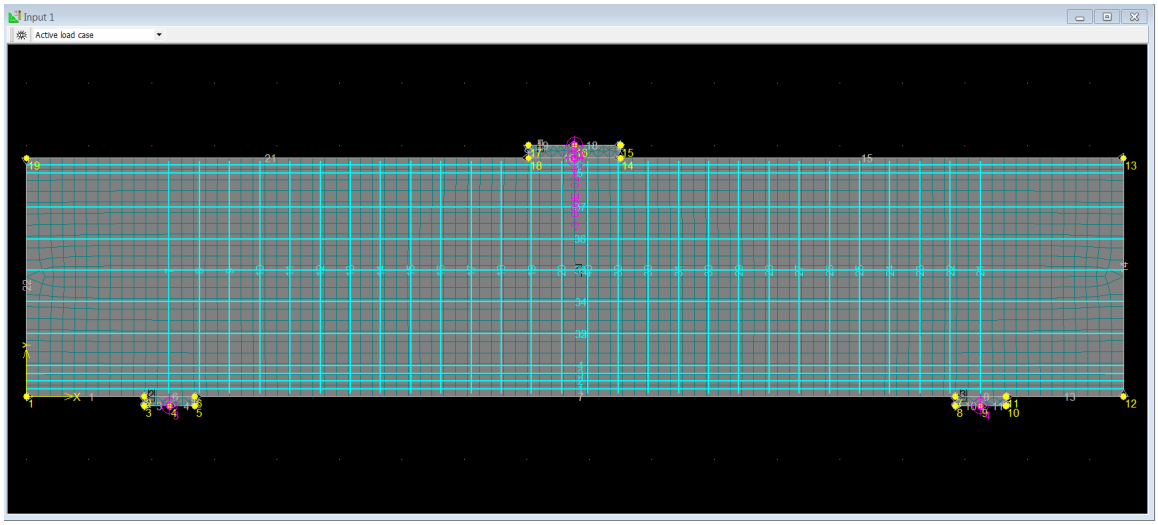

Figure 4.65 Details of the computer model of the beam IV 2175-1.85-03 of Birrcher's tests

The crack pattern at failure of the beam IV 2175-1.85-03 was shown in Fig. 4.66. At failure, there were some inclined cracks forming from the support plate up to the loading plate. These inclined cracks were not parallel, but they converged at the face of

the node region under the loading plate (Fig. 4.66). There was one major inclined crack at failure that extended from the middle of the shear span to inside edge of the loading plate. The mode of failure was shear compression. The failure region was at the outside edge of the loading plate.

It was observed that the computer model of the beam IV 2175-1.85-03 sketched the crack pattern quite accurately (Fig. 4.67). The cracks formed and converged from support plates to loading plate. However, it did show the major inclined crack. The computer model also captured the ultimate load well. The tolerance of value of ultimate load between the beam and its companion computer model is 11% (Fig. 4.68).

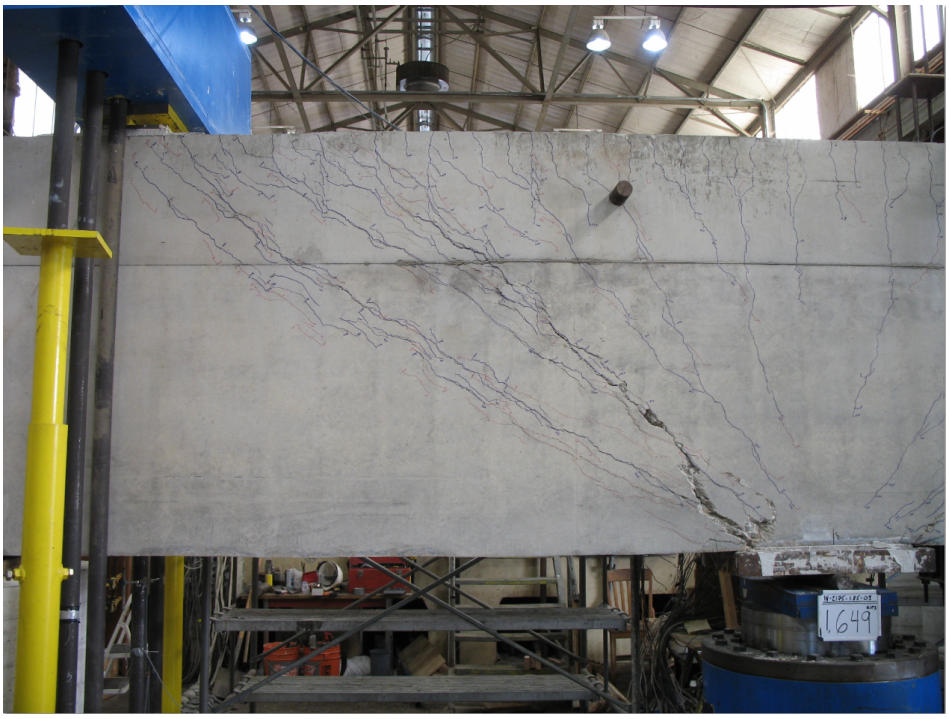

Figure 4.66 Crack pattern at failure of the beam IV 2175-1.85-0.3 of Birrcher's tests

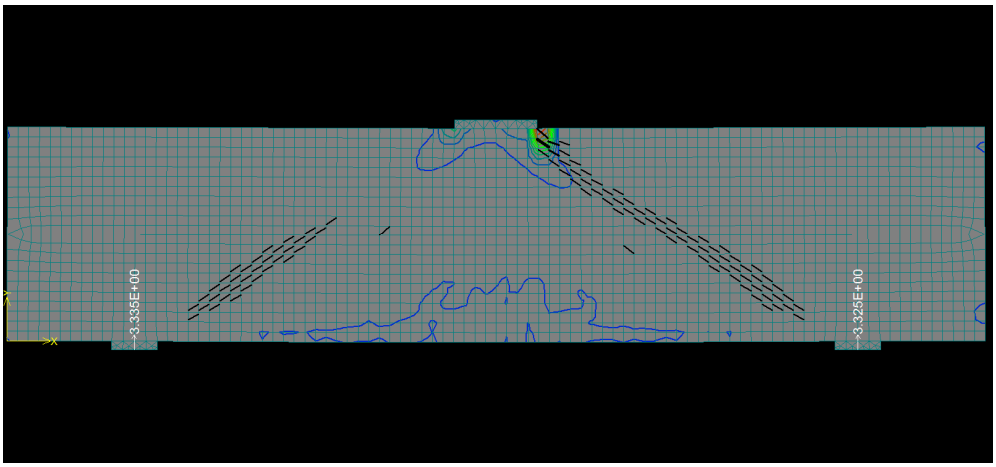

Figure 4.67 Crack pattern (after crack filtering with a minimum crack width = 0.031 in.) at failure of the computer model of the beam IV 2175-1.85-03 of Birrcher's tests

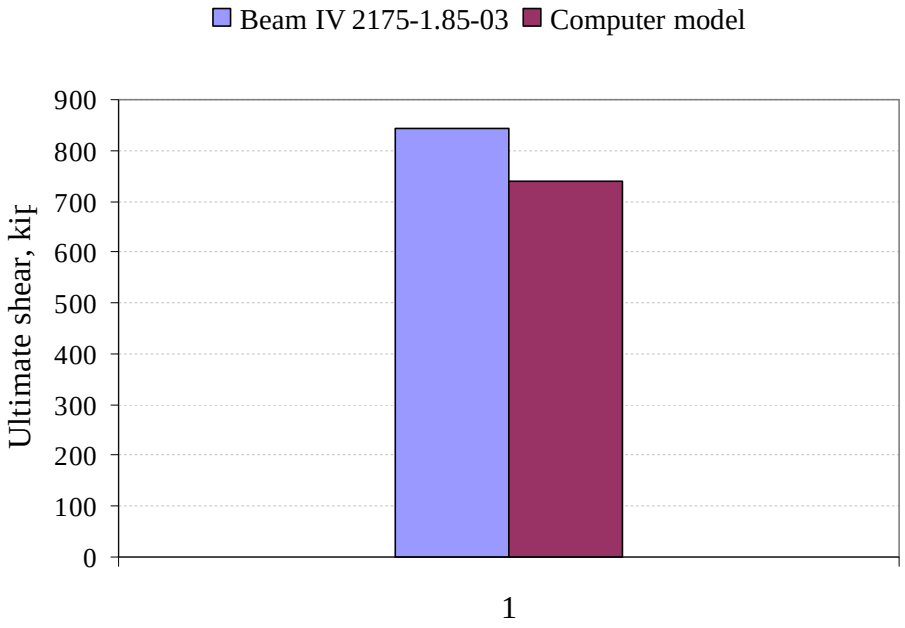

Figure 4.68 Ultimate load of the beam IV 2175-1.85-03 and that of its companion computer model

The comparison between Birrcher deep beam and computer model during of test are shown in Figs. 4.69 to 4.76.

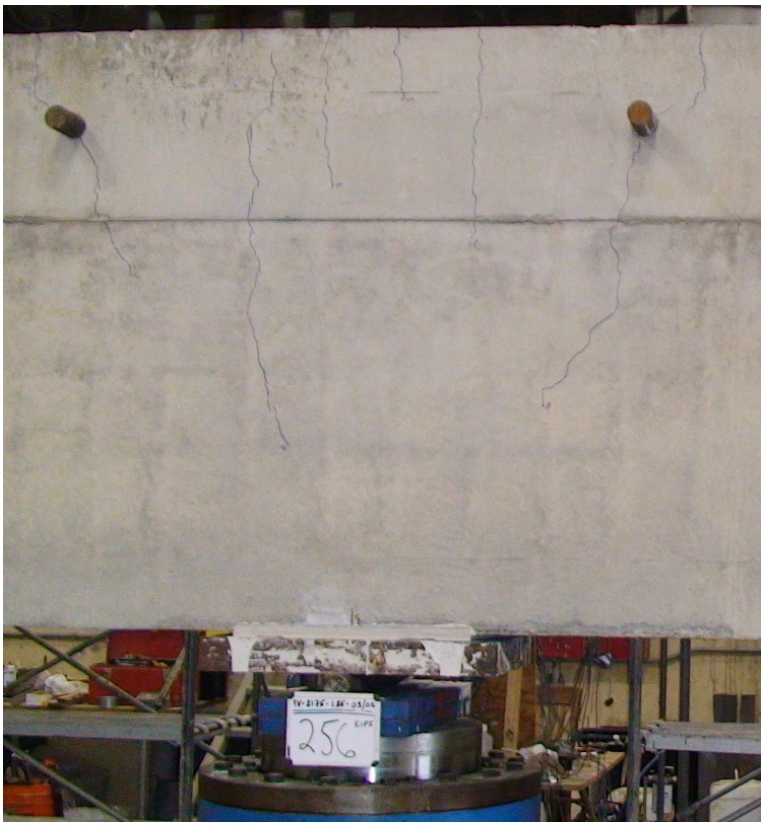

Figure 4.69 Crack pattern of the beam IV 2175-1.85-03 of Birrcher's tests at external load of 256 kips

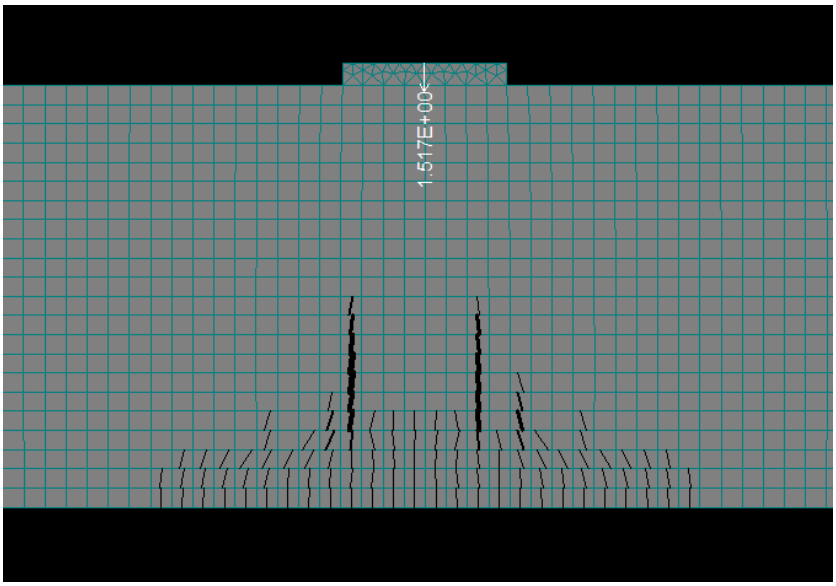

Figure 4.70 Crack pattern of computer model of the beam IV 2175-1.85-03 of Birrcher's tests at external load of 341 kips

Figure 4.71 Crack pattern of the beam IV 2175-1.85-03 of Birrcher's tests at external load of 552 kips

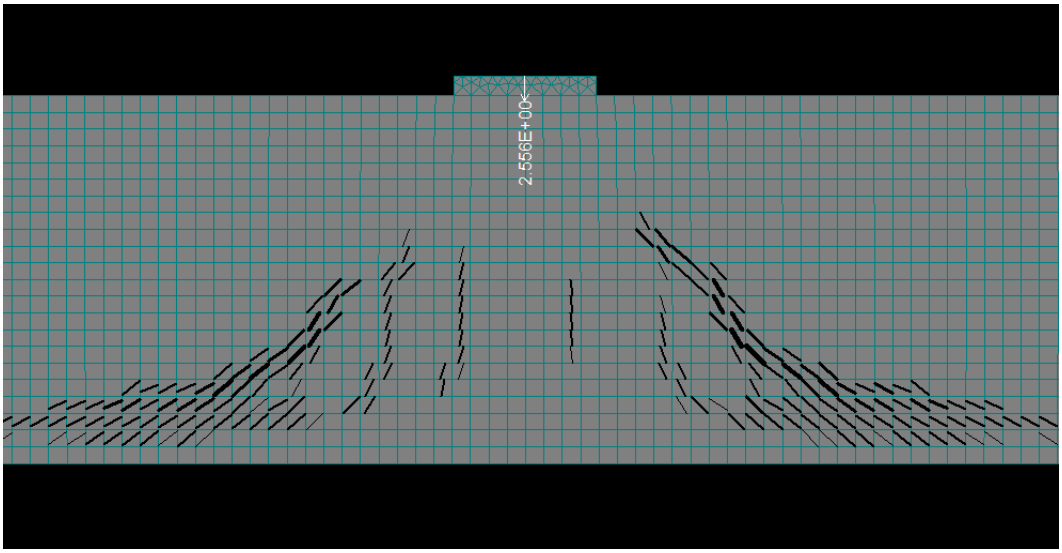

Figure 4.72 Crack pattern of computer model of the beam IV 2175-1.85-03 of Birrcher's tests at external load of 574 kips

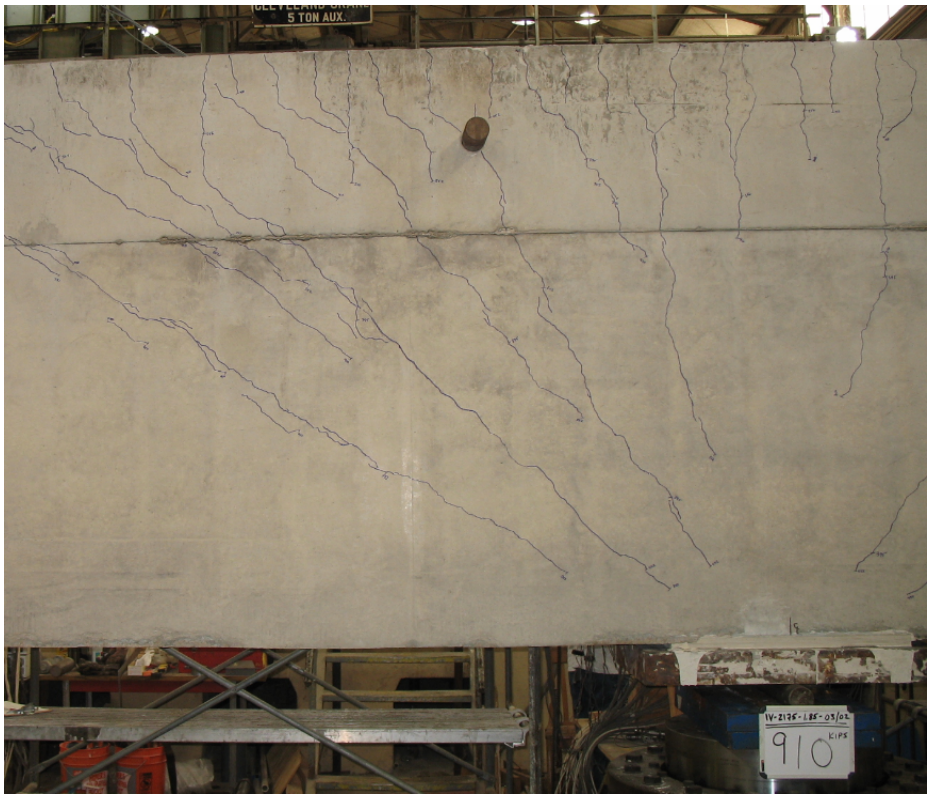

Figure 4.73 Crack pattern of the beam IV 2175-1.85-03 of Birrcher's tests at external load of 910 kips

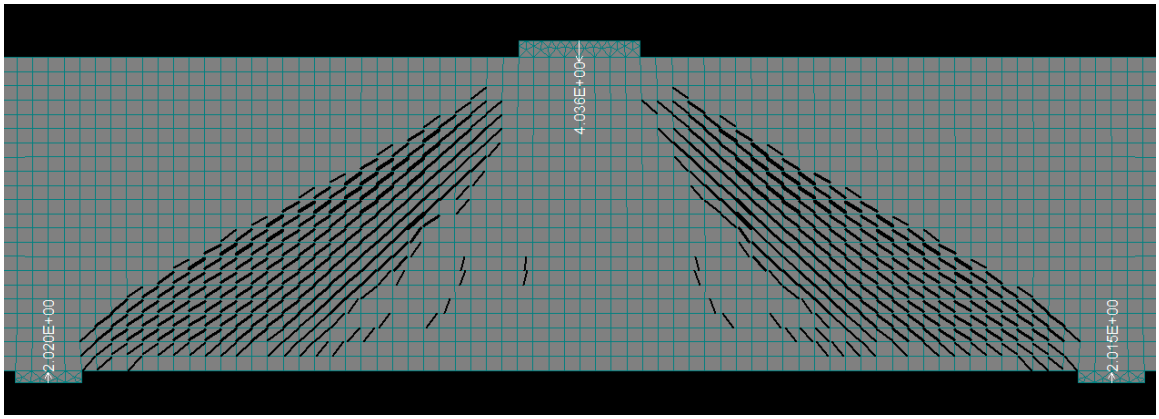

Figure 4.74 Crack pattern of computer model of the beam IV 2175-1.85-03 of Birrcher's tests at external load of 907 kips

Figure 4.75 Crack pattern of the beam IV 2175-1.85-03 of Birrcher's tests at external load of 1476 kips

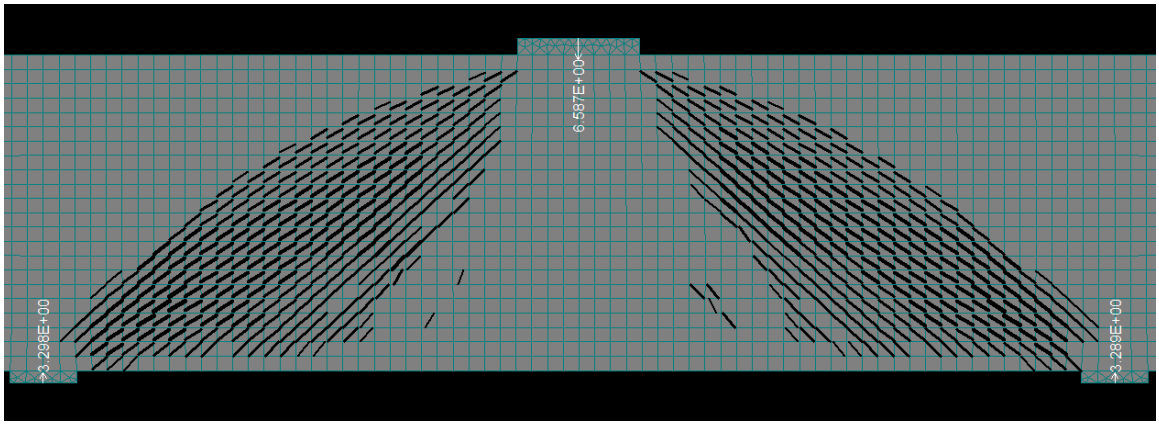

Figure 4.76 Crack pattern of computer model of the beam IV 2175-1.85-03 of Birrcher's tests at external load of 1480 kips

(b) Computer model of the beam IV 2175-2.5-02

The crack pattern at failure of the beam IV 2175-2.5-02 is shown in Fig 4.77. At failure, inclined cracks formed form support plate to loading plate, and there was one

major inclined crack occurred close to middle shear span up to loading plate. The mode of failure is sectional failure.

In Fig. 4.78, the crack pattern at failure of the computer model of the beam IV 2175-2.5-02 was shown. It seemed that the computer model represented the behavior of the beam IV 2175-2.5-02 well. The cracks formed and converged from support plate to loading plate. At failure, there was one major inclined crack forming and the mode of failure was sectional (Fig. 4.78). It was also observed that the model captured the shear capacity. The difference between test shear and model shear is 3%.

Figure 4.77 Crack pattern at failure of the beam IV 2175-2.5-02 of Birrcher's tests

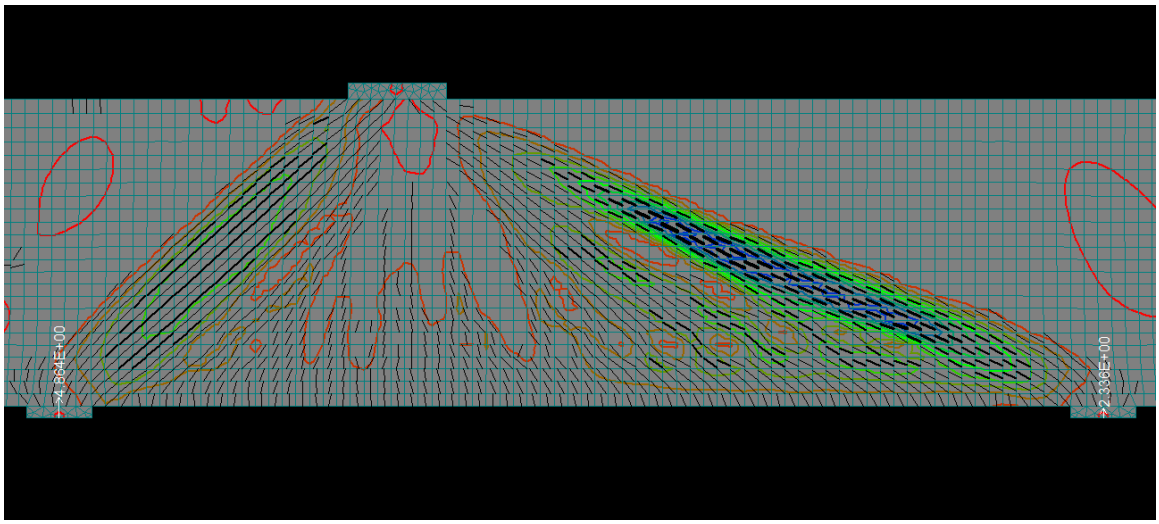

Figure 4.78 Crack pattern at failure of the computer model of the beam IV 2175-2.5-02 of Birrcher's tests

4.4 Summary

In this chapter, a brief introduction of ATENA program was presented. The applicability of ATENA was verified by developing the computer models of simply supported and two span continuous deep beams based on the Birrcher's tests of simply supported deep beams. For the models of two span continuous deep beams, tests by Rogowsky and MacGregor and by Ashour were selected. Those tests were selected because the researchers reported adequate details of the experimental program and on specimen behavior.

Chapter 5 Computer Analyses of Reinforced Concrete Deep Beams

5.1 Overview

In this chapter, a series of computer models were developed to investigate the behavior of reinforced concrete simply supported and continuous deep beams. Parameters investigated included concrete strength, longitudinal reinforcement, web reinforcement, height of beam, and loading conditions.

5.2 Analyses of simply supported deep beam

5.2.1 The influence of concrete strength on the shear strength of deep beams (series A)

In this part, computer models of simply supported deep beams with different values of concrete strength were developed. Dimensions of the computer models were based on the dimensions of Birrcher's tests. The computer models consist of two subsets of deep beams with three different ratios of shear span-to-depth, 1.0, 1.2 and 1.5. The models are simply supported deep beams under a single concentrated load at the middle of the loading plate. Values of concrete strength range from 3000 psi to 6000 psi.

A typical beam of series A was modeled as follows:

(1) Geometric dimensions:

- Shear span length is the distance from the center of the loading plate to the center of the supporting plate.
- Dimensions of cross section: height 75 in., and width 21 in.
- Loading plates: 24x21x4 in.
- Bearing plates: 16x21x3 in.

(2) Constraint conditions:

- One constraint was a perfect pin and the other a perfect roller.

(3) Loading conditions:

- Single load was applied at middle of loading plates. The increment of load was 20 kips.

(4) Materials:

- Concrete model was CCQ10SBeta: f'_c = 3000 - 6000 psi.
- Plates were modeled as a plane stress elastic isotropic material
- Reinforcement was represented as a linear-perfectly plastic material model with f_y = 69 ksi.

(5) Finite element analysis:

- Mesh type: rectangular mesh for reinforced concrete beam with mesh size of 3.3 in.

The dimensions of the computer models are shown in Table 5.1.

Table 5.1 Detail dimensions of series A computer model tests

Beam	**L**, in.	**H**, in	**B**, in	**d**, in	**a**, in	ρ_s
A I-2175-1.0	138	75	21	68.9	68.9	0.0237
A II-2175-1.2	165	75	21	68.9	82	0.0237
A III-2175-1.5	206	75	21	68.9	103	0.0237
Bearing plates	16	21	3			
Loading plate	24	21	4			

The reinforcement detail of the computer models is shown in Fig. 5.1.

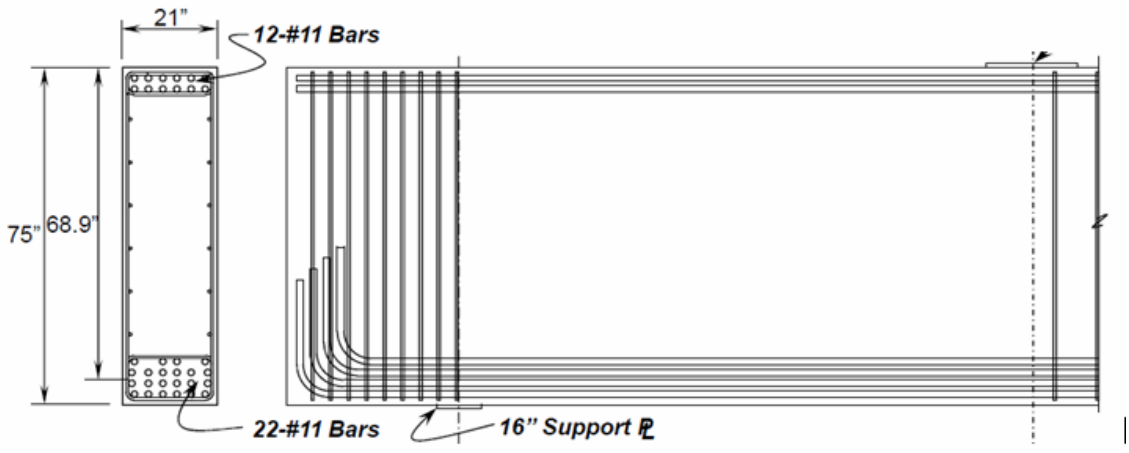

Figure 5.1 Detail reinforcement of computer model

The details of two computer models are shown in Figs. 5.2 and 5.3. The reinforcement is shown as light lines. The moments were computed along the centroidal

axis at the mid-depth extending between supports. The diagonal lines show where compressive stresses were plotted to study the strut forces.

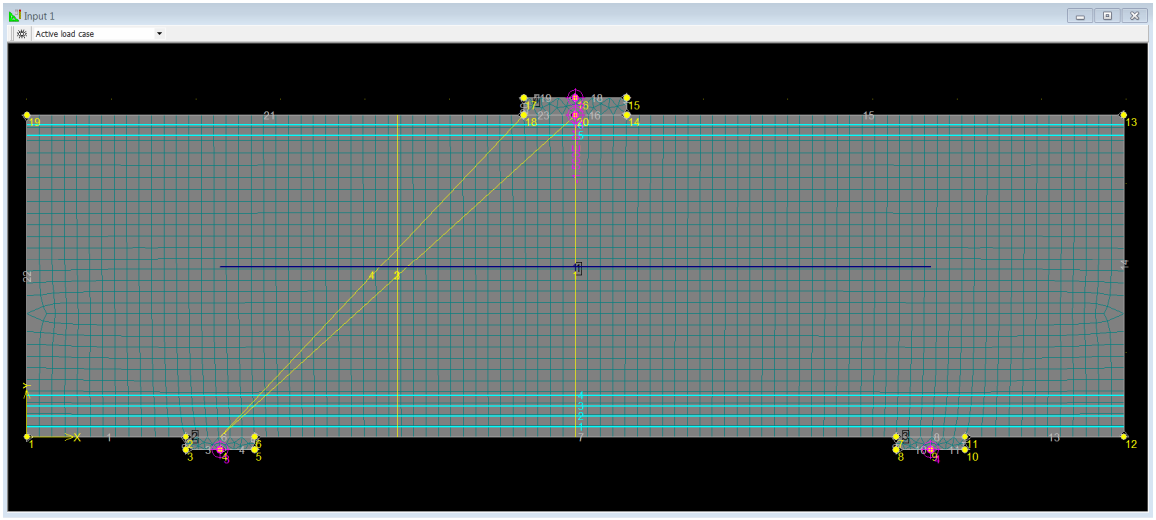

Figure 5.2 Details of computer model beam with a/d = 1.2

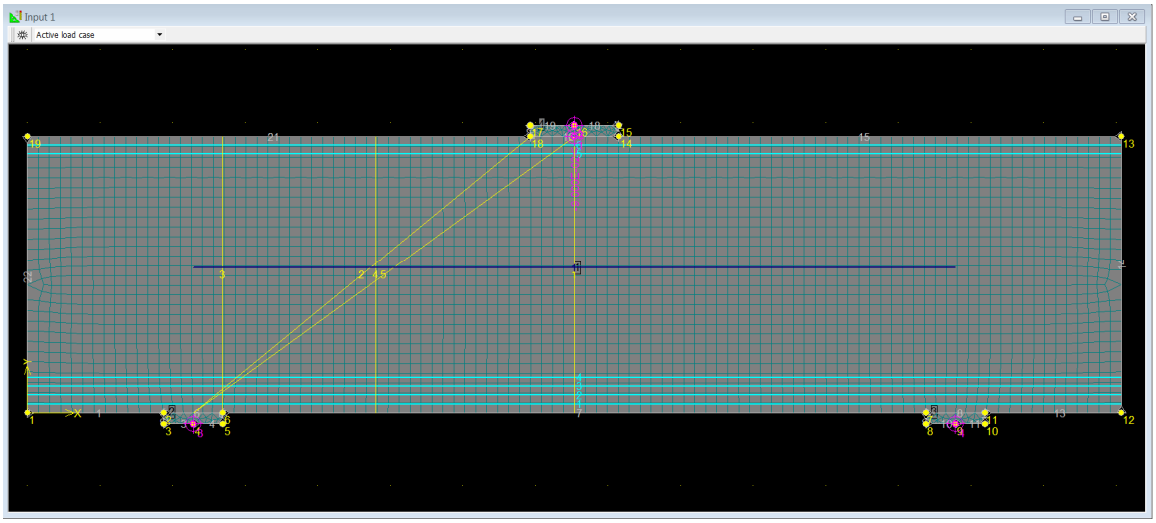

Figure 5.3 Details of computer model beam with a/d = 1.5

The initial flexural cracking shear, an inclined cracking shear, ultimate shear, maximum moments, maximum crack width, and maximum deflection were determined in the analysis in which the concrete strength was varied and the shear strength capacity is plotted for the three cases against f'_c in Fig. 5.4.

The test results of the two subsets are shown in Tables 5.2.

Table 5.2 Shear capacity as a function of f'_c for series A I

Beam	f'_c = 3000 psi	f'_c = 3500 psi	f'_c = 4000 psi	f'_c = 4500 psi	f'_c = 5000 psi	f'_c = 5500 psi	f'_c = 6000 psi
A I-1.0	556	640	725	809	876	977	1045
A II-1.2	472	522	573	674	725	792	859
A III-1.5	404	445	505	556	607	627	687

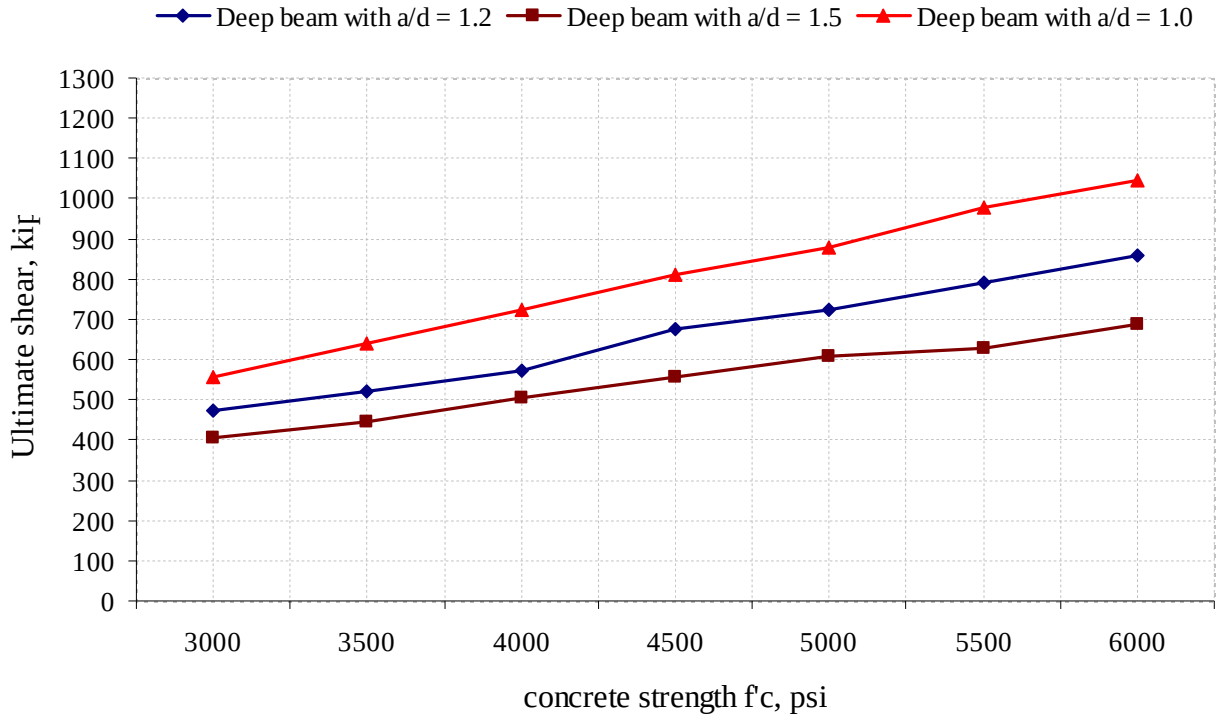

Figure 5.4 The influence of concrete strength on shear strength of deep beam

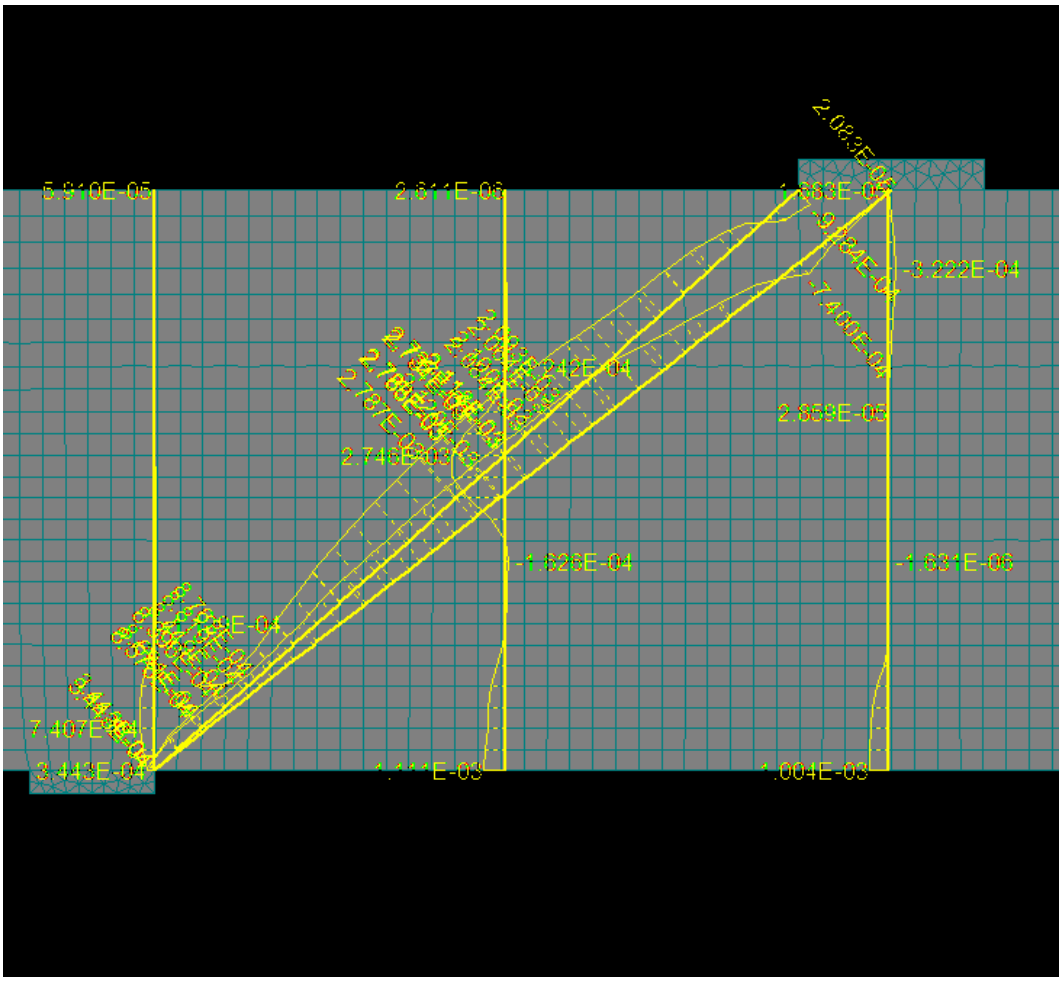

Figure 5.5 Distribution of xx strains of concrete just before failure of computer model beam with a/d = 1.5 and ρ = 2.37%

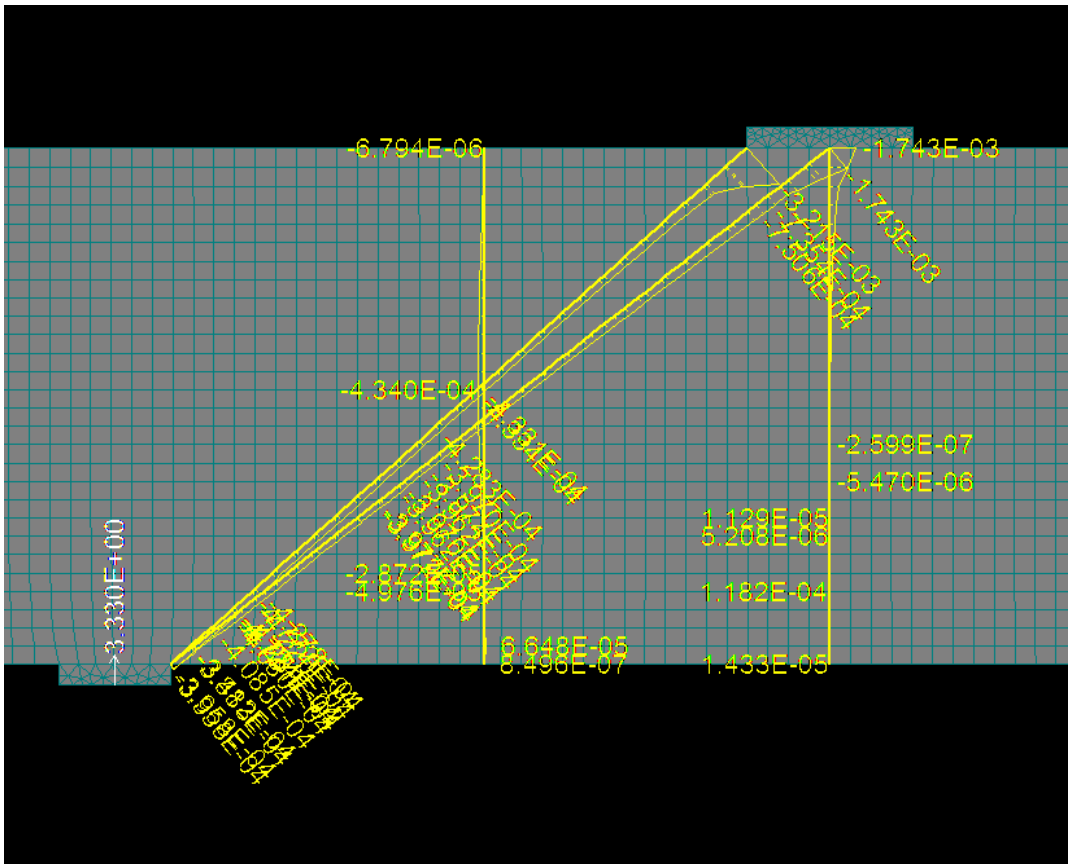

Figure 5.6 Distribution of principal compressive strain of concrete just before failure of the computer model test with a/d = 1.5 and ρ = 2.37%

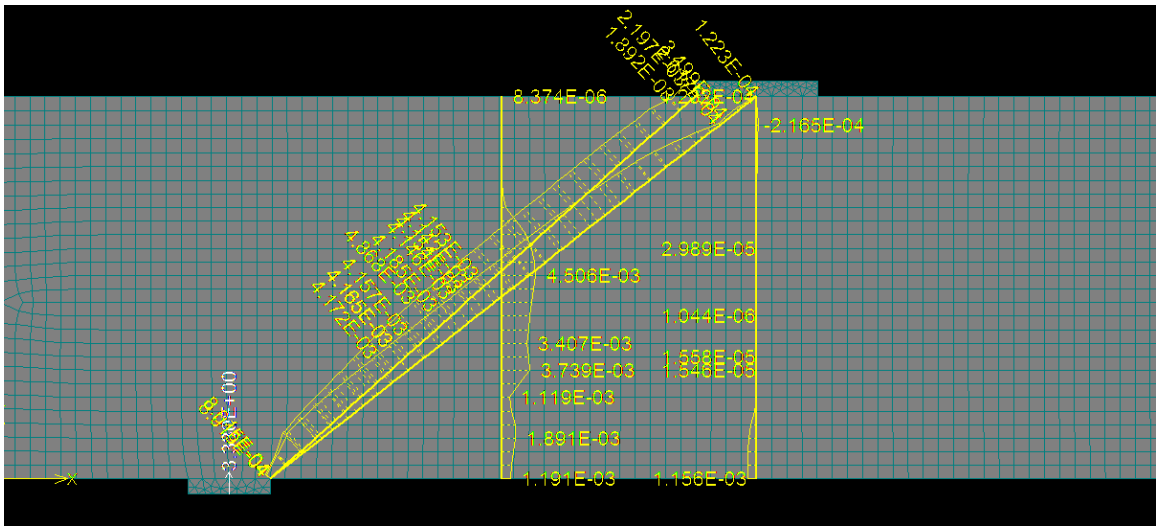

Figure 5.7 Distribution of principal tensile strain in concrete just before failure of the computer model test with a/d = 1.5 and ρ = 2.37%

The shear strength is linearly proportional to concrete strength as shown in Fig. 5.4. However, concrete strength is different for deep beam with different shear span-to-depth ratio. It was observed that the smaller value of a/d the larger rate of contribution of concrete strength on the shear strength deep beam.

Distribution of ε_{xx} (horizontal strain) of concrete just before failure of deep beam a/d = 1.5 is shown in Fig. 5.5. At the middle section of the beam it was observed the depth of compression zone is about 0.8 of height of the beam. However, compressive strain is almost zero in the web of the beam. Compression strain concentrates in the region below loading plate with the centroid of compression force is about 0.11 of the depth of the beam. It showed that tensile strain is distributed almost along diagonal section extending from the inside edge of the support plate to outside edge of the loading plate. But, in the region just at outside edge of the loading plate there is a concentration of strain. This may be a reason for failure of the deep beam begins there first. This is also confirmed on Fig 5.6 and 5.7 which show the distribution of principal compression strain and principal tensile strain.

5.2.2 The influence of longitudinal reinforcement (series B)

In the Section 10.5.1 ACI Code 318-11, the minimum requirement of tensile longitudinal reinforcement in flexural members is:

$$A_{s,\min} = \frac{3\sqrt{f'c}}{f_y} b_w d \tag{5.1}$$

and not less than $\dfrac{200 b_w d}{f_y}$

The maximum requirement based on the ductile failure requirement of flexural member follows (Park and Paulay, 1975)[ ]:

$$\rho_{\max} \le 0.75\rho_b$$

$$\rho_{\max} \le 0.75\left(\frac{0.85 f'_c \beta_1}{f_y} \frac{0.003E_s}{0.003E_s + f_y} + \frac{\rho' f'_s}{f_y} \right) \tag{5.2}$$

where,

ρ is the tensile steel ratio

ρ' is the compression steel ratio

E_s is the modulus of reinforcement, 29000 psi

f_y is the yield strength of steel

f'_s is the stress of compression steel

f'_c is the cylinder strength of concrete

β_1 is the factor relating the depth of equivalent rectangular compressive stress block to the neutral axis depth

where,

$$f'_s = 0.003E_s\left[1 - \frac{d}{d'}\left(\frac{0.003E_s + f_y}{0.003E_s}\right)\right]$$

or $f'_s = f_y$, whichever is least.

The values of minimum and maximum requirements of longitudinal tensile reinforcement provided in Table 5.3, follow Eqs. 5.1 and 5.2 for beams with the cross-section shown in Fig. 5.8 and only the amount of longitudinal reinforcement was varied for the model beams.

Table 5.3 Maximum and minimum requirements of longitudinal reinforcement

$A_{s,\min} = \frac{3\sqrt{f'c}}{f_y} b_w d$, in^2	4.5 (0.3%)
$A_{\min} = \frac{200 b_w d}{f_y}$, in^2	4.2 (0.29%)
$A_{s,\ max}$, in^2, ($\rho_{\max} \le 0.75\rho_b$)	46 (3.16%)
A_b, in^2,(ρ_b)	61 (4.21%)

where,

E_s is equal to 29000 psi

f_y is equal to 69000 psi

f'_c is equal to 5000 psi

β_1 is equal to 0.85

The limitations were used to select the longitudinal tension reinforcement (Fig. 5.8) that ranged from 12 - #11 bars to 24 - #14 bars. The compression reinforcement was kept the same 12 - #11 bars.

For series B, the longitudinal reinforcement ratio of deep beams consists of simply supported deep beam having longitudinal reinforcement ratio ranges 1.29%, 2.1%, 2.37%, 3.0%, 3.5%, and 4.0% and have the same 0.3% vertical reinforcement.

A typical beam of series B was modeled as follows:

(1) Geometric dimensions:

- Shear span length is the distance from the center of the loading plate to the center of the supporting plate.
- Dimensions of cross section: height 75 in., and width 21 in.
- Loading plates: 24x21x4 in.
- Bearing plates: 16x21x3 in.

(2) Constraint conditions:

- One constraint was a perfect pin and the other a perfect roller.

(3) Loading conditions:

- Single load was applied at middle of loading plates. The increment of load was 20 kips.

(4) Materials:

- Concrete model was CCQ10SBeta: f'_c = 5.01 ksi
- Plates were modeled as a plane stress elastic isotropic material
- Reinforcement was represented as a linear-perfectly plastic material model with f_y = 69 ksi and f_{vy} = 67 ksi.

(5) Finite element analysis:

- Mesh type: rectangular mesh for reinforced concrete beam with mesh size of 3.3 in.

Details of reinforcement of this subset computer model are shown in Table 5.3 and Figs. 5.8 and 5.9.

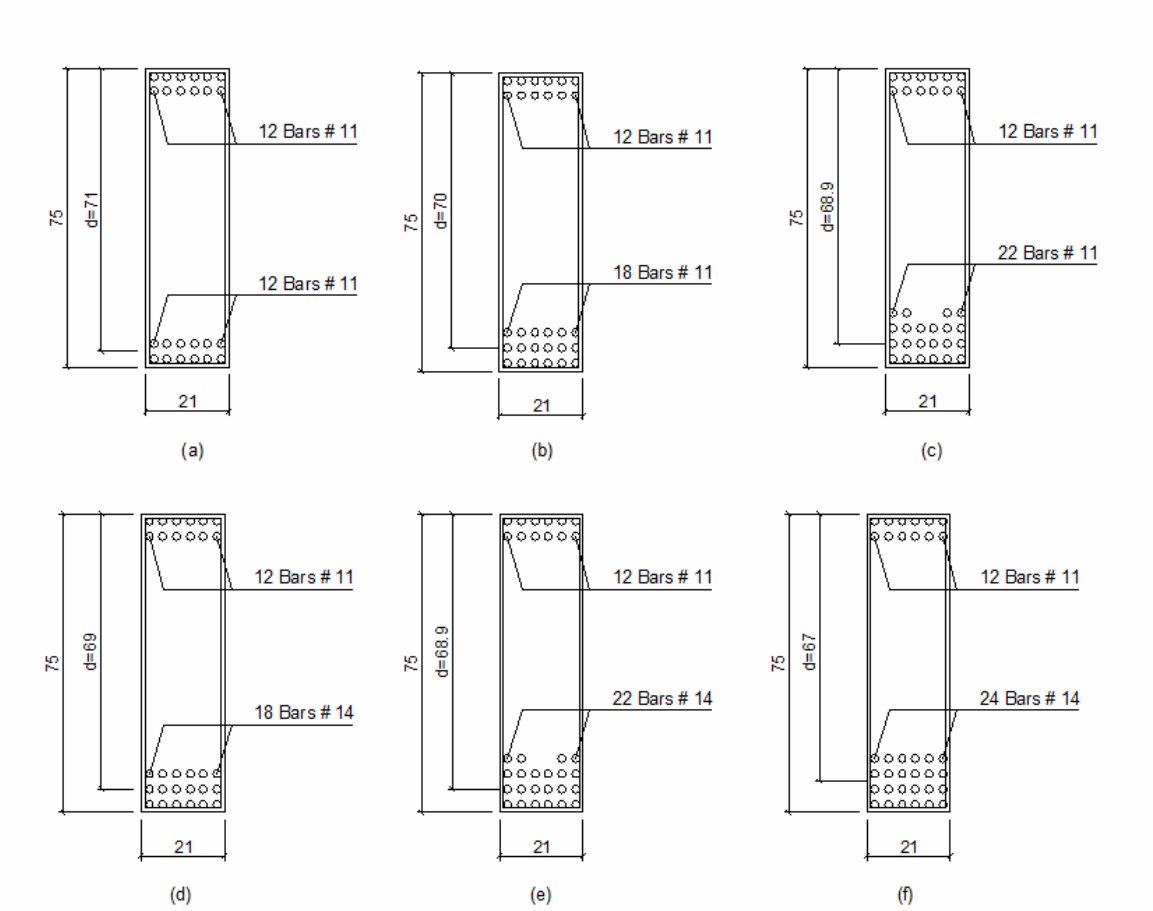

Figure 5.8 Details of reinforcement of computer model test (a) ρ =ρ' =1.29%, (b) ρ = 2.1%, and (c) ρ = 2.37% (d) ρ =3.0%, (e) ρ = 3.5%, and (f) ρ = 4.0%

Details of the models and test results of series B are shown in Table 5.4.

Table 5.4 Details of a series B of models and computed shear capacity

Computer model I.D.	b_w, in	d, in	a/d	ρ_s,%	Ultimate shear, kip
B-1.29	21	71	1.5	1.29	658
B-2.0	21	68.9	1.5	2.1	739
B-2.37	21	69	1.5	2.37	759
B-3.0	21	69	1.5	3.0	789
B-3.5	21	68.9	1.5	3.5	819
B-4.0	21	67	1.5	4.0	819

Two models of beams with different amount of longitudinal reinforcement in series B are shown in Figs. 5.9 and 5.10.

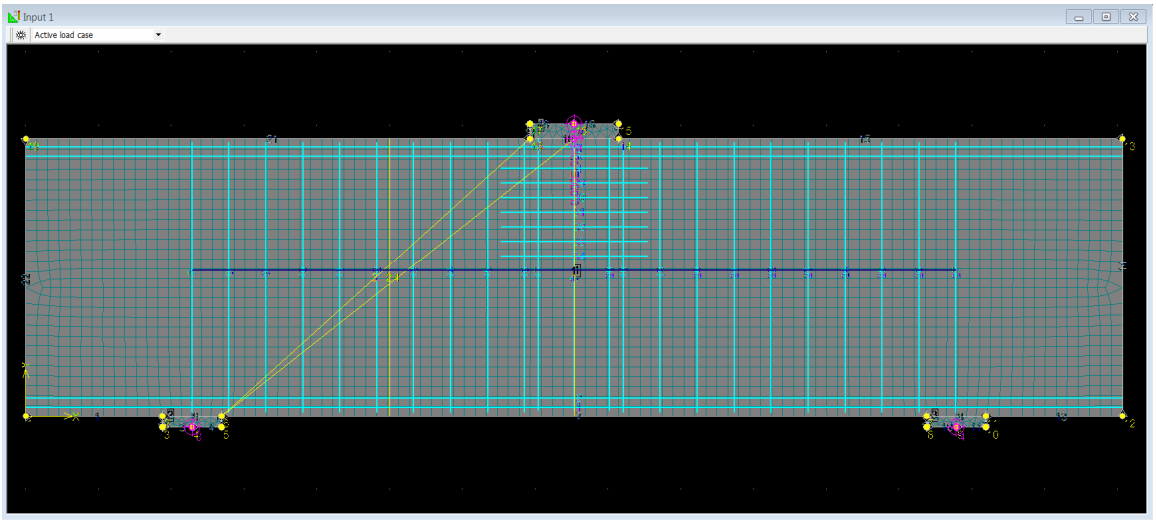

Figure 5.9 A beam of computer model test series B with ρ_s = 1.29% and ρ'_s = 1.29%

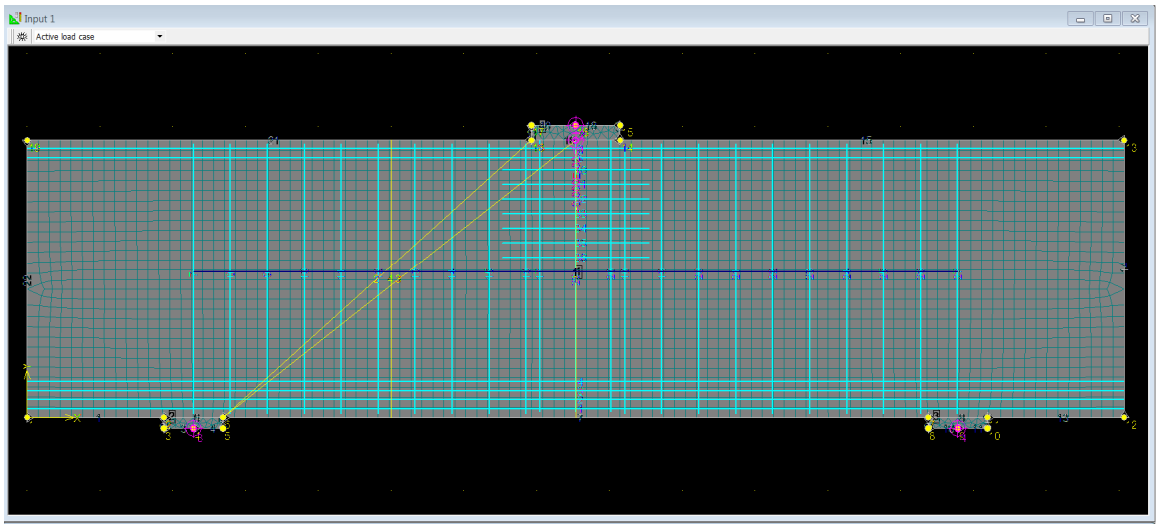

Figure 5.10 A beam of computer model test series B with ρ_s = 4.0% and ρ'_s = 1.29%

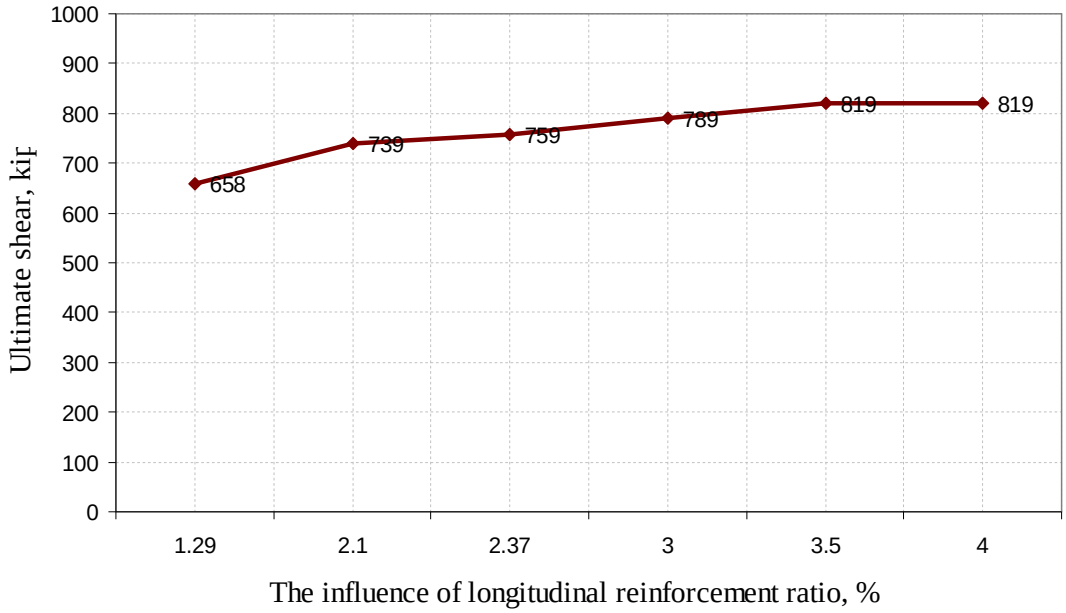

Figure 5.11 The influence of longitudinal reinforcement on shear strength of deep beam

It was observed that the shear capacity of the deep beam increased when the ratio of longitudinal reinforcement increased (Fig. 5.11). The largest increase of capacity occurred between at longitudinal ratios 1.2% and 2.1%. There is not much change of ultimate shear of deep beam for longitudinal reinforcement greater than 2.1%. This is due

to with large longitudinal reinforcement the concrete compression region at outside edge of the loading plate will start to fail before steel reach its yield stress.

5.2.3 The influence of shear span-to-depth ratio

In order to investigate the influence of the shear span-to-depth ratio on the strength of deep beams, series C and D models (twelve models) were developed. The models have values of ratio a/d from 1.0 to 2.5. In series C, there was no web reinforcement and in series D the minimum vertical web reinforcement ratio permitted in ACI 318-11 was used (0.3%). The ratio of longitudinal reinforcement is kept constantly for all models ρ = 2.37%.

A typical beam of series C or D was modeled as follows:

(1) Geometric dimensions:

- Shear span length is the distance from the center of the loading plate to the center of the supporting plate.
- Dimensions of cross section: height of 75 in., and width of 21 in.
- Loading plates: 24x21x4 in.
- Bearing plates: 16x21x4 in.

(2) Constraint conditions:

- One constraint was a perfect pin and the other a perfect roller.

(3) Loading conditions:

- Single load was applied at middle of loading plates. The increment of load was 20 kips.

(4) Materials:

- Concrete model was CCQ10SBeta: f'_c = 5.01 ksi
- Plates were modeled as plane stress elastic isotropic material
- Reinforcement used bilinear material model: f_y = 69 ksi and f_{vy} = 67 ksi.

(5) Finite element analysis:

- Mesh type: rectangular mesh for reinforced concrete beam with mesh size of 3.3 in.

Details of series C and D models are shown in Table 5.5, 5.6 and Figs. 5.12 and 5.13.

Table 5.5 The influence of ratio a/d on the shear strength of deep beams without vertical shear reinforcement (series C)

Computer model I.D.	H, in	b_w, in	d, in	a/d	ρ_v	f'_c, psi	f_y, ksi
C-1.0-00	75	21	68.9	1.0	0.00	5010	69
C-1.2-00	75	21	68.9	1.2	0.00	5010	69
C-1.5-00	75	21	68.9	1.5	0.00	5010	69
C-1.85-00	75	21	68.9	1.85	0.00	5010	69
C-2.0-00	75	21	68.9	2.0	0.00	5010	69
C-2.5-00	75	21	68.9	2.5	0.00	5010	69

Table 5.6 The influence of ratio a/d on the shear strength of deep beams with 0.3% vertical shear reinforcement (series D)

Computer model I.D.	H, in	b_w, in	d, in	a/d	ρ_v	f'_c, psi	f_{vy}, ksi	f_y, ksi
D-1.0-03	75	21	68.9	1.0	0.03	5010	67	69
D-1.2-03	75	21	68.9	1.2	0.03	5010	67	69
D-1.5-03	75	21	68.9	1.5	0.03	5010	67	69
D-1.85-03	75	21	68.9	1.85	0.03	5010	67	69
D-2.0-03	75	21	68.9	2.0	0.03	5010	67	69
D-2.5-03	75	21	68.9	2.5	0.03	5010	67	69

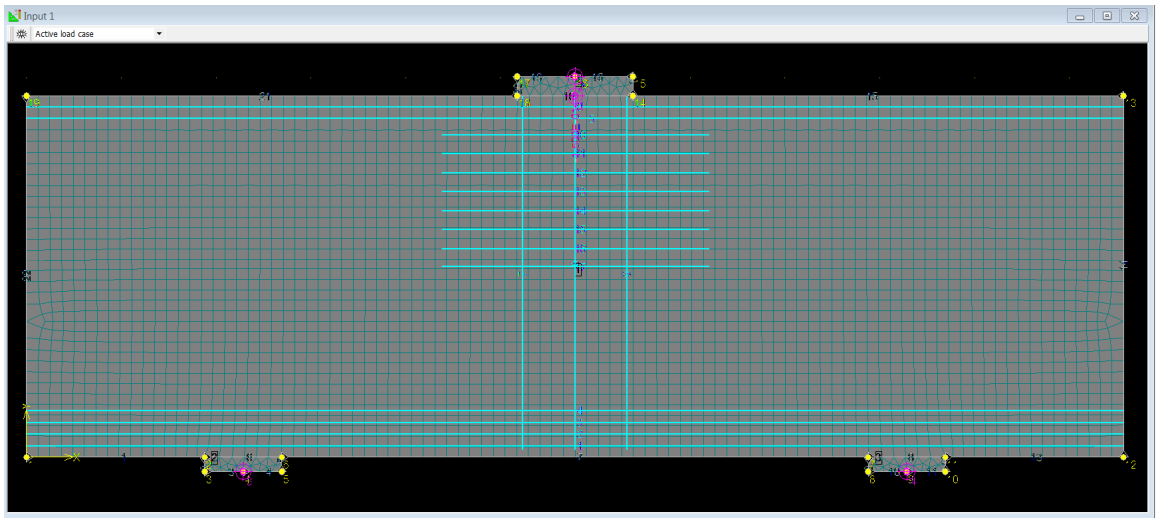

Figure 5.12 A typical beam of computer model series C without web reinforcement

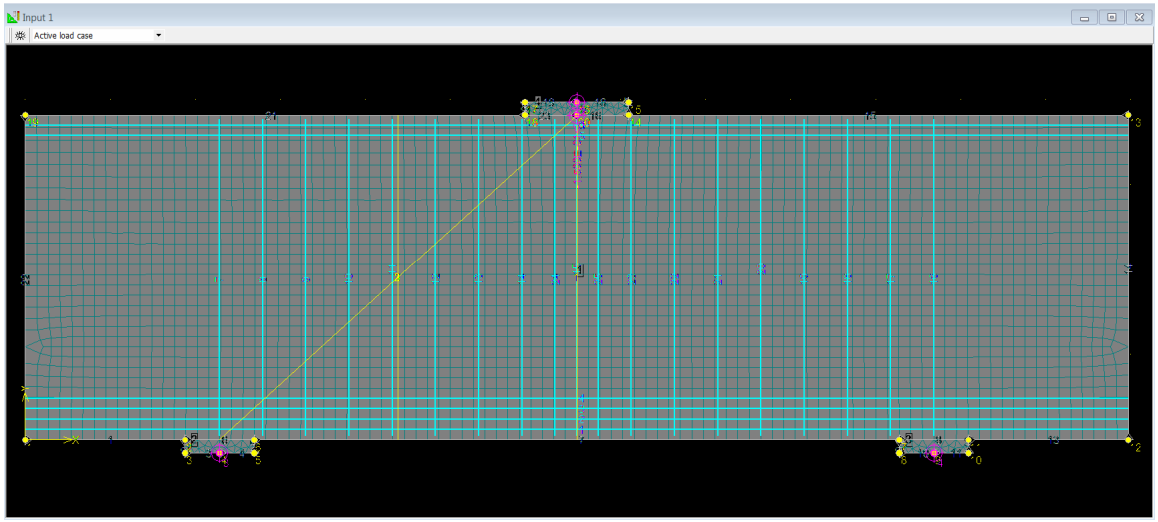

Figure 5.13 A typical beam of computer model series D with 0.3% vertical web reinforcement

The test results of series C and D are shown in Table 5.7.

Table 5.7 Test results of series C and D

a/d	Ultimate shear, kip	
	(without web reinforcement) Series C	(with 0.3% vertical web reinforcement) Series D
1.0	910	991
1.2	718	859
1.5	586	758
1.85	536	708
2.0	515	691
2.5	435	637

A comparison of ultimate shear between deep beams without and with vertical web reinforcement under various shear span-to-depth ratios, a/d, is shown in Fig. 5.15.

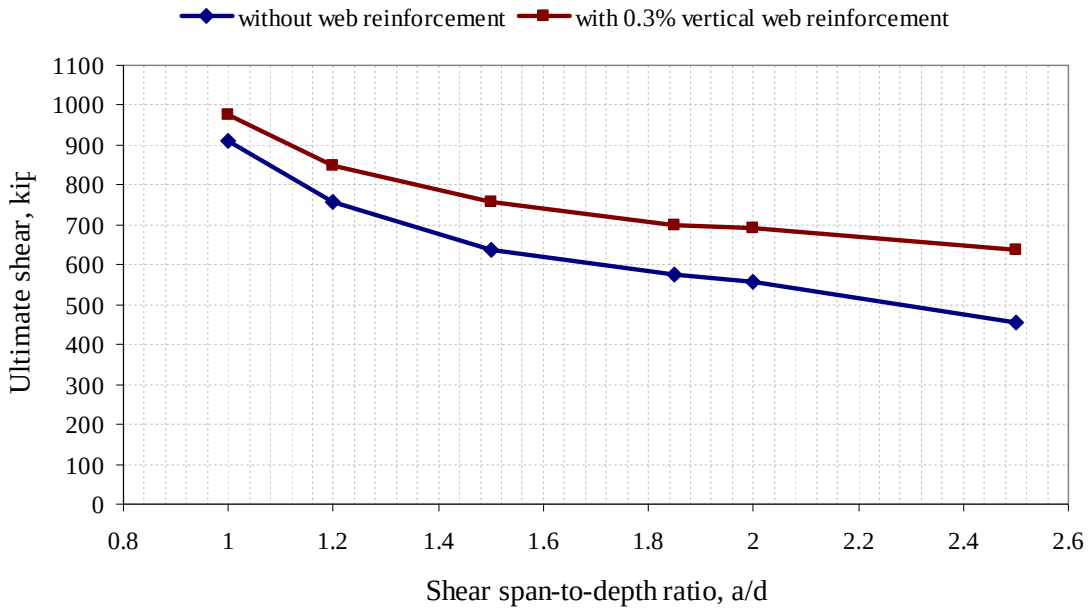

Figure 5.14 The influence of ratio a/d on shear strength of deep beam

From Fig. 5.14 it was observed that shear span-to-depth ratio has considerable influence on the shear strength of deep beam. As the shear span-to-depth ratio, a/d, increases, the

shear capacity is reduced as has been reported in many experimental investigations. The contribution of the web reinforcement to the shear strength of deep beams was proportional to a/d. The larger value of a/d the larger contribution of web reinforcement on the shear strength of deep beam. This has been observed in experimental studies and indicated that with a small a/d ratio the direct compression strut between the load and the reaction contributed most of the shear strength. As the a/d ratio increases, the direct compression strut is less efficient and the vertical web reinforcement is needed to mobilize a more complex truss mechanism. This will become more apparent in the next series of models.

5.2.4 The contribution of web reinforcement (series W)

Series W consisted of models with different details of web reinforcement. As shown in Tables 5.8, 5.9, 5.10, and 5.11. The web reinforcement varied as follows:

Series W I (series D): 0.3% vertical, 0.0% horizontal web reinforcement

Series W II : 0.0% vertical, 0.3% horizontal web reinforcement

Series W III : 0.3% vertical, 0.3% horizontal web reinforcement

Series W IV : 0.0% to 0.6% vertical, 0.0% to 0.6% horizontal web reinforcement

A typical beam of series W was modeled as follows:

(1) Geometric dimensions:

- Shear span length is the distance from the center of the loading plate to the center of the supporting plate.
- Dimensions of cross section: height of 75 in., and width of 21 in.
- Loading plates: 24x21x4 in.
- Bearing plates: 16x21x4 in.

(2) Constraint conditions:

- One constraint was a perfect pin and the other a perfect roller.

(3) Loading conditions:

- Single load was applied at middle of loading plates. The increment of load was 20 kips.

(4) Materials:

- Concrete model was CCQ10SBeta: f'_c = 5.01 ksi
- Plates were modeled as plane stress elastic isotropic material
- Reinforcement used bilinear material model: f_y = 69 ksi and f_{vy} = 67 ksi.

(5) Finite element analysis:

- Mesh type: rectangular mesh for reinforced concrete beam with mesh size of 3.3 in.

Table 5.8 Details of computer model tests of series W I

Computer model I.D.	H, in	b_w, in	d, in	a/d	ρ_v	ρ_h	f'_c, psi	f_y, ksi	f_{vy}, ksi
W I-1.0-03-00	75	21	68.9	1.0	0.03	0.00	5010	69	67
W I-1.2-03-00	75	21	68.9	1.2	0.03	0.00	5010	69	67
W I-1.5-03-00	75	21	68.9	1.5	0.03	0.00	5010	69	67
W I-1.85-03-00	75	21	68.9	1.85	0.03	0.00	5010	69	67
W I-2.0-03-00	75	21	68.9	2.0	0.03	0.00	5010	69	67
W I-2.5-03-00	75	21	68.9	2.5	0.03	0.00	5010	69	67

Table 5.9 Details of computer model tests of series W II

Computer model I.D.	H, in	b_w, in	d, in	a/d	ρ_v	ρ_h	f'_c, psi	f_y, ksi	f_{vy}, ksi
W II-1.0-00-03	75	21	68.9	1.0	0.00	0.03	5010	69	67
W II-1.2-00-03	75	21	68.9	1.2	0.00	0.03	5010	69	67
W II-1.5-00-03	75	21	68.9	1.5	0.00	0.03	5010	69	67
W II-1.85-00-03	75	21	68.9	1.85	0.00	0.03	5010	69	67
W II-2.0-00-03	75	21	68.9	2.0	0.00	0.03	5010	69	67
W II-2.5-00-03	75	21	68.9	2.5	0.00	0.03	5010	69	67

Table 5.10 Details of computer model tests of series W III

Computer model I.D.	H, in	b_w, in	d, in	a/d	ρ_v	ρ_h	f'_c, psi	f_y, ksi	f_{vy}, ksi
W III-1.0-03-03	75	21	68.9	1.0	0.03	0.03	5010	69	67
W III-1.2-03-03	75	21	68.9	1.2	0.03	0.03	5010	69	67
W III-1.5-03-03	75	21	68.9	1.5	0.03	0.03	5010	69	67
W III-1.85-03-03	75	21	68.9	1.85	0.03	0.03	5010	69	67
W III-2.0-03-03	75	21	68.9	2.0	0.03	0.03	5010	69	67
W III-2.5-03-03	75	21	68.9	2.5	0.03	0.03	5010	69	67

Table 5.11 Details of computer model tests of series W IV

Computer model I.D.	H, in	b_w, in	d, in	a/d	ρ_v	ρ_h	f'_c, psi	f_y, ksi	f_{vy}, ksi
W IV-1.0-00-06	75	21	68.9	1.0	0.00	0.06	5010	69	67
W IV-1.2-03-06	75	21	68.9	1.2	0.03	0.06	5010	69	67
W IV-1.5-06-00	75	21	68.9	1.5	0.06	0.00	5010	69	67
W IV-1.5-06-03	75	21	68.9	1.5	0.06	0.03	5010	69	67
W IV-1.5-00-06	75	21	68.9	1.5	0.00	0.06	5010	69	67
W IV-1.85-06-03	75	21	68.9	1.85	0.06	0.03	5010	69	67
W IV-1.85-06-00	75	21	68.9	1.85	0.06	0.00	5010	69	67
W IV-2.0-06-00	75	21	68.9	1.85	0.06	0.00	5010	69	67
W IV-2.0-03-06	75	21	68.9	1.85	0.03	0.06	5010	69	67

Models for selected cases are shown in Figs. 5.15, 5.16, 5.17, 5.18, and 5.19.

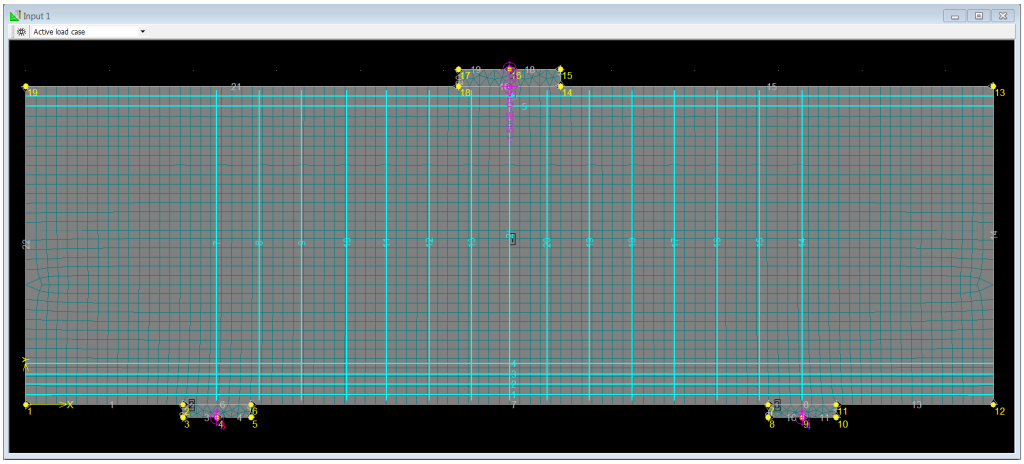

Figure 5.15 Model in series W I with ρ_v = 0.3%

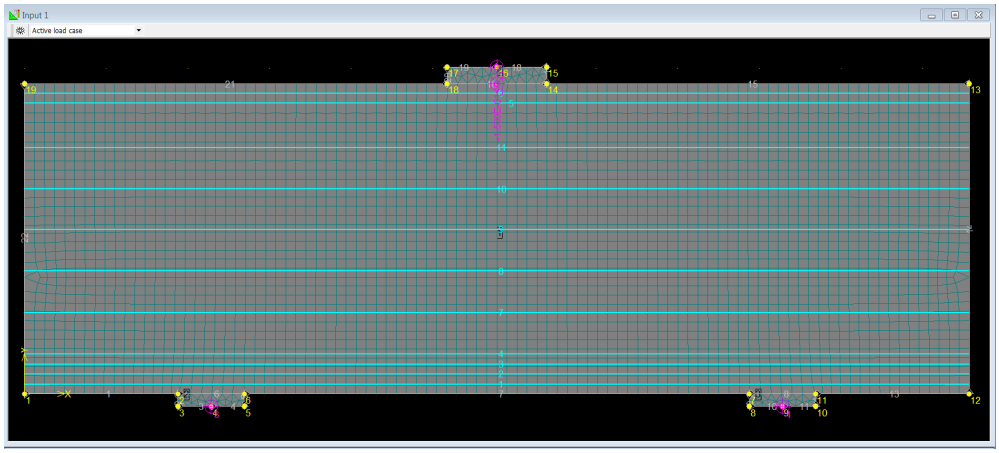

Figure 5.16 A Model in series W II with ρ_h = 0.3%

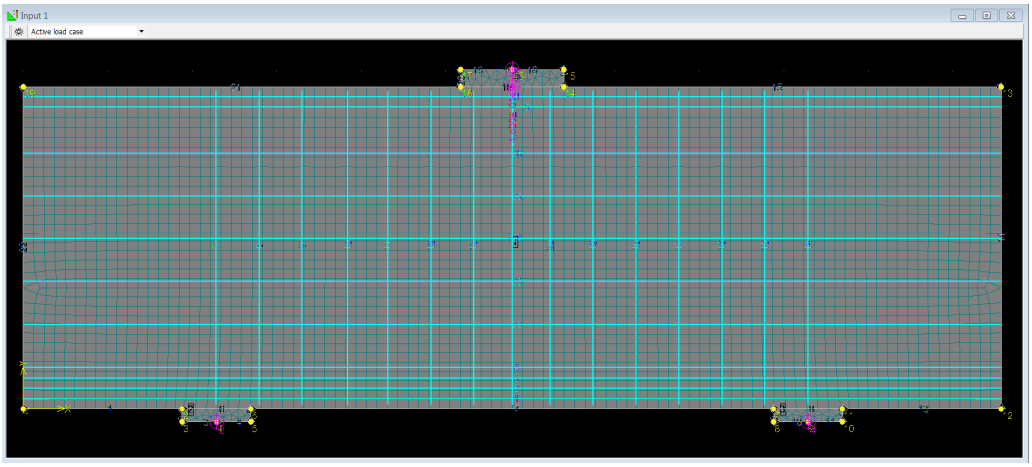

Figure 5.17 Model in series W III with ρ_v = 0.3% and ρ_h = 0.3%

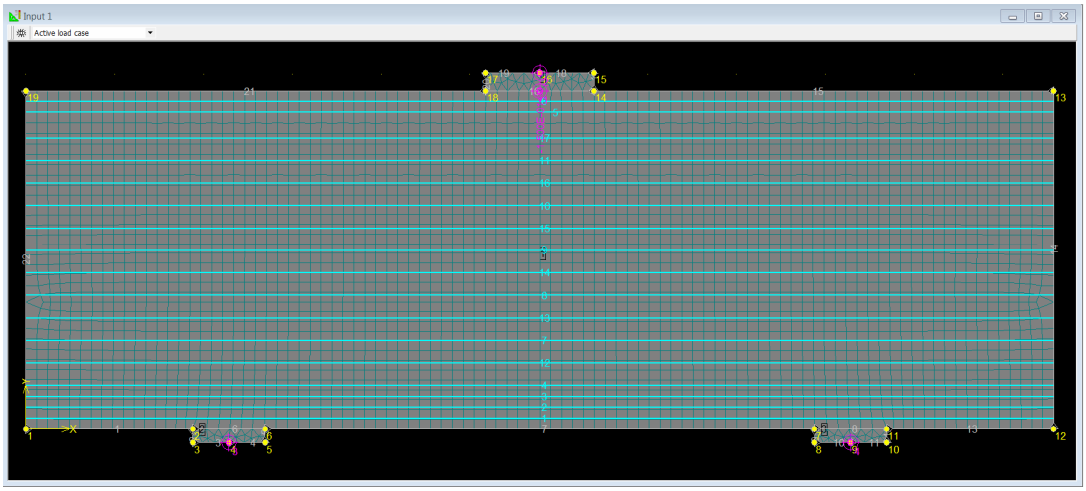

Figure 5.18 Model in series W IV with ρ_v = 0.0% and ρ_h = 0.6%

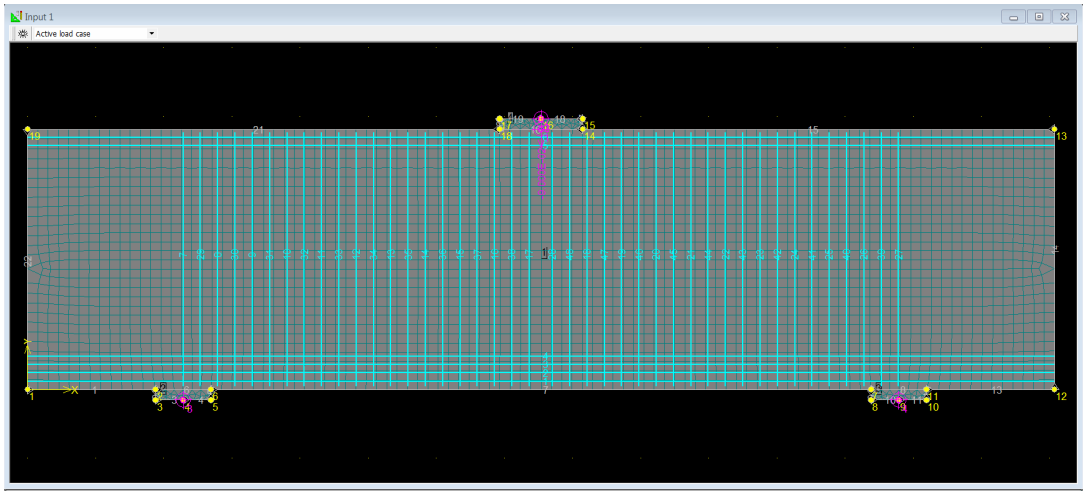

Figure 5.19 Model in series W IV with ρ_v = 0.6% and ρ_h = 0.0%

The shear capacity of models in series W is shown in Table 5.12.

Table 5.12 Contribution of web reinforcement of the shear strength of deep beam

Type of web reinforcement	Ultimate shear, kip					
	a/d = 1.0	a/d = 1.2	a/d = 1.5	a/d = 1.85	a/d = 1.85	a/d = 1.85
None	910	718	587	536	516	435
0.3% horizontal (series W II)	876	725	546	485	-	-
0.3% vertical (series W I)	1052	860	748	698	677	637
0.3% web (series W III)	991	860	738	708	691	637
0.6% horizontal (series W IV)	893	775	586	-	-	-
0.6% vertical (series W IV)	1102	950	849	839	809	718
1.2% vertical	1173	1001	941	920	870	789

A comparison of the web reinforcement contribution to the shear strength of deep beam is shown in Fig. 5.20.

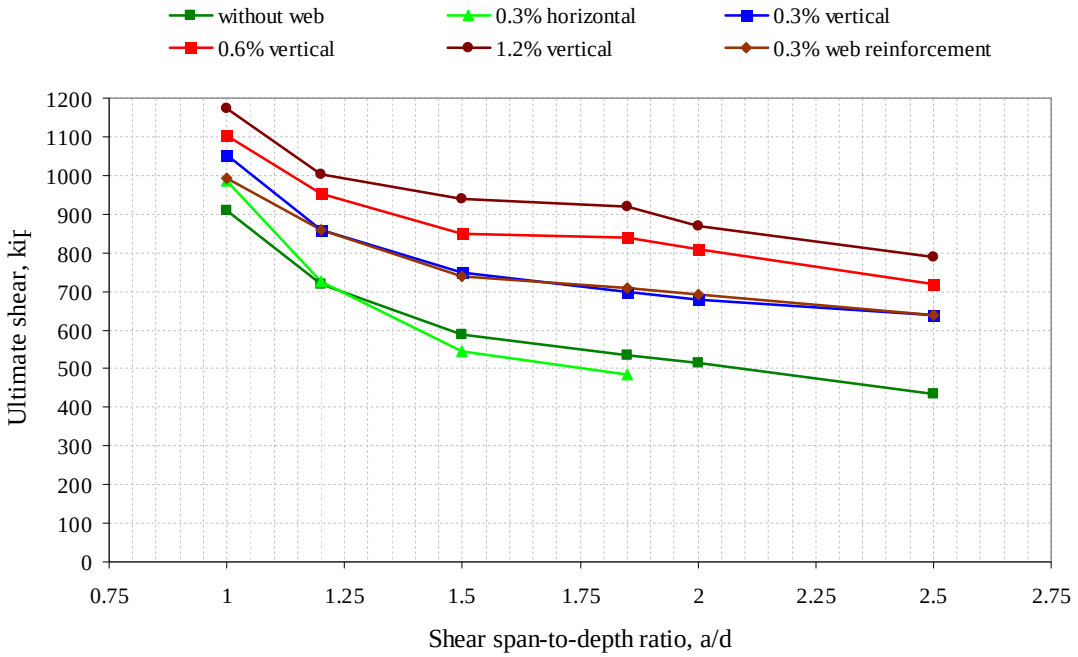

Figure 5.20 Contribution of web reinforcement to the shear strength of deep beam

It was observed that the contribution of horizontal web reinforcement on the shear strength of deep beam was negligible. Beams with a/d = 1.0 to 1.85. The curves for 0.3% vertical and 0.3% vertical and horizontal web reinforcement were identical. Vertical web reinforcement contributed to the shear strength of deep beam, but for low a/d ratios (less than 1.5) the increases were less than for lager a/d ratios (greater than 2.0).

The contributions of vertical web reinforcement to the shear strength of deep beams shown in Table 5.13 and Fig. 5.21 and 5.22 were determined by subtracting the strength of the beam with no web reinforcement from the strength of shear reinforced beam. The percentage increases is the difference divided by the strength of the beam with no web reinforcement.

Maximum strains in vertical reinforcement of deep beams with 0.3% and 0.6% vertical reinforcement are shown in Figs. 5.23 and 5.24.

Table 5.13 Relative contribution of vertical web reinforcement on the shear strength of deep beam

Type of web reinforcement	Ultimate shear, kip/%					
	a/d = 1.0	a/d = 1.2	a/d = 1.5	a/d = 1.85	a/d = 2.0	a/d = 2.5
ΔV_s (0.3% vertical)	141/15	141/19	162/27	161/30	161/31	202/46
%	15	19	27	30	31	46
ΔV_s (0.3% web)	81/9	141/19	151/26	171/32	175/33	202/46
%	9	19	26	32	33	46
ΔV_s (0.6% vertical)	192/21	158/22	263/45	303/56	293/57	283/65
%	21	22	45	56	57	65
ΔV_s (1.2% vertical)	263/28	283/39	354/60	384/71	354/69	354/81
%	28	39	60	71	69	81

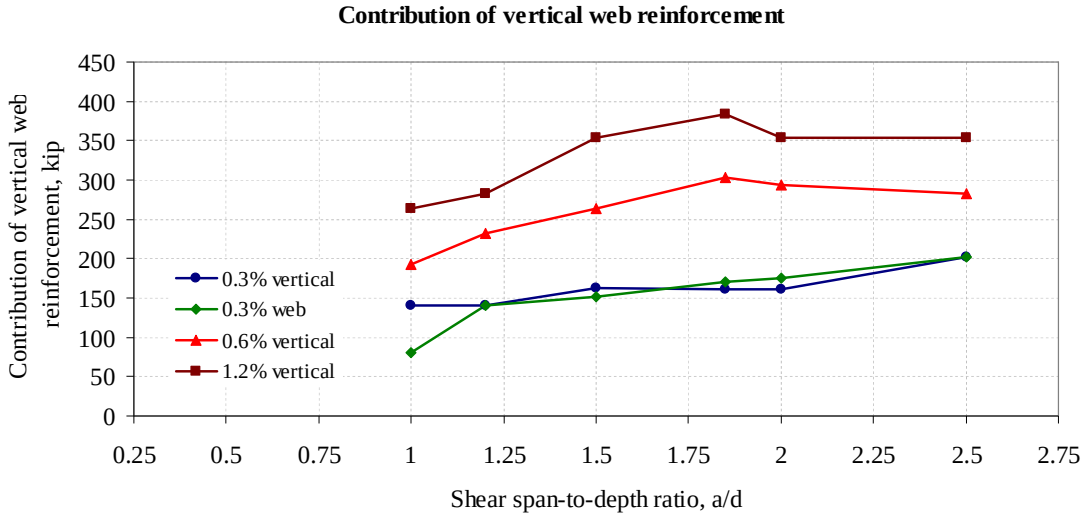

Figure 5.21 Contribution of vertical web reinforcement

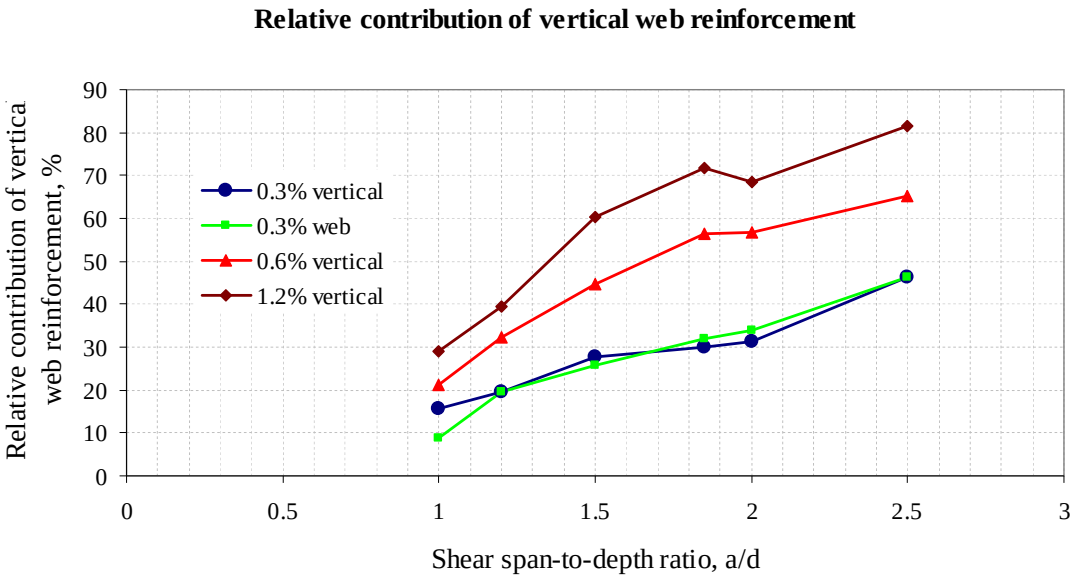

Figure 5.22 Relative contribution of vertical web reinforcement on the shear strength of deep beam

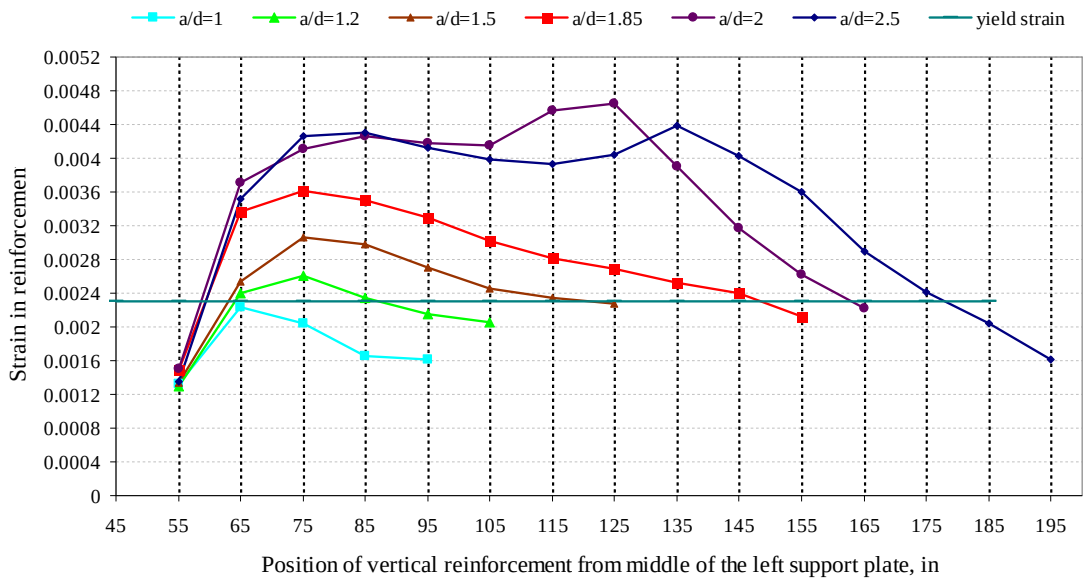

Figure 5.23 Strains in vertical reinforcement of deep beam with 0.3% vertical web reinforcement

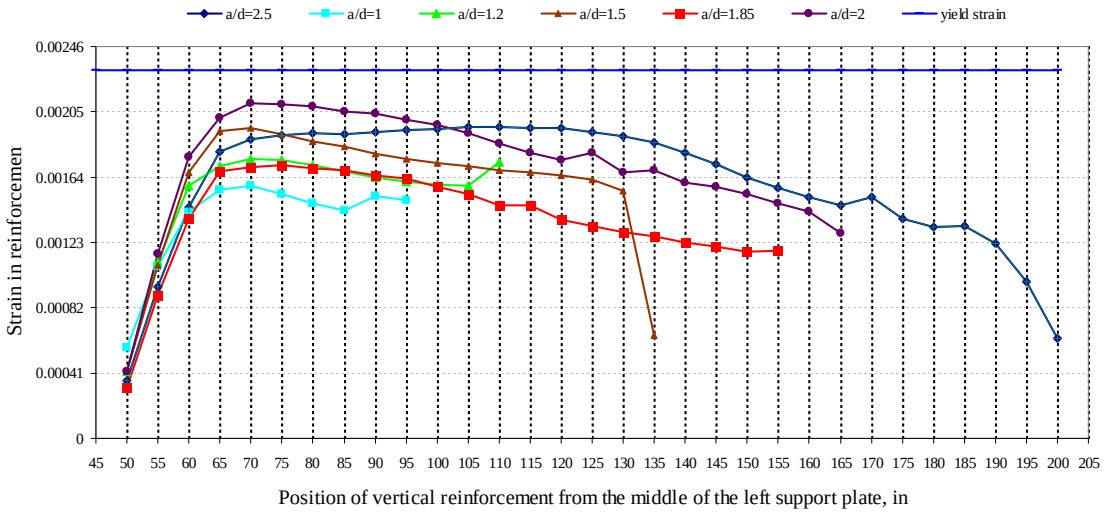

Figure 5.24 Strains in vertical reinforcement of deep beams with 0.6% vertical reinforcement

5.2.5 The influence of loading conditions

Series L consists of simply supported deep beams with different loading conditions. Loading conditions considered were single symmetric loading, single unsymmetric loading, two symmetric loadings, uniform distributed loading, and single loading through monolithic columns. For deep beams under single unsymmetric loading, in order to measure the shear capacity of short span the long span will be clamped with external cable.

A typical beam of series Ls was modeled as follows:

(1) Geometric dimensions:

- Shear span length is the distance from the center of the loading plate to the center of the supporting plate.
- Dimensions of cross section: height of 75 in., and width of 21 in.
- Loading plates:

For deep beams under single concentrated loading: 24x21x4 in.

- For deep beams under two symmetric loading: 16x21x4 in.
- For deep beam loading through column: 24x21x1 in.

- Bearing plates: 16x21x4 in.

(2) Constraint conditions:

- One constraint was a perfect pin and the other a perfect roller.

(3) Loading conditions:

- Single load was applied at middle of loading plates. The increment of load was 20 kips.

(4) Materials:

- Concrete model was CCQ10SBeta: f'_c = 5.01 ksi
- Plates were modeled as plane stress elastic isotropic material
- Reinforcement used bilinear material model: f_y = 69 ksi and f_{vy} = 67 ksi.

(5) Finite element analysis:

- Mesh type: rectangular mesh for reinforced concrete beam with mesh size of 3.3 in.

Details of the beams in L are as follows:

- L I single symmetric load, Fig. 5.25 and Table 5.16.
- L II single unsymmetric load, Fig. 5. 26 and Table 5.17.
- L III two symmetric loads, Fig. 5.27 and Table 5.18.
- L IV loading through column, Fig. 5.28 and Table 5.19.
- L V loading through column, Fig. 5.29 and Table 5.20.

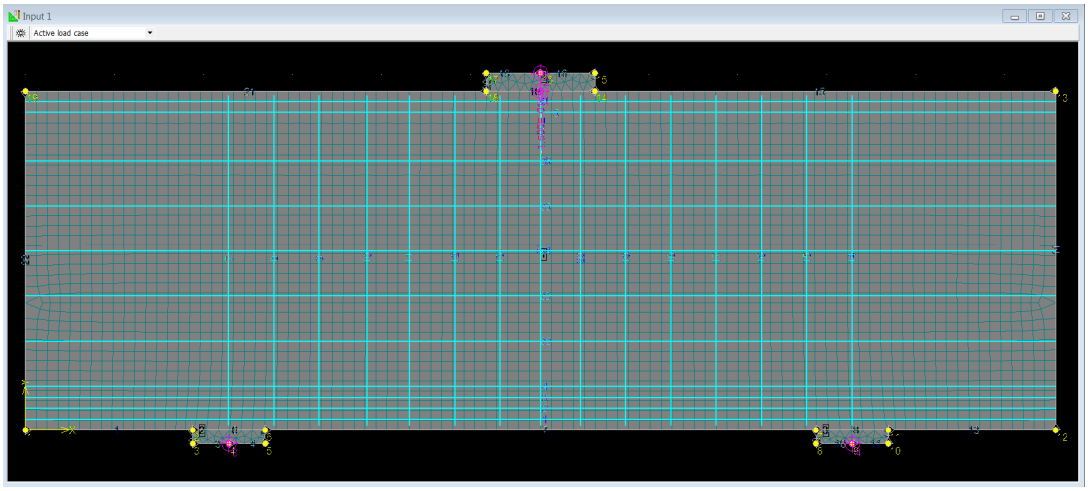

Figure 5.25 Model with single symmetric loading (series L I)

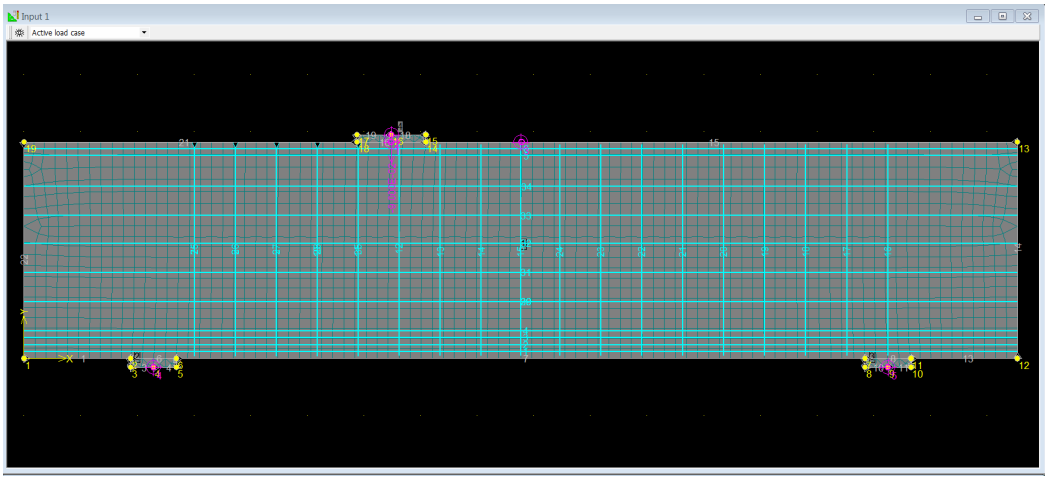

Figure 5.26 Model with unsymmetric loading (series L II)

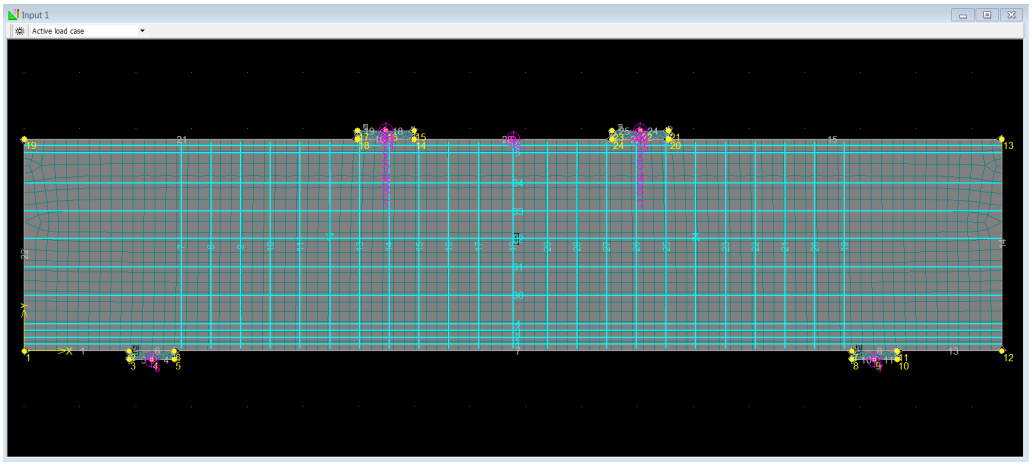

Figure 5.27 Model with two symmetric loadings (series L III)

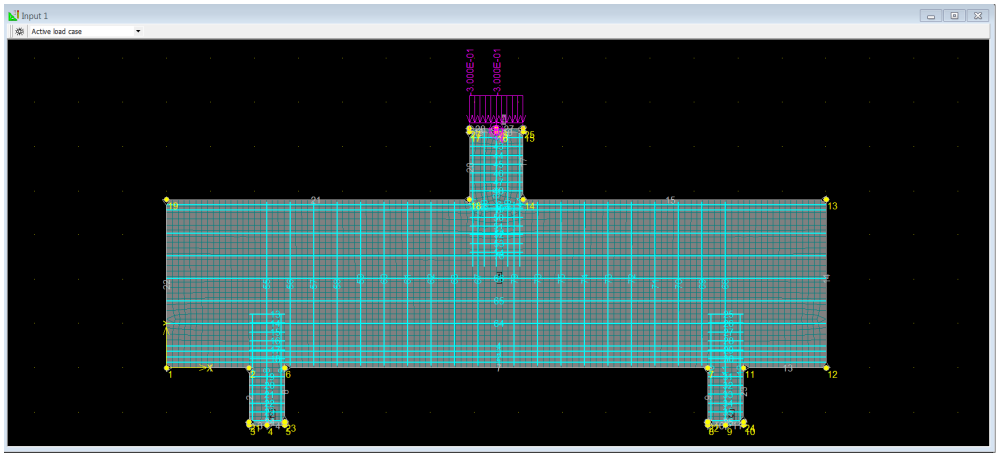

Figure 5.28 Model with loading through monolithic column (series L IV)

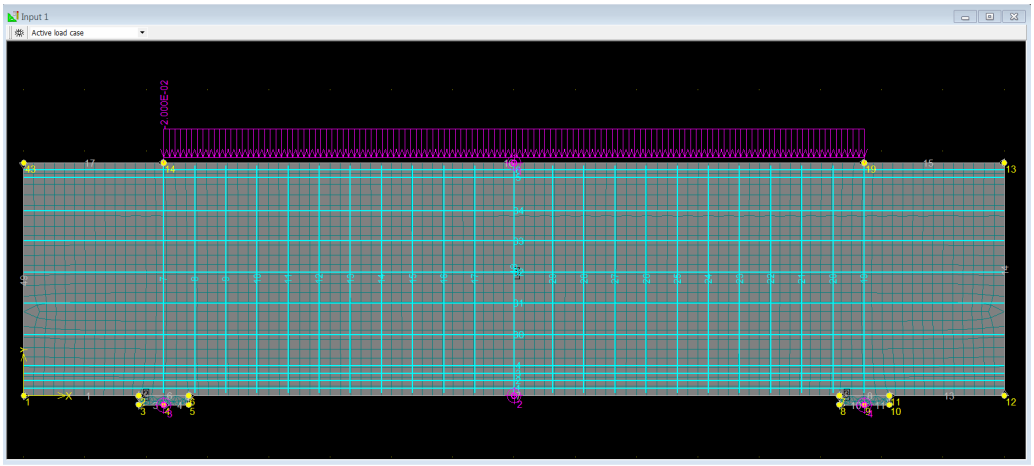

Figure 5.29 Model under uniform distributed loading (series L V)

Table 5.14 Test results of computer model test under uniform distributed loading

L/H	1.0	1.5	2.0	2.5	3.0	3.4
Equivalent a/d*	0.27	0.4	0.54	0.68	0.82	0.93
Ultimate shear, kip	2547	2569	2484	2248	2055	1937

(*): Equivalent shear span, a, for deep beam under uniform distributed loading is calculated equal to L/4.

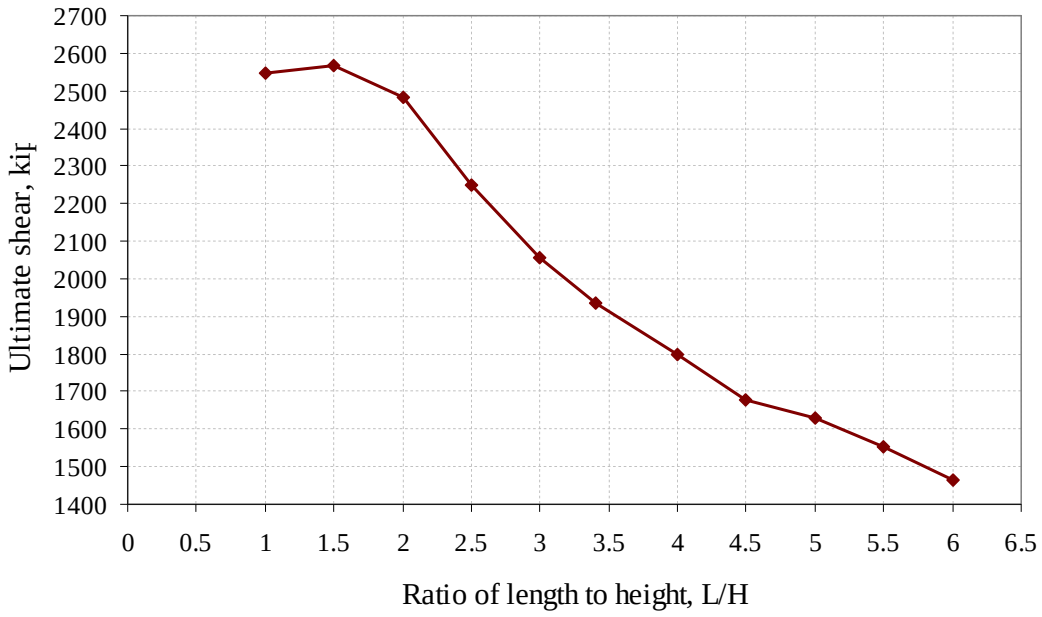

Figure 5.30 Ultimate shear of deep beam under uniform distributed loading

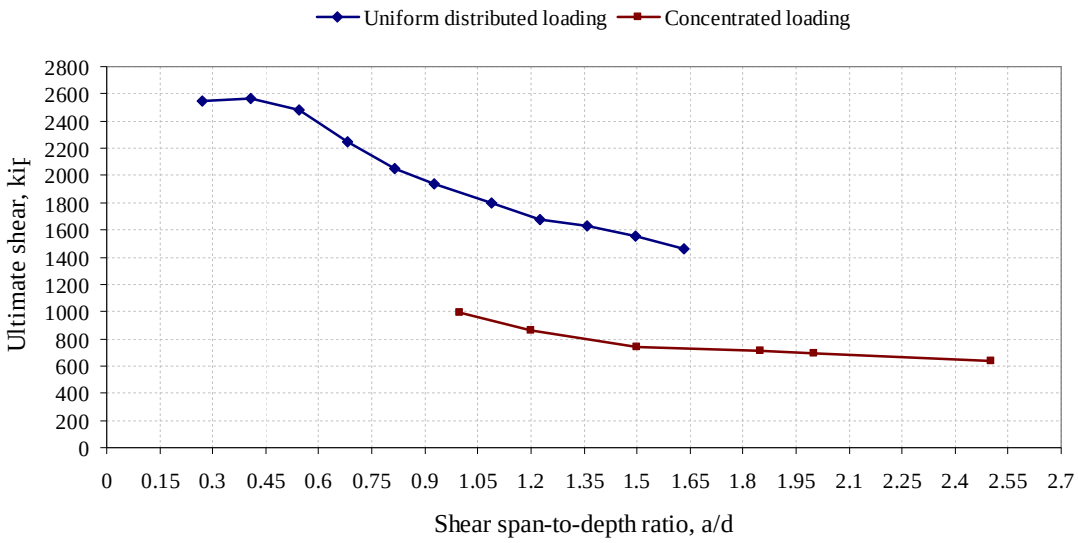

Figure 5.31 The influence of shear span-to-depth ratio on the shear strength of deep beam

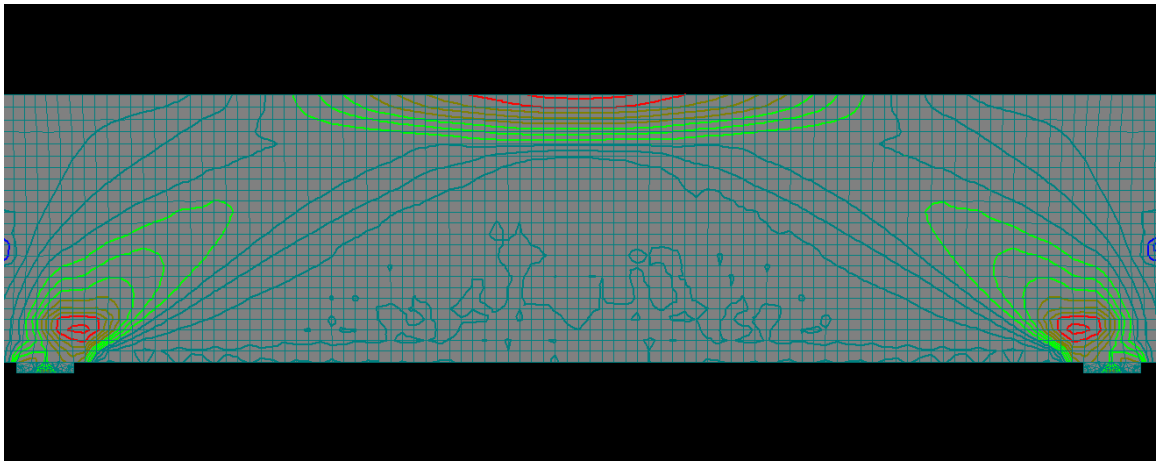

Figure 5.32 The compression arch in simply supported deep beam with L/H=4.0 under uniform distributed loading

Figure 5.30 shows the influence of L/H (a/d) ratio on the shear strength of deep beams under uniform distributed loading. It was observed that the shear strength of deep beam is almost linearly proportional to L/H ratio ranging from 2 to 6. However, for deep beams with L/H less than 2 it seems that L/H has no effect on the shear strength. This behavior may come from different mode of failure for small values of L/H. For L/H is less than 2.0 deep beam fails in manner of shear friction failure (Fig.5.33). While for

deep beam with L/H greater than 2.0 failure mode is splitting shear at outside edge of support plates (Fig.5.34).

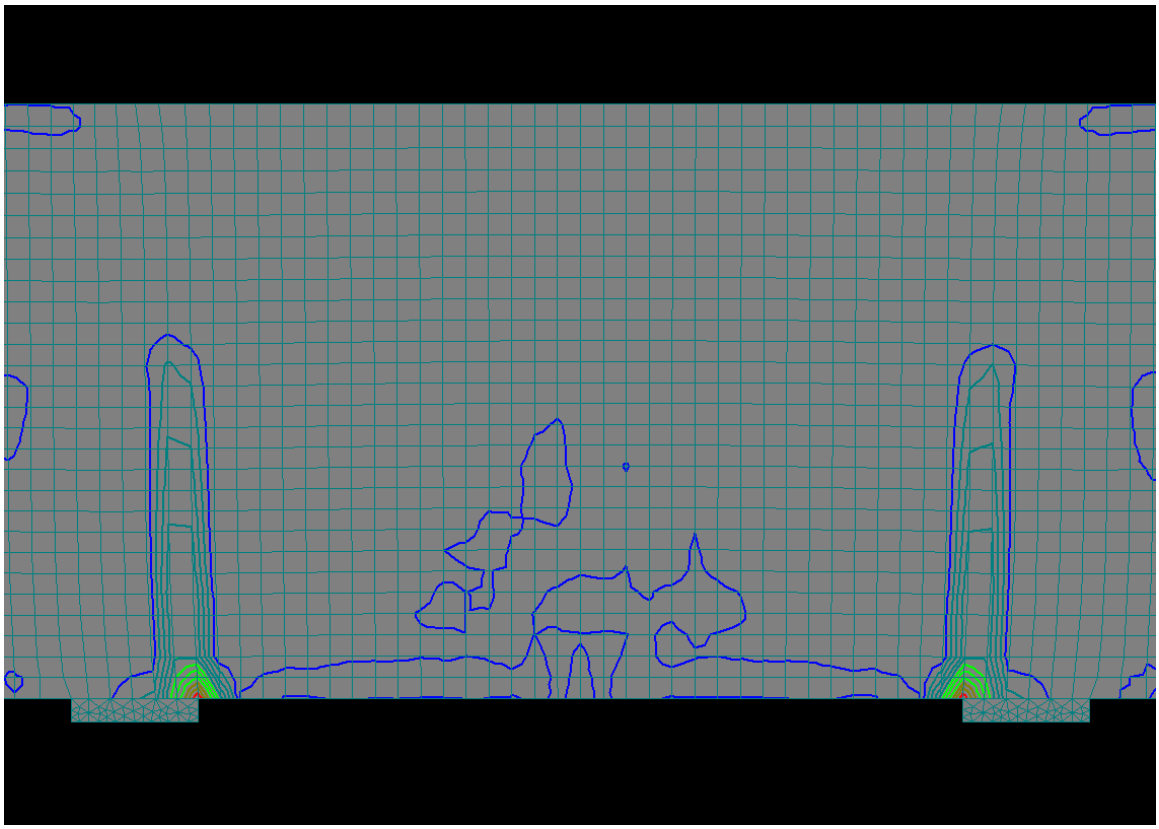

Figure 5.33 Shear friction failure of deep beam L/H = 1.5 under uniform distributed loading

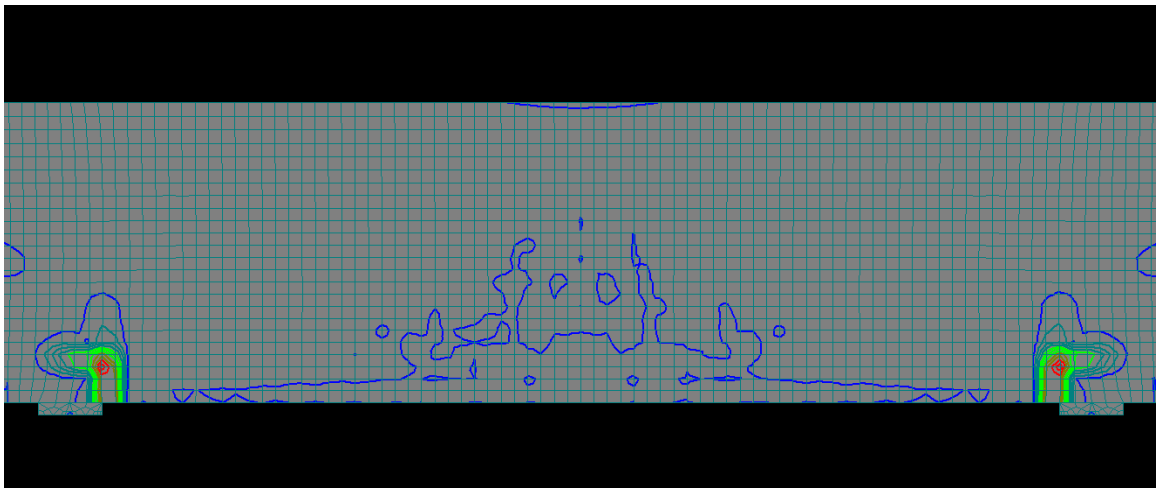

Figure 5.34 Failure of deep beam L/H = 3.4 under uniform distributed loading

Results of computer models in series L V are shown in Table 5.15.

Table 5.15 Test results of computer model test series L V

a/d	Ultimate shear, kip			
	Symmetric loading	Unsymmetric loading	Two loading points	through column
1.0	991	1181	1214	842
1.2	860	889	1133	781
1.5	748	722	870	716
1.85	708	-	809	-

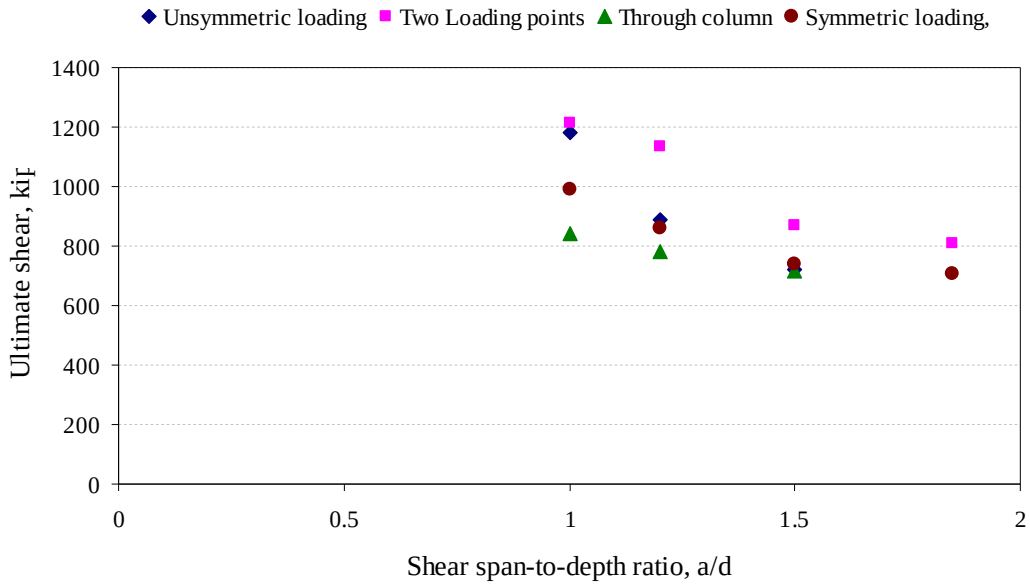

Figure 5.35 Comparison of ultimate shear under different loading conditions

It was observed that the shear strength for loading through a column gave lower results than loading through a bearing plate (Fig. 5.35 and Table 5.14). It seems that a concentration of strain at outside face of loading column is higher than that of loading through a steel plate. It was also observed that a deep beam under uniform distributed loading obtained the highest shear strength for the same geometry. It showed that a deep beam subjected under two symmetric loadings is higher than a deep beam under single loading.

Table 5.16 Details of series L-I (single symmetric loading)

Computer model I.D.	L/H	H, in	b_w, in	d, in	a/d	ρ_v	ρ_h	f'_c, psi	f_y, ksi
L-I-1.0-03-03	1.8	75	21	68.9	1.0	0.03	0.03	5010	69
L-I-1.2-03-03	2.2	75	21	68.9	1.2	0.03	0.03	5010	69
L-I-1.5-03-03	2.8	75	21	68.9	1.5	0.03	0.03	5010	69
L-I-1.85-03-03	3.0	75	21	68.9	1.85	0.03	0.03	5010	69
L-I-2.0-03-03	3.7	75	21	68.9	2.0	0.03	0.03	5010	69
L-I -2.5-03-03	4.6	75	21	68.9	2.5	0.03	0.03	5010	69

Table 5.17 Details of series L-II (single unsymmetric loading)

Computer model I.D.	L/H	H, in	b_w, in	d, in	a/d	ρ_v	ρ_h	f'_c, psi	f_y, ksi
L-II-1.0-03-03	3	75	21	68.9	1.0	0.03	0.03	5010	69
L-II-1.2-03-03	3	75	21	68.9	1.2	0.03	0.03	5010	69
L-II-1.5-03-03	3	75	21	68.9	1.5	0.03	0.03	5010	69
L-II-1.85-03-03	3	75	21	68.9	1.85	0.03	0.03	5010	69
L-II-2.0-03-03	3	75	21	68.9	2.0	0.03	0.03	5010	69
L-II-2.5-03-03	3	75	21	68.9	2.5	0.03	0.03	5010	69

Table 5.18 Details of series L-III (two symmetric loadings)

Computer model I.D.	L/H	H, in	b_w, in	d, in	a/d	ρ_v	ρ_h	f'_c, psi	f_y, ksi
L-III 1.0-03-03	3	75	21	68.9	1.0	0.03	0.03	5010	69
L-III 1.2-03-03	3	75	21	68.9	1.2	0.03	0.03	5010	69
L-III-1.5-03-03	3	75	21	68.9	1.5	0.03	0.03	5010	69
L-III-1.85-03-03	3	75	21	68.9	1.85	0.03	0.03	5010	69

Table 5.19 Details of series L-IV (loading through monolithic column)

Computer model I.D.	L/H	H, in	b_w, in	d, in	a/d	ρ_v	ρ_h	f'_c, psi	f_y, ksi
L-IV-1.0-03-03	1.8	75	21	68.9	1.0	0.03	0.03	5010	69
L-IV-1.2-03-03	2.2	75	21	68.9	1.2	0.03	0.03	5010	69
L-IV-1.5-03-03	2.8	75	21	68.9	1.5	0.03	0.03	5010	69
L-IV-1.85-03-03	3.0	75	21	68.9	1.85	0.03	0.03	5010	69
L-IV-2.0-03-03	3.7	75	21	68.9	2.0	0.03	0.03	5010	69
L-IV-2.5-03-03	4.6	75	21	68.9	2.5	0.03	0.03	5010	69

Table 5.20 Details of series L-V (uniform distributed loading)

Computer model I.D.	L/H	H, in	b_w, in	d, in	a/d	ρ_v	ρ_h	f'_c, psi	f_y, ksi
L-V-1.0-03-03	1.0	75	21	68.9	N/A	0.03	0.03	5010	69
L-V-1.2-03-03	1.5	75	21	68.9	N/A	0.03	0.03	5010	69
L-V-1.5-03-03	2.0	75	21	68.9	N/A	0.03	0.03	5010	69
L-V-1.85-03-03	2.5	75	21	68.9	N/A	0.03	0.03	5010	69
L-V-2.0-03-03	3.0	75	21	68.9	N/A	0.03	0.03	5010	69

5.2.6 The influence of the depth of beam

In series H, models with different heights were studied. The height ranged from 23 in to 75 in.

A typical beam of series H was modeled as follows:

(1) Geometric dimensions:

- Shear span length is the distance from the center of the loading plate to the center of the supporting plate.
- Dimensions of cross sections: 23x21; 33x21; 42x21; 60x21; and 75x21 in.
- Loading plates: 16x21x3 in. for series of 23x21 and 33x21, 24x21x4 in. for series of 42x21, 60x21, and 75x21 in.
- Bearing plates: 16x21x4 in.

(2) Constraint conditions:

- One constraint was a perfect pin and the other a perfect roller.

(3) Loading conditions:

- Single load was applied at middle of loading plates. The increment of load was 20 kips.

(4) Materials:

- Concrete model was CCQ10SBeta: f'_c = 5.01 ksi
- Plates were modeled as plane stress elastic isotropic material
- Reinforcement used an elastic-perfectly plastic material model: f_y = 69 ksi and f_{vy} = 67 ksi.

(5) Finite element analysis:

- Mesh type: rectangular mesh for reinforced concrete beam with mesh size of 3.3 in.

Details of the series H computer model are shown in Tables 5.21 and 5.22.

A typical computer model of series Hs are shown in Figs. 5.36, 5.37, 5.38, 5.39, and 5.40.

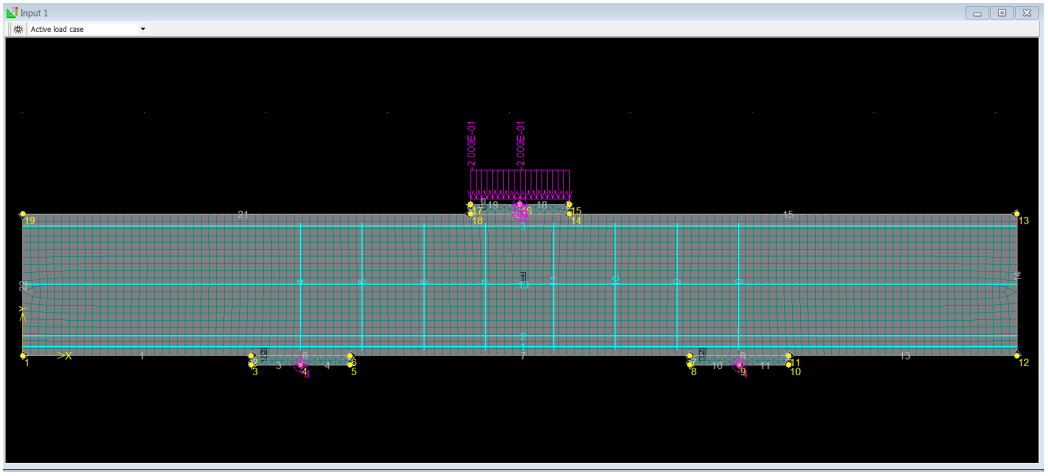

Figure 5.36 Model with H = 23 in. and a/d = 1.2

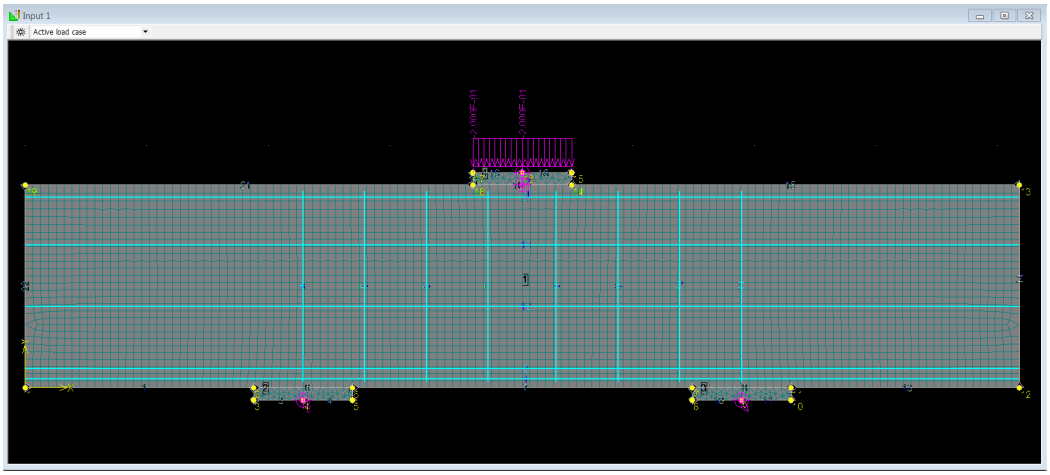

Figure 5.37 Model with H = 33 in. and a/d = 1.2

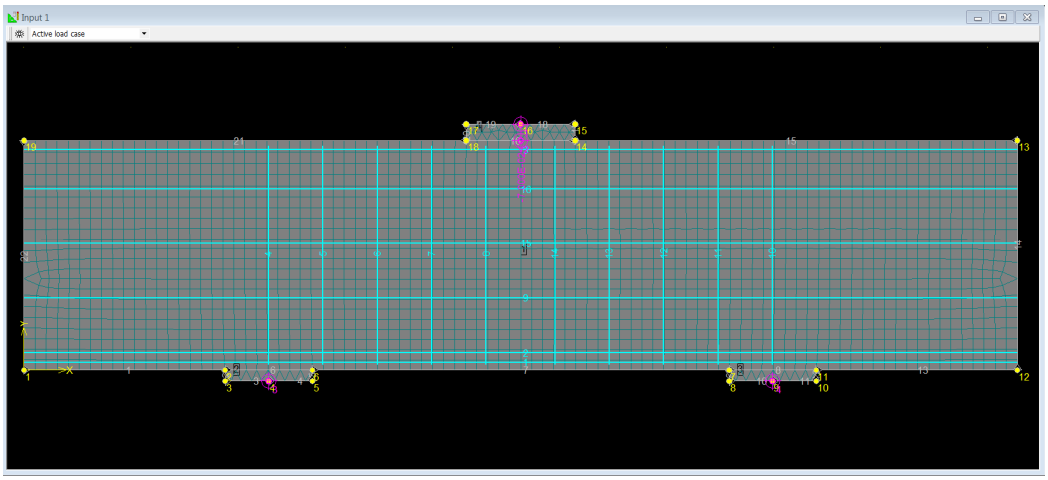

Figure 5.38 Model with H = 42 in. and a/d = 1.2

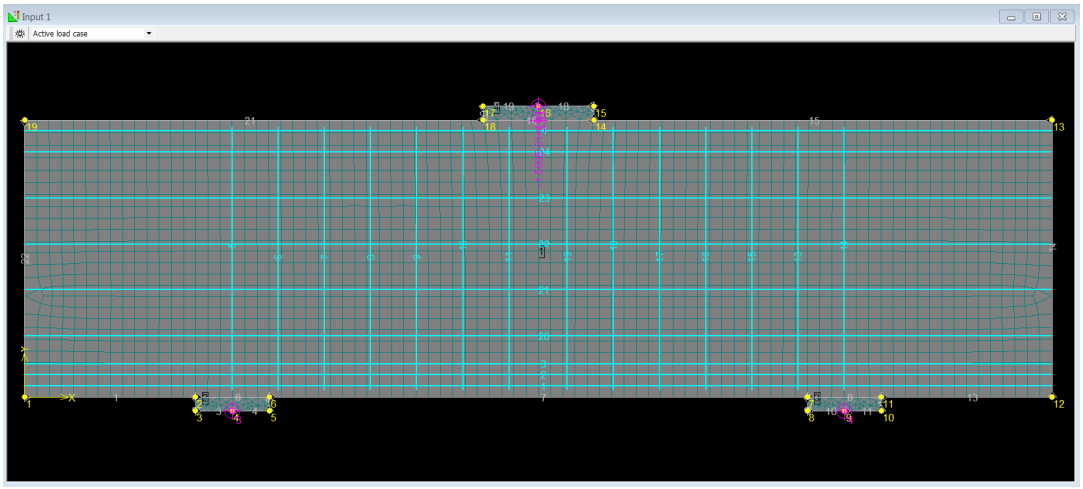

Figure 5.39 Model with H = 60 in. and a/d 1.2

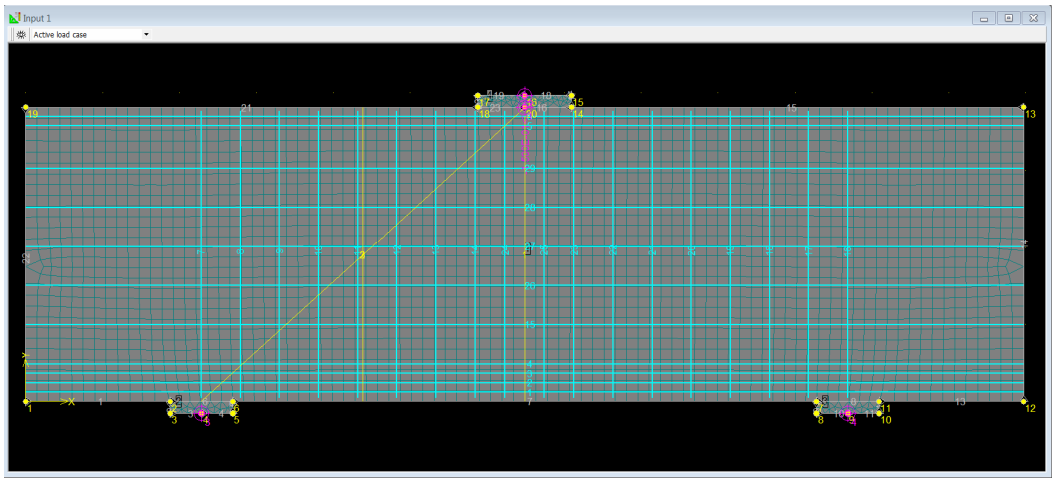

Figure 5.40 Model with H = 75 in. and a/d 1.2

Table 5.21 Details of series H-I with a/d = 1.2

Computer model I.D.	H, in	b_w, in	d, in	a/d	ρ_v	ρ_h	f'_c, psi	f_y, ksi
H-I -2123-1.2-03-03	23	21	19.5	1.2	0.03	0.03	5010	69
H-I -2133-1.2-03-03	33	21	29.6	1.2	0.03	0.03	5010	69
H-I -2142-1.2-03-03	42	21	38.6	1.2	0.03	0.03	5010	69
H-I -2160-1.2-03-03	60	21	55.26	1.2	0.03	0.03	5010	69
H-I -2175-1.2-03-03	75	21	68.9	1.2	0.03	0.03	5010	69

Table 5.22 Details of series H-II with a/d = 1.5

Computer model I.D.	H, in	b_w, in	d, in	a/d	ρ_v	ρ_h	f'_c, psi	f_y, ksi
H-II -2123-1.5-03-03	23	21	19.5	1.5	0.03	0.03	5010	69
H-II -2133-1.5-03-03	33	21	29.6	1.5	0.03	0.03	5010	69
H-II -2142-1.5-03-03	42	21	38.6	1.5	0.03	0.03	5010	69
H-II -2160-1.5-03-03	60	21	55.26	1.5	0.03	0.03	5010	69
H-II -2175-1.5-03-03	75	21	68.9	1.5	0.03	0.03	5010	69

Results of models of series H are shown in Tables 5.23 and 5.24.

Table 5.23 Shear capacity (series H)

a/d	Ultimate shear, kip				
	H = 23 in	H = 33 in	H = 42 in	H = 60 in	H = 75 in
a/d = 1.2	237	429	594	792	826
a/d = 1.5	219	377	487	617	748

Table 5.24 Average shear stress of series H

a/d	V/b_wd, ksi				
	H = 23 in	H = 33 in	H = 42 in	H = 60 in	H = 75 in
a/d = 1.2	0.58	0.69	0.73	0.68	0.57
a/d = 1.5	0.53	0.60	0.60	0.53	0.52

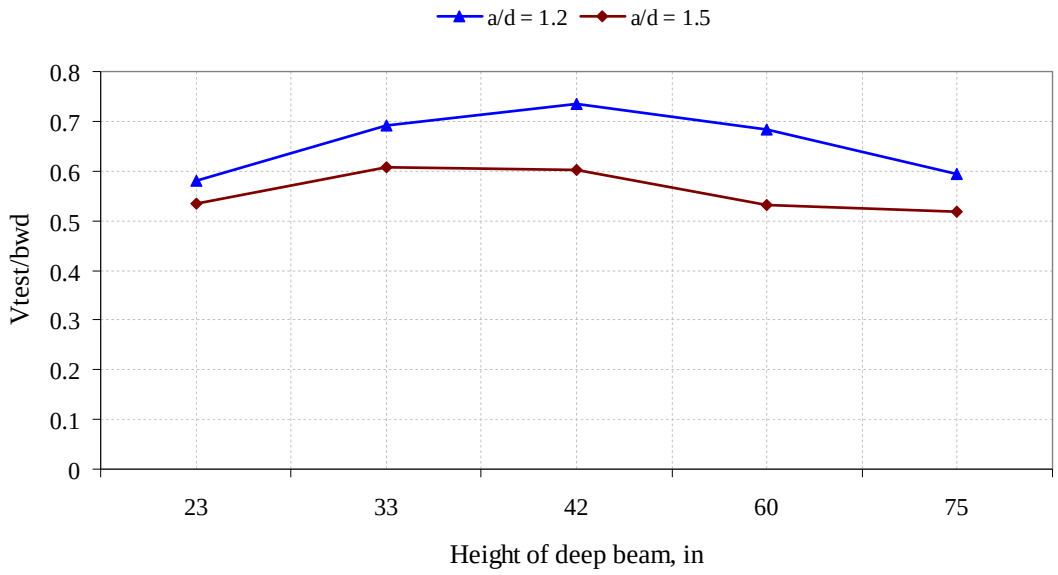

Figure 5.41 Average shear stress of series H computer model test

From Table 5.24 and Fig. 5.41 the effect of size depended on the depth of beam. However, if series of computer model tests are separated into two subsets: one from H = 23 in. to H = 42 in and the other from H = 42 in to H = 75 in. In the second one, it was observed the size effect. The average shear stress decreases when the height of deep beam increases. But for the first one, it seems that average shear stress is proportional to height of deep beam. The reason for this controversy is that ratio of height to width of

deep beam. For the second series, ratios of H/B range from 2 to 3.6 it is a conventional ratio of a beam. While the first has H/B from 1.1 to 1.6 these ratios are typical wide beam.

5.3 Models of two span continuous deep beams

5.3.1 The influence of concrete strength on the shear strength of continuous two span deep beams

Series CB-I models of continuous two span deep beam consists two subsets: with a/d ratios of 1.2 and 1.5. Values of concrete strength used in this series ranged from 3000 psi to 7000 psi.

A typical beam of series CB I was modeled as follows:

(1) Geometric dimensions:

- Shear span length is the distance from the edge of the loading plate to the closest edge of the supporting plate.
- Dimensions of cross section: height of 75 in., and width of 21 in.
- Loading plates: 16x21x4 in.
- Supporting plates: 16x21x3 in.

(2) Constraint conditions:

- One constraint was one perfect pin and two perfect rollers.

(3) Loading conditions:

- Single load was applied at middle of two loading plates. The increment of load was 20 kips.

(4) Materials:

- Concrete model was CCQ10SBeta: f'_c = 3 ksi to 6 ksi
- Plates were modeled as plane stress elastic isotropic material
- Reinforcement used as an elastic-perfectly plastic material model: f_y = 69 ksi and f_{vy} = 67 ksi.

(5) Finite element analysis:

- Mesh type: rectangular mesh for reinforced concrete beam with mesh size of 3.8 in.

Details of series CB-I computer model are shown in Tables 5.25, 5.26 and typical computer models of series CB-I are shown in Figs. 5.42 and 5.43.

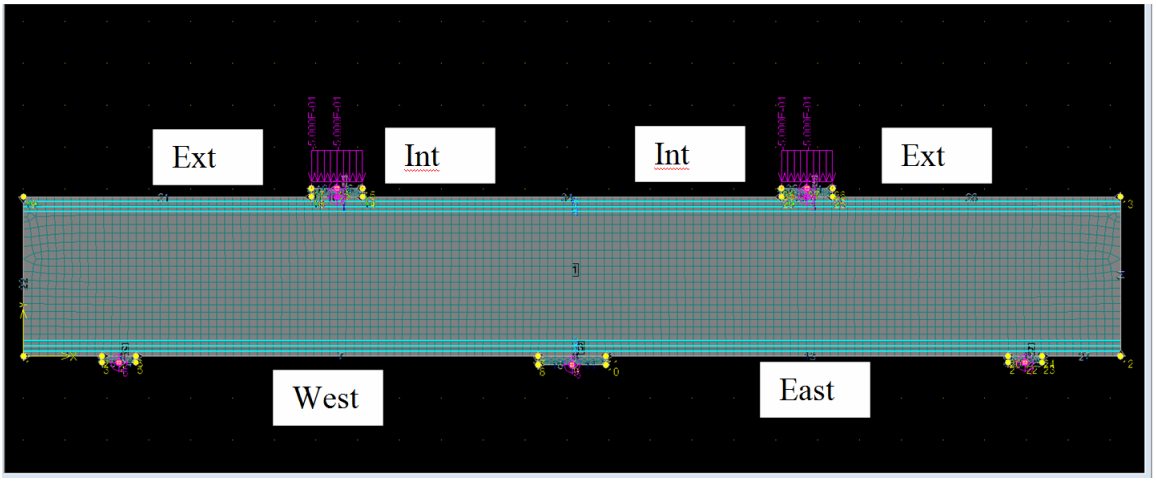

Figure 5.42 Model a/d=1.2, f'c =6000 psi

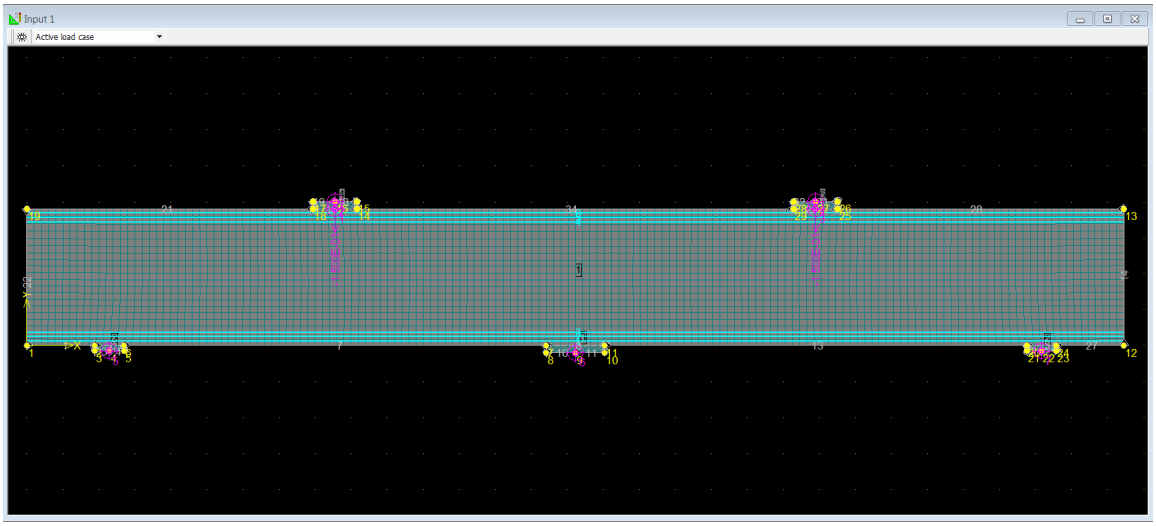

Figure 5.43 Model a/d =1.5, f'c =6000 psi

Results of models series CB-I are shown in Tables 5.25 and Fig. 5.44.

Table 5.25 The influence strength of two span deep beams with a/d = 1.2 and a/d = 1.5

f'c, psi	a/d	West exterior shear, kip	West interior shear, kip	East interior shear, kip	East exterior shear, kip
3000	1.2	313	440	440	313
4000	1.2	458	569	569	458
5000	1.2	469	695	695	469
6000	1.2	549	821	821	549
7000	1.2	592	915	915	592
3000	1.5	294	414	414	294
4000	1.5	352	513	513	352
5000	1.5	424	595	595	424
6000	1.5	442	704	704	442
7000	1.5	492	789	789	492

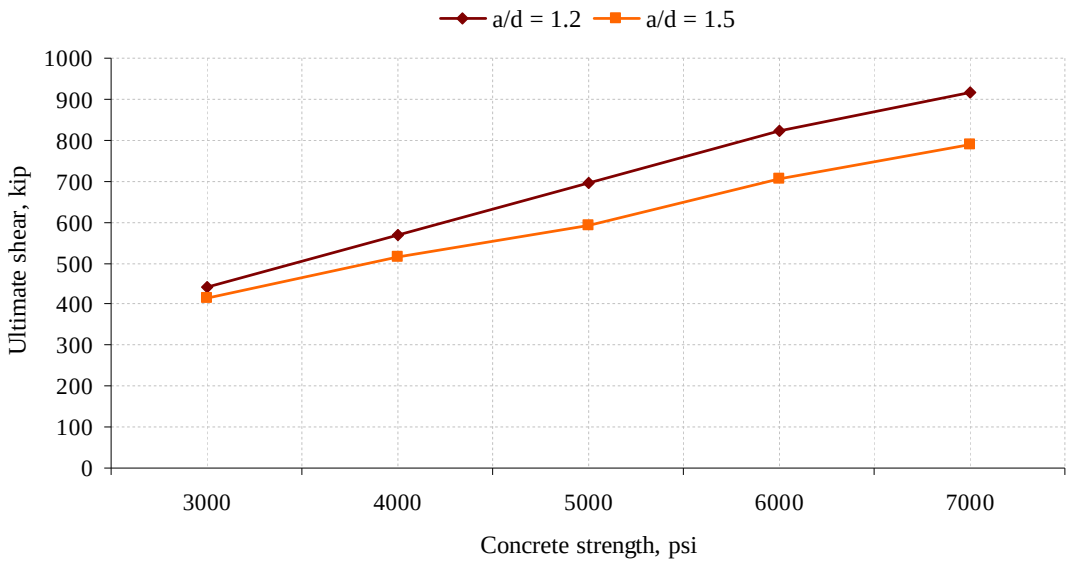

Figure 5.44 The influence of concrete strength on the shear strength of continuous deep beam

It was observed from the models the shear strength of continuous deep beams is proportional to concrete strength. This behavior was also observed in results of models of simply supported deep beam. It also showed that the slope of shear strength is inversely proportional to shear span-to-depth ratio. The strength of continuous deep beams with a/d ratios less than 1.5 is governed by direct compression strut (Fig. 5.44)

Table 5.26 Details of two span beams with a/d = 1.2 (series CB I)

Computer model I.D.	H, in	b_w, in	d, in	a/d	ρ_v	ρ_h	f'_c, psi	f_y, ksi
CB-I-1.2	75	21	68.9	1.2	0.00	0.00	3000	69
CB-I-1.2	75	21	68.9	1.2	0.00	0.00	4000	69
CB-I-1.2	75	21	68.9	1.2	0.00	0.00	5000	69
CB-I-1.2	75	21	68.9	1.2	0.00	0.00	6000	69
CB-I-1.2	75	21	68.9	1.2	0.00	0.00	7000	69

Table 5.27 Details of two span beams with a/d = 1.2 (series CB II)

Computer model I.D.	H, in	b_w, in	d, in	a/d	ρ_v	ρ_h	f'_c, psi	f_y, ksi
CB-I-1.5	75	21	68.9	1.2	0.00	0.00	3000	69
CB-I-1.5	75	21	68.9	1.2	0.00	0.00	4000	69
CB-I-1.5	75	21	68.9	1.2	0.00	0.00	5000	69
CB-I-1.5	75	21	68.9	1.2	0.00	0.00	6000	69
CB-I-1.5	75	21	68.9	1.2	0.00	0.00	7000	69

5.3.2 The influence of web reinforcement on the shear strength of two span deep beams

Series CB-II models of two span deep beams consist of beams with different detail of web reinforcement: without web reinforcement, only vertical shear reinforcement, only horizontal shear reinforcement, and both vertical and horizontal shear reinforcement. The web reinforcement varied as follows:

Series CB II : 0.3% vertical, 0.0% horizontal web reinforcement

Series CB II : 0.0% vertical, 0.3% horizontal web reinforcement

Series CB II : 0.3% vertical, 0.3% horizontal web reinforcement

Series CB II : 0.6% vertical, 0.0% horizontal web reinforcement

Series CB II : 0.0% vertical, 0.6% horizontal web reinforcement

reinforcement

A typical beam of series CB II was modeled as follows:

(1) Geometric dimensions:

- Shear span length is the distance from the edge of the loading plate to the closest edge of the supporting plate.
- Dimensions of cross section: height of 75 in., and width of 21 in.
- Loading plates: 16x21x4 in.
- Supporting plates: 16x21x3 in.

(2) Constraint conditions:

- One constraint was a perfect pin and the other two perfect rollers.

(3) Loading conditions:

- Single load was applied at middle of two loading plates. The increment of load was 20 kips.

(4) Materials:

- Concrete model was CCQ10SBeta: f'_c = 5.01 ksi
- Plates were modeled as plane stress elastic isotropic material
- Reinforcement used as an elastic-perfectly plastic material model: f_y = 69 ksi and f_{vy} = 67 ksi.

(5) Finite element analysis:

- Mesh type: rectangular mesh for reinforced concrete beam with mesh size of 3.8 in.

Details of series CB-II computer model tests are shown in Tables 5.31, 5.32, 5.33, and 5.34 and typical continuous deep beams with different detail of web reinforcement are shown in Figs. 5.45 5.46, 5.47, and 5.48.

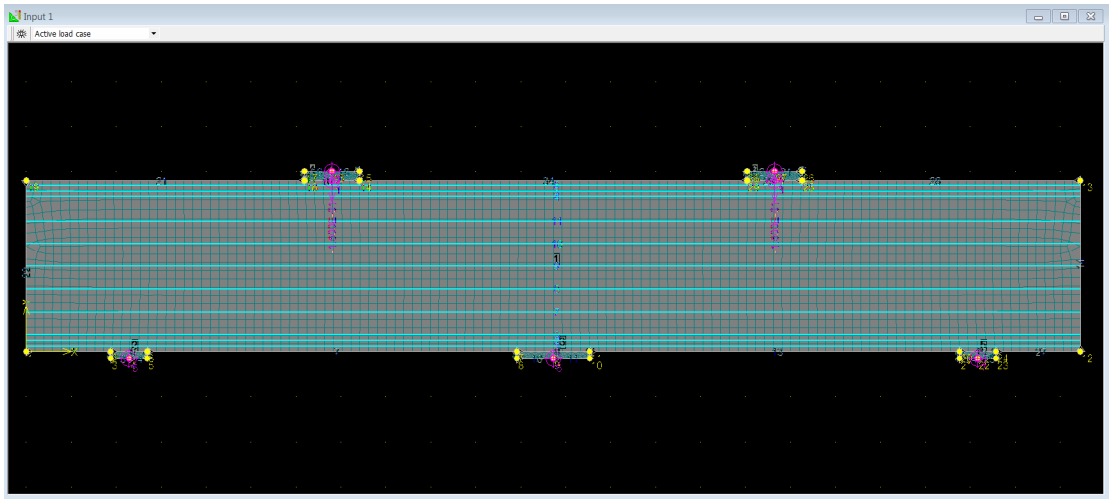

Figure 5.45 Model of CB-II with a/d = 1.0 and 0.3% horizontal reinforcement

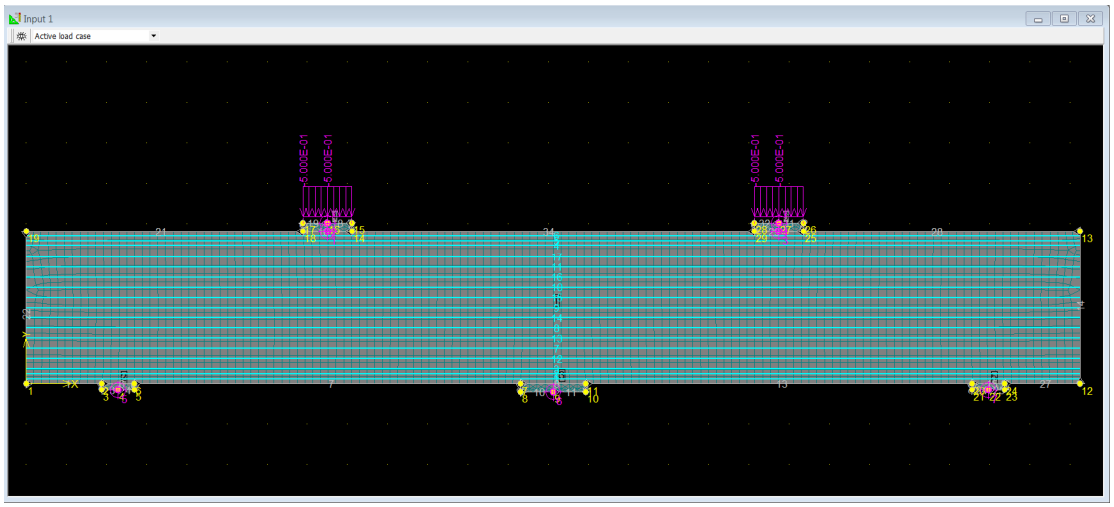

Figure 5.46 Model of CB-II with a/d = 1.2 and 0.6% horizontal reinforcement

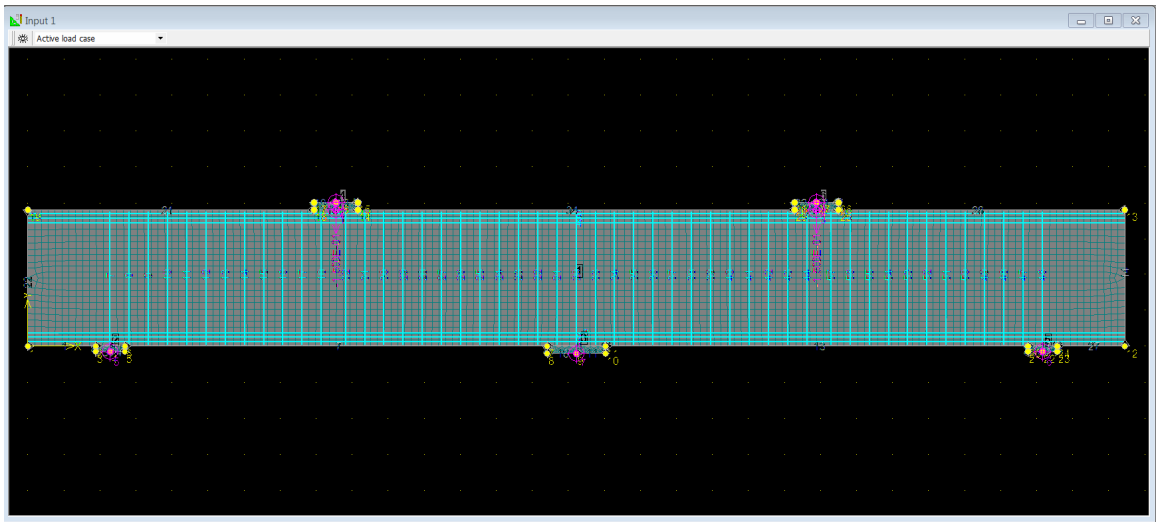

Figure 5.47 Model of CB-II with a/d = 1.5 and 0.6% vertical reinforcement

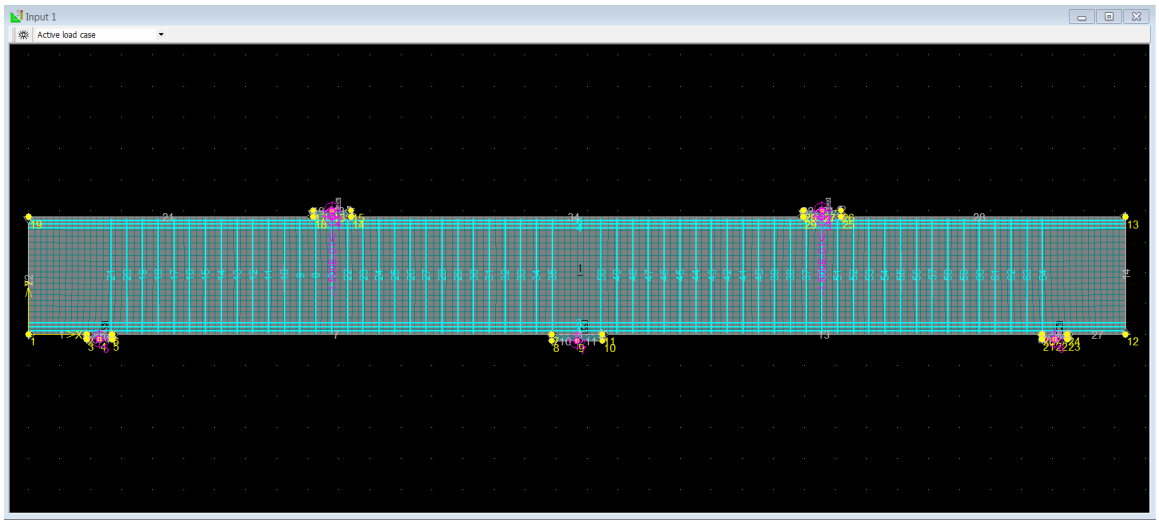

Figure 5.48 Model of CB-II with a/d = 1.85 and 0.3% vertical reinforcement

Results of models of series CB-II are shown in Tables 5.28, 5.29, and 5.30 and Fig. 5.49.

Table 5.28 Contribution of web reinforcement to the shear strength of two span deep beam, without web reinforcement

a/d	West exterior shear, kip	West interior shear, kip	East interior shear, kip	East exterior shear, kip
1	549	816	816	549
1.2	454	678	678	454
1.5	424	595	595	424
1.85	371	612	612	371

Table 5.29 Contribution of web reinforcement to the shear strength of two span deep beam, with 0.3% vertical and 0.3% horizontal web reinforcement

a/d	West exterior shear, kip	West interior shear, kip	East interior shear, kip	East exterior shear, kip
1	643	1034	1034	643
1.2	613	985	985	613
1.5	520	895	895	520
1.85	489	825	825	489

Table 5.30 Contribution of web reinforcement on the shear strength of continuous deep beam, with 0.6% vertical web reinforcement

a/d	West exterior shear, kip	West interior shear, kip	East interior shear, kip	East exterior shear, kip
1	805	1183	1183	805
1.2	613	1154	1154	613
1.5	628	1068	1068	628
1.85	532	985	985	532

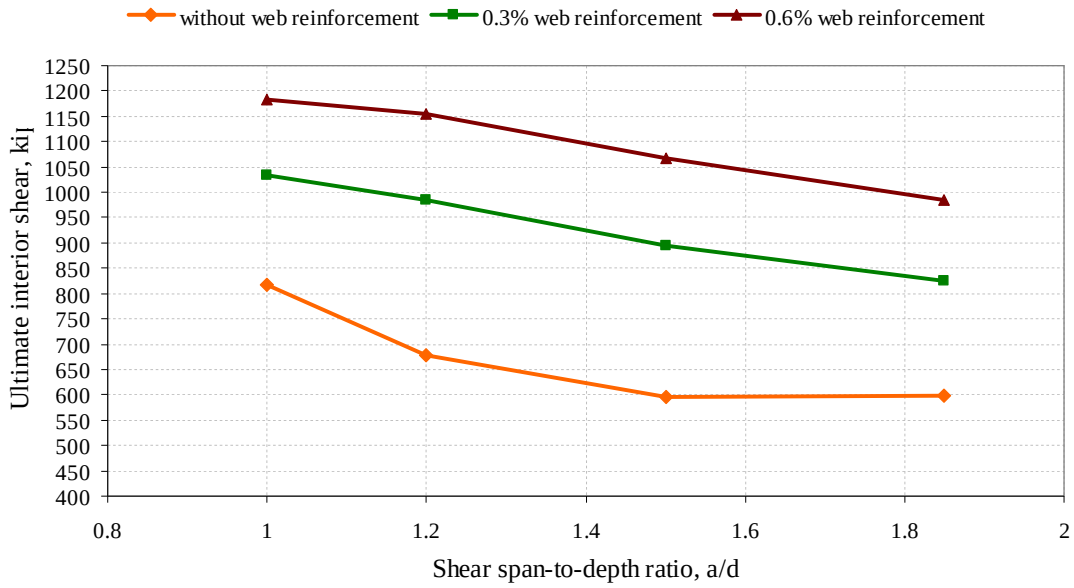

Figure 5.49 Contribution of web reinforcement on the shear strength of continuous deep beam

Figures 5.49, and 5.50 show that vertical web reinforcement is more effective than for simply supported deep beams. In Fig. 5.49 for deep beams without web reinforcements there is little different between simply supported and continuous deep

beams. However, for the same amount vertical web reinforcement used, continuous deep beams gained more shear strength for the same geometry. In Fig. 5.49 it was observed that vertical web reinforcement nearly eliminated the influence of shear span-to-depth ratio on the shear strength of continuous deep beams. This was also observed by Rogowsky and Mac Greogor (1983).

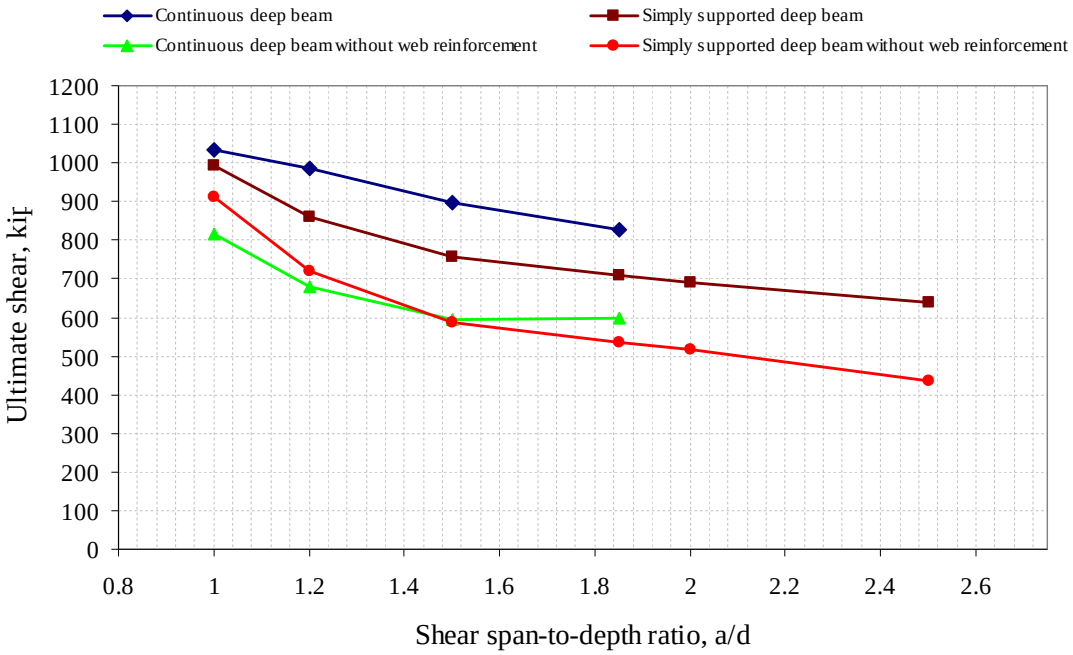

Figure 5.50 Comparison shear capacity between simply supported and two span deep beams

Table 5.31 Details of series CB-II-1.0 computer model tests

Computer model I.D.	H, in	b_w, in	d, in	a/d	ρ_v	ρ_h	f'_c, psi	f_y, ksi
CB-II-1.0	75	21	68.9	1.0	0.00	0.00	3000	69
CB-II-1.0	75	21	68.9	1.0	0.03	0.00	4000	69
CB-II-1.0	75	21	68.9	1.0	0.00	0.03	5000	69
CB-II-1.0	75	21	68.9	1.0	0.06	0.00	6000	69
CB-II-1.0	75	21	68.9	1.0	0.00	0.06	7000	69

Table 5.32 Details of series CB-II-1.2 computer model tests

Computer model I.D.	H, in	b_w, in	d, in	a/d	ρ_v	ρ_h	f'_c, psi	f_y, ksi
CB-II1.2	75	21	68.9	1.2	0.00	0.00	3000	69
CB-II-1.2	75	21	68.9	1.2	0.03	0.00	4000	69
CB-II-1.2	75	21	68.9	1.2	0.00	0.03	5000	69
CB-II-1.2	75	21	68.9	1.2	0.03	0.03	6000	69
CB-II-1.2	75	21	68.9	1.2	0.00	0.06	7000	69

Table 5.33 Details of series CB-II-1.5 computer model tests

Computer model I.D.	H, in	b_w, in	d, in	a/d	ρ_v	ρ_h	f'_c, psi	f_y, ksi
CB-II-1.5	75	21	68.9	1.5	0.00	0.00	3000	69
CB-II-1.5	75	21	68.9	1.5	0.03	0.03	4000	69
CB-II-1.5	75	21	68.9	1.5	0.06	0.03	5000	69
CB-II-1.5	75	21	68.9	1.5	0.06	0.00	6000	69

Table 5.34 Details of series CB-II-1.85 computer model tests

Computer model I.D.	H, in	b_w, in	d, in	a/d	ρ_v	ρ_h	f'_c, psi	f_y, ksi
CB-II-1.85	75	21	68.9	1.85	0.00	0.00	3000	69
CB-II-1.85	75	21	68.9	1.85	0.03	0.00	4000	69

5.3.3 The influence of longitudinal tensile reinforcement on the shear strength of two span deep beam

Series CB-III of models consists of deep beams with different details of longitudinal tensile reinforcements, which place over middle support and bottom (Figs. 5.51 and 5.52).

A typical beam of series CB III was modeled as follows:

(1) Geometric dimensions:

- Shear span length is the distance from the edge of the loading plate to the closest edge of the supporting plate.
- Dimensions of cross section: height of 75 in., and width of 21 in.
- Loading plates: 16x21x4 in.
- Supporting plates: 16x21x3 in.

(2) Constraint conditions:

- One constraint was a perfect pin and the other two perfect rollers.

(3) Loading conditions:

- Single load was applied at middle of two loading plates. The increment of load was 20 kips.

(4) Materials:

- Concrete model was CCQ10SBeta: f'_c = 5.01 ksi
- Plates were modeled as plane stress elastic isotropic material
- Reinforcement used as an elastic-perfectly plastic material model: f_y = 69 ksi and f_{vy} = 67 ksi.

(5) Finite element analysis:

- Mesh type: rectangular mesh for reinforced concrete beam with mesh size of 3.8 in.

Details of CB-III models are shown in Table 5.36 and details of placements of longitudinal reinforcement are shown in Figs. 5.51 and 5.52.

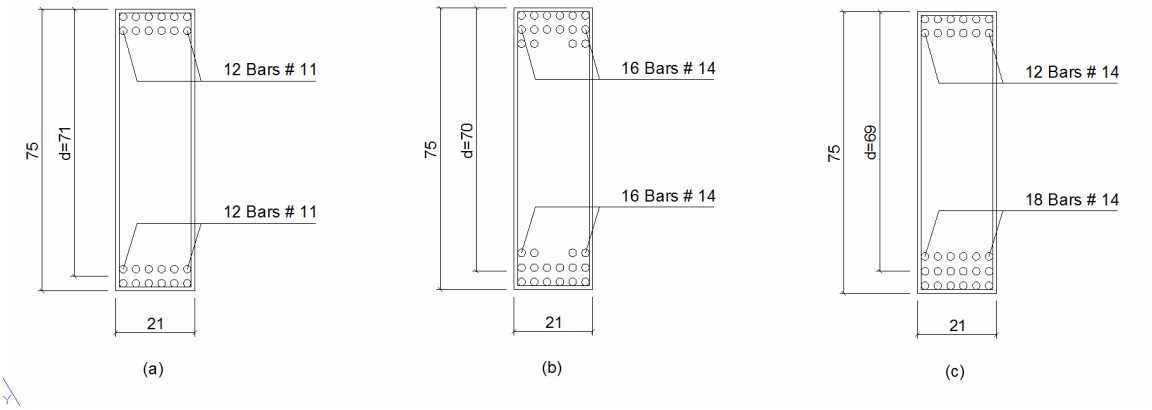

Figure 5.51 Details of placement of longitudinal reinforcement of model CB-III: (a) ρ =ρ' =1.29%, (b) ρ =ρ' =2.5%, and (c) ρ =3.0% and ρ' =1.29%

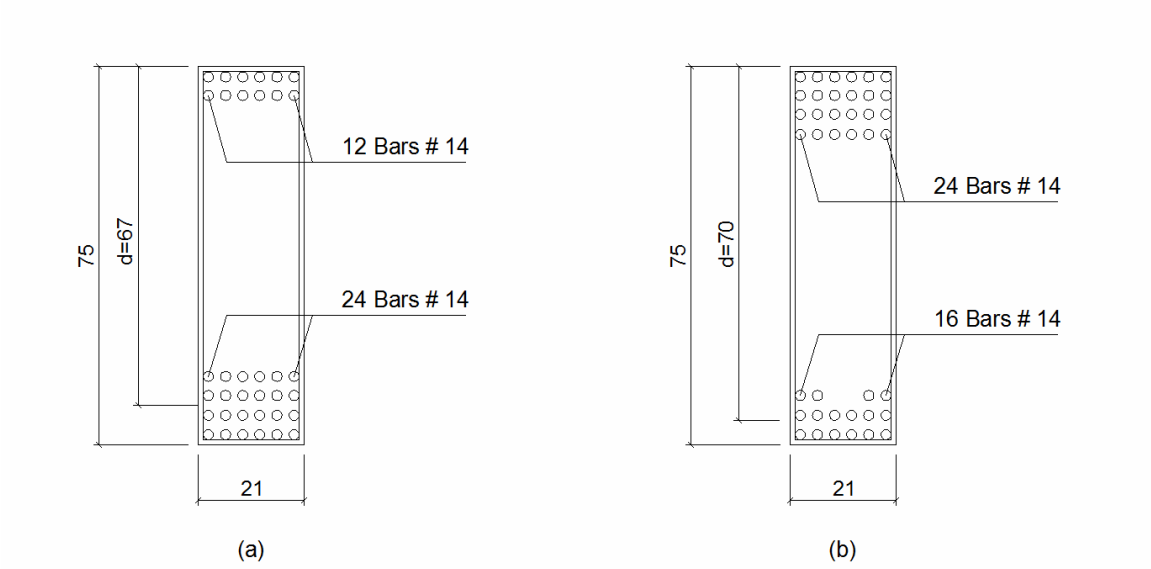

Figure 5.52 Details of placement of longitudinal reinforcement of model CB-III: (a) ρ =4% and ρ' =2.0% and (b) ρ = 2.5% and ρ' =4.0%

Results of models of series CB-III are shown in Table 5.35.

It was observed that two span continuous deep beams with larger top longitudinal reinforcement ratio have higher shear strength. This reflected that a plastic truss forming between two loading plates and middle support governs the shear strength of two span continuous deep beams.

Table 5.35 Results of models of series CB-III

ρ, %	ρ', %	d, in	f_y, ksi	f'_c, psi	Interior ultimate shear, kip	Exterior ultimate shear, kip
1.29	1.29	71	69	5010	874	254
2.5	2.5	70	69	5010	930	293
2.5	4	70	69	5010	955	264
3	2	69	69	5010	899	309
4	2	67	69	5010	911	320

Table 5.36 Details of CB-III computer model tests

Computer model I.D.	H, in	b_w, in	d, in	a/d	ρ	ρ'	f'_c, psi	f_y, ksi
CB-III-1.5	75	21	71	1.5	1.29	1.29	5010	69
CB-III-1.5	75	21	70	1.5	2.5	2.5	5010	69
CB-III-1.5	75	21	69	1.5	3.0	1.29	5010	69
CB-III-1.5	75	21	67	1.5	4.0	2.0	5010	69
CB-III-1.5	75	21	70	1.5	2.5	4.0	5010	69

5.3.4 The influence of shear span-to-depth ratio, a/d, on the shear strength of two span deep beams

Series CB IV of models consist of continuous deep beams with various shear span-to-depth ratios, a/d. Values of a/d investigated are 1.0, 1.2, 1.5 and 1.85.

A typical beam of series CB IV was modeled as follows:

(1) Geometric dimensions:

- Shear span length is the distance from the edge of the loading plate to the closest edge of the supporting plate.
- Dimensions of cross section: height of 75 in., and width of 21 in.
- Loading plates: 16x21x4 in.
- Supporting plates: 16x21x3 in.

(2) Constraint conditions:

- One constraint was a perfect pin and the other two perfect rollers.

(3) Loading conditions:

- Single load was applied at middle of two loading plates. The increment of load was 20 kips.

(4) Materials:

- Concrete model was CCQ10SBeta: f'_c = 5.01 ksi
- Plates were modeled as plane stress elastic isotropic material
- Reinforcement used as an elastic-perfectly plastic material model: f_y = 69 ksi and f_{vy} = 67 ksi.

(5) Finite element analysis:

- Mesh type: rectangular mesh for reinforced concrete beam with mesh size of 3.8 in.

Details of models of series CB IV are shown in Tables 5.40, 5.41 and Figs. 5.53, 5.54, and 5.55.

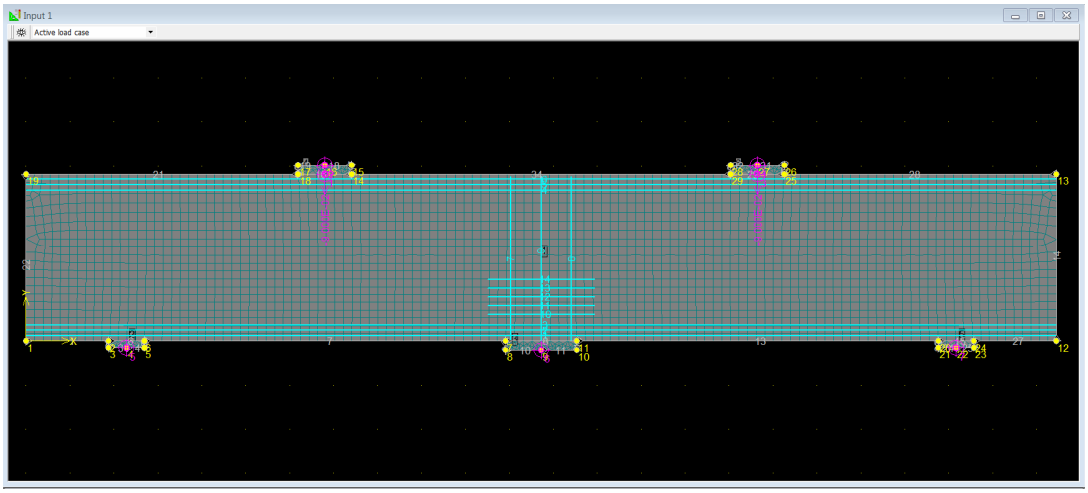

Figure 5.53 Model of series CB IV without web reinforcement and a/d = 1.0

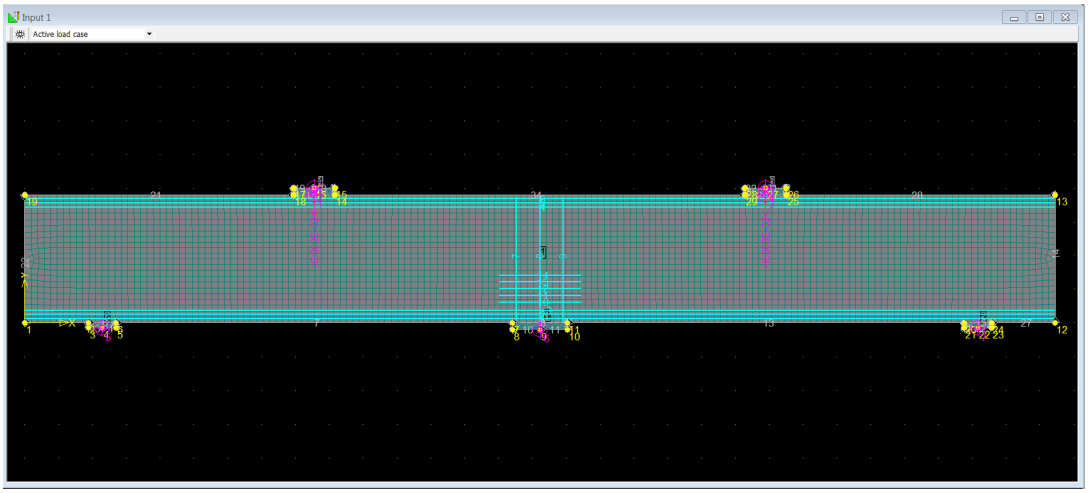

Figure 5.54 Model of series CB IV without web reinforcement and a/d = 1.5

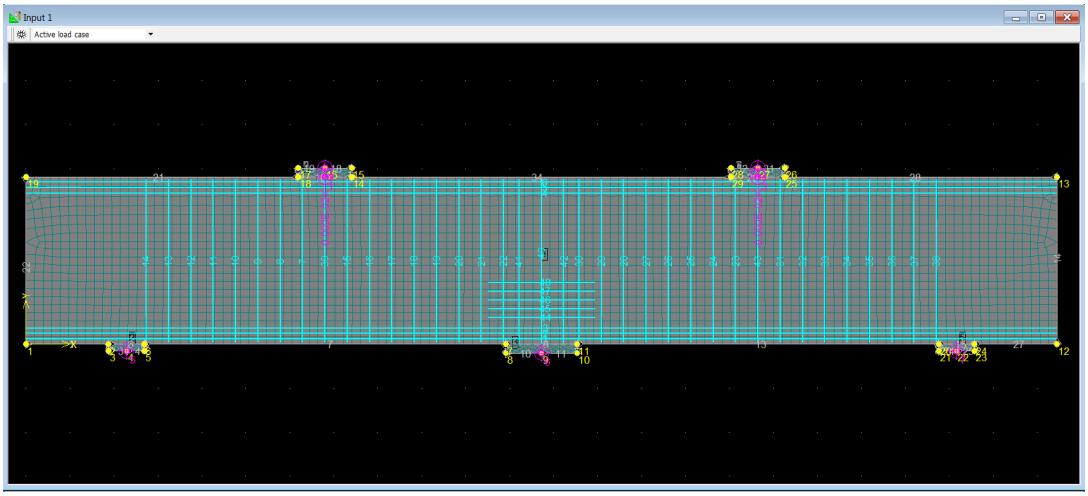

Figure 5.55 Model of series CB IV with web reinforcement and a/d = 1.0

Results of models of series CB-IV are shown in Tables 5.37, 5.38, 5.39 and Fig. 5.56.

Table 5.37 Contribution of web reinforcement to the shear strength of two span deep beam, without web reinforcement

a/d	West exterior shear, kip	West interior shear, kip	East interior shear, kip	East exterior shear, kip
1	601	794	794	601
1.2	465	698	698	465
1.5	424	595	595	424
1.85	371	612	612	371

Table 5.38 Contribution of web reinforcement to the shear strength of two span deep beam, with 0.3% vertical and 0.3% horizontal web reinforcement

a/d	West exterior shear, kip	West interior shear, kip	East interior shear, kip	East exterior shear, kip
1	643	1034	1034	643
1.2	613	985	985	613
1.5	520	895	895	520
1.85	489	825	825	489

Table 5.39 Contribution of web reinforcement to the shear strength of two span deep beam, with 0.6% vertical web reinforcement

a/d	West exterior shear, kip	West interior shear, kip	East interior shear, kip	East exterior shear, kip
1	805	1183	1183	805
1.2	613	1154	1154	613
1.5	628	1068	1068	628
1.85	532	985	985	532

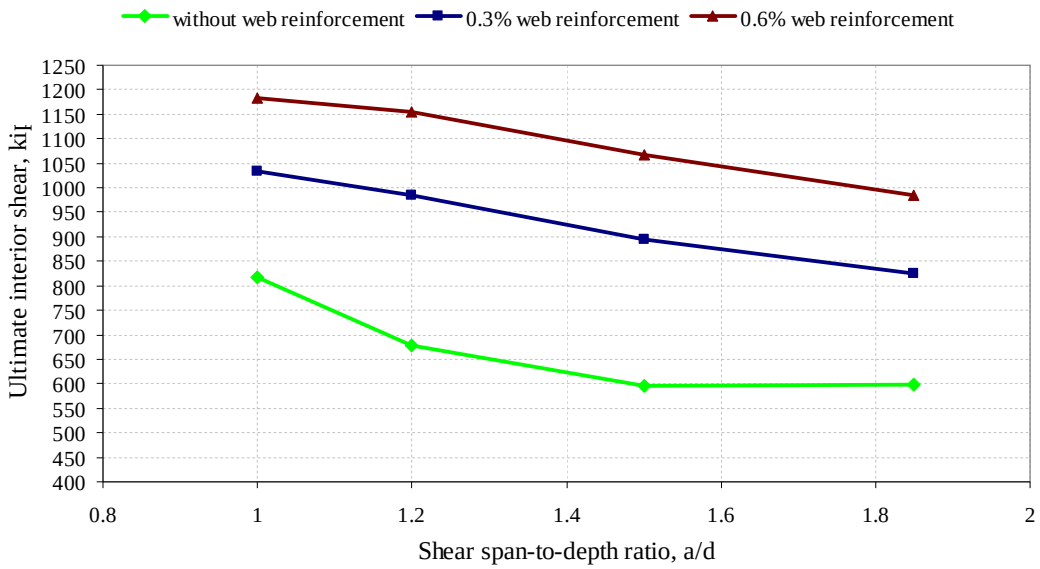

Figure 5.56 The influence of shear span-to-depth ratio on the shear strength of continuous deep beam

Table 5.40 Details of models of series CB IV without web reinforcement

Computer model I.D.	H, in	b_w, in	d, in	d', in	a/d	ρ	ρ'	f'_c, psi	f_y, ksi
CB-IV-1.0	75	21	70	70	1.0	0.02	0.02	5010	69
CB-IV-1.2	75	21	70	70	1.2	0.02	0.02	5010	69
CB-IV-1.5	75	21	70	70	1.5	0.02	0.02	5010	69
CB-IV-1.85	75	21	70	70	1.85	0.02	0.02	5010	69

Table 5.41 Details of models of series CB IV with 0.3% vertical web reinforcement

Computer model I.D.	H, in	b_w, in	d, in	d', in	a/d	ρ	ρ'	f'_c, psi	f_y, ksi
CB-IV-1.0	75	21	70	70	1.0	0.02	0.02	5010	69
CB-IV-1.2	75	21	70	70	1.2	0.02	0.02	5010	69
CB-IV-1.5	75	21	70	70	1.5	0.02	0.02	5010	69
CB-IV-1.85	75	21	70	70	1.85	0.02	0.02	5010	69

5.4 Summary

A series of models were developed for investigating the behavior of reinforced concrete deep beams. The major parameters studied include concrete strength, ratio of longitudinal reinforcement, shear span-to-depth ratio, and web reinforcement.

- Series consisting of twenty-one computer model tests of simply supported and ten computer model tests of two span continuous deep beams were developed to examine the influence of concrete strength on the shear strength of deep beam. It was observed that the shear strength of deep beams is linearly proportional to concrete strength.
- The influence of longitudinal reinforcement on the shear strength of deep beams were analyzed by a series of six computer model tests of simply supported and of five computer model tests of two span continuous deep beams. It was observed that continuous deep beams with larger longitudinal reinforcement ratio have higher shear strength. It also showed that longitudinal reinforcement, top and bottom, affect on the redistribution of reaction forces after inclined cracks formed.
- The contribution of web reinforcement to the shear strength of deep beams was investigated by series consisting of thirty simply supported and seventeen two span continuous deep beams. Some interesting results were gained from investigating of the contribution of web reinforcement on the shear strength of deep beams. It seems that horizontal web reinforcement has an insignificant contribution on the shear strength of deep beam. On the other hand, a major contribution comes from vertical web reinforcement. This is confirmed by experimental investigations (Smith and Vantsiotis 1982 and Rogowsky and MacGregor 1983).
- It was observed in both the models and experimental tests that as the shear span-to-depth ratio, a/d, increased the shear capacity decreased.

Chapter 6 Discussion of Shear Behavior of Deep Beams - Proposed Design Equation for Shear Strength

6.1 Overview

In this chapter, an interpretation of the computer model results will be presented. The behavior of reinforced concrete deep beam, simply supported and continuous two span, are outlined. The contribution of concrete, and flexural longitudinal and web reinforcement to shear strength of deep beams also are discussed. Finally, a proposed design equation for shear strength of deep beams is developed. The database of tests of reinforced concrete beams failing in shear is used to evaluate the proposed design equation.

6.2 Interpretation of test results of computer model tests

6.2.1 Simply supported deep beam

Behavior of simply supported deep beam could be divided into three stages. The first stage is behavior in the elastic range without cracks forming. In this range, concrete and reinforcement behave in elastic manner. Contour lines of principal compression strain radiate from the support and the loading plates and strain strategies form a compression arch (Fig. 6.1). The profile of strain in longitudinal reinforcement is similar to that of bending moment diagram. The second stage starts with flexural cracks forming. Flexural cracks extend up through the web as loading increases (Fig. 6.2). When loading is about 50% - 60% of peak load inclined cracks form (Fig.6.3). After inclined cracks form, strains in the longitudinal reinforcement are almost constant along clear span of deep beam. As loading increases the inclined cracks extend to the support plates and loading plate. There are some parallel inclined cracks that form, as well. Principal compression strain, now changes as a/d ratio changes. For deep beams with a/d less than 1.2 contour lines of principal compression strain form a band from the support plate to the loading plate (Fig. 6.4). However, for deep beams reinforced with vertical web

reinforcement and a/d equal or greater than 1.5 a fan shape of compression forms between the support plate to the loading plate (Fig. 6.5).

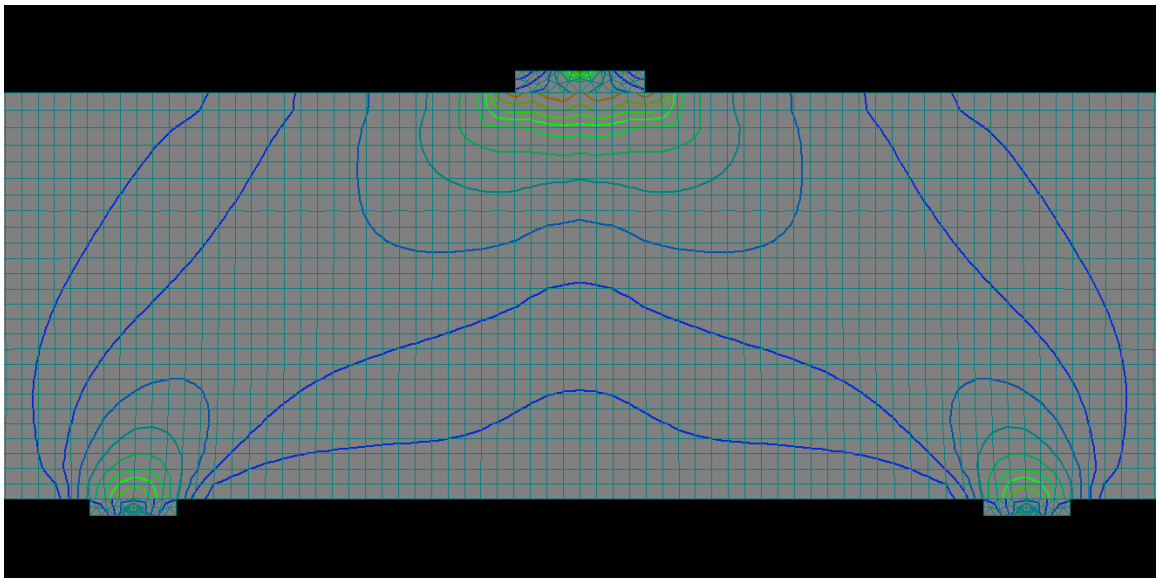

Figure 6.1 A compression arch of simply support deep beam in elastic behavior before cracks forming

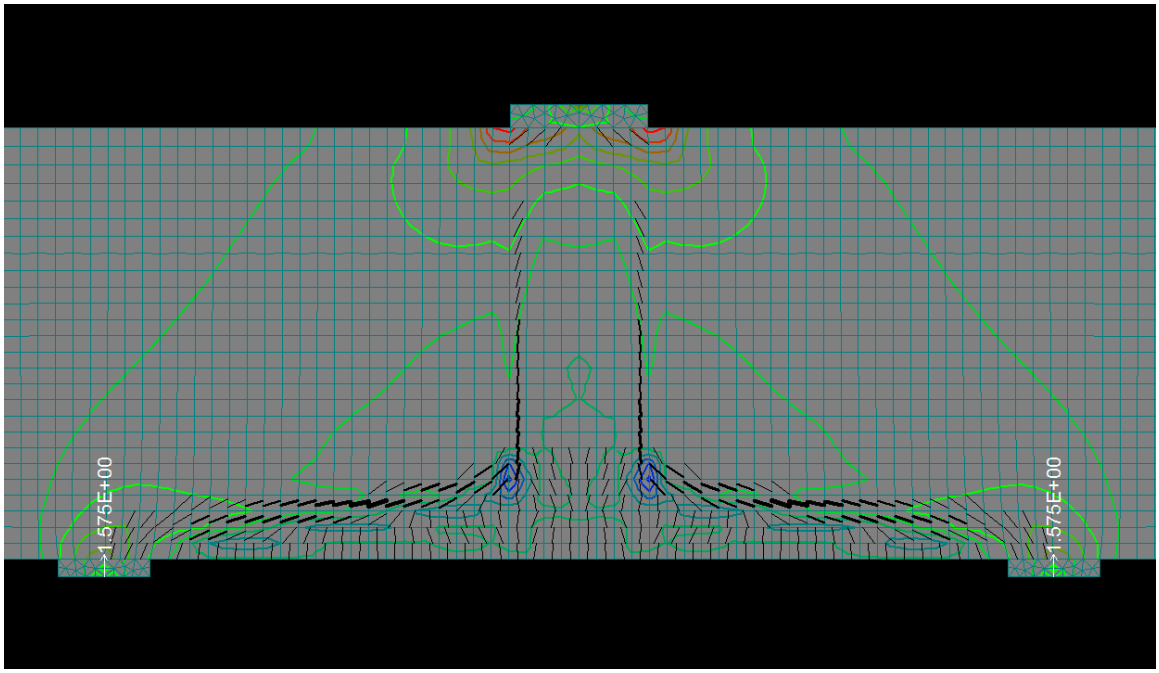

Figure 6.2 Flexural cracks up to web of deep beam as loading

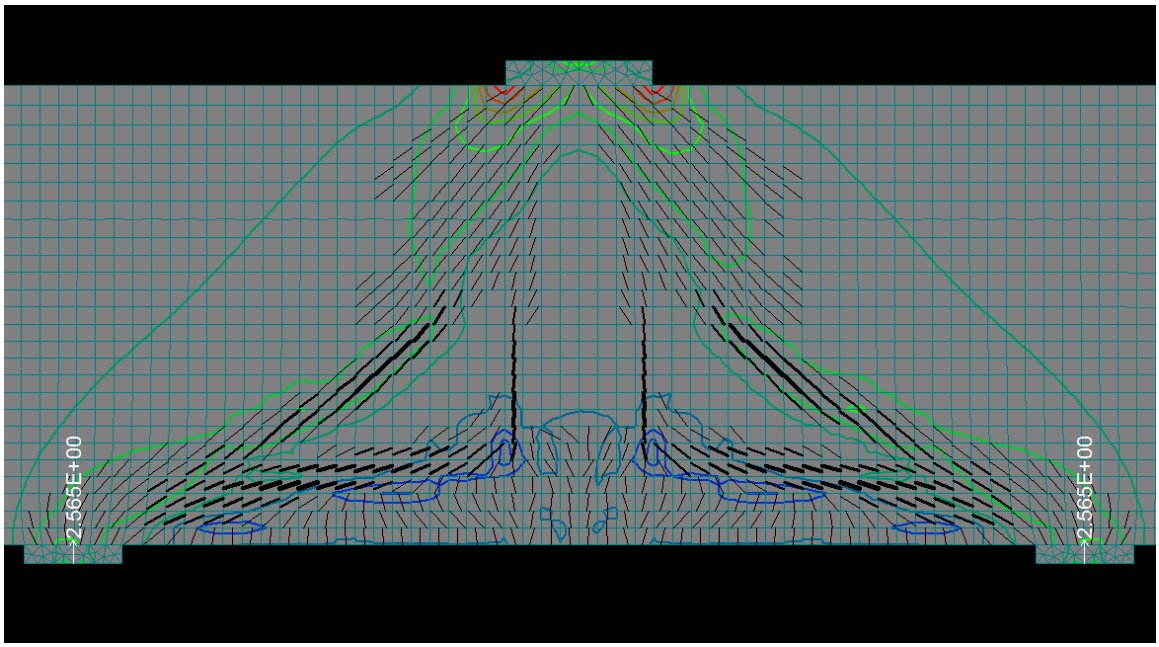

Figure 6.3 Inclined cracks forming

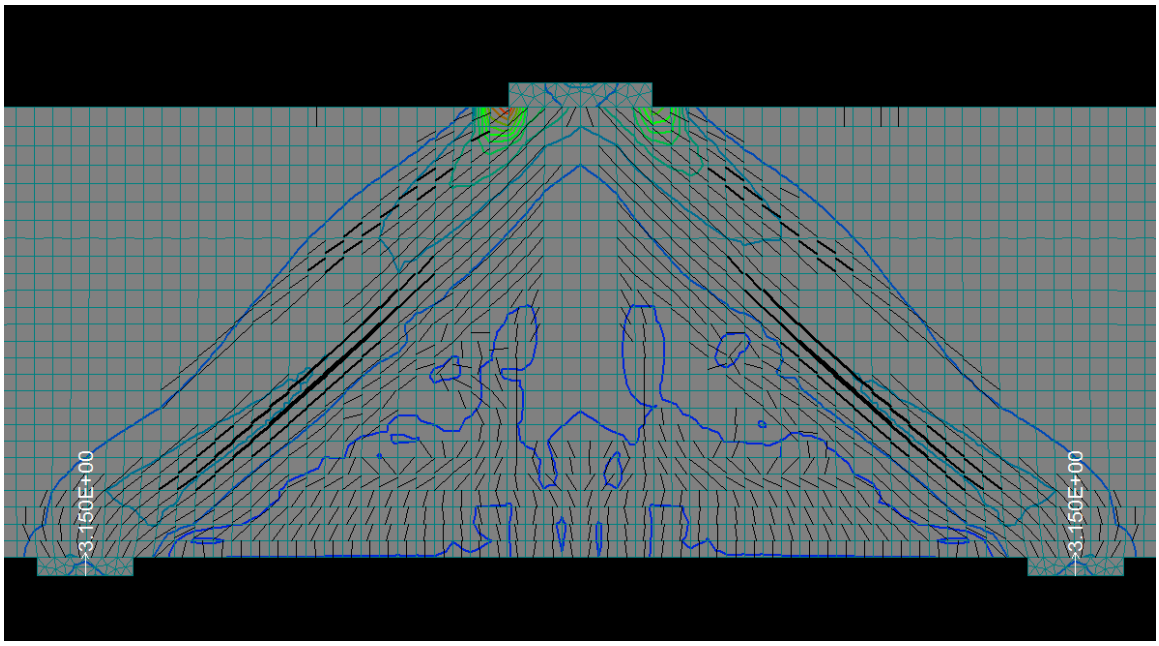

Figure 6.4 Band of principal compression strain in deep beam with a/d = 1.2

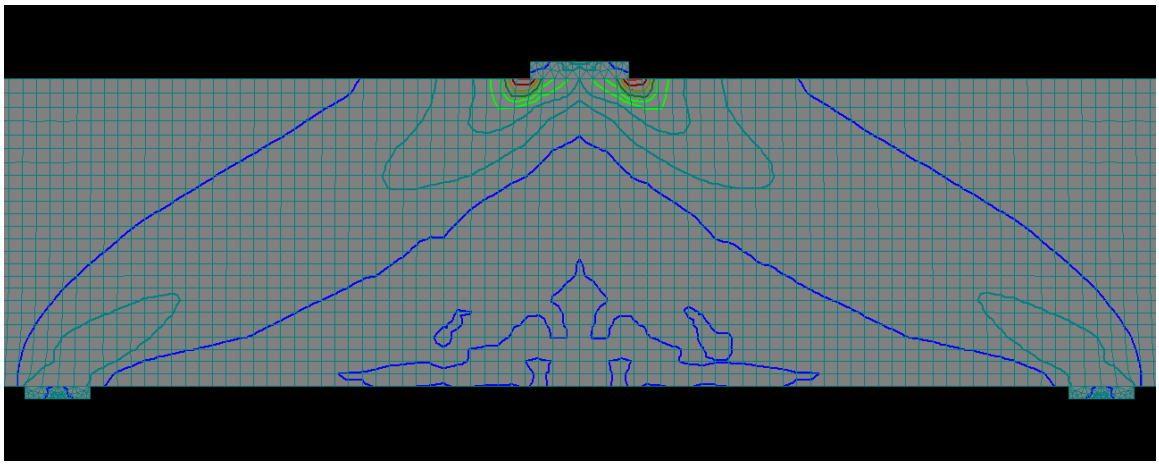

Figure 6.5 Fan shape of principal compression strain in deep beam with a/d = 1.85

The third stage is failure of the deep beam. A deep beam reaches failure when the compression zone at outside edge of the loading plate begins to crush. The predominant mode of failure is shear compression occurring at the edge of the loading plate. The failure is brittle if deep beams have no or minimum vertical web reinforcement. Deep beams with sufficient vertical web reinforcement would have more deformation capacity. The behavior of deep beams under two loading points or uniform distributed loading exhibit similar response. However, deep beams under uniform distributed load have a different mode of failure. It can be considered a shear failure, but the failure zones are located at the inside edge of the support plates (Fig. 6.6) and shear friction failure developed for deep beams with L/H less than 2.0 (Fig. 6.7).

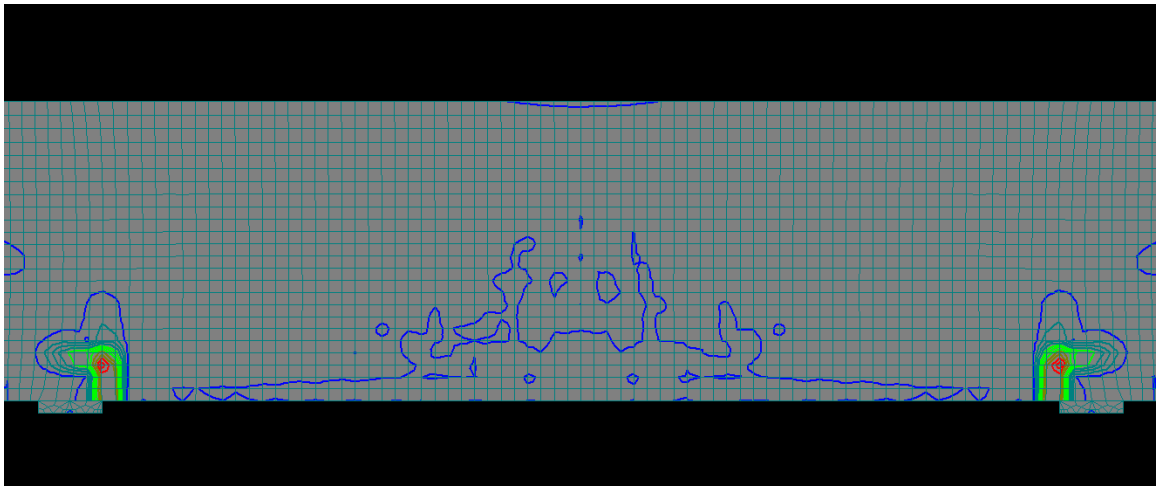

Figure 6.6 Deep beam with L/H = 3.4 under uniform distributed loading at failure

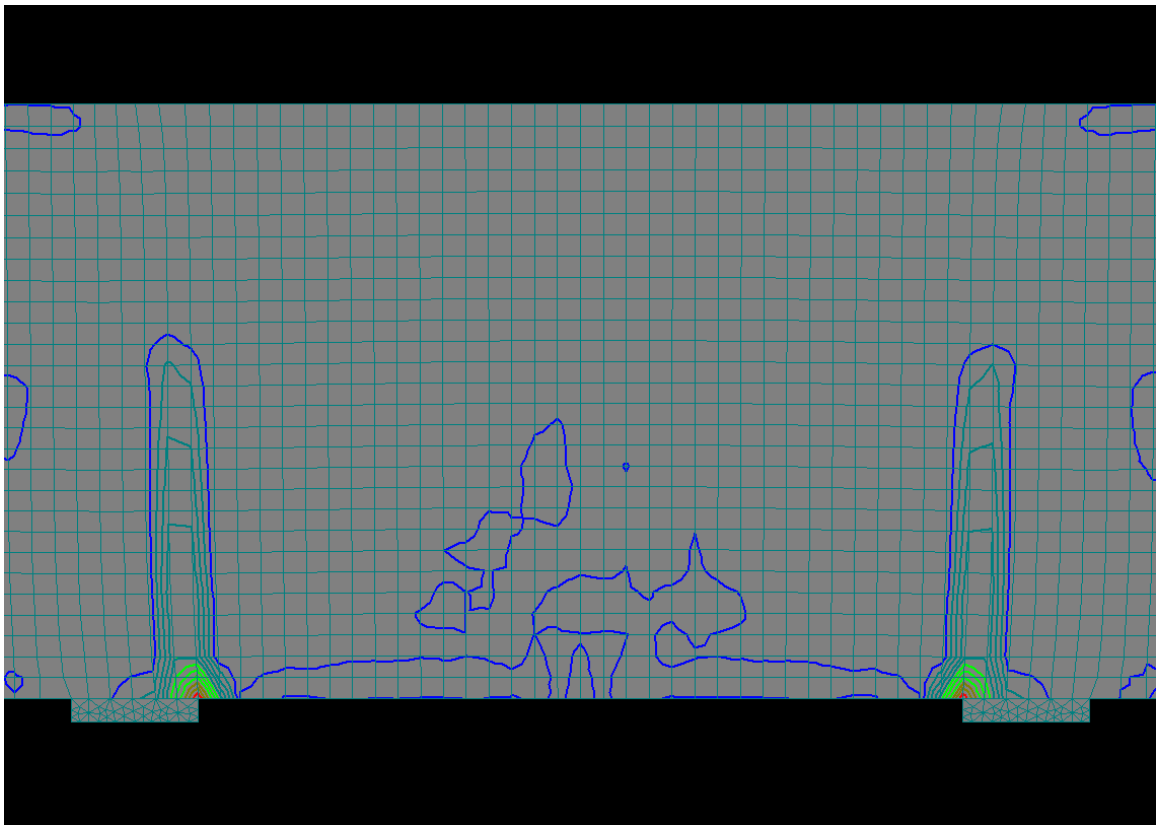

Figure 6.7 Deep beam with L/H=1.5 under uniform distributed loading

(a) The influence of concrete strength on the shear strength of deep beam

The shear strength of deep beams with a/d from 1.0 to 1.5 is linearly proportional to concrete strength (Fig. 6.8). This behavior reflects the dependence of the shear strength on the strength of a truss consisting of concrete struts and a steel tie (Fig. 6.9). The strength of the truss is usually governed by the strength of the concrete strut or the concrete nodes after the steel tie yields (ductile failure).

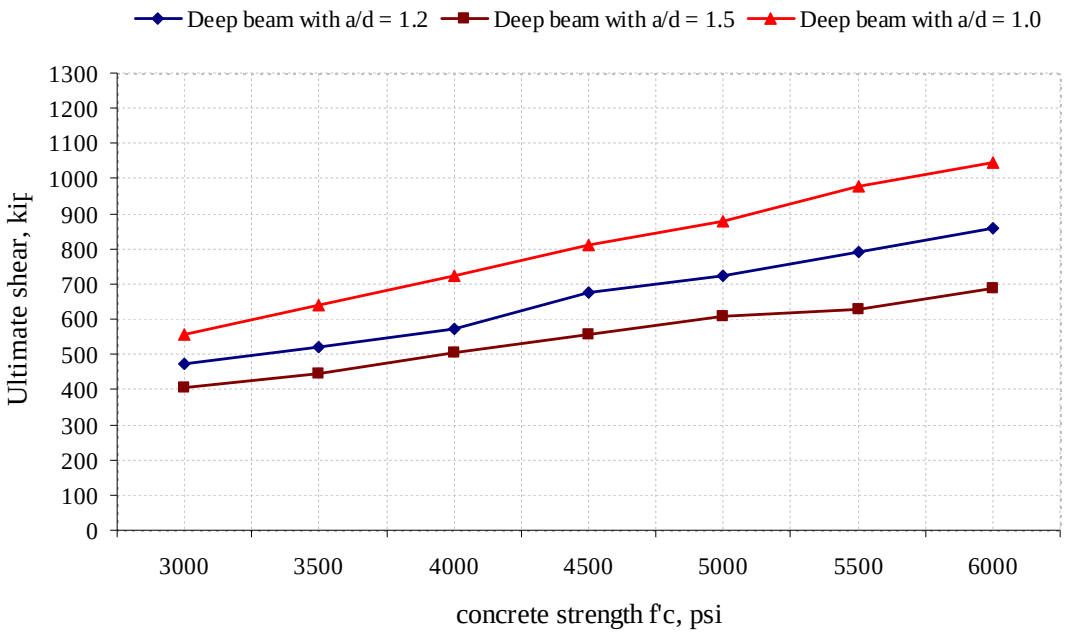

Figure 6.8 Influence of concrete strength on the shear strength of simply supported deep beams

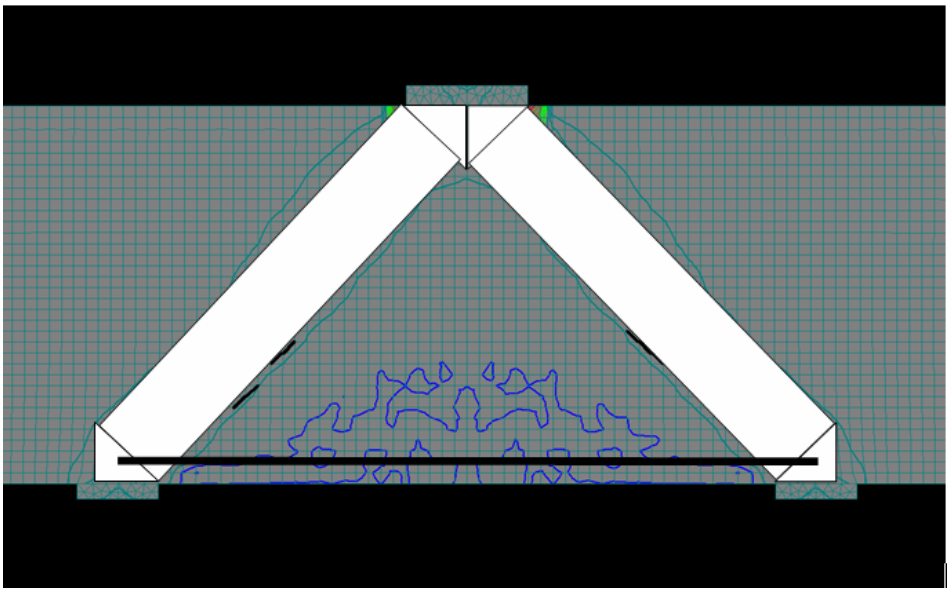

Figure 6.9 A strut-and-tie model of simply supported deep beam with a/d = 1.0

(b) The influence of shear span to depth ratio, a/d, on the shear strength of deep beams

The influence of shear span-to-depth ratio, a/d was observed from experimental results. The smaller the ratio of a/d, the larger the shear strength of a deep beam. The characteristic arch action is shown in Fig. 6.9.

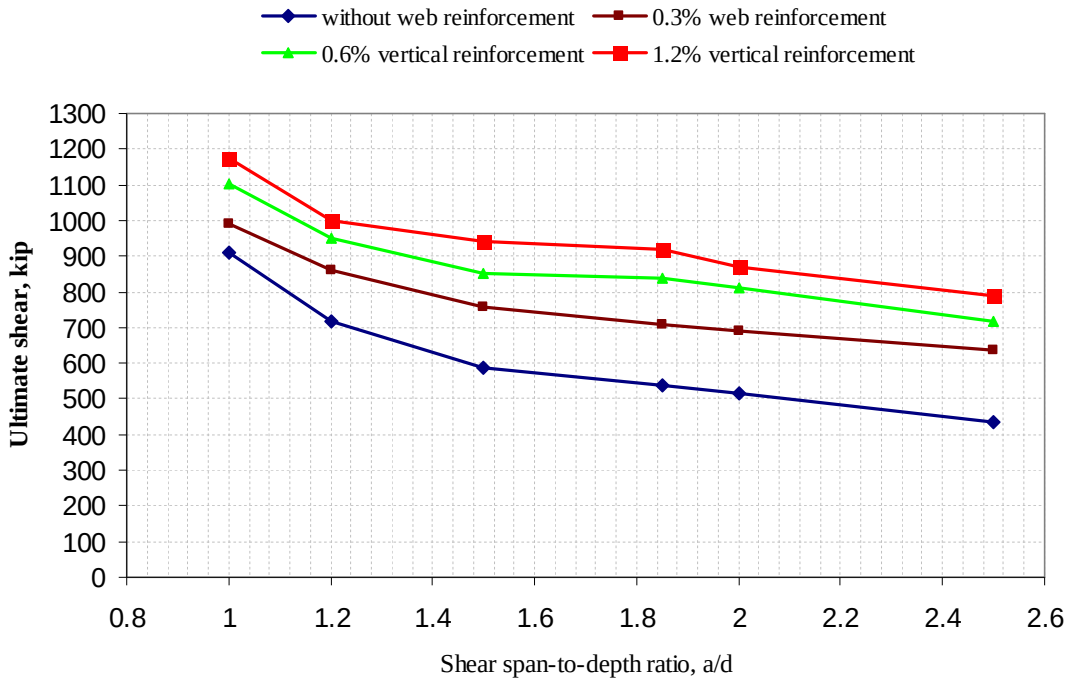

Figure 6.10 The influence of a/d ratio on the shear strength of deep beams

The a/d ratio has more influence on the shear capacity of deep beams with low a/d ratios and without web reinforcement. The influence of a/d ratio on deep beams is moderate for a/d ratios from 1.5 to 2.5, especially for deep beams with web reinforcement.

(c) The influence of web reinforcement on the shear strength of deep beams

From their experimental study, Smith and Vantsiotis (1982) considered that horizontal web reinforcement contributes little to the shear strength of deep beams. This observation was also discussed by Rogowsky and MacGregor (1983) and they comment that in some tests with only horizontal web reinforcement, the shear capacity was slightly reduced. The influence of horizontal web reinforcement was shown in the models

studied. The characteristics of horizontal web reinforcement was explained using a plastic truss model by Rogowsky and Mac Gregor (1983) (Fig. 6.11).

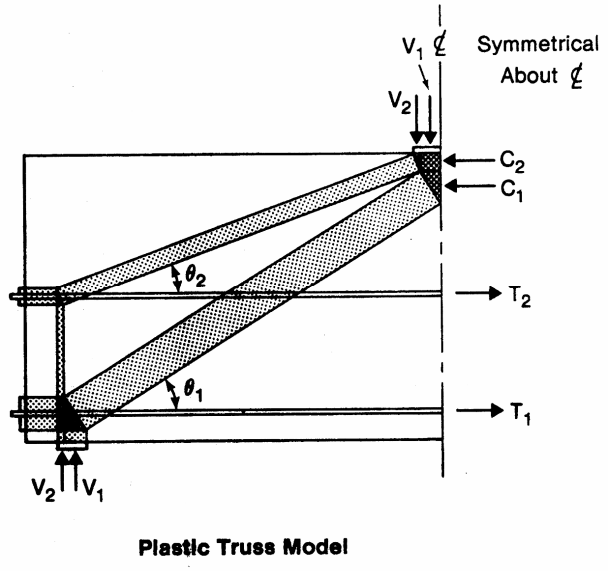

Figure 6.11 Plastic truss model for beam with horizontal web reinforcement (Rogowsky and MacGregor 1983)

In most beams the amount of horizontal web reinforcement is usually small compared to main longitudinal reinforcement, thus it means that $T_2 << T_1$. The contribution of horizontal reinforcement on shear strength transferred by the upper truss is the vertical component of the force in the upper strut. However, the slope of the upper strut, θ_2, may be quite small. As a result, T_2, the horizontal component of the upper strut force is small, and the vertical component of the upper strut force is even smaller. If this mechanism of force transfer exists, contour lines of principal compression strains should be observed in deep beams. Unfortunately, in the models studied there are no contour lines (Figs. 6.12a and 6.12b) but that is not likely when a large number of horizontal bars are present.

From Figs. 6.13, the models show that horizontal reinforcement has little contribution to shear strength of deep beams. On the other hand, vertical web reinforcements have major contribution on the shear strength of deep beams. It also seems that the contribution of vertical reinforcement is proportional to a/d. For a/d less than 1.2 the contribution of vertical reinforcement is about 15% for 0.3% vertical

reinforcement. But for a/d = 1.5 the contribution of vertical reinforcement is 28% and it is 30% for a/d = 1.85 (Fig. 6.14). The difference in the contribution of vertical reinforcement can be explained using the plastic truss concept for the contribution of vertical reinforcement (Fig. 6.15).

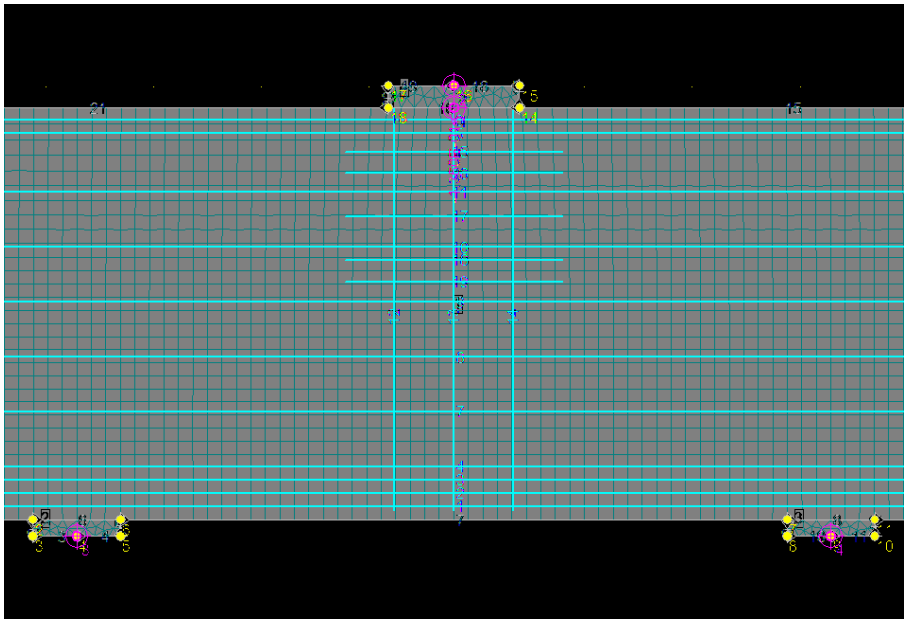

Figure 6.12a Model of deep beam a/d=1.0 with 0.3% horizontal reinforcement

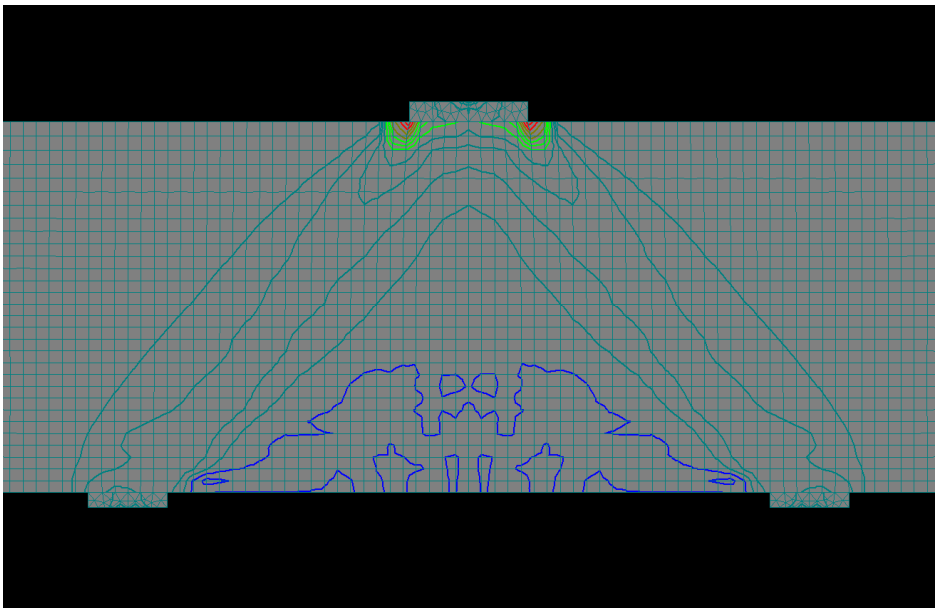

Figure 6.12b Contour lines of principal compression strains in deep beam a/d =1.0 with 0.3% horizontal reinforcement

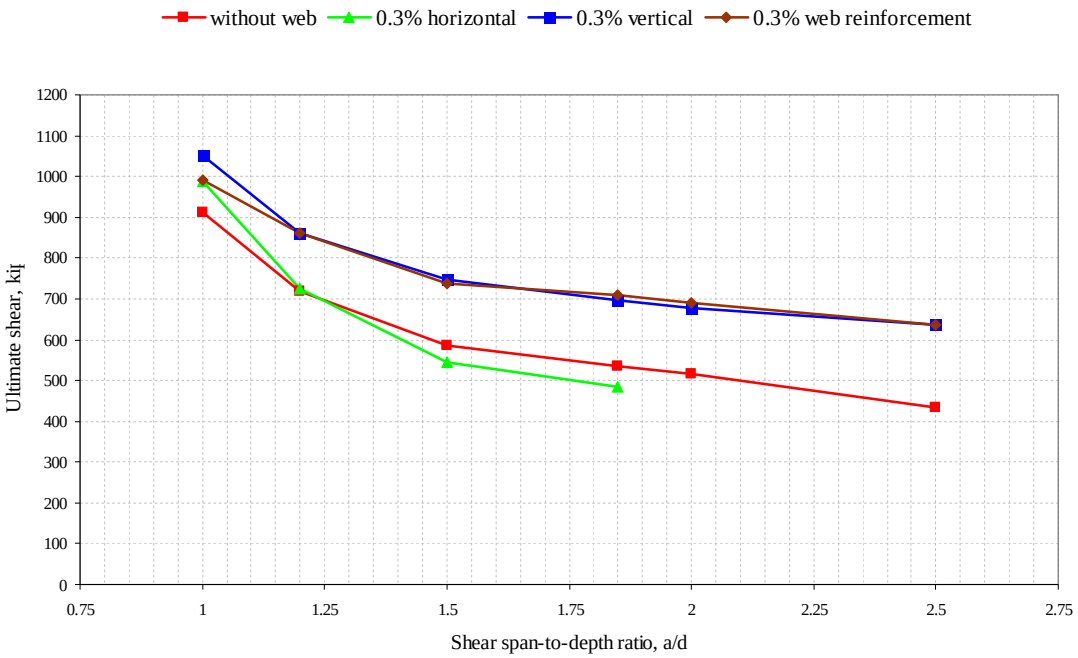

Figure 6.13 Contribution of horizontal web reinforcement to the shear strength of deep beams

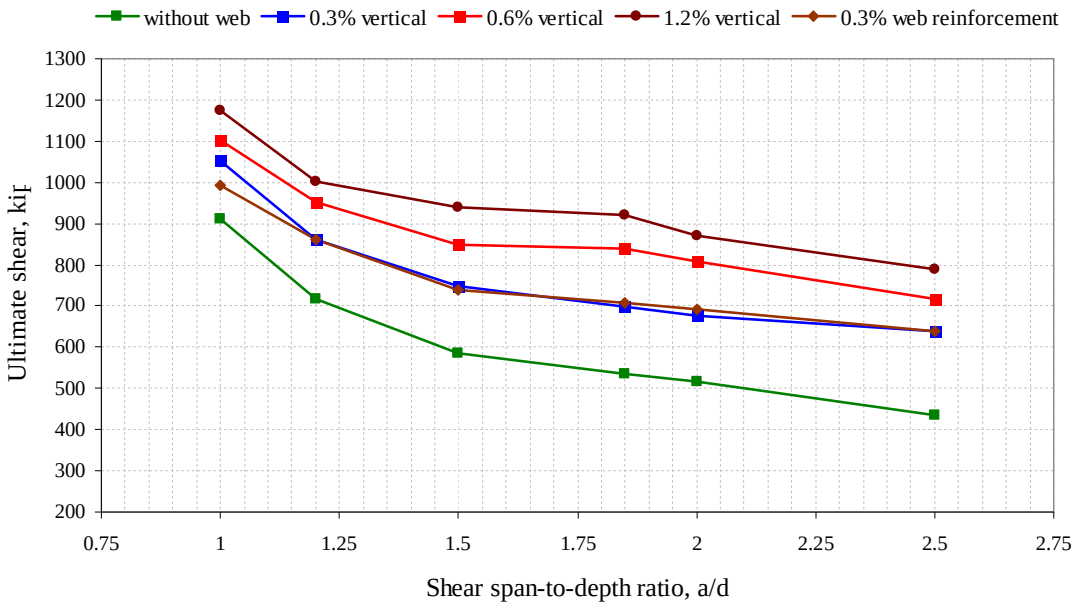

Figure 6.14 Contribution of vertical web reinforcement to shear strength of deep beams

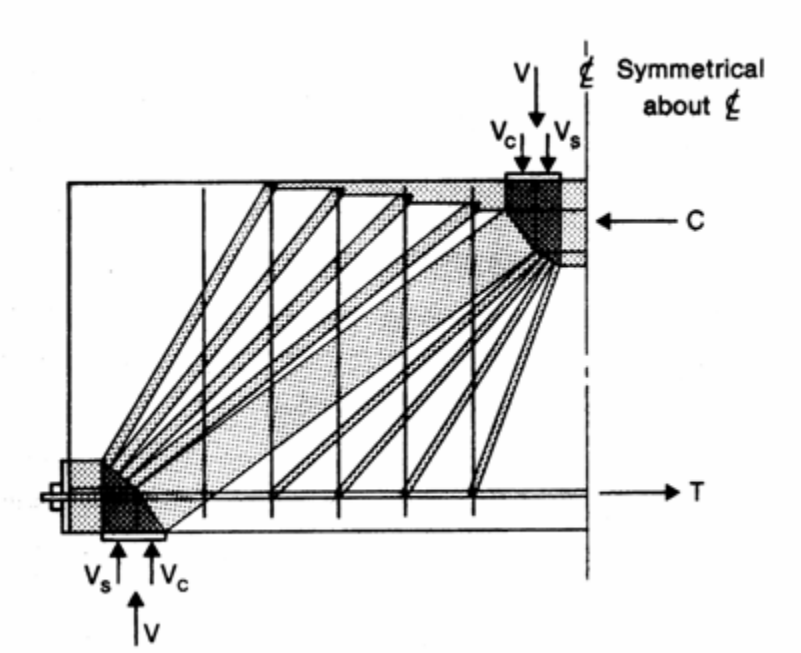

Figure 6.15 Plastic truss model for beam with vertical reinforcement (Rogowsky and Mac Gregor 1983)

In Fig. 6.15, the contribution of vertical reinforcement comes from the plastic truss formed by struts radiating from support and loading plates and vertical reinforcement. However, there are questions regarding the plastic truss: should all of the stirrups be incorporated into the truss? and Will the stirrups and main reinforcement reach yield before beam failure? Figure 6.15 shows that stirrups used in a truss depend on the compression zone at top of the beam and the compression fan that develops from the support and loading plates. Contour lines of principal compression strain of deep beam with various ratios of a/d and companion plastic truss models are shown in Fig. 6.16 to 6.22.

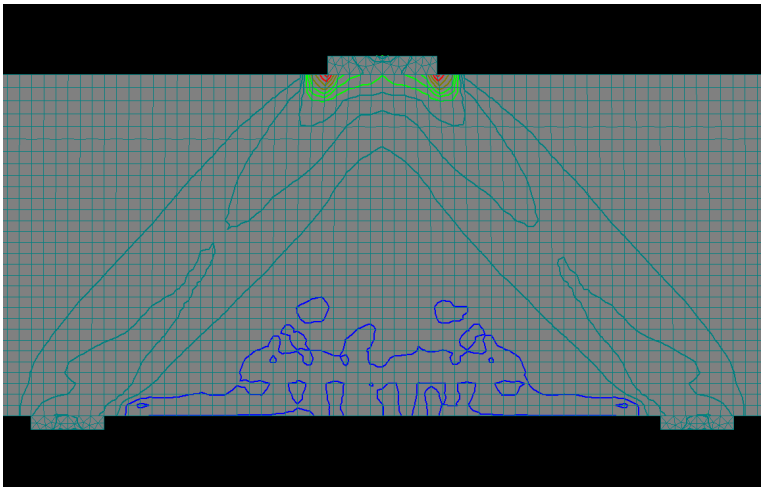

Figure 6.16 Contour lines of principal compression strain in deep beam with a/d=1.0

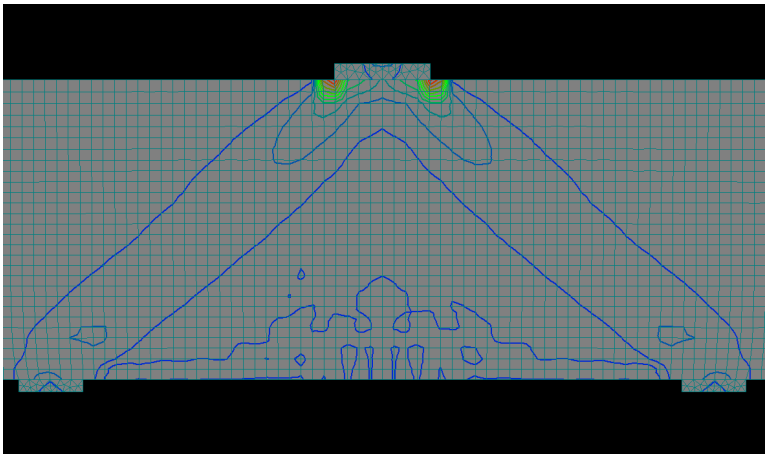

Figure 6.17 Contour lines of principal compression strain in deep beam with a/d=1.2

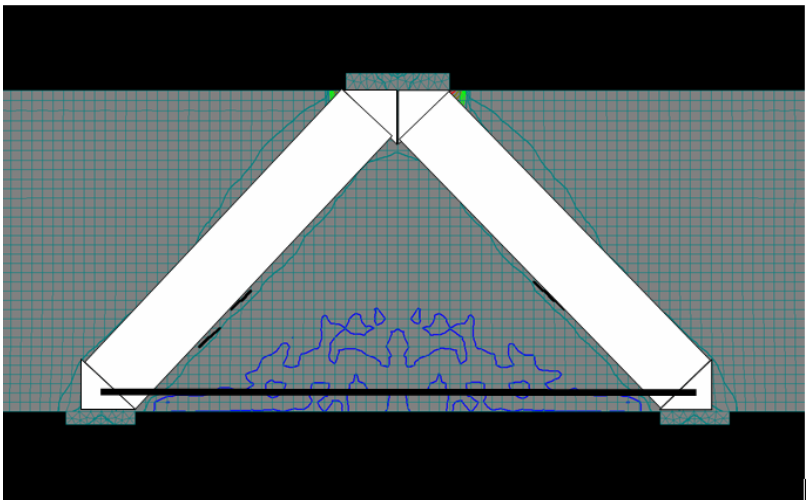

Figure 6.18 A plastic truss model for deep beam with a/d=1.0 and 1.2

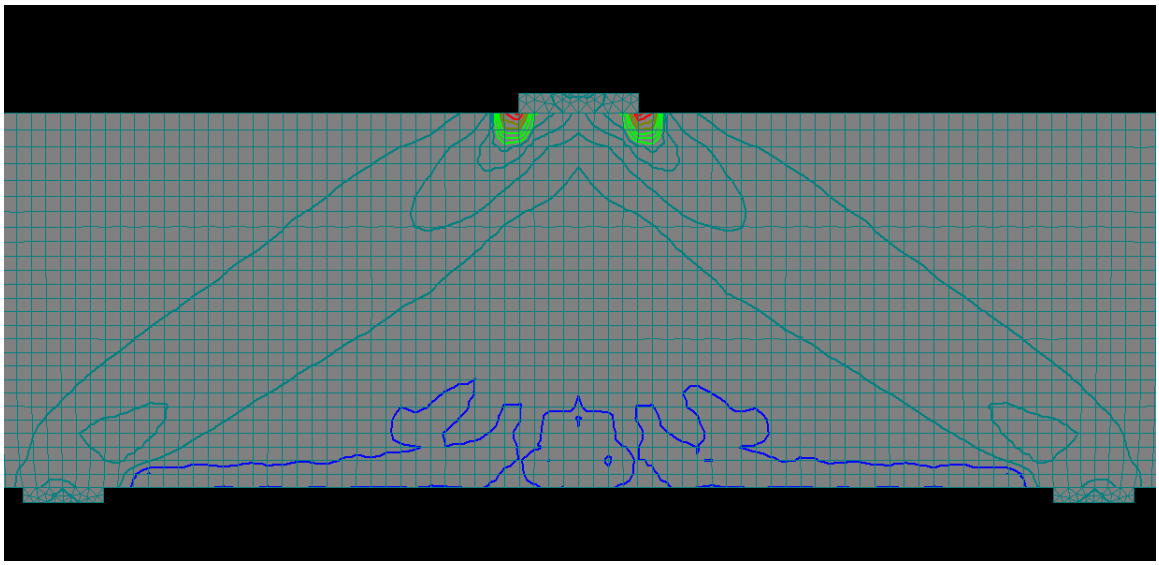

Figure 6.19 Contour lines of principal compression strain in deep beam with a/d=1.5

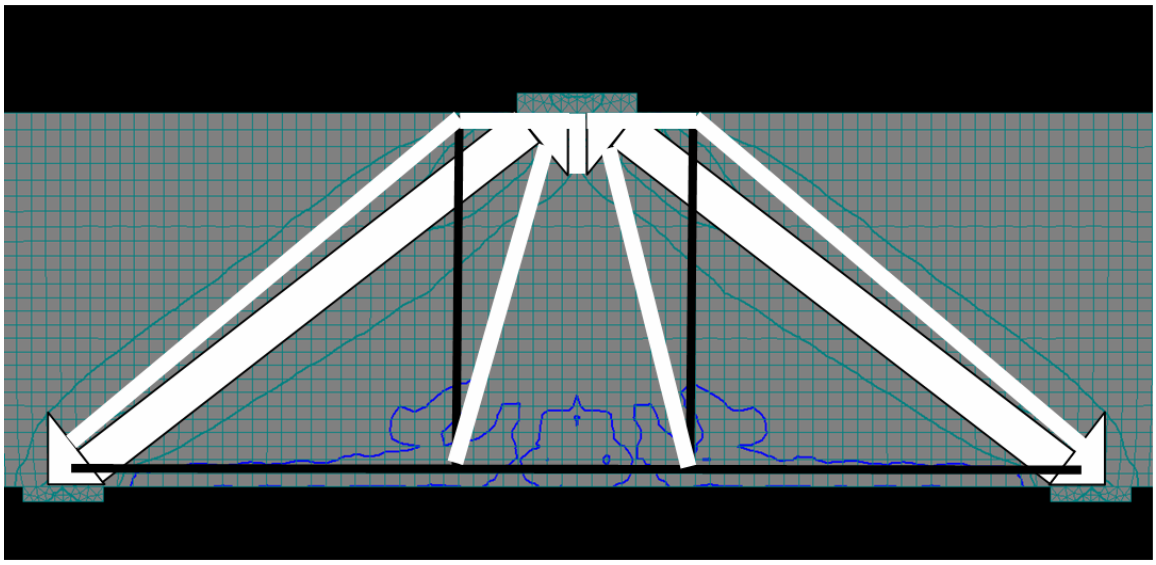

Figure 6.20 A plastic truss model for deep beam with a/d=1.5

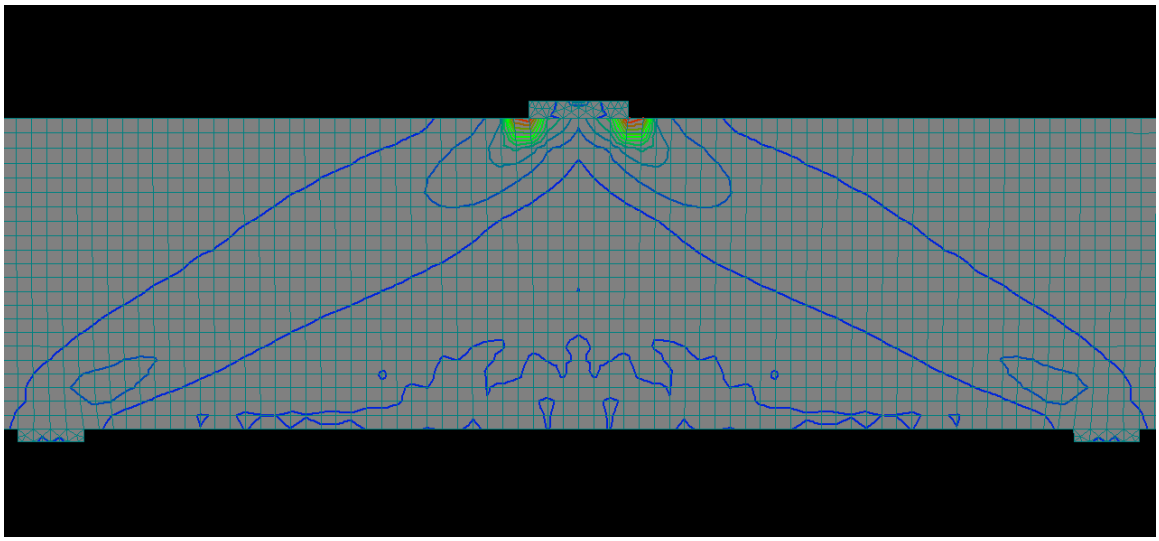

Figure 6.21 Contour lines of principal compression strain in deep beam with a/d=1.85

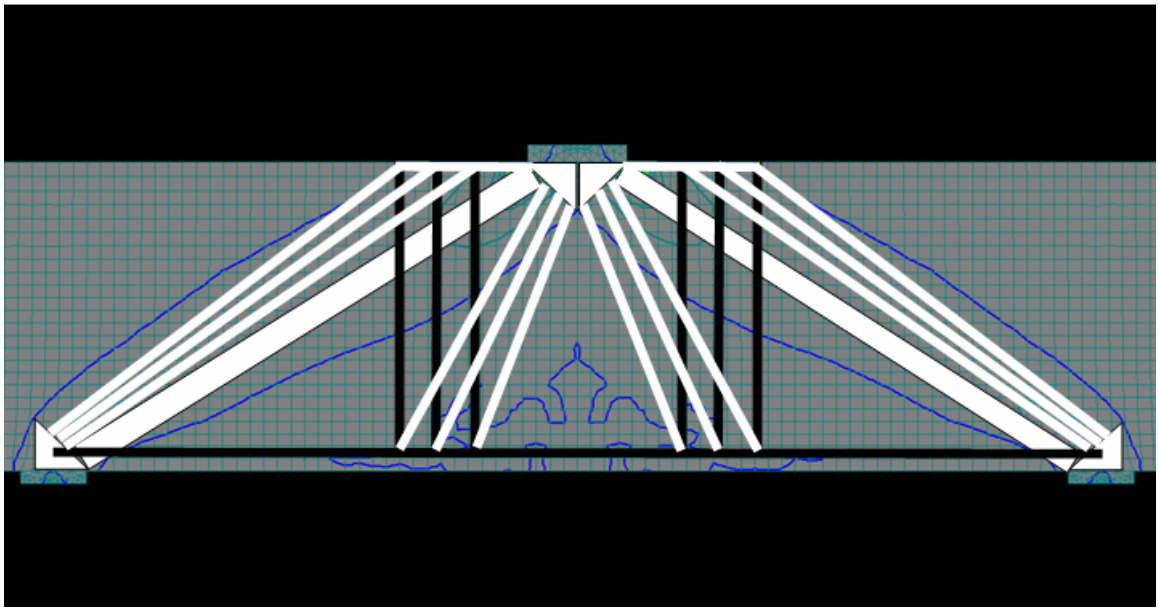

Figure 6.22 A plastic truss model for deep beam with a/d=1.85

Figures 6.23 and 6.24 help to answer the question regarding strains in the vertical reinforcement in deep beams having 0.3% and 0.6% vertical reinforcement. Figure 6.25 shows the strains along vertical reinforcing bars for a deep beam with a/d = 1.85. From the computer models it observed that strains in vertical reinforcement are largest through

the direct compression strut and they decrease rapidly at the upper of strut. It also observed that from Figs. 6.23 and 6.24, that vertical bars have the largest strains around the middle of the shear span. For deep beams with 0.3% vertical reinforcement almost all vertical bars reached yielding before failure. On the other hand, for deep beams with 0.6% vertical reinforcement no stirrups yielded before failure.

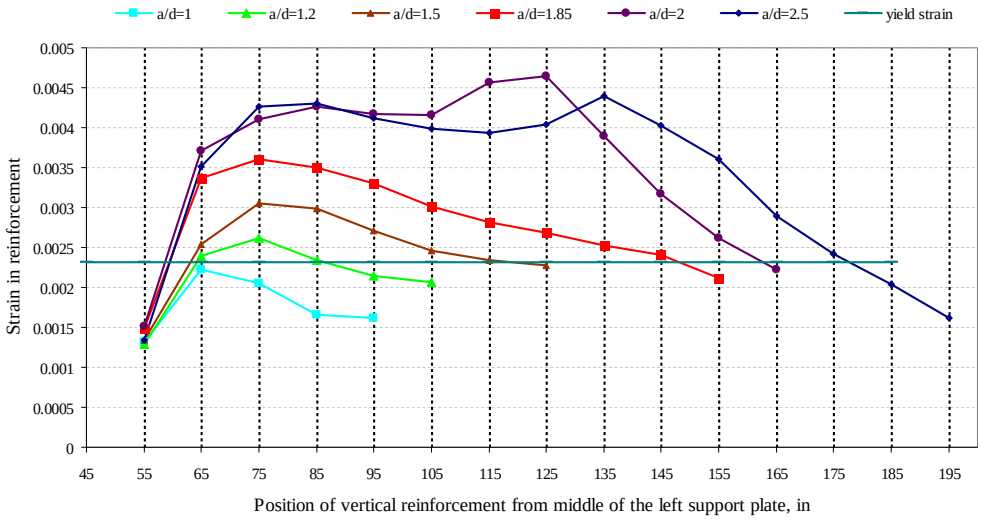

Figure 6.23 Strains in vertical reinforcement just before failure of deep beam having 0.3% vertical reinforcement

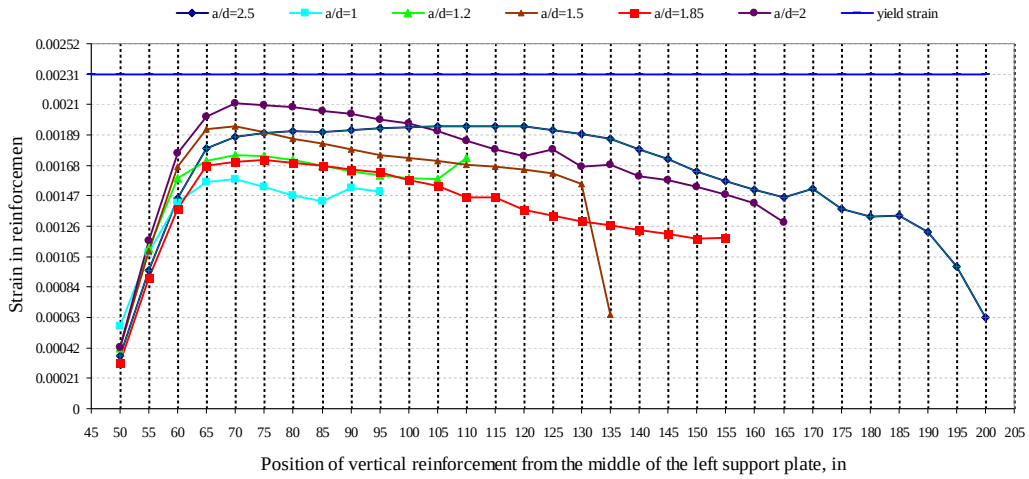

Figure 6.24 Strains in vertical reinforcement just before failure of deep beams having 0.6% vertical reinforcement

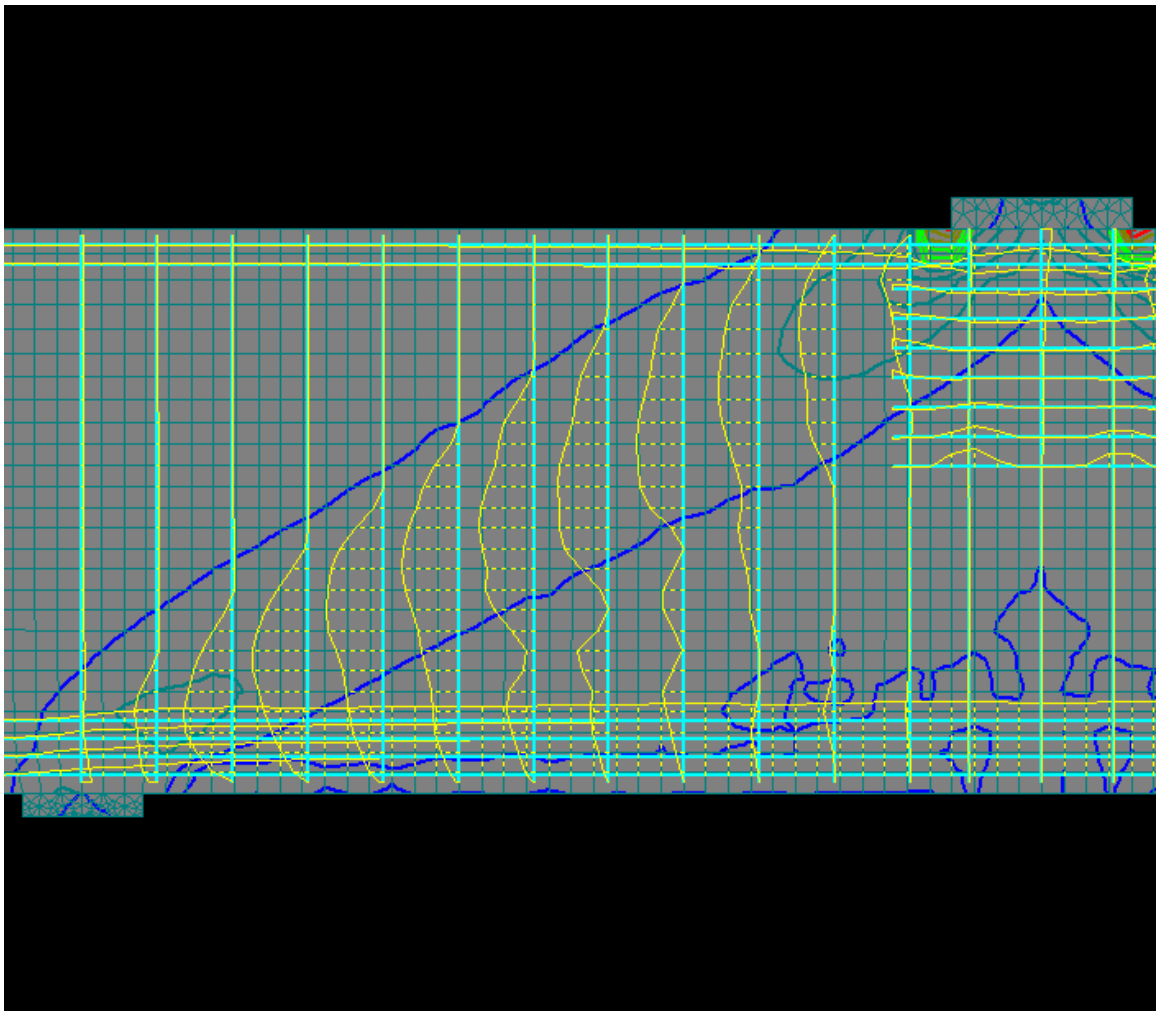

Figure 6.25 Distribution of strains in vertical reinforcement of deep beam a/d=1.85 having 0.3% stirrup

The contribution of vertical reinforcement to the shear capacity and maximum potential forces caused by the vertical reinforcement are shown in Table 6.1. ΔV_s represents the difference between the capacity of a beam without web reinforcement and one with vertical reinforcement. The maximum possible contribution would be given by $A_v f_y$ where A_v is the area of vertical reinforcement in the clear shear span.

Table 6.1 Contribution of vertical reinforcement at failure and total forces of stirrups

Amount of web reinforcement		Shear contribution, kip					
		a/d = 1.0	a/d = 1.2	a/d = 1.5	a/d = 1.85	a/d = 2.0	a/d = 2.5
0.3%	ΔV_s	141	141	162	162	162	202
	Maximum potential	159	223	314	438	482	588
0.6%	ΔV_s	192	232	263	303	293	283
	Maximum potential	246	357	512	547	738	890
1/3 clear shear span		108	124	166	166	166	208
ACI 318-99 steel contribution equation		48	81	95	112	119	143

It was observed from Table 6.1 the contribution of stirrups is close to the total forces in stirrups for deep beam having a/d = 1.0. However, for deep beams with a/d greater than 1.2 the difference between contribution of stirrups and total forces in stirrups is proportional to a/d. The ratio of contribution of stirrups to total forces of stirrups is close to 1/3 when the a/d ratio reaches 2.5 (Fig. 6.26) indicating that the vertical web reinforcement is about 1/3 effective when distributed uniformly along the clear shear span.

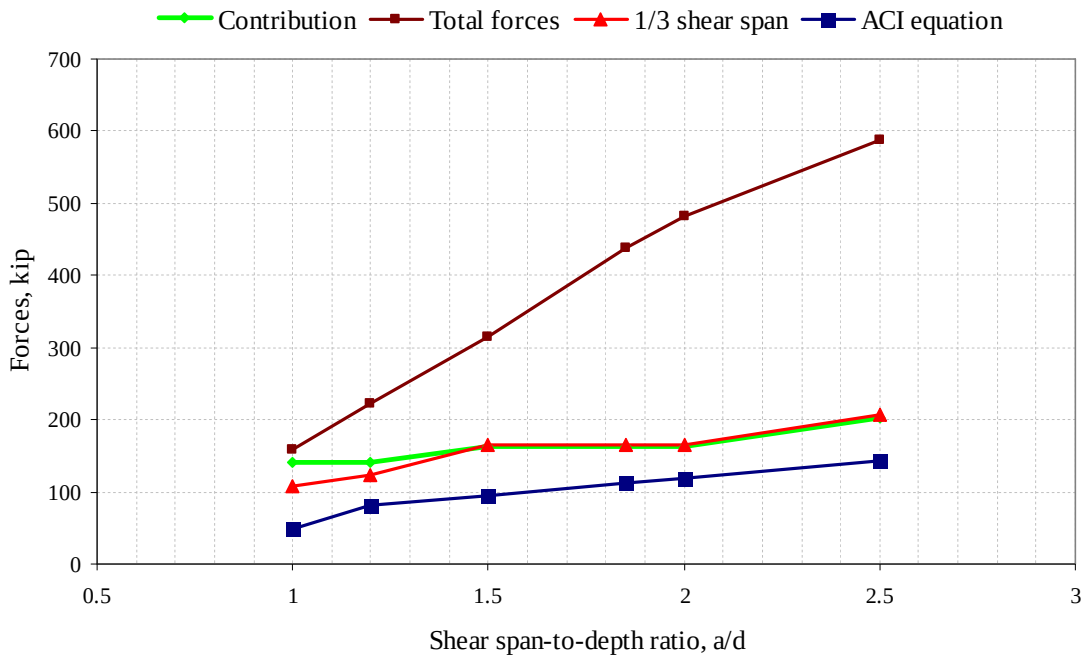

Figure 6.26 Comparison between contribution and total forces of stirrups in deep beams

The models show that the contribution of vertical reinforcement to shear strength of deep beams with a/d less than 1.2 is minimal. In such beams, shear strength is primarily a function of concrete strength and the steel contribution can be ignored.

The plastic truss model for the contribution of vertical reinforcement was validated by models with a/d =1.85 having different details of vertical reinforcement. Three more models with a/d =1.85 were developed. One consists of 0.6% vertical reinforcement placed on one-third of the clear shear span closest to loading plate (Fig. 6.27). Another has 0.6% vertical reinforcement placed one-third of the clear shear span that is closest to the support plates (Fig. 6.28). The third has 0.6% vertical reinforcement placed at the middle third of the clear shear span (Figs. 6.29). In each case, the spacing between stirrups remains the same, so the amount of shear reinforcement is equal to 1/3 of that using uniform spacing over the entire shear span.

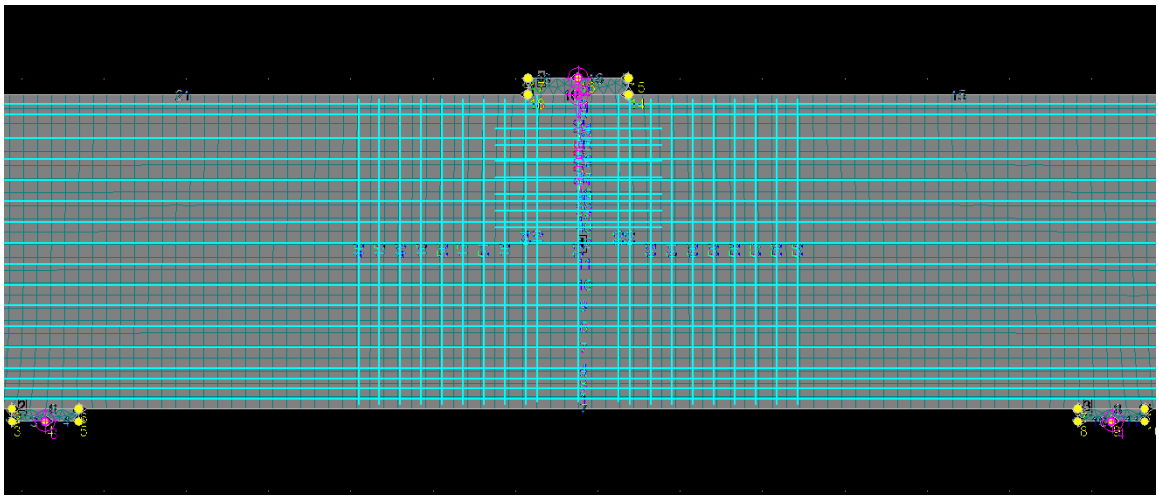

Figure 6.27 Deep beam with a/d=1.85 and vertical reinforcement placed close to loading plate

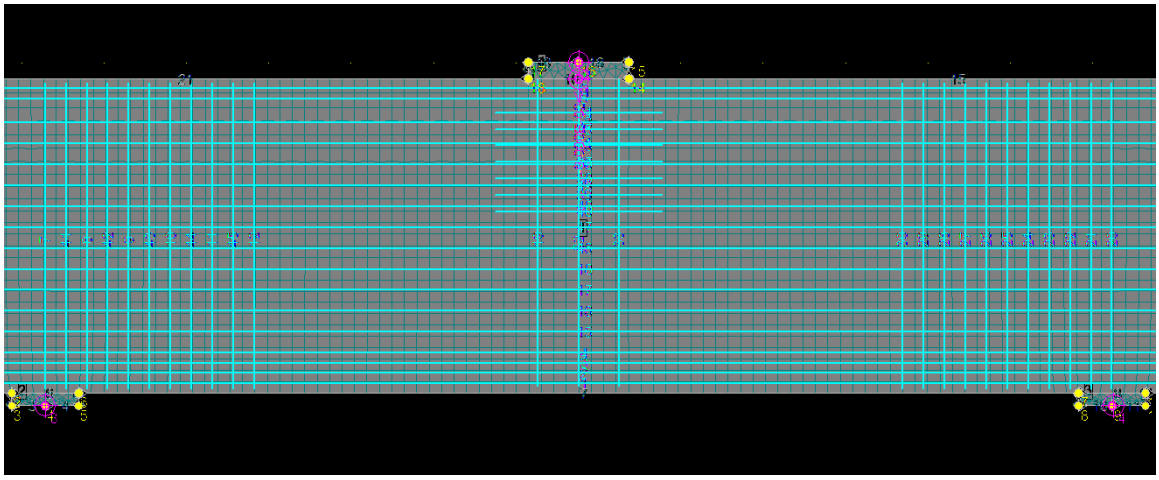

Figure 6.28 Deep beam with a/d=1.85 and vertical reinforcement placed close to support plates

Test results of these three computer models will be compared to the result of deep beam with a/d=1.85 and having 0.6% vertical reinforcement placed on whole of the shear span. This comparison of test results among three computer model tests is shown in Table 6.2.

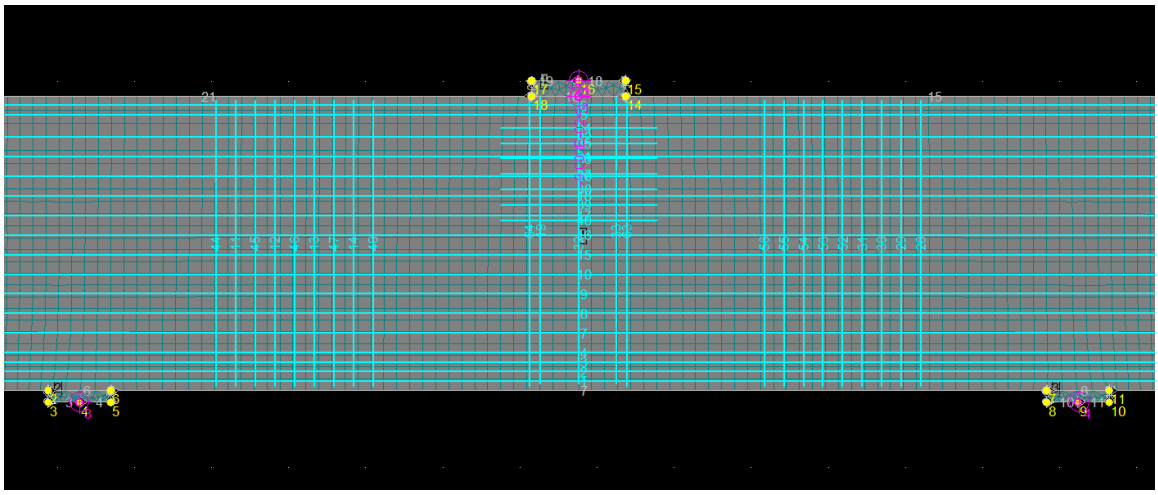

Figure 6.29 Deep beam with a/d=1.85 and 0.6% vertical reinforcement around mid shear span

Table 6.2 Comparison of ultimate shear among deep beams having a/d=1.85

Type of reinforcement	Ultimate shear, kip	V/V_{none}	$V/V_{0.6dist.}$
none	536	-	-
0.6% vertical	839	1.56	1.0
0.6% Close to loading plate	759	1.41	0.91
0.6% Close to support plates	546	1.02	0.65
0.6% around mid shear span	637	1.17	0.76

This result confirms the strength using a plastic truss model for the contribution of vertical reinforcement to the shear strength of deep beam. For deep beam with 0.6% vertical placed close to loading plate the ultimate shear is 759 kip. Difference is 9.6% compare to the deep beam with 0.6% vertical reinforcement placed shear span fully. However, for the deep beam with 0.6% vertical reinforcement placed close to the support plates difference is 35%. For the deep beam with 0.6% vertical reinforcement placed around middle span difference is 25%. The most efficient placement of vertical web reinforcement is adjacent to the loaded area.

6.2.2 Two span continuous deep beams

The behavior of two span continuous deep beams could be also divided into three stages. In the elastic range, continuous deep beams exhibit fan shapes of principal compression strain from support and loading plates (Fig.6.30).

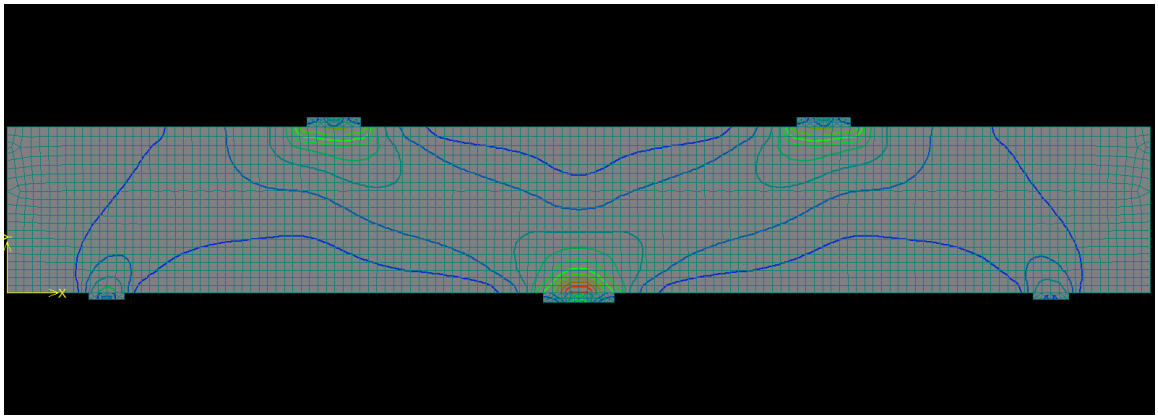

Figure 6.30 Contour lines of elastic principal compression strains of continuous deep beam with a/d = 1.2

In the second stage after flexural cracks form, the behavior of continuous deep beams depends on web reinforcement. For continuous deep beams with minimum 0.3%, web reinforcement, a plastic truss consisting of a concrete strut and steel tie in each span (Fig. 6.30). It was observed that strains in longitudinal reinforcement over middle support and bottom are almost constant along each span. This is confirmed by observations from experimental studies reported in the literature. For deep beams without web reinforcement a plastic truss forms between two loading plates and middle support plate (Fig. 6.31 and 6.32).

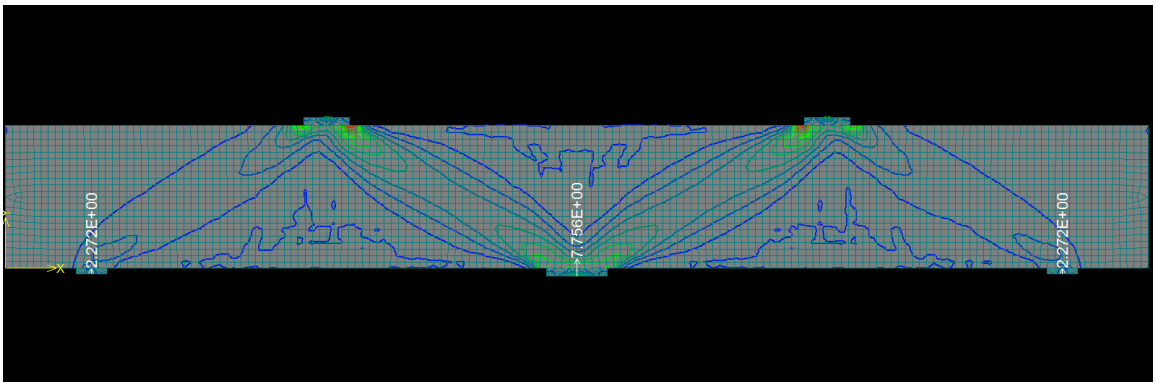

Figure 6.31 A plastic truss of continuous deep beam with a/d = 1.5 and 0.3% web reinforcement forming just before failure

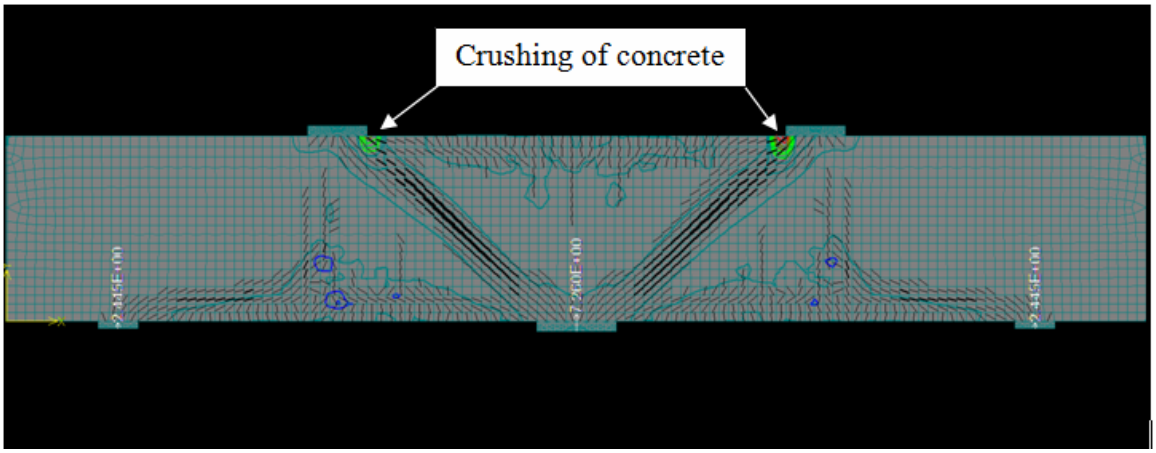

Figure 6.32 A plastic truss of continuous deep beam with a/d = 1.0 and without web reinforcement forming at just before failure

Two span continuous deep beams reach failure when the compression zone at the edge of the loading plates that is between the loading and middle support plate begins to crush. Deformation prior to failure also depends on web reinforcement. For deep beams with no or 0.3% web reinforcement failure occurs suddenly. For deep beams with greater than 0.6% vertical web reinforcement there is more deformation before failure.

(a) The influence of concrete strength on the shear strength of continuous deep beam

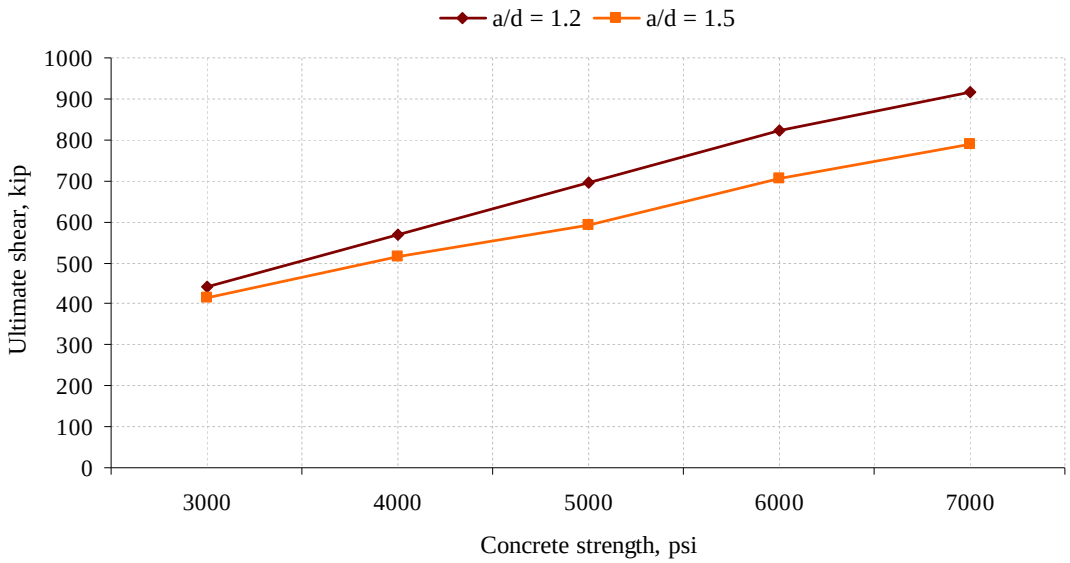

Figure 6.33 The influence of concrete strength on the shear strength of continuous deep beam

It was observed from the models that the shear strength of continuous deep beams is proportional to concrete strength. This behavior was also observed in results of models of simply supported deep beam. It also showed that the slope of shear strength is inversely proportional to shear span-to-depth ratio. The strength of continuous deep beams with a/d ratios less than 1.5 is governed by direct compression strut (Fig. 6.31 and 6.32).

(b) The influence of web reinforcement on the shear strength of continuous deep beam

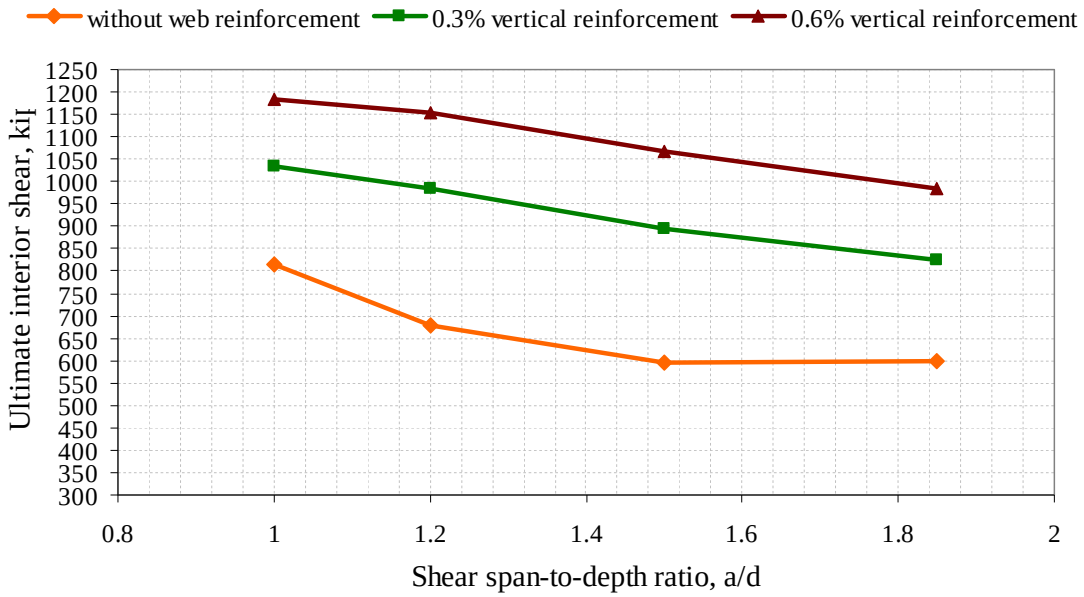

Figure 6.34 The influence of web reinforcement on shear strength of continuous deep beam

Figures 6.34 and 6.35 show that vertical web reinforcement is more effective for two span continuous deep beams. In Fig.6.35 for deep beams without web reinforcements there is little different between simply supported and continuous deep beams. However, for the same amount vertical web reinforcement used, continuous deep beams gained more shear strength for the same geometry. In Fig. 6.34 it was observed that vertical web reinforcement reduced the influence of shear span-to-depth ratio on the shear strength of continuous deep beams. This was also observed by Rogowsky and MacGreogor (1983).

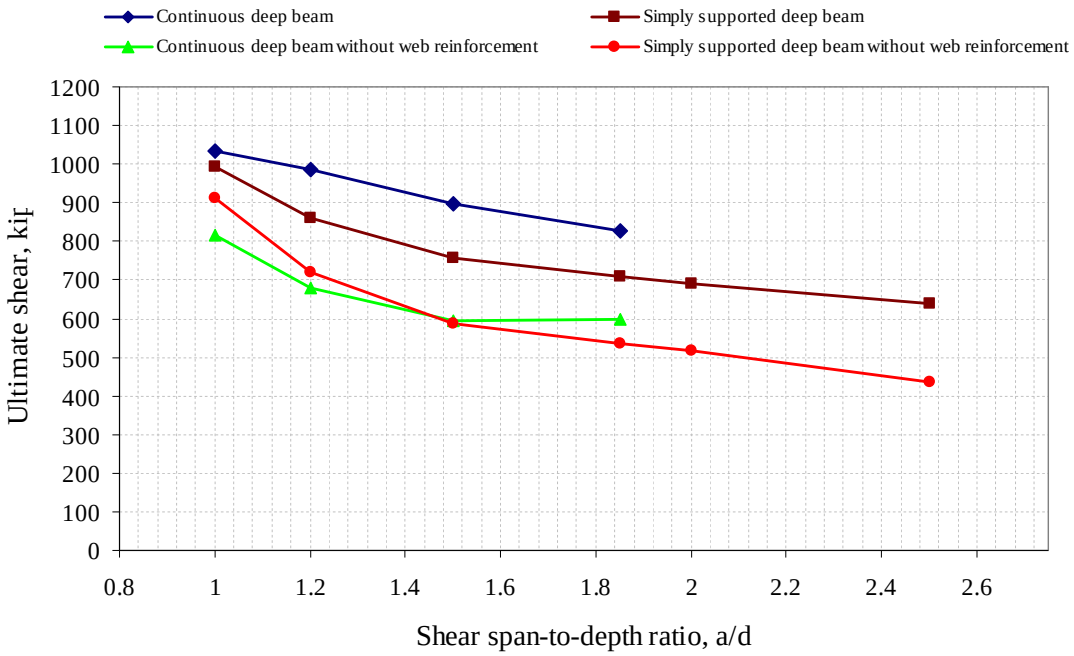

Figure 6.35 Comparison ultimate shear between single and continuous deep beams

6.3 Proposed design equation for shear strength of deep beams

6.3.1 Simply supported deep beams

Shear strength of a deep beam can be expressed as the sum of the contributions of concrete and web reinforcements as follows:

$$V_n = V_c + V_s \qquad (6.1)$$

where,

V_n is the nominal shear strength of a deep beam

V_c is the shear contributed by concrete

V_s is the shear contributed by web reinforcement

(a) Contribution of concrete on the shear strength of deep beam

Based on computer model results (Figs. 6.16 - 6.22) for simply supported deep beams a model of a direct compression strut (Fig. 6.36) could be used to calculate the contribution of concrete to the shear strength of a deep beam. The assumptions made in the calculated strength of a direct compression strut are:

(1) Equilibrium condition must be satisfied.

(2) Strut has the uniaxial compression stress.

(3) Node zone has a plane hydrostatic stress field.

(4)The concrete only resists compression and has an effective compressive strength $f^*_c = \nu f'_c$, where, $\nu < 1.0$ and discussed below.

(5) Steel is required to resist all tensile forces and is assumed to be at yield.

(6) Failure of model occurs by crushing of concrete in strut or node zone after steel yields.

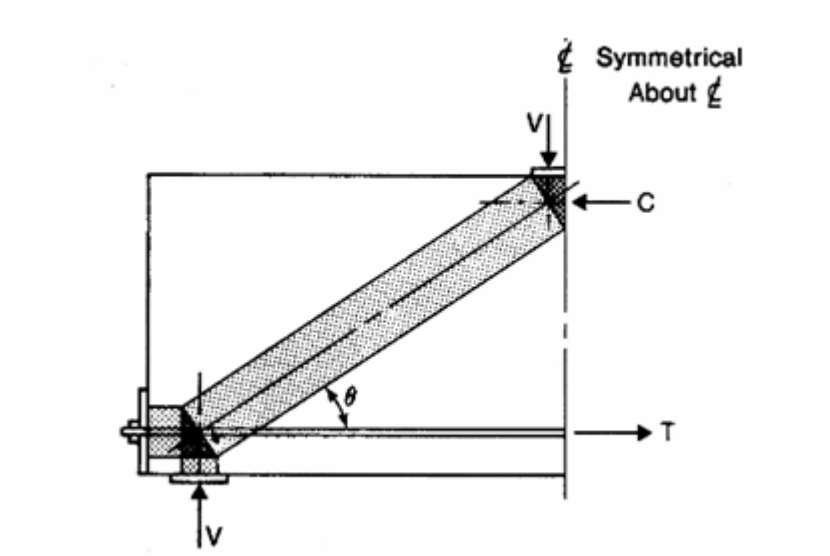

Figure 6.36 A direct compression strut model (Rogowsky 1983)

Strength can be calculated using a direct compression strut model shown in Fig. 6.37.

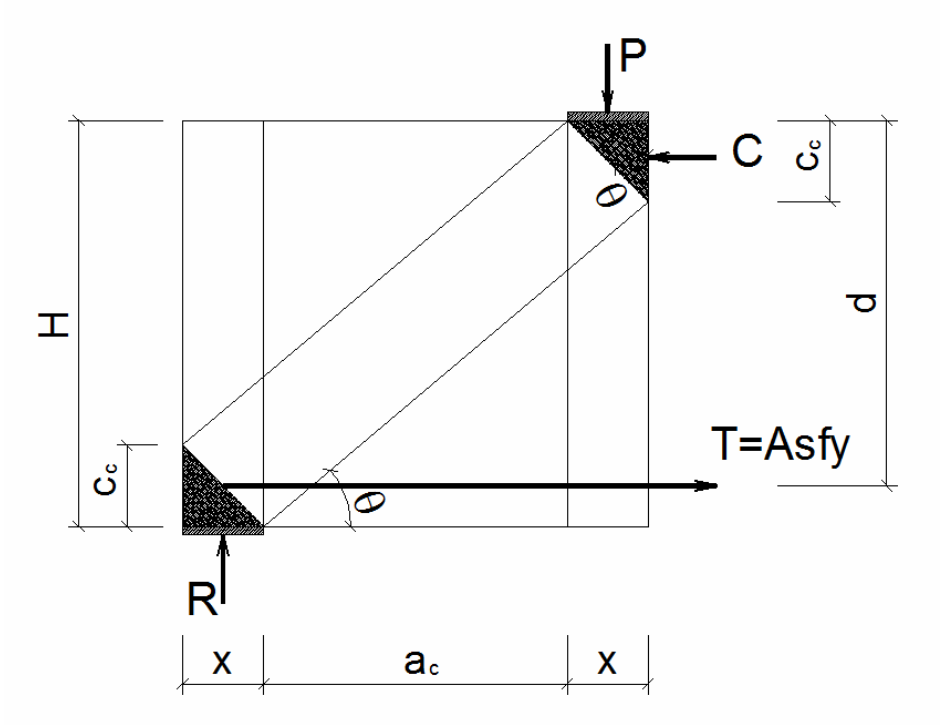

Figure 6.37 Details of the model of direct strut

Assuming that a single shear span of a deep beam under single loading is shown in Fig. 6.37. The deep beam has:

a_c is the clear shear span of horizontal length from the face of support to the face of loading plate,

d is the effective depth of beam,

H is the total height of beam,

b_w is the width of beam,

x is the length of support plate satisfying bearing stress limits,

A_s is the longitudinal steel area.

A relationship between θ and the beam geometry is as follows:

$$\tan\theta = \frac{H - c_c}{a_c + x} = \frac{x}{c_c} \tag{6.2}$$

Before failure, it is assumed that the steel tie has yielded and stresses in strut and node zone reach the concrete compressive strength f_c'. The tensile force of longitudinal

steel is T = $A_s f_y$, and the compression force of concrete is C = $f_c' c_c b_w$, and external load P = $f_c' x b_w$.

To maintain equilibrium condition:

$$C = T \tag{6.3}$$

For a deep beam with given geometric dimensions and longitudinal steel area, the maximum shear capacity of the shear span (P or R) that the deep beam can carry can be obtained from Eq. (6.2) and lead to a quadratic equation in (*x*/H) as follows:

$$\left(\frac{x}{H}\right)^2 + \left(\frac{a_c}{H}\right)\left(\frac{x}{H}\right) - \left(\frac{c_c}{H}\right)\left(1 - \frac{c_c}{H}\right) = 0 \tag{6.4}$$

Solving Eq.(6.4) for (*x*/H), the following equation is obtained:

$$\left(\frac{x}{H}\right) = \frac{1}{2}\left(\sqrt{\left(\frac{a_c}{H}\right)^2 + 4\left(\frac{c_c}{H}\right)\left(1 - \frac{c_c}{H}\right)} - \frac{a_c}{H}\right) \tag{6.5a}$$

Multiplying both sides of Eq. (6.5a) with (H/d), one obtained:

$$\left(\frac{x}{d}\right) = \frac{1}{2}\left(\sqrt{\left(\frac{a_c}{d}\right)^2 + 4\left(\frac{c_c}{d}\right)\left(1 - \frac{c_c}{d}\right)} - \frac{a_c}{d}\right) \tag{6.5b}$$

From Eq. (6.3) it obtained:

$$T = C \rightarrow \alpha_1 f_c' c_c b_w = A_s f_y$$

and,

$$c_c = \frac{A_s f_y}{\alpha_1 f_c' b_w} \tag{6.6}$$

and,

$$\frac{c_c}{d} = \frac{A_s}{b_w d}\frac{f_y}{\alpha_1 f_c'} = \frac{1}{\alpha_1}\rho\frac{f_y}{f_c'} \tag{6.7}$$

finally, it obtained the maximum external load P that the deep beam carried:

$$P_{\max} = x b_w v f_c' = b_w d \frac{x}{d} v f_c' = \left(\sqrt{\left(\frac{a_c}{2d}\right)^2 + \frac{1}{\alpha_1}\rho\frac{f_y}{f_c'}\left(1 - \frac{1}{\alpha_1}\rho\frac{f_y}{f_c'}\right)} - \left(\frac{a_c}{2d}\right)\right) b_w d v f_c' \tag{6.8}$$

hence,

$$V_c = \left(\sqrt{\left(\frac{a_c}{2d}\right)^2 + \frac{1}{\alpha_1}\rho\frac{f_y}{f_c^{'}}\left(1 - \frac{1}{\alpha_1}\rho\frac{f_y}{f_c^{'}}\right)} - \left(\frac{a_c}{2d}\right) \right) b_w d \nu f_c^{'} \qquad (6.9)$$

where,

a_c is a clear shear span, in

d is an effective depth of cross section, in

b_w is a width of deep beam, in

α_1 is the 0.85 factor in ACI Section 10.2.7.1

ρ is a ratio of tensile longitudinal reinforcement

f_y is yielding strength of longitudinal reinforcement, ksi

$f^*_c = \nu f'_c$ is an effective compressive strength, ksi

Using Eq. (6.9), the maximum shear force of a given deep beam depends on the: shear span-to-depth ratio, a/d; flexural reinforcement ratio; ratio of yield strength of steel to compressive strength of concrete; and compressive concrete strength. It showed that in Eq. (6.9) the shear strength of a deep beam is proportional to compressive concrete strength, not to the square root of compressive concrete strength. The influence of parameters identified above on V_c are shown in Figs. 6.38, 6.39, and 6.40. This is confirmed by experimental studies (Smith and Vantsiotis) and computer model tests of deep beams.

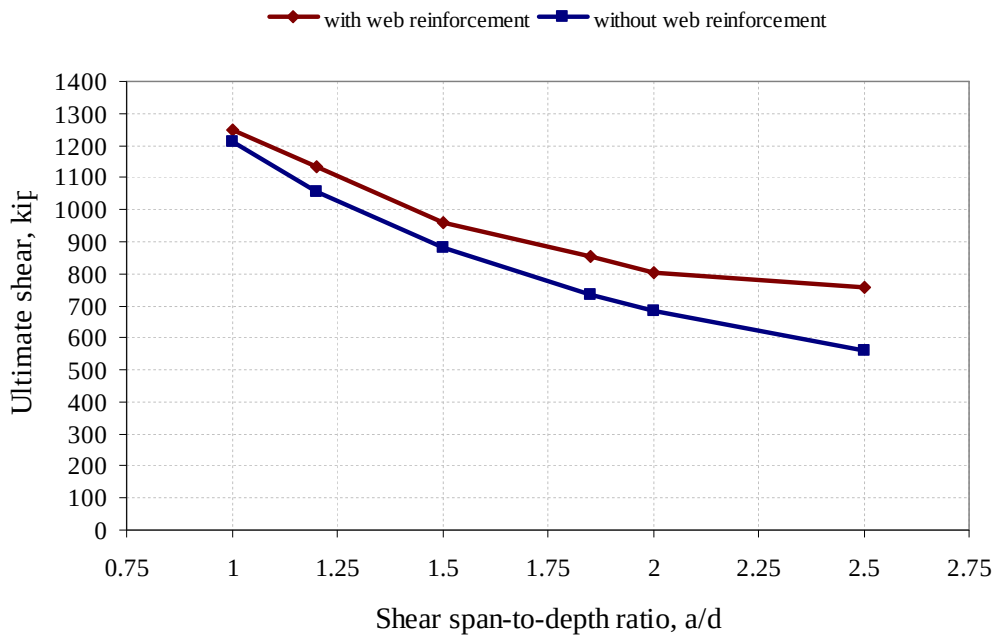

Figure 6.38 The influence of a/d ratio on the V_c

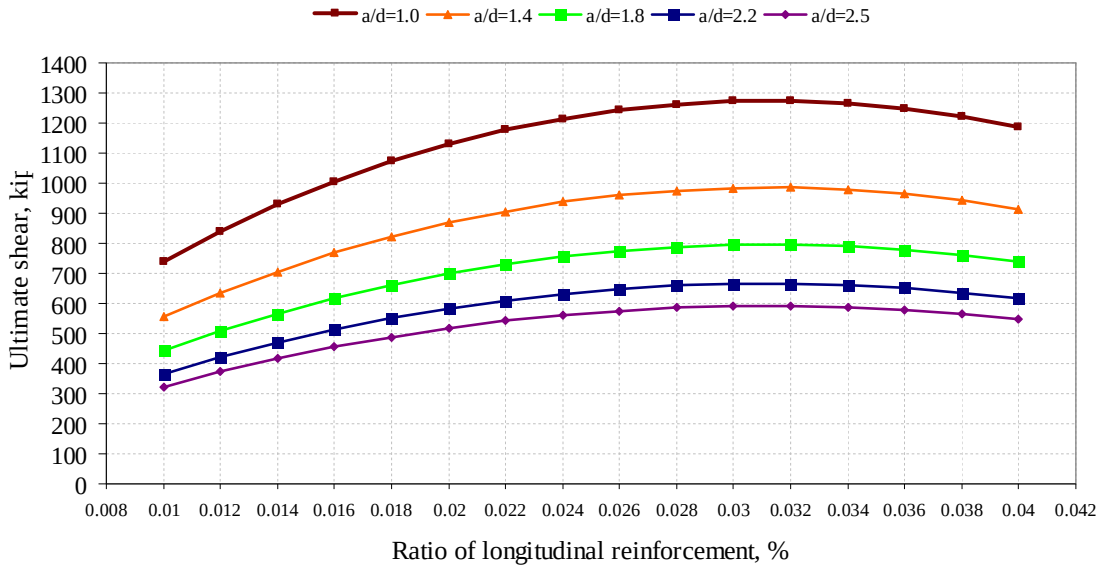

Figure 6.39 The influence of longitudinal reinforcement ratio on V_c

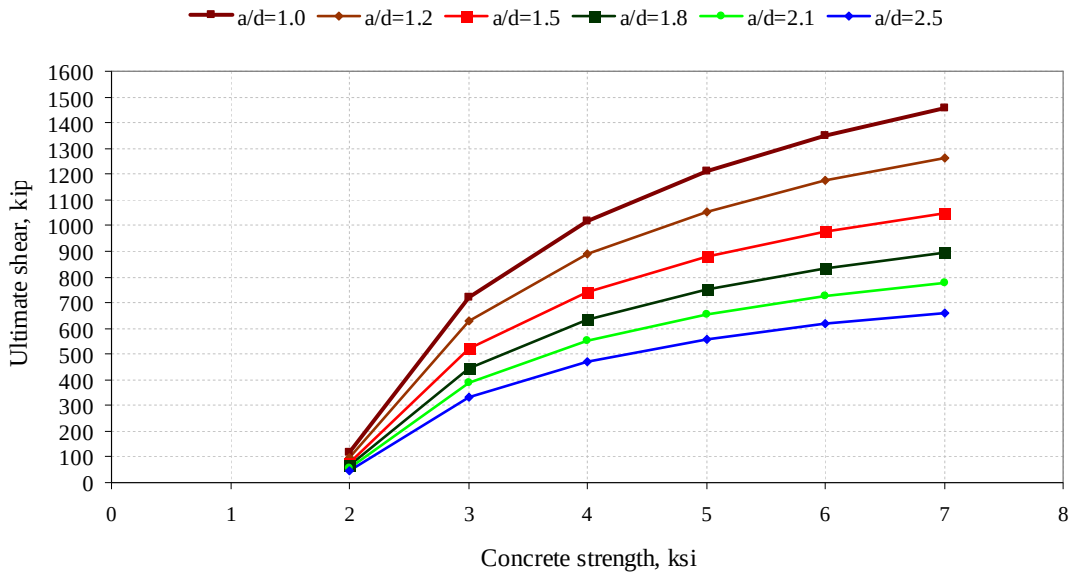

Figure 6.40 The influence of concrete strength on V_c

Details of effective compressive strength of struts were presented in ACI SP - 208, 2002. and ACI-ASCE committee on Shear and Torsion 1997.

(b) The contribution of vertical web reinforcement

The contribution of vertical web reinforcement is calculated based on a model of the plastic truss shown in Fig. 6.14.

Results of models of simply supported deep beams with 0.3% and 0.6% vertical reinforcement are shown in Figs. 6.23 and 6.24. It showed that from Fig. 6.23 a plastic truss formed in deep beams with 0.3% vertical reinforcement. But for deep beams with 0.6% vertical reinforcement all stirrups did not yield before the deep beams failed. It was observed from Table 6.1 and Fig. 6.26 the contribution of vertical reinforcement is about one-third of total capacity of the stirrups. It also shows that the ACI 318-99 for calculating contribution of vertical reinforcement is quite conservative.

It could be concluded from computer models and comparison of the contribution of vertical reinforcements that a plastic truss could be developed to reflect the contribution of all vertical reinforcements. However, for simplicity a conservative

estimate of the contribution of vertical reinforcement is to consider only 1/3 of the vertical reinforcement to be effective. The equation for contribution of vertical reinforcement is:

$$V_s = \frac{1}{3} f_y A_s \frac{a_c}{s} \tag{6.10}$$

where,

V_s is the contribution of vertical reinforcement, kip

f_y is the yield strength of vertical reinforcement, ksi

A_s is area of vertical reinforcement, in^2

s is spacing c-c of vertical reinforcement, in

a_c is the clear shear span, in

6.3.2 Validation of the proposed equations for shear strength of simply supported deep beams

In this part, the equations of shear strength of deep beams developed above will be compared with ACI 318-99 using shear database mentioned in Chapter 3.

Before applying the proposed equation for calculating shear strength of simply supported deep beams on effectiveness factor is needed to determine the concrete contribution. From tests and literature, various investigators have proposed different values of the effectiveness factor ν. Rogowsky and MacGregor (1986) proposed ν = 0.85 based on their experimental tests of simply and continuous deep beams. Risketts (1985) indicated that ν was closer to 1.0 than 0.6. Marti (1985) recommended a constant value of ν = 0.6. In 1991, Ramirez and Breen suggested a relation ship between ν and $\sqrt{f'_c}$ with ν ranging form 0.55 to 0.39 for f'_c ranging from 3000 to 6000 psi. From the test results a constant value of ν = 0.6 is proposed.

The comparison between shear strength of Smith and Vantsiotis's tests (1982) and the shear strength using the proposed equation is shown in Fig. 6.41.

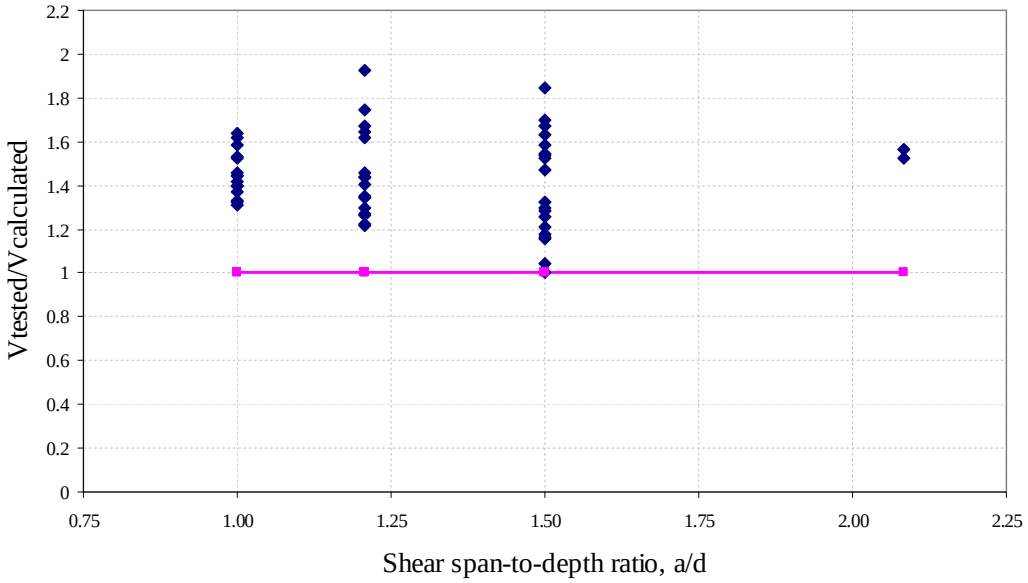

Figure 6.41 Comparison between shear strength of Smith and Vantsiotis beams and calculated shear using the proposed equation

The comparison between shear strength of Rogowsky and MacGregor (1983) beams and calculated shear strength using the proposed equation is shown in Fig. 6.42.

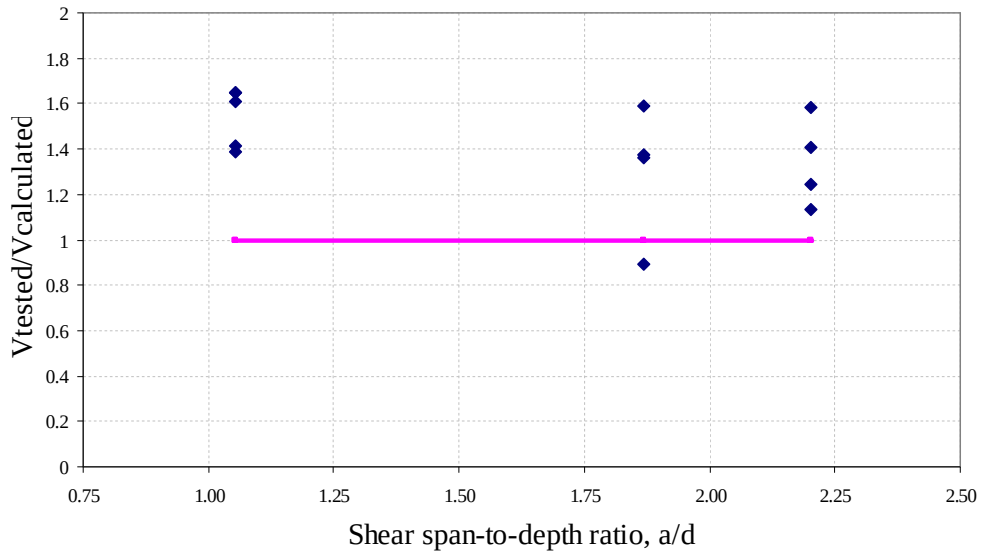

Figure 6.42 Comparison between shear strength of Rogowsky and MacGregor beams and calculated shear using the proposed equation

The comparison between shear strength of Birrcher (2008) beams and calculated shear using the proposed equation is shown in Fig. 6.43.

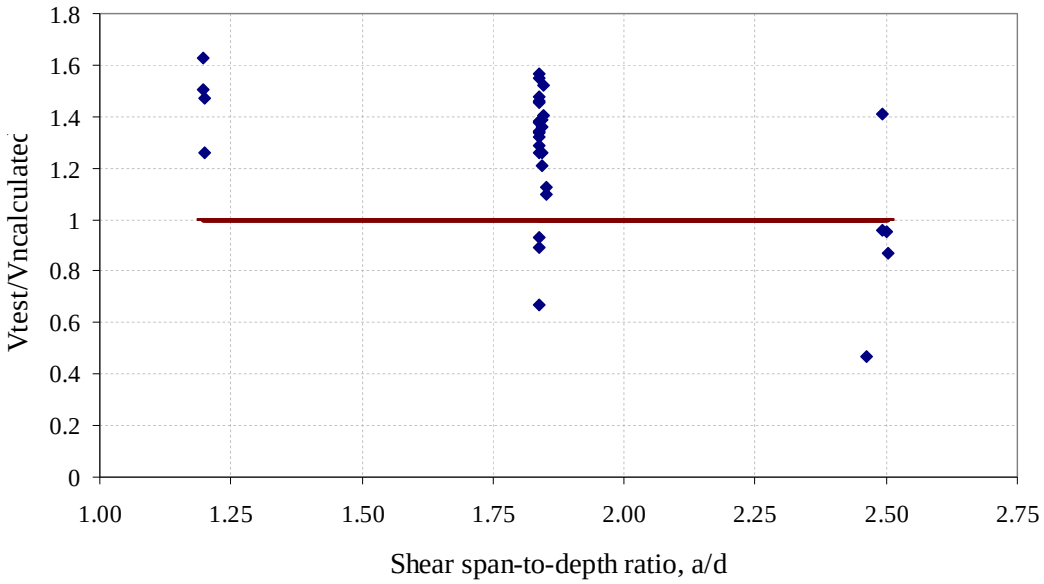

Figure 6.43 Comparison between shear strength of Birrcher beams and calculated shear using the proposed equation

It was observed that there are three unsafe cases in the Birrcher beams with a/d = 1.84 when using the proposed equation. However, it showed from database that these cases have the shear strength is unusually low compare to other beams the same geometry and details of reinforcement. One is a deep beam with a/d = 18.4, ρ = 0.0231, and ρ_v = 0.001 having tested shear of 272.6 kip. While other deep beams the same geometry and ρ_v = 0.002 having tested shear around of 400 kip.

In Figure 6.44, the comparison between shear strength of Birrcher (2008) beams using the proposed equation and ACI 318-99 equation.

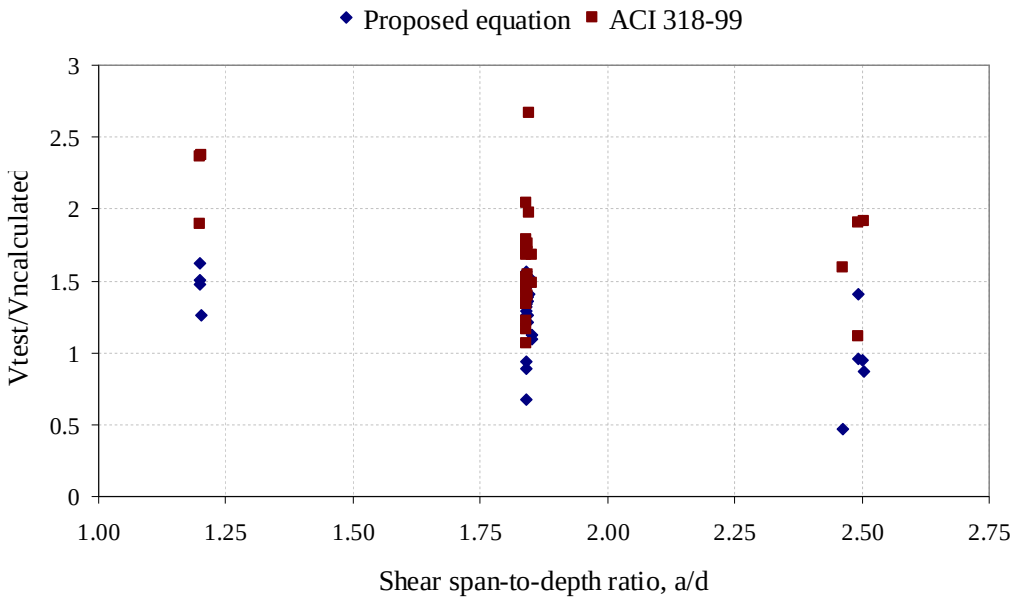

Figure 6.44 Comparison between proposed equation and ACI 318-99 by Birrcher's tests

The comparison between shear strength of Quintero Febres et al. (2006) beams and calculated shear using the proposed equation is shown in Fig. 6.45.

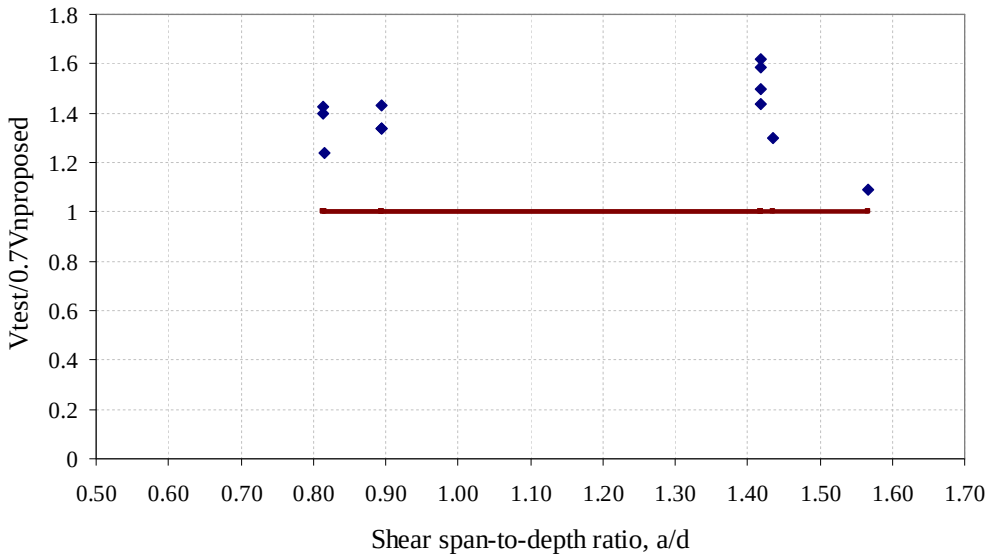

Figure 6.45 Comparison between shear strength of Quintero Febres et al (2006) beams and calculated shear using the proposed equation

The comparison between shear strength of beams in whole of shear database and calculated shear using the proposed equation is shown in Fig. 6.46.

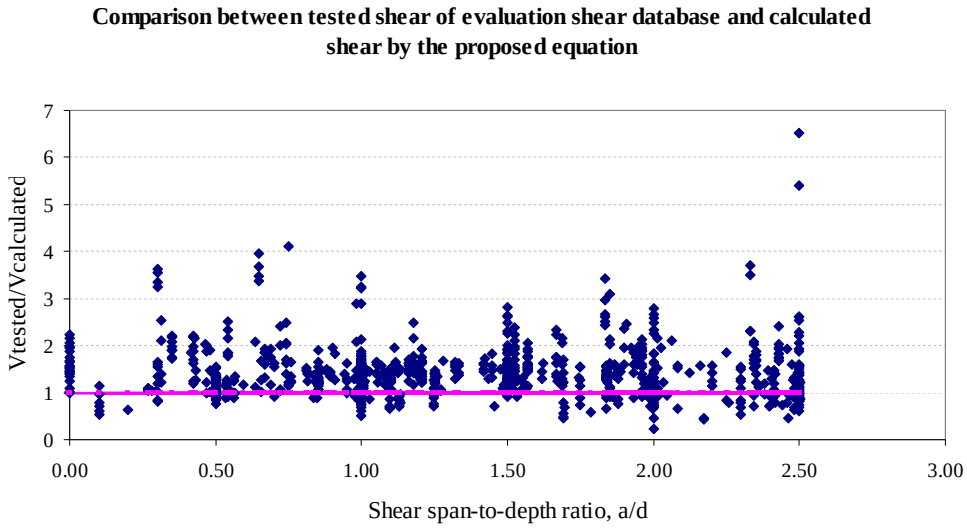

Figure 6.46 Comparison between shear strength of beams in whole database and calculated shear capacity using the proposed equations with ν = 0.6

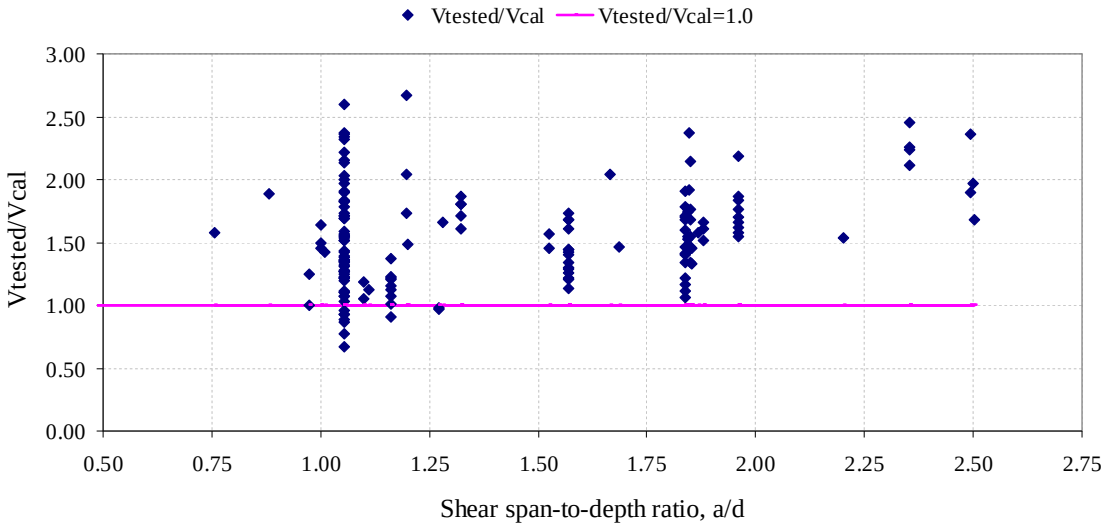

Figure 6.47 Comparison between shear capacity of beams in evaluation shear database and calculated shear capacity using ACI 318-99 equation

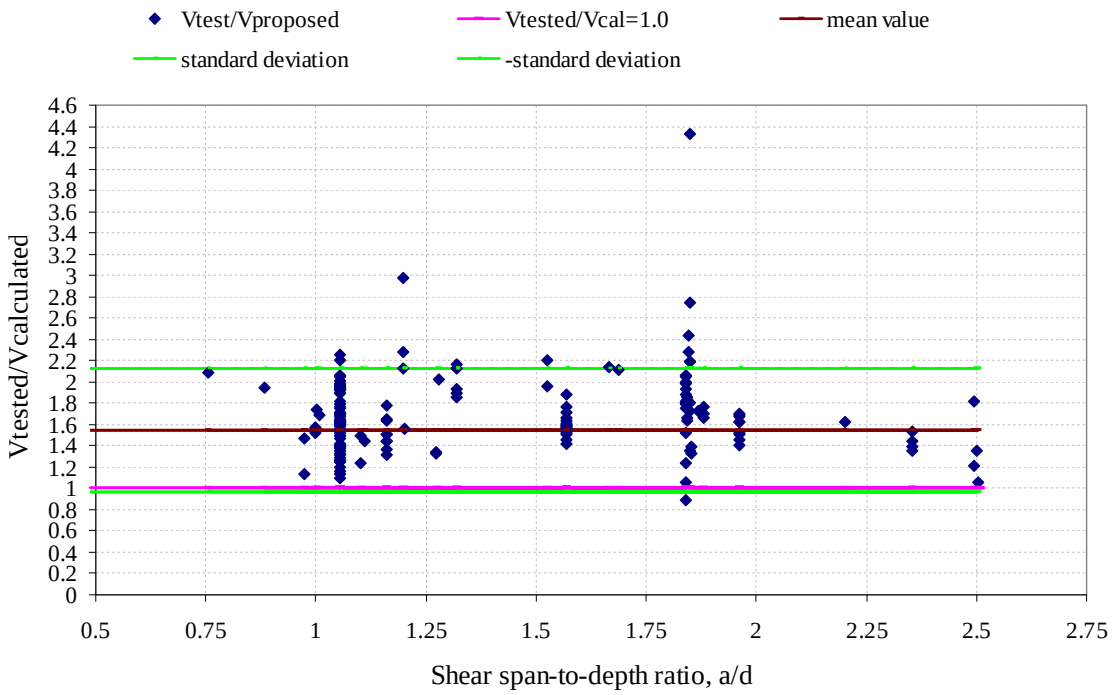

Figure 6.48 Comparison between shear capacity of beams in evaluation shear database and calculated shear capacity using the proposed equations with ν = 0.6

It was observed that the proposed design equation for shear strength of deep beams captured the shear strength of tested deep beams quite accurately (Figs. 6.41, 6.42, 6.43, and 6.44). The mean value of the proposed equation is 1.42 and standard deviation is 0.57. However, it still shows that there are ratios of tested shear to calculated shear less than 1.0. This result may come from the scattering behavior of reinforced concrete elements and there are still tested beams failing to filter criteria for evaluation shear database. The proposed equation predicts quite accurately the shear strength of deep beams with a/d less than 1.85, particularly for deep beams with a/d less than 1.5 (Figs. 6.41 and 6.42). But it shows unsafe prediction for deep beams with a/d greater than 1.85, especially for deep beams with a/d = 2.5 (Fig. 6.43). This result may come from the fundamental model of the proposed equation. The proposed equation has a good prediction for a beam behaving arch action predominantly. For deep beams with a/d equal to or greater than 2.0 the shear strength is governed primarily by a beam action. Thus, the ACI 318-99 equation predict shear strength of these beams pretty well (Fig. 6.47). Fig.

6.48 shows the comparison between shear capacity and calculated shear capacity of beams in the evaluation shear database. It shows that the proposed equations have a much better prediction than ACI 318-99 equation. The mean value of ratio of tested shear capacity to calculated shear capacity is 1.55 and standard deviation is 0.58. The statistical comparisons of the two approaches are summarized in Table 6.3.

Table 6.3 Comparison of proposed equation and ACI 318-99 equation

Equation	Number of tests	Average value V_{test}/V_{cal}	Standard deviation
Proposed	306	1.42	0.57
ACI 318-99	306	1.55	0.58

6.3.3 Two span continuous deep beams

It was observed that in a two span symmetrical continuous deep beam failure is governed by the shear strength of two direct struts forming between two loading plates and the mid support plate. One again, a fan shape compression stress field radiates from two loading plates and the mid support plate (Fig. 6.49).

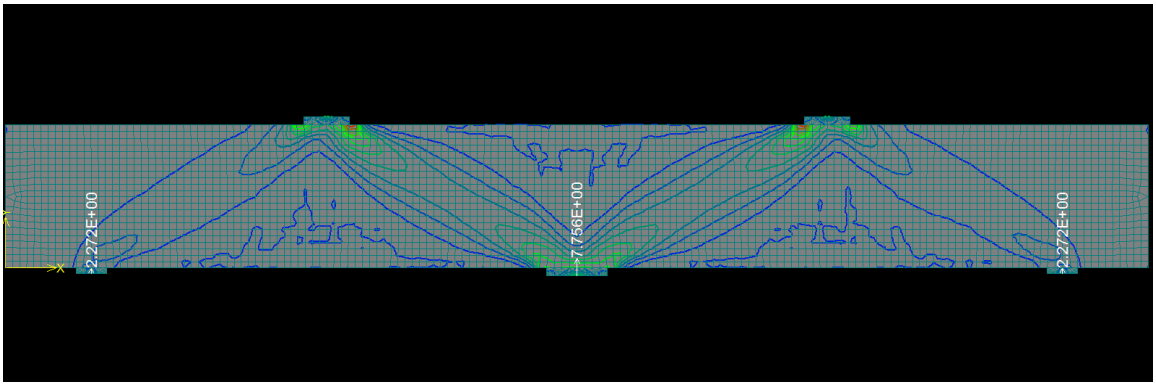

Figure 6.49 A plastic truss of continuous deep beam with a/d=1.5 and 0.3% vertical reinforcement

Strains in vertical reinforcement of continuous deep beams having 0.3% vertical reinforcement yielded along the entire clear shear span (Fig. 6.50). It means that shear

strength of continuous deep beams could be calculated by using a plastic truss as following (Fig. 6.51):

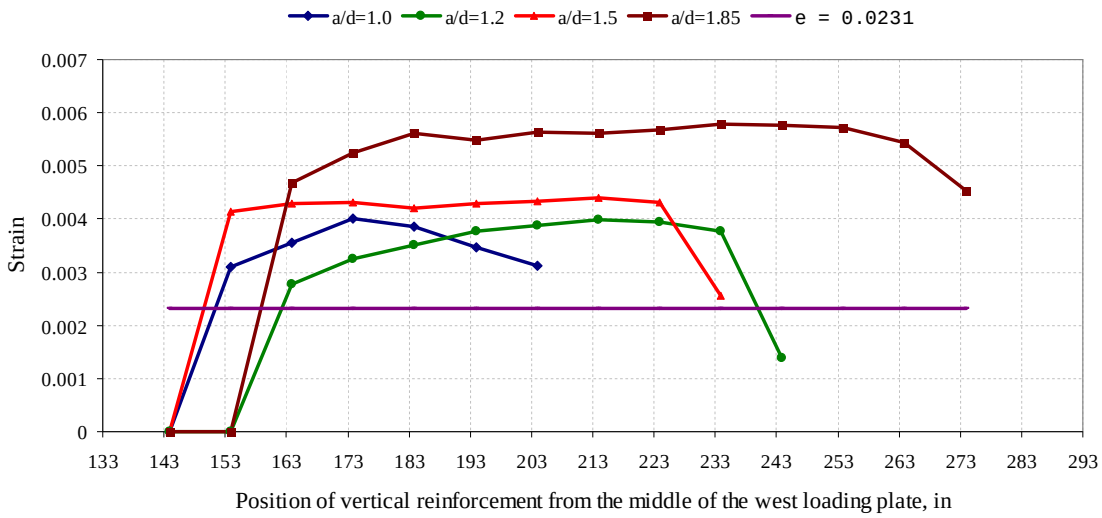

Figure 6.50 Strains in vertical reinforcement of continuous deep beams with 0.3% vertical reinforcement

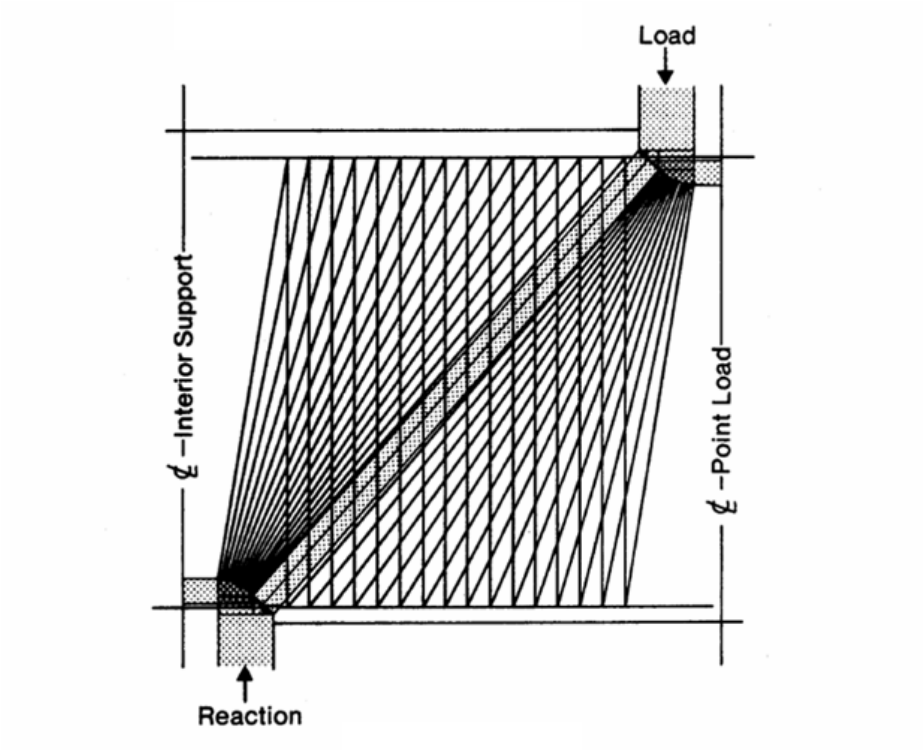

Figure 6.51 A plastic truss model for shear strength of continuous deep beams

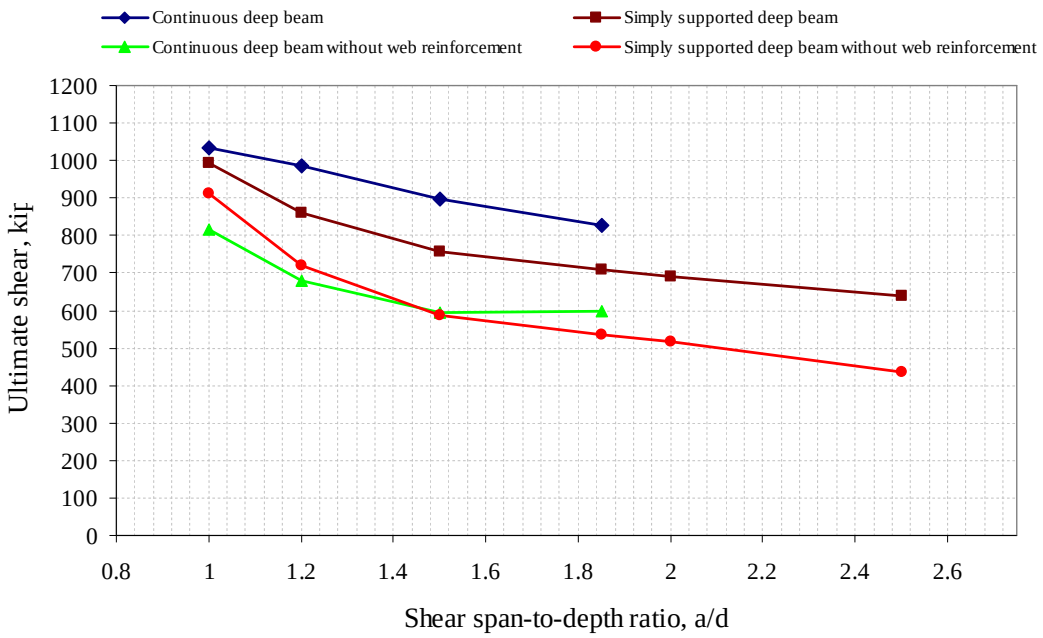

Figure 6.52 Comparison of the contribution of vertical reinforcement in a simply supported and continuous deep beam

In Fig. 6.52, it could be seen that for continuous deep beams with a/d ratios less than 1.2 the shear strength of continuous deep beam with web reinforcement is similar to the shear strength of simply supported deep beam with the same a/d ratio and web reinforcement. For a/d ratios greater than 1.2, the difference in shear strength between continuous deep beams and simply supported deep beams is about 15%. The proposed equations for predicting shear strength of simply supported deep beams appear to applicable to the shear strength of two span continuous deep beams.

6.3.4 Validation of the proposed equations for shear strength of continuous deep beams

In this part, the calculated shear strength of two span continuous deep beams of Rogowsky and MacGregor's tests and Ashour's tests using the proposed equations will be compared with the measured shear strength.

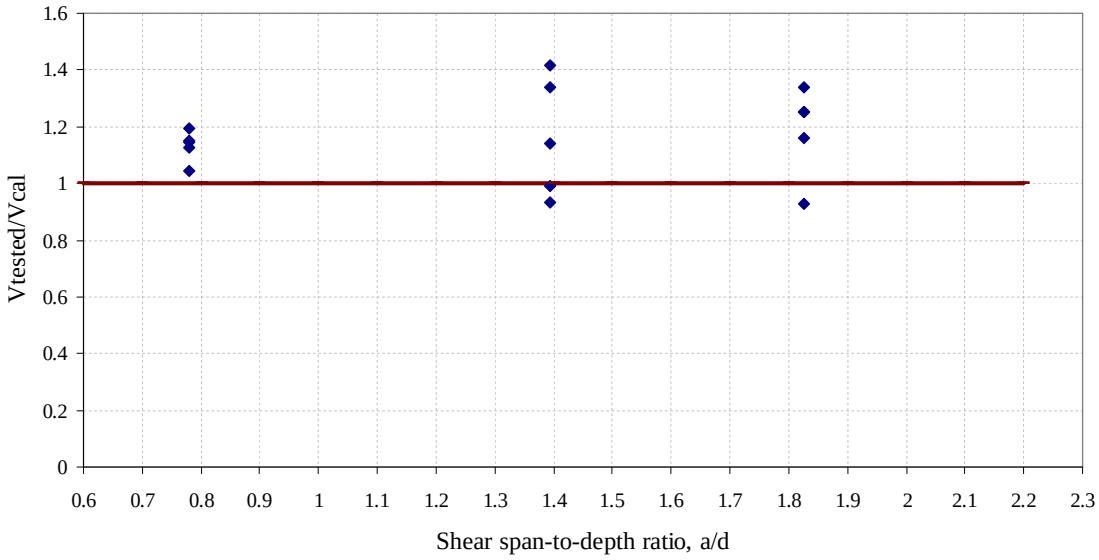

Figure 6.53 Comparison between tested shear of Rogowsky and MacGregor' tests and calculated shear capacity using the proposed equations with ν = 1.0

Figure 6.53 shows the comparison between measured and calculated shear capacity of Rogowsky and MacGregor's tests with an effectiveness factor ν = 1.0. Three tests without vertical reinforcement fell below 1.0; two are deep beams with a/d ratio of

1.4 and the other with a/d ratio of 1.83. However, when ν is 0.9 all tests are above 1.0 (Fig. 6.31). The mean value of ratio test to calculated shear capacity is 1.27 and standard variation is 0.15.

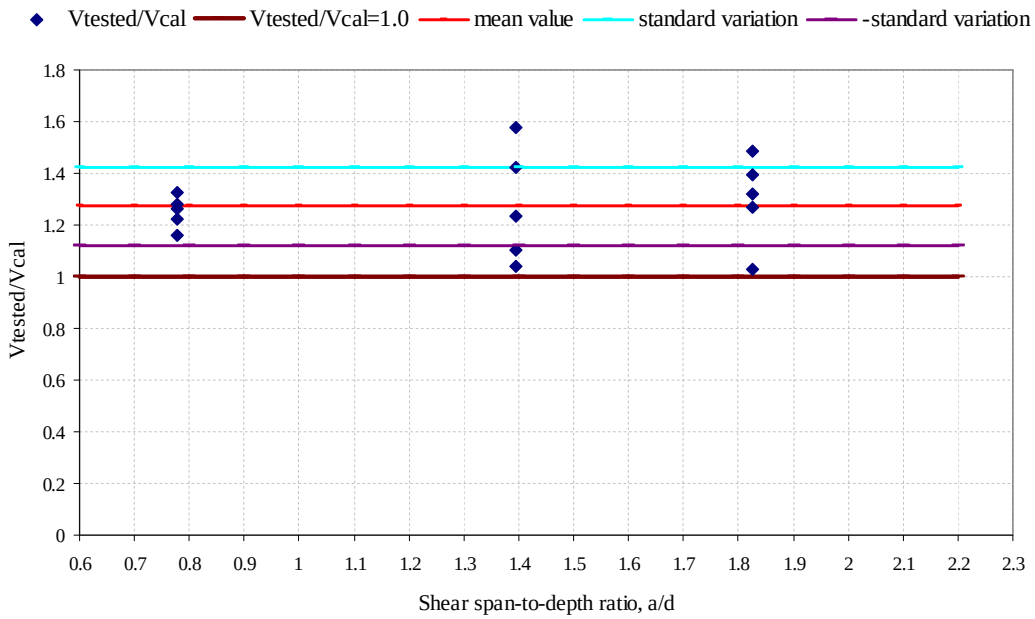

Figure 6.54 Comparison between tested shear of Rogowsky and MacGregor' tests and calculated shear capacity using the proposed equations with ν = 0.9

In Figures 6.55 and 6.56, the applicability of the proposed equations is evaluated for Ashour's tests. For an effectiveness factor ν = 1.0 the calculated strength is in poor agreement with the test shear capacity. However, the proposed equations are in good agreement when the effectiveness factor ν is 0.7. The mean value of ratio of tested shear capacity to calculated shear capacity is 1.31 and standard deviation is 0.35. Figure 6.57 shows the comparison between shear capacity of Yang beams and calculated shear using the proposed equations. It was observed that the proposed equations are in good agreement with ν = 0.7. The mean value of ratio of tested shear capacity to calculated shear capacity is 1.3 and standard deviation is 0.22. In Figure 6.58, the comparison between tested shear of continuous deep beams in evaluation database and calculated shear capacity using the ACI 318-99 equations. The mean value of ratio of tested shear capacity to calculated shear capacity is 1.43 and standard deviation is 0.34.

The proposed equations have a good agreement for calculating shear strength of reinforced concrete deep beams. The proposed equations provide reliable estimates of the shear strength of simply supported deep beams using an effectiveness factor $\nu = 0.6$. For two span continuous deep beams, the proposed equations were in a good agreement using as an effectiveness factor ranging from 0.7 to 0.9.

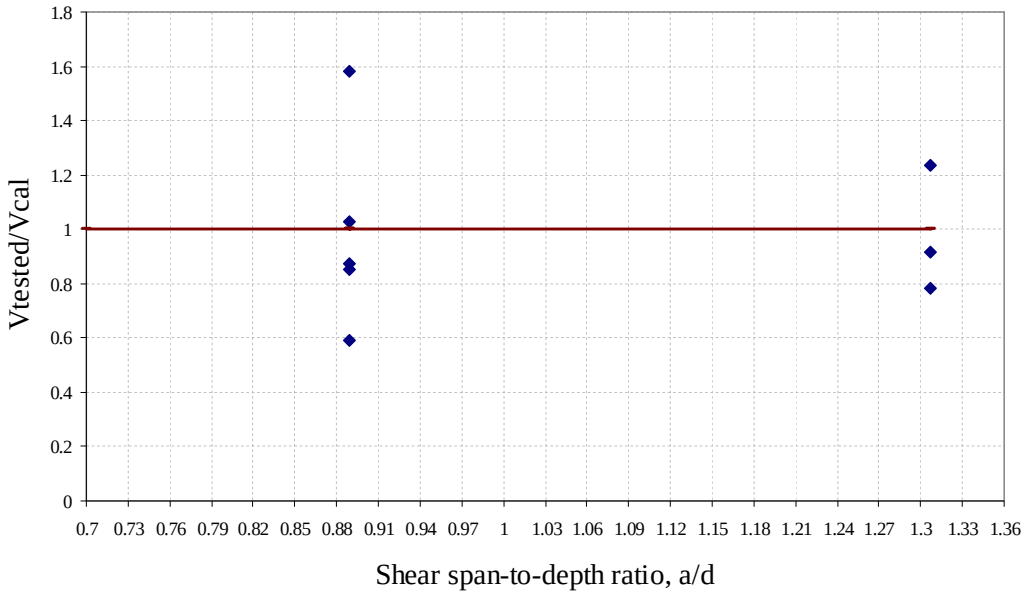

Figure 6.55 Comparison between tested shear of Ashour's tests and calculated shear capacity using the proposed equations with $\nu = 1.0$

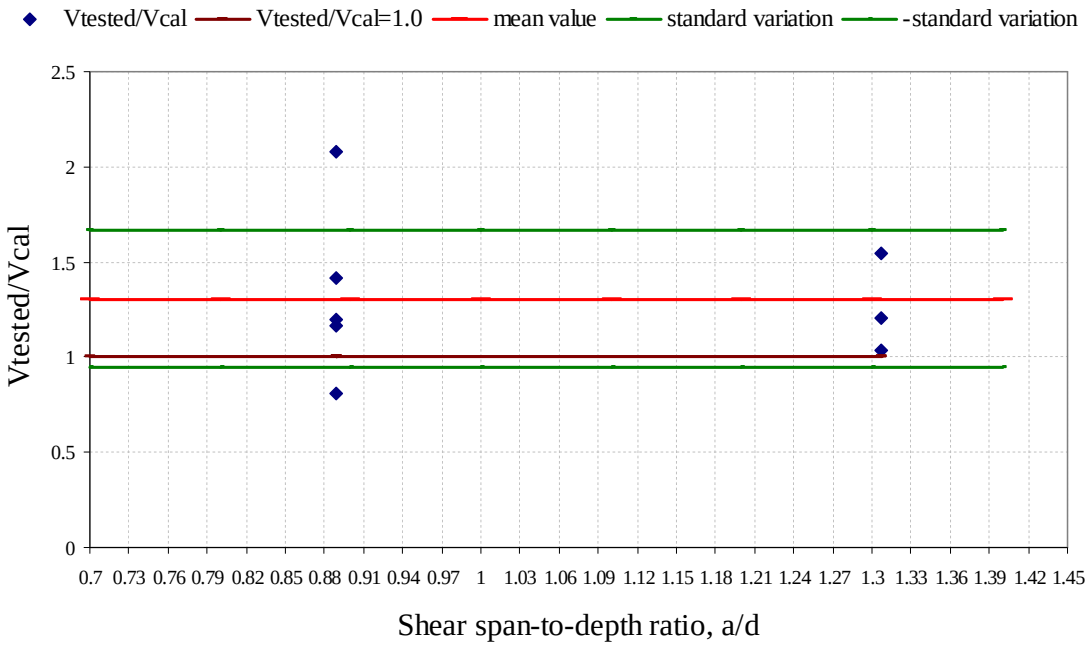

Figure 6.56 Comparison between tested shear of Ashour's tests and calculated shear capacity using the proposed equations with ν = 0.7

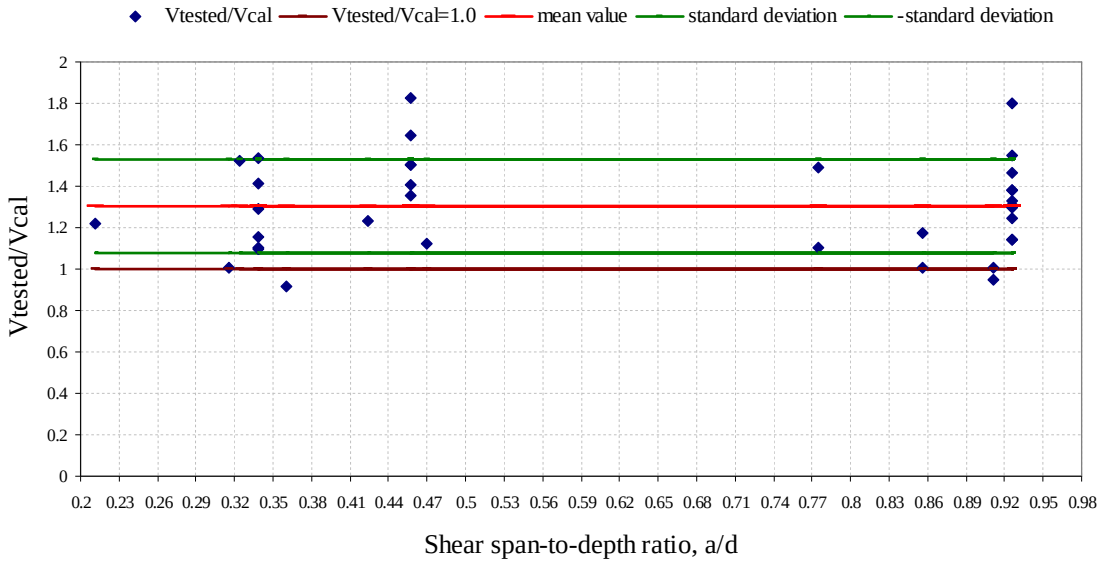

Figure 6.57 Comparison between tested shear of Yang's tests and calculated shear capacity using the proposed equations with ν = 0.7

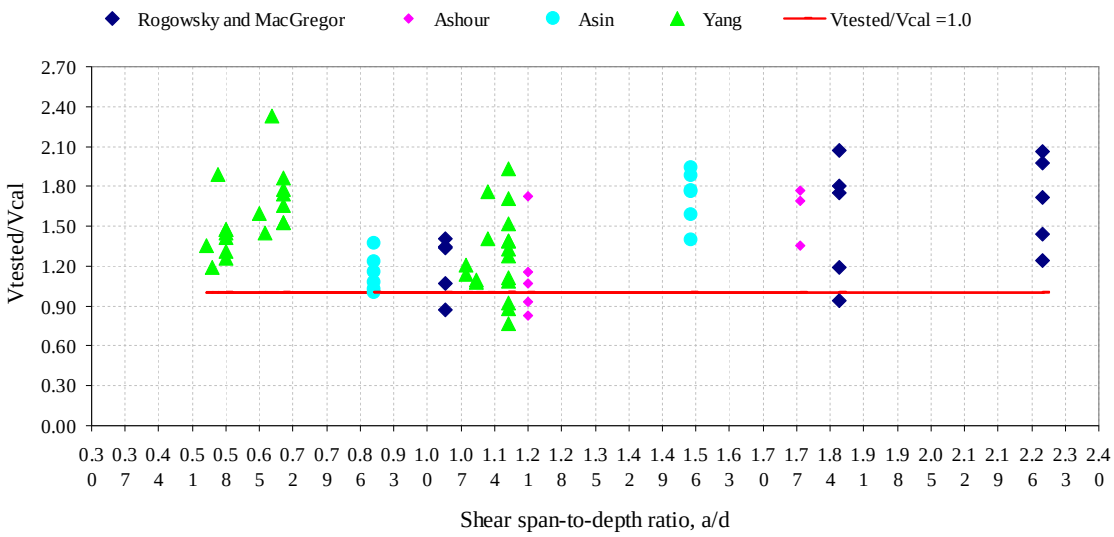

Figure 6.58 Comparison between tested shear of continuous beams in evaluation database and calculated shear capacity using the ACI 318-99 equations

6.4 Recommendations for design of reinforced concrete deep beams

For deep beams with a/d ratios greater than 2.0 the ACI 318-99 equation has a good prediction for the contribution of concrete. Using the analyses of beams with a plane stress field assumed in this study for a/d from 1.0 to 2.5, the following recommendation for the contribution of the concrete is proposed. In the analyses, concrete compressive strengths between 3 and 6ksi were studied.

6.4.1 Simply supported deep beams

- For deep beams as defined in ACI Code 318 Section 11.7.1 the shear strength can be calculated by using the proposed equations Eqs. 6.9 and 6.10:

$$V_c = \left(\sqrt{\left(\frac{a_c}{2d}\right)^2 + \frac{1}{\alpha_1}\rho\frac{f_y}{f_c'}\left(1 - \frac{1}{\alpha_1}\rho\frac{f_y}{f_c'}\right)} - \left(\frac{a_c}{2d}\right) \right) b_w d v f_c' \qquad (6.9)$$

and,

$$V_s = \frac{1}{3} f_y A_s \frac{a_c}{s} \qquad (6.10)$$

The proposed equations were in a good agreement with tests of simply supported deep beams with a/d ratios ranging from 1.0 to 1.85.

- An effectiveness factor ν for simply supported deep beams 0.6 is proposed.
- Vertical web reinforcement should meet minimum requirement mentioned in ACI 318-11 Section 11.7.4 and 11.7.5. The contribution of vertical reinforcement to the shear strength of deep beam is calculated by using the Eq. 6.10.
- Horizontal web reinforcement could be used for limiting crack width. However, it should not be included in calculating the shear strength of deep beams.
- For deep beams with a/d ratios less than 1.2 is quite small and can be ignored the contribution of vertical reinforcement to the shear strength. Web reinforcement should be used to satisfy the minimum requirements for limiting crack width.
- The proposed equations are applicable to simply supported deep beams under a single concentrated loading, multiple concentrated loads, or uniform distributed loading.
- For simply supported deep beams having the same geometry, the shear capacity under uniform distributed loading is higher than that under an equivalent single load or two concentrated loads.
- For simply supported deep beams load through a concrete column or other concrete element, a smaller effectiveness factor should be used for calculating the contribution of concrete to the shear strength. The effectiveness factor for deep beams loaded through a monolithic concrete member bearing on the top of the beam should be reduced 10% to 15% compare to that for deep beams under loading through a rigid steel plate.
- For deep beams under uniform distributed loading l_n can not be greater than five times the overall member depth.
- For simply supported deep beams with l_n/h less than 2.0 the shear strength should be based on a friction shear mechanism.

6.4.2 Two span continuous deep beams

- Shear strength of two span continuous deep beams can be calculated by using the Eqs. 6.9 and 6.10. An effectiveness factor for concrete compressive strength ranged from 0.7 to 0.9. A conservative value for designing is 0.7.
- Vertical and horizontal web reinforcement should not be less than the minimum requirement in ACI 318-11 Section 11.7.4 and 11.7.5. However, similar to simply supported deep beams, horizontal reinforcement should not be included in the contribution of web reinforcement to the shear strength of continuous deep beams.

6.5 Summary

- In this chapter, proposed equations for calculating the contribution of concrete and web reinforcement to the shear strength of deep beams were developed by using a plastic truss model.
- The proposed equations for shear strength of deep beams were verified by comparing measured shear capacities of deep beams reported in the literature to calculated shear capacity by using the proposed equations. The proposed equations showed good agreement with the test values.
- Finally, recommendations for design of deep beams for shear were presented.

Chapter 7 Summary and Conclusions

7.1 Summary

Reinforced concrete deep beams are vital structural members serving as load transferring elements. The behavior of reinforced concrete deep beams is complex. Nonlinear distribution of strain and stress must be considered. Prior to 1999, ACI 318 Codes included an empirical design equation for reinforced concrete deep beams. Since 2002, the strut and tie model and nonlinear analysis have been required. However, both methods have disadvantages of complexity or lack of transparency.

The objective of this study was to develop a simple, reliable design equation for reinforced concrete deep beams as an alternative to current design procedures. A nonlinear finite element program, ATENA, was used to simulate the behavior of concrete and reinforced concrete structures. ATENA was developed specially for reinforced concrete structures. A series of tests reported in the literature were used to calibrate the models for specific test specimens. Simply supported deep beams models were verified using Birrcher's tests, and two span continuous beams were verified using tests by Rogowsky and MacGregor and by Ashour. Those tests were selected because the researchers reported adequate of information on details an on specimen behavior.

Once the calibration process was complete, a systematic study of parameters influencing deep beam behavior was carried out. The parameters investigated were the compressive strength of concrete, shear span to depth ratios, longitudinal reinforcement ratios, horizontal and vertical web reinforcement, member depth, and loading conditions. A series of simply supported and two span continuous deep beams models were developed based on the details and geometry of Birrcher's beams. The details and geometry of Birrcher's beams were selected because these beams were among largest ones reported in the literature. In addition, behavior of large scale tests was considered to better reflect the behavior of real elements.

Finally, a proposed design equation for shear strength of reinforced concrete deep beams has been derived based on the observed the behavior of reinforced concrete deep

beam tests, the results of the analytical study, and a plastic truss model. The proposed equations agreed well with test values.

7.2 Conclusions

7.2.1 Computer analyses of reinforced concrete deep beams

Using ATENA to study the parameters influencing of simply supported and two span continuous deep beam shear behavior, the findings can be summarized as follows:

1. For deep beams, the concrete strength is the primary variable because the shear strength was governed by a direct compression strut forming between the loading and support plates. It was observed that the shear strength of deep beams is linearly proportional to concrete strength. The influence of concrete strength on the shear strength of deep beams is inversely proportional to a/d ratios.
2. Although horizontal web reinforcement may contribute to limit crack width the contribution to the shear strength of deep beams is very small. It was observed that the contribution of web reinforcement to shear strength of deep beams primarily comes from vertical web reinforcement. Vertical web reinforcement was most efficient if placed near the point of load application.
3. The manner in which loads are applied may influence the shear capacity by 10-20%. The lowest capacity was obtained under a single concentrated load. A uniform distributed loading gave the highest shear capacity.
4. It was found that loads through a column resulted in lower capacity than loading through a thick steel plate. This should be considered when reviewing test data which in nearly cases involved load through plates.

7.2.2 A proposed equation for contribution of concrete and web reinforcement to the shear strength of deep beams

Based on the model analyses (assuming a plane stress field and concrete strengths up to 7 ksi) and observed test data, a design approach was developed that involved the following approach:

1. Plastic truss model was used to determine the concrete contribution to the shear strength of a deep beam. It was observed that a compression arch consisting of compression struts and steel tie formed in deep beams. This mechanism governed the shear capacity of deep beams. A proposed equation for concrete contribution to the shear strength of a deep beam was derived as follows:

$$V_c = \left(\sqrt{\left(\frac{a_c}{2d}\right)^2 + \frac{1}{\alpha_1}\rho\frac{f_y}{f_c'}\left(1 - \frac{1}{\alpha_1}\rho\frac{f_y}{f_c'}\right)} - \left(\frac{a_c}{2d}\right) \right) b_w d \nu f_c'$$

   where,

   a_c is a clear shear span, in. (distance between face or edge of support and face of edge of loaded area)

   d is an effective depth of cross section, in.

   b_w is a width of deep beam, in.

   α_1 is the 0.85 factor in ACI Section 10.2.7.1

   ρ is a ratio of tensile longitudinal reinforcement

   f_y is yielding strength of longitudinal reinforcement, ksi

   $f^*_c = \nu f'_c$ is an effective compressive strength, ksi

2. Steel contribution is based on the vertical web reinforcement. The steel near the point of load application is most efficient. The proposed equation for steel contribution was derived as follows:

$$V_s = \frac{1}{3} f_y A_s \frac{a_c}{s}$$

3. The proposed equation could be used for calculating the steel contribution to the shear strength of a deep beam under uniform distributed loading. In this

case, a_c clear shear span should be considered equal to an equivalent shear span a = l_n/4.

4. Validation of the proposed equations was based on comparison between shear strength of deep beams in the database and calculated shear capacity using the proposed equations, and between the proposed equation and equations in ACI 318-99. It was observed that the proposed equations are in good agreement with test values.

The proposed equations give designers a simple, reliable alternative procedure beside a strut-and-tie model and a nonlinear analysis for designing shear strength of deep beams.

APPENDIX A
ATENA Program

1.1 ATENA

ATENA is a non-linear finite element program developed by Cervenka [9]. ATENA is a program designed especially for analysis of concrete and reinforced concrete structures. The program can be used to check and verify the behavior of concrete and reinforced concrete structures in a user friendly graphical environment. Currently, there are over 1000 ATENA users around the world. Figures A1 and A2 show examples of the types of the problems that can be addressed by ATENA.

ATENA can simulate behavior of concrete and reinforced concrete structures including concrete cracking, crushing and reinforcement yielding. ATENA is a powerful tool for experimental researchers to test and to conduct analytical parametric studies.

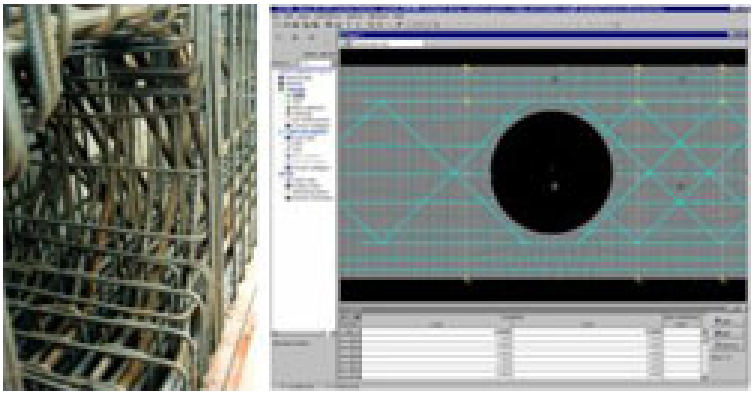

Figure A1 ATENA program for analysis of complicated D-regions (Cervenka's website)

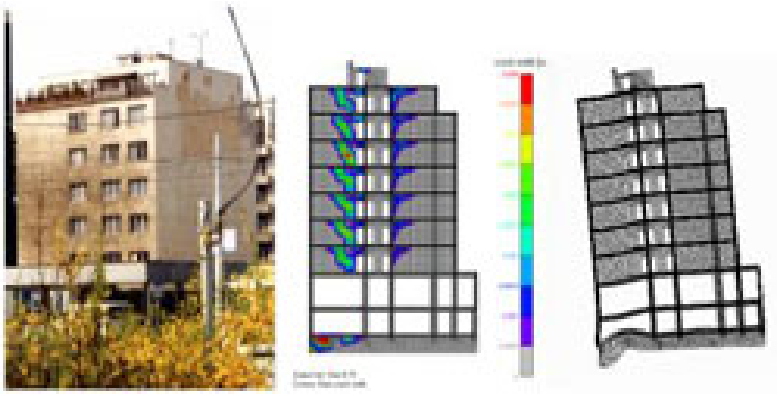

Figure A2 ATENA for analysis of a historical infilled reinforced concrete frame building in Prague (Cervenka's website)

1.1.1 Material Model SBETA

The capacity of ATENA is based on the material model SBETA that can simulate the following characteristics of concrete materials:

- Non-linear behavior in compression including hardening and softening,
- Fracture of concrete in tension based on a non-linear fracture mechanism,
- Biaxial strength failure criterion,
- Reduction of compressive strength after cracking,
- Tension stiffening effect,
- Reduction of the shear stiffness after cracking (variable shear retension),
- Two crack models: fixed crack direction and rotated crack direction.

Reinforcement in both smeared and discrete forms is in a uniaxial stress state and its constitutive law is a multi-linear stress-strain diagram. Perfect bond behavior between concrete and reinforcement is assumed within the smear concept. No bond slip can be directly modeled except for that included inherently in tension stiffening. However, on a macro-level a relative slip displacement of reinforcement with respect to concrete over a certain distance can arise, if concrete is cracked or crushed.

The material matrix is derived using a non-linear elastic approach. In this approach the elastic constants are derived from a stress-strain function called the equivalent uniaxial law. This approach is similar to the non-linear hypoelastic constitutive model, except that different laws are used here for loading and unloading,

causing the dissipation of energy to be exhausted as damage to the material increases. The detailed treatment of the theoretical background of this subject can be found in Chen (1982).

1.1.2 Stress-strain relationship of Concrete

1.1.2.1 Equivalent uniaxial law

The non-linear behavior of concrete in the biaxial stress state is expressed by effective stress σ^{ef}_c, and equivalent uniaxial strain ε^{eq}. The effective stress is, in most cases, a principal stress. The equivalent uniaxial strain is introduced in order to eliminate the Poison's effect in a plane stress state.

$$\varepsilon^{eq} = \frac{\sigma_{ci}}{E_{ci}} \tag{1.1}$$

The equivalent unixial strain can be considered as the strain that would be produced by the stress σ_{ci} in a uniaxial test with modulus E_{ci} associated with the direction *i*.

The complete equivalent uniaxial stress-strain diagram for concrete is shown in Fig. A3.

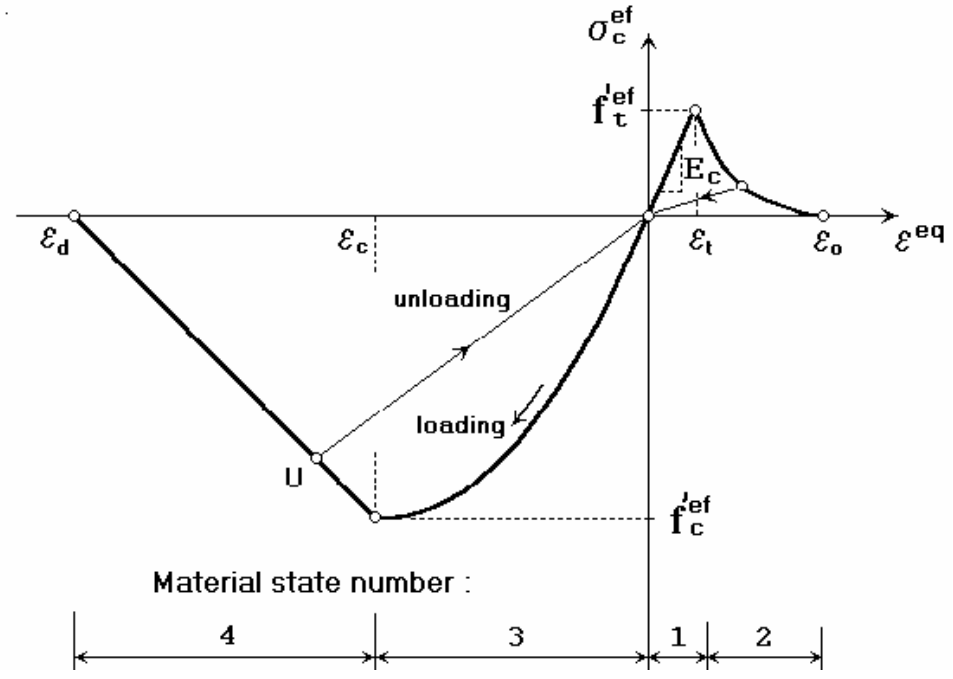

Figure A3 Uniaxial stress-strain law for concrete (Cervenka)

Unloading is a linear function to the origin. Thus, the relationship between stress σ^{ef}_c and strain ε^{eq} is not unique and depends on the load history. A change from loading to unloading occurs when the increment of the effective strain changes sign.

1.1.2.2. Behavior of concrete material model in tension

(a) Before cracking

The behavior of concrete in tension without cracks is assumed linear elastic. E_c is the initial elastic modulus of concrete, f'^{ef}_t is the effective tensile strength derived from the biaxial failure function.

$$\sigma_t^{ef} = E_c \varepsilon^{eq},\ 0 \le \sigma_c \le f_t^{'eq} \tag{1.2}$$

$$f_t^{eq} = f_t^{'} r_{et} \tag{1.3}$$

where r_{et} is the reduction factor of the tensile strength in direction 1 due to the compressive stress in direction 2. The reduction factor has the following forms:

$$r_{et} = 1 - 0.95\frac{\sigma_{c2}}{f'_c} \tag{1.4}$$

$$r_{et} = \frac{A + (A-1)B}{AB},\ B = Kx + A,\ x = \frac{\sigma_{c2}}{f'_c} \tag{1.5}$$

The relation in Eq.(1.4) is the linear decrease of the tensile strength and in Eq.(1.5) is the hyperbolic decrease as shown in Fig. A4. Two predefined shapes of the hyperbola are given by the position of an intermediate point r, x. Constants K and A define the shape of the hyperbola. The values of constants for the two positions of the intermediate point are given in Table A1.1.

Table A1 Types and parameters for tensile failure

Type	point		parameters	
	r	x	A	K
a	0.5	0.4	0.75	
b	0.5	0.2	1.0625	6.0208

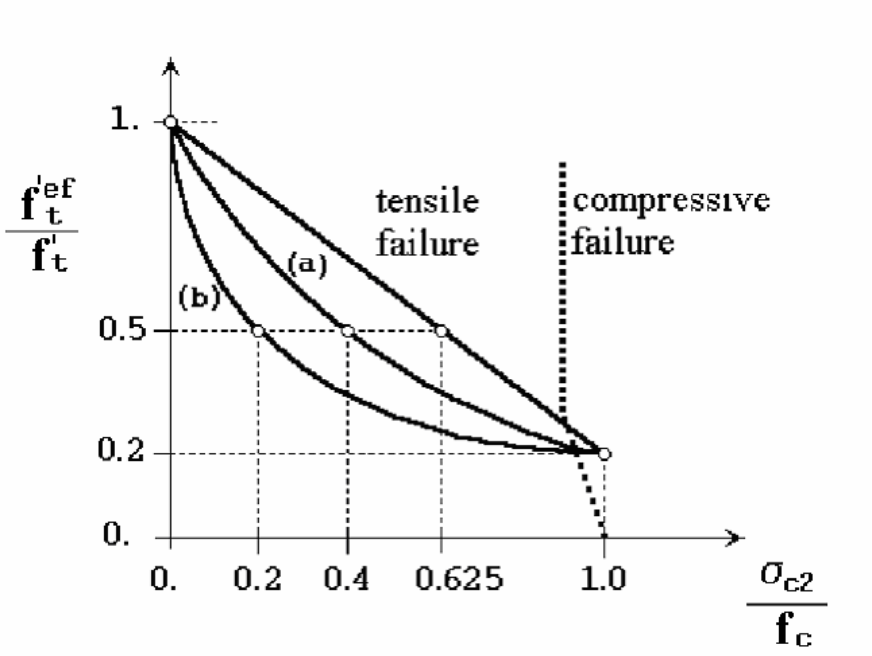

Figure A4 Tension-Compression failure function for concrete material model (Cervenka)

(b) After cracking

After cracking, two types of formulations are used for the crack opening:

- A fictitious crack model based on a crack-opening law and fracture energy. This formulation is suitable for modeling crack propagation in concrete.
- A stress-strain relation in a material point. This formulation is not suitable for normal cases of crack propagation in concrete and should be used only in some special cases.

Details of softening models included in SBETA material model are provided in reference [10].

1.1.2.3 Behavior of concrete material model in compression

(a) Before peak stress

The formula recommended by CEB-FIB Model Code 1990 has been adopted for the ascending branch of the concrete stress-strain law in compression, Fig. A5. This

formula enables a wide range of curve forms, from linear to curved, and is appropriate for normal as well as high strength concrete materials.

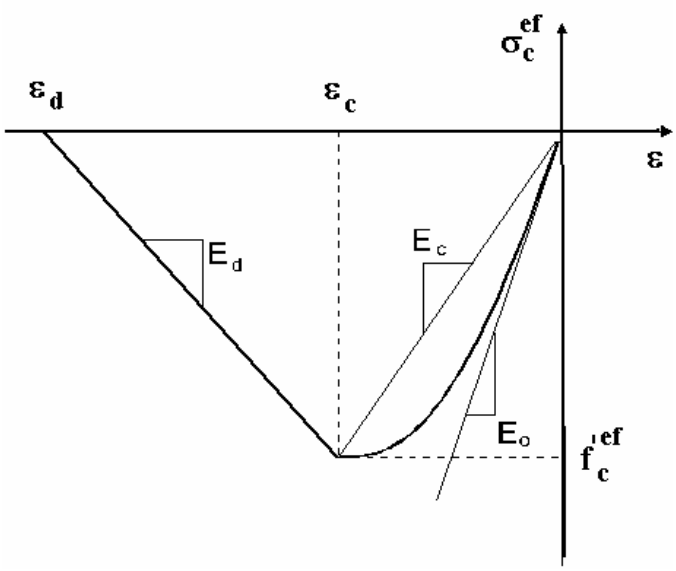

Figure A5 Compressive stress-strain diagram (Cervenka)

where,

$$\sigma_c^{ef} = f'^{ef}_c \frac{kx - x^2}{1 + (k-2)x},\ x = \frac{\varepsilon}{\varepsilon_c},\ k = \frac{E_0}{E_c} \qquad (1.6)$$

where,

σ^{ef}_c is concrete compressive stress,

f'^{ef}_c is concrete effective compressive strength,

x is normalized strain,

ε_c is the strain at peak stress,

k is the shape parameter, greater than or equal to 1,

E_0 is the initial elastic modulus of concrete,

E_c is the secant elastic modulus at the peak stress, $E_c = \frac{f'^{ef}}{\varepsilon_c}$

(b) After peak stress

The softening law in compression is linearly descending. There are two models of strain softening in compression, one based on dissipated energy, and the other based on local strain softening.

- The fictitious compression plane model is based on the assumption, that compression failure is localized in a plane normal to the direction of compressive principal stress. All post-peak compressive displacements and energy dissipation are localized in this plane.

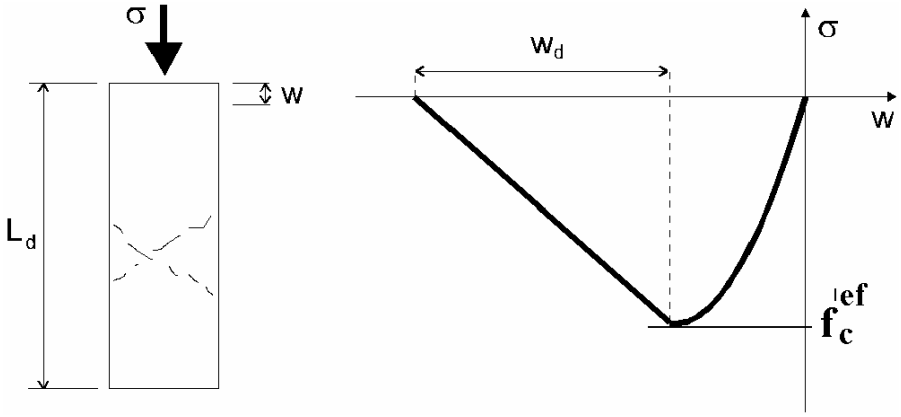

Figure A6 Softening displacement law in compression (Cervenka)

where,

$$\varepsilon_d = \varepsilon_c + \frac{w_d}{L_d'} \tag{1.7}$$

where,

ε_d is the limit compressive strain at the zero compressive stress,

w_d is a plastic displacement,

L'_d is the band size of the element in the direction of compression.

- The compression strain softening law based on strain. In this model, the slope of the softening curve is defined by means of a softening modulus E_d.

1.1.3 Fracture process, crack width

The process of crack formation can be divided into three stages, Fig. A7. The uncracked stage exists before tensile strength is reached. The crack formation takes place in the process zone of a potential crack with decreasing tensile stress on a crack face due to a bridging effect. Finally, after a complete release of the stress, the crack opening continues without stress.

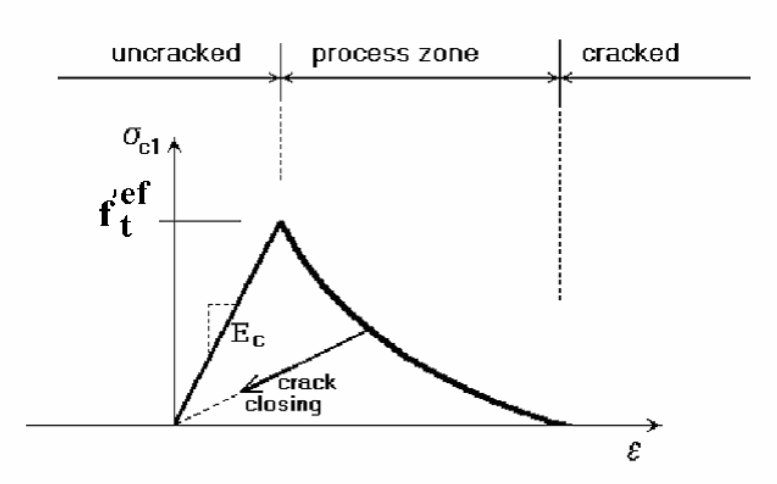

Figure A7 Stages of crack opening (Cervenka)

The crack width w is calculated as a total crack opening displacement within the crack band.

$$w = \varepsilon_{cr} L_t^{'} \tag{1.8}$$

where,

ε_{cr} is the crack opening strain, which is equal to the strain normal to the crack direction in the cracked state after complete stress release,

L'_t is the band size of the element in the direction of tension.

1.1.4 Two models of smeared cracks

1.1.4.1 Fixed crack model

In the fixed crack model, crack direction is given by the principal stress direction at the moment of crack initiation. During further loading this direction is fixed and represents the material axis of orthotropy.

The principal stress and strain directions coincide in the uncracked concrete, because of the assumption of isotropy in the concrete component. After cracking, the orthotropy is introduced. The weak material axis m_1 is normal to the crack direction, the strong axis m_2 is parallel with the cracks, Fig. A8.

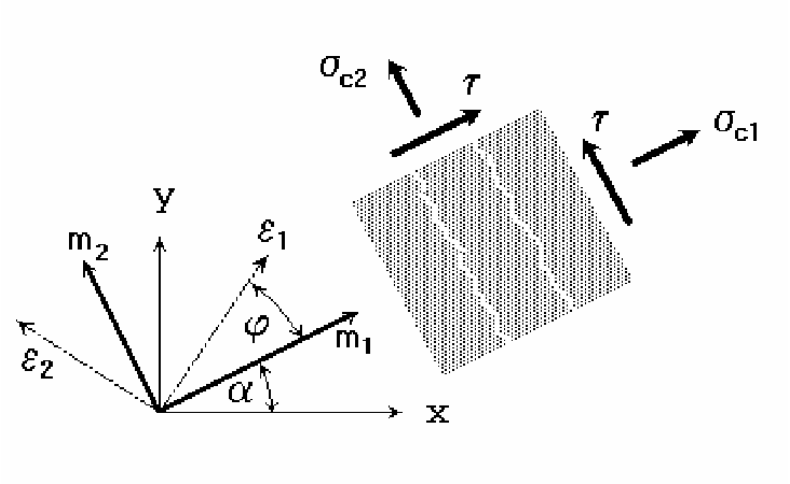

Figure A8 Fixed crack model. Stress and strain state (Cervenka)

In a general case the principal strain axes ε_1 and ε_2 rotate and need not coincide with the axes of orthotropy m_1 and m_2. This produces a shear stress on the crack plane. The stress component σ_{c1} and σ_{c2} denote, respectively, the stresses normal and parallel to the crack plane and, due to shear stress, they are not the principal stresses.

1.1.4.2 Rotated crack model

In the rotated crack model, the direction of the principal stress coincides with the direction of the principal strain. Thus, no shear strain occurs on the crack plane and only two normal stress components must be defined, Fig. A9.

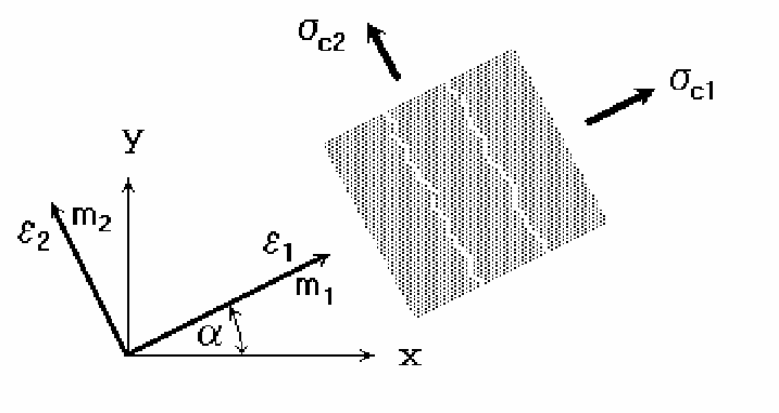

Figure A9 Rotated crack model. Stress and strain state

If the principal strain axes rotate during loading, the direction of cracks rotates, as well.

APPENDIX B
Evaluation Database

1. Overview

The following details are presented in Table 0.1 for the 304 specimens in the *evaluation database*:

b = beam width, in.

h = beam height, in.

d = distance form extreme compression fiber to centroid of tensile reinforcement, in.

f_c = compressive strength of concrete at the time of testing, psi.

Note: if the compressive strength was measured based on the test of astandard 100 or 150-mm cube, then it was converted to the equivalent 6-inch cylinder strength according to fib (1999).

f_y = yield strength of tensile reinforcement, ksi.

f_{yv} = yield strength of vertical transverse reinforcement, ksi

ρ_l = ratio of longitudinal tensile reinforcement to effective area, A_s/bd

ρ'_l = ratio of longitudinal compression reinforcement to effective area, A'_s/bd

ρ_v = ratio of vertical transverse reinforcement to effective area, A_v/bs

ρ_h = ratio of horizontal transverse reinforcement to effective area, A_{vh}/bs_{vh}

s = spacing of vertical stirrups, in.

s_{vh} = spacing of horizontal stirrups, in.

Load plate = dimensions of the load bearing plate measured in the longitudinal, in.

Support plate = dimensions of the support bearing plate measured in the longitudinal, in.

a/d ratio = shear span-to-depth ratio

V_{test} = maximum shear carried in test region, including the estimated self weight of the specimen, kips

V_{crack} = shear in test region at first diagonal cracking, including the estimated self weight of the specimen, kips

Table B1 Evaluation Database of simply supported deep beams (1 of 11)

Beam I.D.	b, in	h, in	d, in	f'_c, psi	f_y, ksi	f_{yv}, ksi	r_l	r'	r_v	r_{vh}	Stirrup spacing, s, in	Load plate l_l, in	Bearing plate l_b, in	a/d	V_{test}, kip	Vcrack, kip
Rogowsky, MacGregor, & Ong, 1986																
1/1.0N	7.9	39.4	37.4	3785	55.4	83.00	0.0094	0.0000	0.0015	0.0000	7.38	11.81	7.87	1.05	136.31	73.70
1/1.0S	7.9	39.4	37.4	3785	55.4	83.00	0.0094	0.0000	0.0000	0.0000	-10	11.81	7.87	1.05	158.12	0.00
2/1.0N	7.9	39.4	37.4	3887	55.4	83.00	0.0094	0.0003	0.0015	0.0006	7.38	11.81	7.87	1.05	169.59	113.38
2/1.0S	7.9	39.4	37.4	3887	55.4	83.00	0.0094	0.0003	0.0000	0.0006	-10	11.81	7.87	1.05	169.59	0.00
1A/1.0S	7.9	39.4	37.4	3829	53.4	83.00	0.0094	0.0000	0.0000	0.0000	-10	11.81	7.87	1.05	135.86	79.68
1/1.5N	7.9	23.6	21.1	6150	65.6	83.00	0.0112	0.0000	0.0019	0.0000	5.91	11.81	7.87	1.87	80.13	0.00
1/1.5S	7.9	23.6	21.1	6150	65.6	83.00	0.0112	0.0000	0.0000	0.0000	-10	11.81	7.87	1.87	68.67	54.55
2/1.5N	7.9	23.6	21.1	6150	65.6	83.00	0.0112	0.0005	0.0019	0.0011	5.91	11.81	7.87	1.87	78.79	0.00
2/1.5S	7.9	23.6	21.1	6150	65.6	83.00	0.0112	0.0005	0.0000	0.0011	-10	11.81	7.87	1.87	51.36	62.35
1/2.0N	7.9	19.7	17.9	6266	65.6	83.00	0.0088	0.0000	0.0014	0.0000	7.87	7.87	7.87	2.20	45.21	0.00
1/2.0S	7.9	19.7	17.9	6266	65.6	83.00	0.0088	0.0000	0.0000	0.0000	-10	7.87	7.87	2.20	40.26	0.00
2/2.0N	7.9	19.7	17.9	6266	65.6	83.00	0.0088	0.0006	0.0014	0.0012	7.87	7.87	7.87	2.20	46.33	0.00
2/2.0S	7.9	19.7	17.9	6266	65.6	83.00	0.0088	0.0006	0.0000	0.0012	-10	7.87	7.87	2.20	42.06	27.47
Tan & Lu, 1996																
1-500/0.50	5.51	19.69	17.48	7120	75.4	75.40	0.0260	0.0009	0.0000	0.0000	-10	9.84	9.84	0.56	190.64	60.94
1-500/0.75	5.51	19.69	17.48	6163	75.4	75.40	0.0260	0.0009	0.0000	0.0000	-10	9.84	9.84	0.84	157.08	33.98
1-500/1.00	5.51	19.69	17.48	5423	75.4	75.40	0.0260	0.0009	0.0000	0.0000	-10	9.84	9.84	1.13	128.00	31.82
2-1000/0.50	5.51	39.37	34.8	4524	75.4	75.40	0.0260	0.0005	0.0012	0.0012	13.77	9.84	9.84	0.57	196.63	96.13
2-1000/0.75	5.51	39.37	34.8	4742	75.4	75.40	0.0260	0.0005	0.0012	0.0012	13.77	9.84	9.84	0.84	146.39	51.39
2-1000/1.00	5.51	39.37	34.8	4473	75.4	75.40	0.0260	0.0005	0.0012	0.0012	13.77	9.84	9.84	1.13	98.39	50.45
3-1400/0.50	5.51	55.12	49.25	4756	75.4	75.40	0.0260	0.0003	0.0012	0.0012	13.77	9.84	9.84	0.56	264.28	113.48
3-1400/0.75	5.51	55.12	49.25	5249	75.4	75.40	0.0260	0.0003	0.0012	0.0012	13.77	9.84	9.84	0.84	214.19	80.09
3-1400/1.00	5.51	55.12	49.25	5120	75.4	75.40	0.0260	0.0003	0.0012	0.0012	13.77	9.84	9.84	1.14	180.92	69.12
4-1750/0.50	5.51	68.9	61.4	6177	75.4	75.40	0.0260	0.0003	0.0012	0.0012	13.77	9.84	9.84	0.56	368.01	68.94
4-1750/0.75	5.51	68.9	61.4	5858	75.4	75.40	0.0260	0.0003	0.0012	0.0012	13.77	9.84	9.84	0.85	279.79	91.93
4-1750/1.00	5.51	68.9	61.4	6496	75.4	75.40	0.0260	0.0003	0.0012	0.0012	13.77	9.84	9.84	1.13	226.53	47.53

Table B2 Evaluation Database of simply supported deep beams (1 of 11)

Beam I.D.	b, in	h, in	d, in	f'_c, psi	f_y, ksi	f_{yv}, ksi	ρ_l	ρ'	ρ_v	ρ_{vh}	Stirrup spacing, s, in	Load plate l_l, in	Bearing plate l_b, in	a/d	V_{test}, kip	Vcrack, kip
Oh & Shin, 2001																
N4200	5.11	22.05	19.68	3440	60	60.00	0.0156	0.0022	0.0000	0.0000	-10	7.09	5.12	0.85	59.84	21.15
N42A2	5.11	22.05	19.68	3440	60	60.00	0.0156	0.0022	0.0012	0.0043	16	7.09	5.12	0.85	64.07	12.70
N42B2	5.11	22.05	19.68	3440	60	60.00	0.0156	0.0022	0.0022	0.0043	8.7	7.09	5.12	0.85	84.93	28.09
N42C2	5.11	22.05	19.68	3440	60	60.00	0.0156	0.0022	0.0034	0.0043	5.7	7.09	5.12	0.85	80.55	27.18
H4100	5.11	22.05	19.68	7121	60	60.00	0.0156	0.0022	0.0000	0.0000	-10	7.09	5.12	0.50	144.44	61.98
H41A2(1)	5.11	22.05	19.68	7121	60	60.00	0.0156	0.0022	0.0012	0.0043	16	7.09	5.12	0.50	160.34	55.94
H41B2	5.11	22.05	19.68	7121	60	60.00	0.0156	0.0022	0.0022	0.0043	8.7	7.09	5.12	0.50	158.74	48.10
H41C2	5.11	22.05	19.68	7121	60	60.00	0.0156	0.0022	0.0034	0.0043	5.7	7.09	5.12	0.50	159.32	45.39
H4200	5.11	22.05	19.68	7121	60	60.00	0.0156	0.0022	0.0000	0.0000	-10	7.09	5.12	0.85	90.33	30.00
H42A2(1)	5.11	22.05	19.68	7121	60	60.00	0.0156	0.0022	0.0012	0.0043	16	7.09	5.12	0.85	109.87	45.39
H42B2(1)	5.11	22.05	19.68	7121	60	60.00	0.0156	0.0022	0.0022	0.0043	8.7	7.09	5.12	0.85	102.73	47.40
H42C2(1)	5.11	22.05	19.68	7121	60	60.00	0.0156	0.0022	0.0034	0.0043	5.7	7.09	5.12	0.85	94.70	26.78
H4300	5.11	22.05	19.68	7121	60	60.00	0.0156	0.0022	0.0000	0.0000	-10	7.09	5.12	1.25	76.03	30.00
H43A2(1)	5.11	22.05	19.68	7121	60	60.00	0.0156	0.0022	0.0012	0.0043	16	7.09	5.12	1.25	78.22	28.19
H43B2	5.11	22.05	19.68	7121	60	60.00	0.0156	0.0022	0.0022	0.0043	8.7	7.09	5.12	1.25	85.81	38.45
H43C2	5.11	22.05	19.68	7121	60	60.00	0.0156	0.0022	0.0034	0.0043	5.7	7.09	5.12	1.25	90.62	30.00
H4500	5.11	22.05	19.68	7121	60	60.00	0.0156	0.0022	0.0000	0.0000	-10	7.09	5.12	2.00	25.57	16.52
H45A2	5.11	22.05	19.68	7121	60	60.00	0.0156	0.0022	0.0012	0.0043	16	7.09	5.12	2.00	47.59	17.13
H45B2	5.11	22.05	19.68	7121	60	60.00	0.0156	0.0022	0.0022	0.0043	8.7	7.09	5.12	2.00	53.57	23.66
H45C2	5.11	22.05	19.68	7121	60	60.00	0.0156	0.0022	0.0034	0.0043	5.7	7.09	5.12	2.00	53.13	32.41
N33A2	5.11	22.05	19.68	3440	60	60.00	0.0156	0.0022	0.0012	0.0043	16	7.09	5.12	1.25	51.45	21.27
N43A2	5.11	22.05	19.68	3440	60	60.00	0.0156	0.0022	0.0012	0.0043	16	7.09	5.12	1.25	57.51	24.17
N53A2	5.11	22.05	19.68	3440	60	60.00	0.0156	0.0022	0.0012	0.0043	16	7.09	5.12	1.25	46.94	15.30
H31A2	5.11	22.05	19.68	7121	60	60.00	0.0156	0.0022	0.0012	0.0043	16	7.09	5.12	0.50	167.55	50.13
H32A2	5.11	22.05	19.68	7121	60	60.00	0.0156	0.0022	0.0012	0.0043	16	7.09	5.12	0.85	119.12	39.57
H33A2	5.11	22.05	19.68	7121	60	60.00	0.0156	0.0022	0.0012	0.0043	16	7.09	5.12	1.25	84.99	34.64
H51A2	5.11	22.05	19.68	7121	60	60.00	0.0156	0.0022	0.0012	0.0043	16	7.09	5.12	0.50	157.94	45.07
H52A2	5.11	22.05	19.68	7121	60	60.00	0.0156	0.0022	0.0012	0.0043	16	7.09	5.12	0.85	127.75	39.23
H53A2	5.11	22.05	19.68	7121	60	60.00	0.0156	0.0022	0.0012	0.0043	16	7.09	5.12	1.25	81.80	28.27

Table B3 Evaluation Database of simply supported deep beams (1 of 11)

Beam I.D.	b, in	h, in	d, in	f'_c, psi	f_y, ksi	f_{yv}, ksi	ρ_l	ρ'	ρ_v	ρ_{vh}	Stirrup spacing, s, in	Load plate l_l, in	Bearing plate l_b, in	a/d	V_{test}, kip	Vcrack, kip
HJS - 2, 2001																
III-2	8	18	16	3882	68	0.00	0.0309	0.0000	0.0000	0.0000	-10	8	8	1.50	64.62	0.00
I-CL-8.5-0	6	30	27	2584	68	73.00	0.0195	0.0014	0.0043	0.0000	8.5	6	6	1.11	79.91	41.92
I-CL-0-0	6	30	27	2368	68	73.00	0.0195	0.0014	0.0000	0.0000	-10	6	6	1.11	93.01	69.12
I-2C-8.5-0	6	30	27	3208	68	73.00	0.0195	0.0014	0.0043	0.0000	8.5	12	6	1.67	121.63	55.42
I-2C-0-0	6	30	27	3208	68	73.00	0.0195	0.0014	0.0000	0.0000	-10	12	6	1.67	91.88	83.42
II-N-E-5.8-8	18	18	16	2850	68	73.00	0.0219	0.0008	0.0015	0.0000	8	10	6	1.69	104.25	55.85
II-N-F-5.8-8	18	18	16	2851	68	73.00	0.0219	0.0008	0.0015	0.0000	8	10	6	1.69	111.35	61.35
II-N-F-5.8-3	18	18	16	2880	68	73.00	0.0219	0.0008	0.0041	0.0000	3	10	6	1.69	180.75	51.15
II-N-C-4.6-8	18	18	16	2880	68	73.00	0.0219	0.0008	0.0015	0.0000	8	10	6	1.69	188.31	67.01
II-N-E-4.6-8	18	18	16	2880	68	73.00	0.0219	0.0008	0.0015	0.0000	8	10	6	1.69	139.91	72.81
II-N-F-4.6-8	18	18	16	3130	68	73.00	0.0219	0.0008	0.0015	0.0000	8	10	6	1.69	112.31	62.71
Moody, Viest, Elstner & Hognestad, 1954																
III-24a	7	24	21	2580	45.7	0.00	0.0272	0.0136	0.0000	0.0000	-10	8	8	1.52	67.09	20.59
III-24b	7	24	21	2990	45.7	0.00	0.0272	0.0136	0.0000	0.0000	-10	8	8	1.52	68.59	25.59
III-25a	7	24	21	3530	45.4	0.00	0.0346	0.0173	0.0000	0.0000	-10	8	8	1.52	60.59	28.09
III-25b	7	24	21	2500	45.4	0.00	0.0346	0.0173	0.0000	0.0000	-10	8	8	1.52	65.59	23.09
III-26a	7	24	21	3140	43.8	0.00	0.0425	0.0213	0.0000	0.0000	-10	8	8	1.52	95.09	30.59
III-26b	7	24	21	2990	43.8	0.00	0.0425	0.0213	0.0000	0.0000	-10	8	8	1.52	89.59	25.59
III-27a	7	24	21	3100	45.7	0.00	0.0272	0.0136	0.0000	0.0000	-10	8	8	1.52	78.59	23.09
III-27b	7	24	21	3320	45.7	0.00	0.0272	0.0136	0.0000	0.0000	-10	8	8	1.52	80.59	25.59
III-28a	7	24	21	3380	45.4	0.00	0.0346	0.0173	0.0000	0.0000	-10	8	8	1.52	68.59	25.59
III-28b	7	24	21	3250	45.4	0.00	0.0346	0.0000	0.0000	0.0000	-10	8	8	1.52	77.09	23.09
III-29a	7	24	21	3150	43.8	0.00	0.0425	0.0213	0.0000	0.0000	-10	8	8	1.52	88.09	30.59
III-29b	7	24	21	3620	43.8	0.00	0.0425	0.0213	0.0000	0.0000	-10	8	8	1.52	98.59	30.59
III-30	7	24	21	3680	43.8	47.30	0.0425	0.0213	0.0052	0.0000	6	8	8	1.52	108.09	25.59
III-31	7	24	21	3250	43.8	44.00	0.0425	0.0213	0.0095	0.0000	6	8	8	1.52	114.59	25.59

Table B4 Evaluation Database of simply supported deep beams (1 of 11)

Beam I.D.	b, in	h, in	d, in	f'_c, psi	f_y, ksi	f_{yv}, ksi	ρ_l	ρ'	ρ_v	ρ_{vh}	Stirrup spacing, s, in	Load plate l_l, in	Bearing plate l_b, in	a/d	V_{test}, kip	Vcrack, kip
Foster & Gilbert, 1998																
B1.2-3	4.92	47.2	44.2	11603	58	62.30	0.0134	0.0017	0.0067	0.0028	3	9.842	9.842	0.76	292.91	0.00
B2.0-1	4.92	27.6	24.6	12038	58	62.30	0.0241	0.0030	0.0067	0.0037	3	9.842	9.842	1.32	179.03	0.00
B2.0-2	4.92	27.6	24.6	17404	58	62.30	0.0241	0.0030	0.0067	0.0037	3	9.842	9.842	1.32	185.83	0.00
B2.0-3	4.92	27.6	24.6	11313	58	62.30	0.0241	0.0030	0.0067	0.0037	3	9.842	9.842	1.32	157.73	0.00
B2.0A-4	4.92	27.6	24.6	12473	58	62.30	0.0241	0.0030	0.0067	0.0037	3	3.937008	9.842	0.88	213.93	0.00
B2.0B-5	4.92	27.6	24.6	12908	58	62.30	0.0241	0.0030	0.0000	0.0000	-10	9.842	9.842	1.32	131.83	0.00
B2.0C-6	4.92	27.6	24.6	13489	58	62.30	0.0241	0.0030	0.0100	0.0000	2	9.842	9.842	1.32	164.43	0.00
B2.0D-7	4.92	27.6	24.6	15084	58	62.30	0.0241	0.0030	0.0067	0.0000	3	9.842	9.842	1.32	162.23	0.00
B3.0-1	4.92	27.6	24.6	11603	58	62.30	0.0241	0.0030	0.0067	0.0037	3	9.842	9.842	1.88	115.17	0.00
B3.0-2	4.92	27.6	24.6	17404	58	62.30	0.0241	0.0030	0.0067	0.0037	3	9.842	9.842	1.88	118.47	0.00
B3.0-3	4.92	27.6	24.6	11168	58	62.30	0.0241	0.0030	0.0067	0.0037	3	9.842	9.842	1.88	118.47	0.00
B3.0A-4	4.92	27.6	24.6	12763	58	62.30	0.0241	0.0030	0.0067	0.0037	3	3.937008	9.842	1.28	174.67	0.00
B3.0B-5	4.92	27.6	24.6	12908	58	62.30	0.0241	0.0030	0.0000	0.0000	-10	9.842	9.842	1.88	98.27	0.00
Watstein & Mathey, 1958																
A-15	6	15	13.1	3450	40	0.00	0.0153	0.0000	0.0000	0.0000	-10	3.5	3.5	2.06	30.36	0.00
B-18-1	8	18	15.9	3680	38.7	0.00	0.0305	0.0000	0.0000	0.0000	-10	3.5	3.5	1.51	70.38	0.00
B-18-2	8	18	15.9	3330	38.7	0.00	0.0305	0.0000	0.0000	0.0000	-10	3.5	3.5	1.51	69.88	0.00
C-18-1	8	18	15.9	3710	71	0.00	0.0185	0.0000	0.0000	0.0000	-10	3.5	3.5	1.51	65.38	0.00
C-18-2	8	18	15.9	3830	67.5	0.00	0.0188	0.0000	0.0000	0.0000	-10	3.5	3.5	1.51	70.38	0.00
D-18-1	8	18	15.9	3720	105.15	0.00	0.0117	0.0000	0.0000	0.0000	-10	3.5	3.5	1.51	60.38	0.00
D-18-2	8	18	15.9	3910	96.9	0.00	0.0116	0.0000	0.0000	0.0000	-10	3.5	3.5	1.51	60.38	0.00
E-18-1	8	18	15.9	3250	99.5	0.00	0.0075	0.0000	0.0000	0.0000	-10	3.5	3.5	1.51	50.03	0.00
E-18-2	8	18	15.9	3870	99.5	0.00	0.0075	0.0000	0.0000	0.0000	-10	3.5	3.5	1.51	50.38	0.00

Table B5 Evaluation Database of simply supported deep beams (1 of 11)

Beam I.D.	b, in	h, in	d, in	f'_c, psi	f_y, ksi	f_{yv}, ksi	ρ_l	ρ'	ρ_v	ρ_{vh}	Stirrup spacing, s, in	Load plate l_l, in	Bearing plate l_b, in	a/d	V_{test}, kip	Vcrack, kip
Morrow & Viest, 1957																
B14B2	12	16	14.5	2120	67.6	0.00	0.0185	0.0000	0.0000	0.0000	-10	14	4	1.45	82.81	35.31
B14A4	12	16	14.25	3270	61.7	0.00	0.0250	0.0000	0.0000	0.0000	-10	14	4	1.47	115.30	50.30
B14B4	12	16	14.5	3820	58.6	0.00	0.0185	0.0000	0.0000	0.0000	-10	14	4	1.45	112.81	50.31
B14E4	12	16	14.5	4190	61.2	0.00	0.0124	0.0000	0.0000	0.0000	-10	14	4	1.45	115.31	52.81
B14A6	12	16	14	6590	65	0.00	0.0383	0.0000	0.0000	0.0000	-10	14	4	1.50	202.80	62.80
B14B6	12	16	14.5	6780	65.9	0.00	0.0185	0.0000	0.0000	0.0000	-10	14	4	1.45	175.31	50.31
B21B2	12	16	14.44	2010	63.4	0.00	0.0186	0.0000	0.0000	0.0000	-10	14	4	1.94	53.91	35.41
B21A4	12	16	14.5	4320	58.7	0.00	0.0246	0.0000	0.0000	0.0000	-10	14	4	1.93	117.91	45.41
B21B4	12	16	14.5	3930	61.3	0.00	0.0185	0.0000	0.0000	0.0000	-10	14	4	1.93	89.41	40.41
B21E4	12	16	14.38	3510	62.4	0.00	0.0124	0.0000	0.0000	0.0000	-10	14	4	1.95	95.41	44.91
B21E4R	12	16	14.5	4630	60.4	0.00	0.0124	0.0000	0.0000	0.0000	-10	14	4	1.93	97.91	40.41
B21F4	12	16	14.56	4560	66.2	0.00	0.0117	0.0000	0.0000	0.0000	-10	14	4	1.92	105.41	45.41
B21G4	12	16	14.69	4580	67.8	0.00	0.0058	0.0000	0.0000	0.0000	-10	14	4	1.91	79.91	37.91
B21A6	12	16	14	6570	64.9	0.00	0.0383	0.0000	0.0000	0.0000	-10	14	4	2.00	130.39	49.89
B21B6	12	16	14.75	6600	63.4	0.00	0.0182	0.0000	0.0000	0.0000	-10	14	4	1.90	130.42	50.42
B28B2	12	16	14.25	2130	68.3	0.00	0.0188	0.0000	0.0000	0.0000	-10	14	4	2.46	45.50	28.00
B28A4	12	16	14.5	3990	48.2	0.00	0.0246	0.0000	0.0000	0.0000	-10	14	4	2.41	73.01	34.51
B28B4	12	16	14.5	4690	64	0.00	0.0185	0.0000	0.0000	0.0000	-10	14	4	2.41	58.01	30.51
B28E4	12	16	14.5	4800	62.2	0.00	0.0124	0.0000	0.0000	0.0000	-10	14	4	2.41	60.51	28.01
B28B6	12	16	14.5	6360	65.5	0.00	0.0185	0.0000	0.0000	0.0000	-10	14	4	2.41	73.01	40.51

Table B6 Evaluation Database of simply supported deep beams (1 of 11)

Beam I.D.	b, in	h, in	d, in	f'_c, psi	f_y, ksi	f_{yv}, ksi	ρ_l	ρ'	ρ_v	ρ_{vh}	Stirrup spacing, s, in	Load plate l_l, in	Bearing plate l_b, in	a/d	V_{test}, kip	Vcrack, kip
Clark, 1951																
A1-1	8	18	15.3	3575	46.5	48.00	0.0310	0.0018	0.0038	0.0000	7.2	3.5	3.5	2.35	50.39	0.00
A1-2	8	18	15.3	3430	46.5	48.00	0.0310	0.0018	0.0038	0.0000	7.2	3.5	3.5	2.35	47.39	0.00
A1-3	8	18	15.3	3395	46.5	48.00	0.0310	0.0018	0.0038	0.0000	7.2	3.5	3.5	2.35	50.39	0.00
A1-4	8	18	15.3	3590	46.5	48.00	0.0310	0.0018	0.0038	0.0000	7.2	3.5	3.5	2.35	55.39	0.00
B1-1	8	18	15.3	3388	46.5	48.00	0.0310	0.0018	0.0037	0.0000	7.5	3.5	3.5	1.96	63.05	0.00
B1-2	8	18	15.3	3680	46.5	48.00	0.0310	0.0018	0.0037	0.0000	7.5	3.5	3.5	1.96	58.05	0.00
B1-3	8	18	15.3	3435	46.5	48.00	0.0310	0.0018	0.0037	0.0000	7.5	3.5	3.5	1.96	64.40	0.00
B1-4	8	18	15.3	3380	46.5	48.00	0.0310	0.0018	0.0037	0.0000	7.5	3.5	3.5	1.96	60.65	0.00
B1-5	8	18	15.3	3570	46.5	48.00	0.0310	0.0018	0.0037	0.0000	7.5	3.5	3.5	1.96	54.65	0.00
B2-1	8	18	15.3	3370	46.5	48.00	0.0310	0.0018	0.0073	0.0000	3.75	3.5	3.5	1.96	68.05	0.00
B2-2	8	18	15.3	3820	46.5	48.00	0.0310	0.0018	0.0073	0.0000	3.75	3.5	3.5	1.96	72.81	0.00
B2-3	8	18	15.3	3615	46.5	48.00	0.0310	0.0018	0.0073	0.0000	3.75	3.5	3.5	1.96	75.65	0.00
B6-1	8	18	15.3	6110	46.5	48.00	0.0310	0.0018	0.0037	0.0000	7.5	3.5	3.5	1.96	85.65	0.00
C1-1	8	18	15.3	3720	46.5	48.00	0.0207	0.0018	0.0034	0.0000	8	3.5	3.5	1.57	62.80	0.00
C1-2	8	18	15.3	3820	46.5	48.00	0.0207	0.0018	0.0034	0.0000	8	3.5	3.5	1.57	70.30	0.00
C1-3	8	18	15.3	3475	46.5	48.00	0.0207	0.0018	0.0034	0.0000	8	3.5	3.5	1.57	55.65	0.00
C1-4	8	18	15.3	4210	46.5	48.00	0.0207	0.0018	0.0034	0.0000	8	3.5	3.5	1.57	64.65	0.00
C2-1	8	18	15.3	3430	46.5	48.00	0.0207	0.0018	0.0069	0.0000	4	3.5	3.5	1.57	65.56	0.00
C2-2	8	18	15.3	3625	46.5	48.00	0.0207	0.0018	0.0069	0.0000	4	3.5	3.5	1.57	68.05	0.00
C2-3	8	18	15.3	3500	46.5	48.00	0.0207	0.0018	0.0069	0.0000	4	3.5	3.5	1.57	73.15	0.00
C2-4	8	18	15.3	3910	46.5	48.00	0.0207	0.0018	0.0069	0.0000	4	3.5	3.5	1.57	65.15	0.00
C3-1	8	18	15.3	2040	46.5	48.00	0.0207	0.0018	0.0034	0.0000	8	3.5	3.5	1.57	50.65	0.00
C3-2	8	18	15.3	2000	46.5	48.00	0.0207	0.0018	0.0034	0.0000	8	3.5	3.5	1.57	45.40	0.00
C3-3	8	18	15.3	2020	46.5	48.00	0.0207	0.0018	0.0034	0.0000	8	3.5	3.5	1.57	42.65	0.00
C4-1	8	18	15.3	3550	46.5	48.00	0.0310	0.0018	0.0034	0.0000	8	3.5	3.5	1.57	69.90	0.00
C6-2	8	18	15.3	6560	46.5	48.00	0.0310	0.0018	0.0034	0.0000	8	3.5	3.5	1.57	95.65	0.00
C6-3	8	18	15.3	6480	46.5	48.00	0.0310	0.0018	0.0034	0.0000	8	3.5	3.5	1.57	98.15	0.00
C6-4	8	18	15.3	6900	46.5	48.00	0.0310	0.0018	0.0034	0.0000	8	3.5	3.5	1.57	96.73	0.00
D1-1	8	18	15.5	3800	48.6	48.00	0.0163	0.0018	0.0046	0.0000	6	3.5	3.5	1.16	68.06	0.00
D1-2	8	18	15.5	3790	48.6	48.00	0.0163	0.0018	0.0046	0.0000	6	3.5	3.5	1.16	80.56	0.00
D1-3	8	18	15.5	3560	48.6	48.00	0.0163	0.0018	0.0046	0.0000	6	3.5	3.5	1.16	58.06	0.00
D2-1	8	18	15.5	3480	48.6	48.00	0.0163	0.0018	0.0061	0.0000	4.5	3.5	3.5	1.16	65.56	0.00
D2-2	8	18	15.5	3755	48.6	48.00	0.0163	0.0018	0.0061	0.0000	4.5	3.5	3.5	1.16	70.56	0.00
D2-3	8	18	15.5	3595	48.6	48.00	0.0163	0.0018	0.0061	0.0000	4.5	3.5	3.5	1.16	75.56	0.00

Table B7 Evaluation Database of simply supported deep beams (1 of 11)

Beam I.D.	b, in	h, in	d, in	f'_c, psi	f_y, ksi	f_{yv}, ksi	r_l	r'	r_v	r_{vh}	Stirrup spacing, s, in	Load plate l_l, in	Bearing plate l_b, in	a/d	V_{test}, kip	Vcrack, kip
Clark, 1951, continued . . .																
D2-4	8	18	15.5	3550	48.6	48.00	0.0163	0.0018	0.0061	0.0000	4.5	3.5	3.5	1.16	75.66	0.00
D3-1	8	18	15.5	4090	48.6	48.00	0.0244	0.0018	0.0092	0.0000	3	3.5	3.5	1.16	89.16	0.00
D4-1	8	18	15.5	3350	48.6	48.00	0.0163	0.0018	0.0122	0.0000	2.25	3.5	3.5	1.16	70.56	0.00
A0-1	8	18	15.3	3120	53.7	0.00	0.0098	0.0018	0.0000	0.0000	-10	3.5	3.5	2.35	20.39	0.00
A0-2	8	18	15.3	3770	53.7	0.00	0.0098	0.0018	0.0000	0.0000	-10	3.5	3.5	2.35	24.64	0.00
A0-3	8	18	15.3	3435	53.7	0.00	0.0098	0.0018	0.0000	0.0000	-10	3.5	3.5	2.35	27.14	0.00
B0-1	8	18	15.3	3420	53.7	0.00	0.0098	0.0018	0.0000	0.0000	-10	3.5	3.5	1.96	27.58	0.00
B0-2	8	18	15.3	3468	53.7	0.00	0.0098	0.0018	0.0000	0.0000	-10	3.5	3.5	1.96	21.55	0.00
B0-3	8	18	15.3	3410	53.7	0.00	0.0098	0.0018	0.0000	0.0000	-10	3.5	3.5	1.96	29.15	0.00
C0-1	8	18	15.3	3580	53.7	0.00	0.0098	0.0018	0.0000	0.0000	-10	3.5	3.5	1.57	39.55	0.00
C0-2	8	18	15.3	3405	53.7	0.00	0.0098	0.0018	0.0000	0.0000	-10	3.5	3.5	1.57	40.30	0.00
C0-3	8	18	15.3	3420	53.7	0.00	0.0098	0.0018	0.0000	0.0000	-10	3.5	3.5	1.57	37.90	0.00
D0-1	8	18	15.3	3750	53.7	0.00	0.0098	0.0018	0.0000	0.0000	-10	3.5	3.5	1.18	50.18	0.00
D0-2	8	18	15.3	3800	53.7	0.00	0.0098	0.0018	0.0000	0.0000	-10	3.5	3.5	1.18	58.80	0.00
D0-3	8	18	15.3	3765	53.7	0.00	0.0098	0.0018	0.0000	0.0000	-10	3.5	3.5	1.18	50.55	0.00
Uribe & Alcocer, 2001																
MR	13.78	47	43.3	5134	64.6	62.10	0.0158	0.0079	0.0053	0.0029	6	15.75	15.75	1.27	363.35	58.85
MT	13.78	47	43.3	5076	64.6	62.10	0.0158	0.0079	0.0053	0.0029	6	15.75	15.75	1.27	358.25	64.65
Yang, Chung, Lee & Eun, 2003																
L5-60	6.3	23.62	21.85	4554	116.6	0.00	0.0098	0.0017	0.0000	0.0000	-10	3.94	3.94	0.54	120.78	65.47
L5-60R	6.3	23.62	21.85	4554	116.6	0.00	0.0098	0.0017	0.0000	0.0000	-10	3.94	3.94	0.54	108.07	57.62
L5-75	6.3	29.53	26.97	4554	116.6	0.00	0.0100	0.0014	0.0000	0.0000	-10	3.94	3.94	0.55	134.54	64.72
L5-100	6.3	39.37	36.81	4554	83.4	0.00	0.0090	0.0010	0.0000	0.0000	-10	3.94	3.94	0.53	131.47	84.33
L10-60	6.3	23.62	21.85	4554	116.6	0.00	0.0098	0.0017	0.0000	0.0000	-10	3.94	3.94	1.08	84.85	37.93
L10-75	6.3	29.53	26.97	4554	116.6	0.00	0.0100	0.0014	0.0000	0.0000	-10	3.94	3.94	1.09	61.63	40.70
L10-75R	6.3	29.53	26.97	4554	116.6	0.00	0.0100	0.0014	0.0000	0.0000	-10	3.94	3.94	1.09	74.84	40.25
L10-100	6.3	39.37	36.81	4554	83.4	0.00	0.0090	0.0010	0.0000	0.0000	-10	3.94	3.94	1.07	123.27	51.67
UH5-60	6.3	23.62	21.85	11385	116.6	0.00	0.0098	0.0017	0.0000	0.0000	-10	3.94	3.94	0.54	185.54	78.69
UH5-75	6.3	29.53	26.97	11385	116.6	0.00	0.0100	0.0014	0.0000	0.0000	-10	3.94	3.94	0.55	227.53	95.11
UH5-100	6.3	39.37	36.81	11385	83.4	0.00	0.0090	0.0010	0.0000	0.0000	-10	3.94	3.94	0.53	231.94	121.78
UH10-60	6.3	23.62	21.85	11385	116.6	0.00	0.0098	0.0017	0.0000	0.0000	-10	3.94	3.94	1.08	129.36	57.76
UH10-75	6.3	29.53	26.97	11385	116.6	0.00	0.0100	0.0014	0.0000	0.0000	-10	3.94	3.94	1.09	76.60	56.77
UH10-75R	6.3	29.53	26.97	11385	116.6	0.00	0.0100	0.0014	0.0000	0.0000	-10	3.94	3.94	1.09	81.66	56.77
UH10-100	6.3	39.37	36.81	11385	83.4	0.00	0.0090	0.0010	0.0000	0.0000	-10	3.94	3.94	1.07	173.95	74.80

Table B8 Evaluation Database of simply supported deep beams (1 of 11)

Beam I.D.	b, in	h, in	d, in	f'_c, psi	f_y, ksi	f_{yv}, ksi	ρ_l	ρ'	ρ_v	ρ_{vh}	Stirrup spacing, s, in	Load plate l_l, in	Bearing plate l_b, in	a/d	V_{test}, kip	Vcrack, kip
Tanimura and Sato, 2005																
1A	11.81	17.72	15.75	3365	66.4	0.00	0.0214	0.0033	0.0000	0.0000	-10	3.94	3.94	0.50	192.05	0.00
2A	11.81	17.72	15.75	3365	66.4	53.70	0.0214	0.0033	0.0021	0.0000	3.94	3.94	3.94	0.50	184.85	0.00
3A	11.81	17.72	15.75	3365	66.4	56.30	0.0214	0.0033	0.0048	0.0000	3.94	3.94	3.94	0.50	187.55	0.00
4A	11.81	17.72	15.75	3365	66.4	53.40	0.0214	0.0033	0.0084	0.0000	3.94	3.94	3.94	0.50	195.65	0.00
5A	11.81	17.72	15.75	4206	66.4	0.00	0.0214	0.0033	0.0000	0.0000	-10	3.94	3.94	1.00	142.47	0.00
6A	11.81	17.72	15.75	4206	66.4	53.70	0.0214	0.0033	0.0021	0.0000	3.94	3.94	3.94	1.00	164.67	0.00
7A	11.81	17.72	15.75	4206	66.4	56.30	0.0214	0.0033	0.0048	0.0000	3.94	3.94	3.94	1.00	168.97	0.00
8A	11.81	17.72	15.75	4206	66.4	53.40	0.0214	0.0033	0.0084	0.0000	3.94	3.94	3.94	1.00	181.07	0.00
9A	11.81	17.72	15.75	3321	66.4	0.00	0.0214	0.0033	0.0000	0.0000	-10	3.94	3.94	1.50	64.29	0.00
10A	11.81	17.72	15.75	3263	66.4	53.70	0.0214	0.0033	0.0021	0.0000	3.94	3.94	3.94	1.50	104.79	0.00
11A	11.81	17.72	15.75	3336	66.4	56.30	0.0214	0.0033	0.0048	0.0000	3.94	3.94	3.94	1.50	110.89	0.00
12A	11.81	17.72	15.75	3408	66.4	53.40	0.0214	0.0033	0.0084	0.0000	3.94	3.94	3.94	1.50	128.59	0.00
13B	11.81	17.72	15.75	4641	66.4	0.00	0.0214	0.0000	0.0000	0.0000	-10	3.94	3.94	1.00	148.97	0.00
14B	11.81	17.72	15.75	4641	66.4	53.70	0.0214	0.0000	0.0021	0.0000	3.94	3.94	3.94	1.00	169.17	0.00
15B	11.81	17.72	15.75	4641	66.4	56.30	0.0214	0.0000	0.0048	0.0000	3.94	3.94	3.94	1.00	174.37	0.00
16B	11.81	17.72	15.75	4641	66.4	53.40	0.0214	0.0000	0.0084	0.0000	3.94	3.94	3.94	1.00	191.27	0.00
17C	11.81	17.72	15.75	4540	66.4	53.70	0.0214	0.0033	0.0021	0.0000	3.94	3.94	3.94	1.00	128.47	0.00
18C	11.81	17.72	15.75	4569	66.4	56.30	0.0214	0.0033	0.0048	0.0000	3.94	3.94	3.94	1.00	174.17	0.00
19C	11.81	17.72	15.75	4612	66.4	53.40	0.0214	0.0033	0.0084	0.0000	3.94	3.94	3.94	1.00	170.37	0.00
20D	11.81	17.72	15.75	3524	101.8	138.00	0.0214	0.0033	0.0048	0.0000	3.94	3.94	3.94	1.00	149.87	0.00
21D	11.81	17.72	15.75	3902	101.8	152.40	0.0214	0.0033	0.0084	0.0000	3.94	3.94	3.94	1.00	148.97	0.00
22D	11.81	17.72	15.75	3800	101.8	138.00	0.0214	0.0033	0.0048	0.0000	3.94	3.94	3.94	1.50	121.19	0.00
23D	11.81	17.72	15.75	3814	101.8	152.40	0.0214	0.0033	0.0084	0.0000	3.94	3.94	3.94	1.50	127.69	0.00
24F	11.81	17.72	15.75	11589	101.8	0.00	0.0214	0.0033	0.0000	0.0000	-10	3.94	3.94	0.50	440.45	0.00
25F	11.81	17.72	15.75	11081	101.8	0.00	0.0214	0.0033	0.0000	0.0000	-10	3.94	3.94	1.00	315.77	0.00
26F	11.81	17.72	15.75	11356	101.8	0.00	0.0214	0.0033	0.0000	0.0000	-10	3.94	3.94	1.50	203.69	0.00
27F	11.81	17.72	15.75	11284	101.8	0.00	0.0214	0.0033	0.0000	0.0000	-10	3.94	3.94	2.00	169.71	0.00
28A	11.81	17.72	15.75	3698	66.4	56.30	0.0214	0.0033	0.0048	0.0000	3.94	3.94	3.94	0.75	145.81	0.00
29A	11.81	17.72	15.75	3800	66.4	53.40	0.0214	0.0033	0.0084	0.0000	3.94	3.94	3.94	0.75	150.01	0.00
30A	11.81	17.72	15.75	3829	66.4	56.40	0.0214	0.0033	0.0088	0.0000	5.91	3.94	3.94	0.75	157.91	0.00
31A	11.81	17.72	15.75	3858	101.8	56.30	0.0214	0.0033	0.0048	0.0000	3.94	3.94	3.94	2.00	94.11	0.00
32A	11.81	17.72	15.75	3974	101.8	53.40	0.0214	0.0033	0.0084	0.0000	3.94	3.94	3.94	2.00	99.51	0.00
33A	11.81	17.72	15.75	3582	66.4	56.30	0.0214	0.0033	0.0095	0.0000	1.97	3.94	3.94	1.00	145.87	0.00
34A	11.81	17.72	15.75	3597	66.4	54.40	0.0214	0.0033	0.0095	0.0000	7.87	3.94	3.94	1.00	134.77	0.00

Table B9 Evaluation Database of simply supported deep beams (1 of 11)

Beam I.D.	b, in	h, in	d, in	f'_c, psi	f_y, ksi	f_{yv}, ksi	r_l	r'	r_v	r_{vh}	Stirrup spacing, s, in	Load plate l_l, in	Bearing plate l_b, in	a/d	V_{test}, kip	Vcrack, kip
Tanimura and Sato, 2005																
35E	11.81	17.72	15.75	3669	192.9	0.00	0.0042	0.0033	0.0000	0.0000	-10	3.94	3.94	0.50	132.45	0.00
36E	11.81	17.72	15.75	3553	192.9	56.30	0.0042	0.0033	0.0048	0.0000	3.94	3.94	3.94	0.50	121.45	0.00
37E	11.81	17.72	15.75	3742	192.9	53.40	0.0042	0.0033	0.0084	0.0000	3.94	3.94	3.94	0.50	124.75	0.00
38E	11.81	17.72	15.75	3655	192.9	0.00	0.0042	0.0033	0.0000	0.0000	-10	3.94	3.94	1.00	80.87	0.00
39E	11.81	17.72	15.75	3684	192.9	56.30	0.0042	0.0033	0.0048	0.0000	3.94	3.94	3.94	1.00	106.07	0.00
40E	11.81	17.72	15.75	3756	192.9	53.40	0.0042	0.0033	0.0084	0.0000	3.94	3.94	3.94	1.00	106.07	0.00
41A	11.81	17.72	15.75	2988	108.8	56.30	0.0214	0.0033	0.0048	0.0000	3.94	3.94	3.94	2.50	73.54	0.00
42A	11.81	17.72	15.75	3104	108.8	53.40	0.0214	0.0033	0.0084	0.0000	3.94	3.94	3.94	2.50	85.24	0.00
45F	11.81	17.72	15.75	14098	108.8	0.00	0.0214	0.0033	0.0000	0.0000	-10	3.94	3.94	2.50	78.34	0.00
46F	11.81	17.72	15.75	14141	108.8	138.80	0.0214	0.0033	0.0021	0.0000	3.94	3.94	3.94	1.00	279.77	0.00
47F	11.81	17.72	15.75	13967	108.8	138.20	0.0214	0.0033	0.0048	0.0000	3.94	3.94	3.94	1.00	292.67	0.00
48F	11.81	17.72	15.75	13706	108.8	138.80	0.0214	0.0033	0.0021	0.0000	3.94	3.94	3.94	1.50	209.99	0.00
49F	11.81	17.72	15.75	13663	108.8	138.20	0.0214	0.0033	0.0048	0.0000	3.94	3.94	3.94	1.50	220.79	0.00
L6	7.87	41.3	39.37	4525	147.4	56.40	0.0040	0.0020	0.0029	0.0000	9.84	5.91	5.91	1.00	150.73	0.00
L7	15.75	80.71	78.74	4424	147.4	54.40	0.0040	0.0005	0.0029	0.0000	19.69	11.81	11.81	1.00	589.91	0.00
Matsuo et al., 2002																
D600	5.91	25.59	23.62	5918	145.9	0.00	0.0176	0.0006	0.0000	0.0000	-10	5.91	5.91	1.00	95.67	0.00
D604	5.91	25.59	23.62	4960	145.9	48.00	0.0176	0.0006	0.0042	0.0000	3.94	5.91	5.91	1.00	132.13	0.00
D608	5.91	25.59	23.62	5120	145.9	48.00	0.0176	0.0006	0.0084	0.0000	1.97	5.91	5.91	1.00	149.46	0.00
Brown, Sankovich, Bayrak, and Jirsa, 2006																
B	6	36	36	4200	0	73.00	0.0000	0.0000	0.0000	0.0000	-10	12	12	0.00	196.30	0.00
G	6	36	36	4300	0	73.00	0.0005	0.0000	0.0031	0.0031	6	12	12	0.00	264.50	0.00
L	6	36	36	5290	0	73.00	0.0005	0.0000	0.0000	0.0031	-10	12	12	0.00	366.80	0.00
M	6	36	36	4300	0	73.00	0.0005	0.0000	0.0000	0.0031	-10	12	12	0.00	283.20	0.00
N	6	36	36	4300	0	73.00	0.0005	0.0000	0.0000	0.0031	-10	6	6	0.00	202.10	0.00
O	6	36	36	5500	0	73.00	0.0002	0.0000	0.0000	0.0027	-10	12	12	0.00	352.40	0.00
P	6	36	36	5500	0	73.00	0.0005	0.0000	0.0000	0.0061	-10	12	12	0.00	377.00	0.00
Q	6	36	36	4200	0	73.00	0.0000	0.0000	0.0000	0.0010	-10	12	12	0.00	224.00	0.00
S	6	36	36	5290	0	73.00	0.0000	0.0000	0.0000	0.0008	-10	12	12	0.00	322.50	0.00
T	6	36	36	5290	0	73.00	0.0000	0.0000	0.0000	0.0046	-10	12	12	0.00	343.10	0.00
U	6	36	36	4350	0	73.00	0.0000	0.0000	0.0000	0.0023	-10	6	6	0.00	189.00	0.00
V	6	36	36	4350	0	73.00	0.0000	0.0000	0.0046	0.0015	4	12	12	0.00	259.70	0.00
W	6	36	36	4350	0	73.00	0.0005	0.0000	0.0000	0.0031	-10	16	16	0.00	370.10	0.00
X	6	36	36	4350	0	73.00	0.0005	0.0000	0.0000	0.0031	-10	12	12	0.00	246.70	0.00
Y	10	36	36	4350	0	73.00	0.0010	0.0000	0.0000	0.0037	-10	12	12	0.00	299.50	0.00
Z	10	36	36	4350	0	73.00	0.0010	0.0000	0.0000	0.0037	-10	12	12	0.00	303.80	0.00

Table B10 Evaluation Database of simply supported deep beams (1 of 11)

Beam I.D.	b, in	h, in	d, in	f'_c, psi	f_y, ksi	f_{yv}, ksi	ρ_l	ρ'	ρ_v	ρ_{vh}	Stirrup spacing, s, in	Load plate l_l, in	Bearing plate l_b, in	a/d	V_{test}, kip	Vcrack, kip
Walraven and Lehwalter, 1994																
V022	9.84	15.75	14.17	3608	60	0.00	0.0113	0.0000	0.0000	0.0000	-10	3.5425	3.5425	1.00	60.87	28.27
V511	9.84	23.62	22.05	3590	60	0.00	0.0112	0.0000	0.0000	0.0000	-10	5.5125	5.5125	1.00	79.10	34.12
V411	9.84	31.5	29.13	3518	60	0.00	0.0110	0.0000	0.0000	0.0000	-10	7.2825	7.2825	1.00	82.80	51.28
V211	9.84	39.37	36.61	3626	60	0.00	0.0108	0.0000	0.0000	0.0000	-10	9.1525	9.1525	1.00	114.61	55.06
V711/4b	9.84	15.75	14.17	3300	60	60.00	0.0113	0.0000	0.0013	0.0000	3.94	3.5425	3.5425	1.00	71.43	0.00
V511/4	9.84	23.62	22.05	3390	60	60.00	0.0112	0.0000	0.0014	0.0000	5.91	5.5125	5.5125	1.01	104.95	0.00
V411/4	9.84	31.5	29.92	3083	60	60.00	0.0107	0.0000	0.0017	0.0000	7.48	7.48	7.48	0.97	105.71	0.00
V022/3	9.84	15.75	14.17	3554	60	60.00	0.0113	0.0000	0.0035	0.0000	3.94	3.5425	3.5425	1.00	85.60	0.00
V511/3	9.84	23.62	22.05	3861	60	60.00	0.0112	0.0000	0.0033	0.0000	5.91	5.5125	5.5125	1.01	130.80	0.00
V411/3	9.84	31.5	29.92	3590	60	60.00	0.0107	0.0000	0.0033	0.0000	7.48	7.48	7.48	0.97	150.22	0.00
Zhang & Tan, 2007																
1DB70bw	6.3	27.56	25.28	4104	75.7	53.70	0.0111	0.0010	0.0045	0.0000	5.91	4.13	4.13	1.10	96.21	31.66
1DB100bw	9.06	39.37	35.59	4162	75.4	66.00	0.0123	0.0007	0.0041	0.0000	5.91	5.91	5.91	1.10	174.86	77.06
3DB70b	6.3	27.56	25.28	4162	75.7	0.00	0.0111	0.0000	0.0000	0.0000	-10	4.13	4.13	1.10	81.25	36.18
3DB100b	9.06	39.37	35.59	4249	77.1	0.00	0.0123	0.0000	0.0000	0.0000	-10	5.91	5.91	1.10	151.66	50.07
Hassan et al., 2008																
G-1.9-51	18	36	33.5	7400	68	0.00	0.0072	0.0036	0.0000	0.0000	-10	10	6	1.88	99.27	75.00
M-1.9-51	18	36	33.5	7400	120	0.00	0.0044	0.0022	0.0000	0.0000	-10	10	6	1.88	176.77	75.00
G-1.9-38	18	36	33.5	5500	68	0.00	0.0072	0.0036	0.0000	0.0000	-10	10	6	1.88	86.77	75.00
M-1.9-38	18	36	33.5	5500	120	0.00	0.0044	0.0022	0.0000	0.0000	-10	10	6	1.88	154.77	75.00
Huizinga, 2007																
M-03-4-CC0	36	48	40	4100	67	61.00	0.0293	0.0043	0.0031	0.0030	11	24	16	1.85	1128.30	354.00
M-09-4-CC0	36	48	40	4100	67	61.00	0.0293	0.0043	0.0086	0.0030	4	24	16	1.85	1415.00	0.00
M-03-2-CC0	36	48	40	4900	68	62.00	0.0293	0.0022	0.0031	0.0027	11	24	16	1.85	1096.00	0.00
M-02-4-CC0	36	48	40	2800	65	62.50	0.0293	0.0043	0.0022	0.0022	10	24	16	1.85	1102.00	256.00
M-03-4-CC0	36	48	40	3000	65	62.50	0.0293	0.0043	0.0031	0.0030	11	8	16	1.85	930.00	0.00
Deschenes, 2008																
Validation B	21	42	36.14	5061	66	65.00	0.0310	0.0100	0.0030	0.0058	9.5	20	16	1.85	576.60	151.20
nR1	21	42	36.14	7250	66	65.00	0.0310	0.0100	0.0030	0.0058	9.5	20	16	1.85	560.83	0.00

Table B11 Evaluation Database of simply supported deep beams (1 of 11)

Beam I.D.	b, in	h, in	d, in	f'_c, psi	f_y, ksi	f_{yv}, ksi	r_l	r'	r_v	r_{vh}	Stirrup spacing, s, in	Load plate l_l, in	Bearing plate l_b, in	a/d	V_{test}, kip	Vcrack, kip
Birrcher and Tuchscherer, 2008																
II-03-CCC20	21	42	38.6	3290	64	65.00	0.0231	0.0115	0.0031	0.0045	9.5	20	10	1.84	499.47	139.00
II-030CCC1	21	42	38.6	3480	64	65.00	0.0231	0.0115	0.0031	0.0045	9.5	10	10	1.84	477.40	0.00
III-1.85-00	21	42	38.6	3170	66	0.00	0.0231	0.0115	0.0000	0.0000	-10	20	10	1.84	365.30	98.00
III-2.5-00	21	42	38.6	3200	66	0.00	0.0231	0.0115	0.0000	0.0000	-10	20	10	2.46	81.90	0.00
II-03-CCT10	21	42	38.6	4410	66	71.00	0.0231	0.0115	0.0031	0.0045	9.5	36	10	1.84	635.40	0.00
II-03-CCT05	21	42	38.6	4210	66	71.00	0.0231	0.0115	0.0031	0.0045	9.5	36	5	1.84	597.40	146.00
III-1.85-02	21	42	38.6	4100	66	64.00	0.0231	0.0115	0.0020	0.0019	14.5	20	16	1.84	487.80	112.00
III-1.85-025	21	42	38.6	4100	66	64.00	0.0231	0.0115	0.0024	0.0014	12	20	16	1.84	515.60	0.00
III-1.85-03	21	42	38.6	4990	69	64.00	0.0231	0.0115	0.0029	0.0029	10	20	16	1.84	412.30	137.00
III-1.85-01	21	42	38.6	5010	69	63.00	0.0231	0.0115	0.0010	0.0014	18	20	16	1.84	272.60	0.00
II-02-CCT05	21	42	38.6	3120	69	64.00	0.0231	0.0115	0.0020	0.0019	15	36	5	1.84	401.40	94.00
II-02-CCC10	21	42	38.6	3140	69	64.00	0.0231	0.0115	0.0020	0.0019	15	10	10	1.84	334.80	0.00
I-03-2	21	44	38.5	5240	73	67.00	0.0229	0.0116	0.0029	0.0033	6.5	20	16	1.84	569.20	144.00
I-03-4	21	44	38.5	5330	73	73.00	0.0229	0.0116	0.0030	0.0033	7	20	16	1.84	657.40	0.00
I-02-2	21	44	38.5	3950	73	67.00	0.0229	0.0116	0.0020	0.0020	9.5	20	16	1.84	453.70	121.00
I-02-4	21	44	38.5	4160	73	73.00	0.0229	0.0116	0.0021	0.0020	10	20	16	1.84	528.10	0.00
III-1.85-03b	21	42	38.6	3300	69	62.00	0.0231	0.0115	0.0031	0.0029	6	20	16	1.84	471.10	114.00
III-1.85-02b	21	42	38.6	3300	69	62.00	0.0231	0.0115	0.0020	0.0018	9.5	20	16	1.84	467.60	0.00
III-1.2-02	21	42	38.6	4100	66	60.00	0.0231	0.0115	0.0020	0.0018	9.5	20	16	1.20	846.47	165.00
III-1.2-03	21	42	38.6	4220	66	68.00	0.0231	0.0115	0.0031	0.0029	9.5	20	16	1.20	829.20	0.00
III-2.5-02	21	42	38.6	4630	66	62.00	0.0231	0.0115	0.0020	0.0018	9.5	20	16	2.49	298.30	105.00
III-2.5-03	21	42	38.6	5030	66	65.00	0.0231	0.0115	0.0031	0.0029	9.5	20	16	2.49	516.00	0.00
II-02-CCC10	21	42	38.6	4620	69	67.00	0.0231	0.0115	0.0020	0.0019	15	10	10	1.84	329.00	132.00
II-02-CCT05	21	42	38.6	4740	69	67.00	0.0231	0.0115	0.0020	0.0019	15	20	5	1.84	567.40	0.00
IV-2175-1.8	21	74.5	68.9	4930	68	66.00	0.0237	0.0129	0.0020	0.0018	9.5	29	16	1.85	762.70	216.00
IV-2175-1.8	21	74.5	68.9	4930	68	66.00	0.0237	0.0129	0.0031	0.0029	9.5	29	16	1.85	842.40	218.00
IV-2175-2.5	21	74.5	68.9	5010	68	64.00	0.0237	0.0129	0.0021	0.0021	14.25	24	16	2.50	509.90	144.00
IV-2175-1.2	21	74.5	68.9	5010	68	64.00	0.0237	0.0129	0.0021	0.0021	14.25	24	16	1.20	1222.80	262.00
IV-2123-1.8	21	22.5	19.5	4160	66	66.00	0.0232	0.0116	0.0030	0.0030	6.25	16.5	16	1.85	328.50	60.00
IV-2123-1.8	21	22.5	19.5	4220	66	81.00	0.0232	0.0116	0.0020	0.0017	5.25	16.5	16	1.85	347.00	65.00
IV-2123-2.5	21	22.5	19.5	4570	65	58.00	0.0232	0.0116	0.0020	0.0017	5.25	15.5	16	2.50	160.70	51.00
IV-2123-1.2	21	22.5	19.5	4630	65	58.00	0.0232	0.0116	0.0020	0.0017	5.25	18	16	1.20	591.60	124.00

Table B12 Evaluation Database of two span continuous deep beams (1 of 02)

Beam I.D.	b, in	h, in	d, in	f'_c, psi	f_y, ksi	f_{yv}, ksi	ρ_l	ρ'	ρ_v	ρ_{vh}	Stirrup spacing, s, in	Load plate l_l, in	Bearing plate l_b, in	a/d	V_{test}, kip	Vcrack, kip
Rogowsky and MacGregor, 1983																
3/1.0	7.87	39.37	37.91	4.19	55.04	80.51	0.0063	0.0046	0.0015	0.0000	-	11.81	7.87	0.78	154.00	89.93
4/1.0	7.87	39.37	37.91	4.13	55.04	80.51	0.0063	0.0046	0.0000	0.0006	-	11.81	7.87	0.78	149.06	83.18
5/1.0	7.87	39.37	37.91	5.35	58.42	80.51	0.0063	0.0046	0.0060	0.0000	-	11.81	7.87	0.78	196.72	92.18
6/1.0	7.87	39.37	37.91	5.19	58.42	80.51	0.0063	0.0046	0.0000	0.0013	-	11.81	7.87	0.78	142.76	59.58
7/1.0	7.87	39.37	37.91	5.00	58.42	80.51	0.0063	0.0046	0.0000	0.0000	-	11.81	7.87	0.78	156.25	24.73
3/1.5	7.87	23.62	21.18	2.10	65.63	80.51	0.0072	0.0096	0.0019	0.0000	-	11.81	7.87	1.39	64.52	33.72
4/1.5	7.87	23.62	21.18	4.71	65.63	80.51	0.0072	0.0096	0.0000	0.0011	-	11.81	7.87	1.39	52.16	40.47
5/1.5	7.87	23.62	21.18	5.74	65.63	80.51	0.0072	0.0096	0.0060	0.0000	-	11.81	7.87	1.39	127.25	33.72
6/1.5	7.87	23.62	21.18	6.53	65.63	80.51	0.0072	0.0096	0.0000	0.0032	-	11.81	7.87	1.39	58.00	33.72
7/1.5	7.87	23.62	21.18	4.41	65.63	80.51	0.0072	0.0096	0.0000	0.0000	-	11.81	7.87	1.39	78.24	-
3/2.0	7.87	19.69	17.24	6.16	66.68	80.51	0.0088	0.0119	0.0014	0.0012	-	7.87	7.87	1.83	62.28	29.23
4/2.0	7.87	19.69	17.24	5.55	66.68	80.51	0.0088	0.0119	0.0000	0.0000	-	7.87	7.87	1.83	54.63	56.21
5/2.0	7.87	19.69	17.24	5.96	66.68	80.51	0.0088	0.0119	0.0057	0.0013	-	7.87	7.87	1.83	102.52	35.97
6/2.0	7.87	19.69	17.24	5.42	66.68	80.51	0.0088	0.0119	0.0000	0.0000	-	7.87	7.87	1.83	58.00	42.72
7/2.0	7.87	19.69	17.24	6.79	66.68	80.51	0.0088	0.0119	0.0000	0.0039	-	7.87	7.87	1.83	41.59	53.96
Ashour, 1997																
CB1	4.70	24.61	22.15	4.35	80.76	53.67	0.0070	0.0090	0.0080	0.0100	-	7.87	4.72	1.21	78.91	-
CB2	4.70	24.61	22.15	4.80	80.76	53.67	0.0070	0.0090	0.0040	0.0050	-	7.87	4.72	1.21	68.79	-
CB3	4.70	24.61	22.15	3.19	80.76	53.67	0.0070	0.0090	0.0000	0.0050	-	7.87	4.72	1.21	40.51	-
CB4	4.70	24.61	22.15	4.06	80.76	53.67	0.0070	0.0090	0.0040	0.0000	-	7.87	4.72	1.21	63.83	-
CB5	4.70	24.61	22.15	4.16	72.60	53.67	0.0030	0.0030	0.0040	0.0050	-	7.87	4.72	1.21	58.00	-
CB6	4.70	16.73	15.06	3.26	85.57	53.67	0.0080	0.0080	0.0050	0.0030	-	7.87	4.72	1.78	35.09	-
CB7	4.70	16.73	15.06	3.87	85.57	53.67	0.0080	0.0080	0.0020	0.0010	-	7.87	4.72	1.78	31.59	-
CB8	4.70	16.73	15.06	3.42	80.76	53.67	0.0050	0.0050	0.0020	0.0010	-	7.87	4.72	1.78	27.81	-
Asin, 1999																
1.0/1/1	5.91	39.37	37.91	5.38	91.45	80.69	0.0030	0.0040	0.0050	0.0000	-	11.81	7.87	0.89	118.93	-
1.0/1/2	5.91	39.37	37.91	4.38	90.86	72.25	0.0030	0.0040	0.0040	0.0000	-	11.81	7.87	0.89	111.29	-
1.0/1/3	5.91	39.37	37.91	4.41	90.36	90.36	0.0030	0.0040	0.0020	0.0000	-	11.81	7.87	0.89	87.23	-
1.0/2/1	5.91	39.37	37.91	4.09	88.60	80.96	0.0040	0.0030	0.0050	0.0000	-	11.81	7.87	0.89	132.19	-
1.0/2/2	5.91	39.37	37.91	4.97	89.52	72.12	0.0040	0.0030	0.0040	0.0000	-	11.81	7.87	0.89	105.44	-
1.0/2/3	5.91	39.37	37.91	5.34	88.93	90.71	0.0040	0.0030	0.0020	0.0000	-	11.81	7.87	0.89	94.87	-
1.5/1/1	5.91	23.62	21.18	5.06	85.47	80.97	0.0070	0.0090	0.0050	0.0000	-	11.81	7.87	1.55	90.38	-
1.5/1/2	5.91	23.62	21.18	4.83	85.30	72.43	0.0070	0.0090	0.0040	0.0000	-	11.81	7.87	1.55	78.01	-
1.5/1/3	5.91	23.62	21.18	4.73	85.61	89.81	0.0070	0.0090	0.0020	0.0000	-	11.81	7.87	1.55	58.68	-
1.5/2/1	5.91	23.62	21.18	4.81	80.03	80.88	0.0100	0.0080	0.0050	0.0000	-	11.81	7.87	1.55	84.31	-
1.5/2/2	5.91	23.62	21.18	4.81	80.03	72.21	0.0100	0.0080	0.0040	0.0000	-	11.81	7.87	1.55	76.21	-
1.5/2/3	5.91	23.62	21.18	4.99	79.81	89.78	0.0100	0.0080	0.0020	0.0000	-	11.81	7.87	1.55	55.31	-

Table B13 Evaluation Database of two span continuous deep beams (1 of 02)

Beam I.D.	b, in	h, in	d, in	f'_c, psi	f_y, ksi	$f_{yv,}$ ksi	r_l	r'	r_v	r_{vh}	Stirrup spacing, s, in	Load plate l_l, in	Bearing plate l_b, in	a/d	V_{test}, kip	Vcrack, kip
Yang et al., 2007																
L5-40	6.30	15.75	13.98	4.70	81.49	0.00	0.0100	0.0100	0.0000	0.0000	-	5.91	3.94	0.56	91.05	41.14
L5-60	6.30	23.62	21.85	4.70	81.49	0.00	0.0097	0.0097	0.0000	0.0000	-	5.91	3.94	0.54	102.52	57.33
L5-72	6.30	28.35	25.71	4.70	81.49	0.00	0.0110	0.0110	0.0000	0.0000	-	5.91	3.94	0.55	110.61	64.07
L10-40	6.30	15.75	13.98	4.65	81.49	0.00	0.0100	0.0100	0.0000	0.0000	-	5.91	3.94	1.13	45.19	20.91
L10-60	6.30	23.62	21.85	4.65	81.49	0.00	0.0097	0.0097	0.0000	0.0000	-	5.91	3.94	1.08	58.90	38.89
L10-72	6.30	28.35	25.71	4.65	81.49	0.00	0.0110	0.0110	0.0000	0.0000	-	5.91	3.94	1.10	67.45	43.62
H6-40	6.30	15.75	13.98	9.44	81.49	0.00	0.0100	0.0100	0.0000	0.0000	-	5.91	3.94	0.68	132.64	60.70
H6-60	6.30	23.62	21.85	9.44	81.49	0.00	0.0097	0.0097	0.0000	0.0000	-	5.91	3.94	0.65	142.54	77.56
H6-72	6.30	28.35	25.71	9.44	81.49	0.00	0.0110	0.0110	0.0000	0.0000	-	5.91	3.94	0.66	156.92	92.40
H10-40	6.30	15.75	13.98	9.79	81.49	0.00	0.0100	0.0100	0.0000	0.0000	-	5.91	3.94	1.13	75.31	31.92
H10-60	6.30	23.62	21.85	9.89	81.49	0.00	0.0097	0.0097	0.0000	0.0000	-	5.91	3.94	1.08	83.63	51.26
H10-72	6.30	28.35	25.71	9.79	81.49	0.00	0.0110	0.0110	0.0000	0.0000	-	5.91	3.94	1.10	88.13	56.65
L5-NN	6.30	23.62	20.36	4.70	81.49	70.04	0.0100	0.0100	0.0000	0.0000	-	5.91	3.94	0.58	102.52	57.33
L5-NS	6.30	23.62	20.36	4.70	81.49	70.04	0.0100	0.0100	0.0030	0.0000	-	5.91	3.94	0.58	106.79	55.53
L5-NT	6.30	23.62	20.36	4.70	81.49	70.04	0.0100	0.0100	0.0060	0.0000	-	5.91	3.94	0.58	115.11	62.50
L5-SN	6.30	23.62	20.36	4.70	81.49	70.04	0.0100	0.0100	0.0000	0.0030	-	5.91	3.94	0.58	120.73	57.33
L5-SS	6.30	23.62	20.36	4.70	81.49	70.04	0.0100	0.0100	0.0030	0.0030	-	5.91	3.94	0.58	136.47	55.53
L5-TN	6.30	23.62	20.36	4.70	81.49	70.04	0.0100	0.0100	0.0000	0.0060	-	5.91	3.94	0.58	143.88	59.80
L10-NN	6.30	23.62	20.19	4.65	81.49	70.04	0.0100	0.0100	0.0000	0.0000	-	5.91	3.94	1.17	59.35	38.89
L10-NS	6.30	23.62	20.19	4.65	81.49	70.04	0.0100	0.0100	0.0030	0.0000	-	5.91	3.94	1.17	78.24	35.07
L10-NT	6.30	23.62	20.19	4.65	81.49	70.04	0.0100	0.0100	0.0060	0.0000	-	5.91	3.94	1.17	100.27	46.31
L10-SN	6.30	23.62	20.19	4.65	81.49	70.04	0.0100	0.0100	0.0000	0.0030	-	5.91	3.94	1.17	59.58	34.40
L10-SS	6.30	23.62	20.19	4.65	81.49	70.04	0.0100	0.0100	0.0030	0.0030	-	5.91	3.94	1.17	79.14	37.32
L10-TN	6.30	23.62	20.19	4.65	81.49	70.04	0.0100	0.0100	0.0000	0.0060	-	5.91	3.94	1.17	64.75	39.34
H6-NN	6.30	23.62	20.25	9.44	81.49	70.04	0.0100	0.0100	0.0000	0.0000	-	5.91	3.94	0.70	142.31	68.57
H6-NS	6.30	23.62	20.25	9.44	81.49	70.04	0.0100	0.0100	0.0030	0.0000	-	5.91	3.94	0.70	153.55	85.21
H6-NT	6.30	23.62	20.25	9.44	81.49	70.04	0.0100	0.0100	0.0060	0.0000	-	5.91	3.94	0.70	170.19	72.84
H6-SN	6.30	23.62	20.25	9.44	81.49	70.04	0.0100	0.0100	0.0000	0.0030	-	5.91	3.94	0.70	158.05	88.35
H6-SS	6.30	23.62	20.25	9.44	81.49	70.04	0.0100	0.0100	0.0030	0.0030	-	5.91	3.94	0.70	179.63	82.51
H6-TN	6.30	23.62	20.25	9.44	81.49	70.04	0.0100	0.0100	0.0000	0.0060	-	5.91	3.94	0.70	191.55	98.70
H10-NN	6.30	23.62	20.19	9.89	81.49	70.04	0.0100	0.0100	0.0000	0.0000	-	5.91	3.94	1.17	83.63	51.26
H10-NS	6.30	23.62	20.19	9.89	81.49	70.04	0.0100	0.0100	0.0030	0.0000	-	5.91	3.94	1.17	92.85	53.28
H10-NT	6.30	23.62	20.19	9.89	81.49	70.04	0.0100	0.0100	0.0060	0.0000	-	5.91	3.94	1.17	143.21	56.43
H10-SN	6.30	23.62	20.19	9.89	81.49	70.04	0.0100	0.0100	0.0000	0.0030	-	5.91	3.94	1.17	87.01	57.33
H10-SS	6.30	23.62	20.19	9.89	81.49	70.04	0.0100	0.0100	0.0030	0.0030	-	5.91	3.94	1.17	110.61	52.16
H10-TN	6.30	23.62	20.19	9.89	81.49	70.04	0.0100	0.0100	0.0000	0.0060	-	5.91	3.94	1.17	87.23	52.61

References

1. ACI Committee 318-99, *Building Code Requirements for Reinforced Concrete (ACI 318-99)*, American Concrete Institute Detroit, MI, 1999.
1. ACI Committee 318-08, *Building Code Requirements for Reinforced Concrete (ACI 318-08)*, American Concrete Institute, Farmington Hills, MI, 2008.
2. ACI Committee 318-11, *Building Code Requirements for Reinforced Concrete (ACI 318-11)*, American Concrete Institute, Farmington Hills, MI, 2011.
3. ACI-ASCE Committee 326, "Shear and Diagonal Tension", Report of ACI-ASCE Committee 326, Part 1- General Principles, Chapters 1-4, Jan, 1962.
4. ACI-ASCE Committee 326, "Shear and Diagonal Tension", Report of ACI-ASCE Committee 326, Part 2- Beams and Frames, Chapters 5-7, Feb, 1962.
5. ACI-ASCE Committee, "326 Shear and Diagonal Tension", Report of ACI-ASCE Committee 326, Part 3- Slabs and Footings, Chapter 8, March 1962.
6. ACI-ASCE Committee 426, "The Shear Strength of Reinforced Concrete Members", Journal of the Structural Division ASCE Vol. 99, No. ST6, June, 1973.
7. ACI-ASCE Committee 445R-99, "Recent Approaches to Shear Design of Structural Concrete", Report of ACI-ASCE Committee 445, Nov 1999.
8. ATENA Program Documentation, Cervenka Consulting Ltd., Prague, Czech Republic, 2000.
9. Cervenka, V., Jendele, L., and Cervenka, J., ATENA Program Documentation, Part 1- Theory, Cervenka Consulting Ltd., Prague, Czech Republic, March 2012.
10. Cervenka, J., ATENA Program Documentation, Part 4-1- User's Manual for ATENA 2D, Cervenka Consulting Ltd., Prague, Czech Republic, May 2001.
11. Cervenka, V., and Cervenka, J., ATENA Program Documentation, Part 2-1- Tutorial for Program ATENA 2D, Cervenka Consulting Ltd., Prague, Czech Republic, January 2012.
12. CEB-FIP Model Code 1990, Thomas Telford Services, Ltd., London, for Comite' Euro-International du Beton, Lausanne, 1993, 437 pp.

13. ACI SP-208, "Examples for the Design of Structural Concrete with Strut-and-Tie Models", American Concrete Institute, Farmington Hills, MI, 2002, 242 pp.
14. Ashour, A. F., and Morley, C. T., "Effectiveness Factor of Concrete in Continuous Deep Beams," *Journal of Structural Engineering*, ASCE, Vol. 122, No. 2, Feb. 1996, pp. 169-178.
15. Ashour, A., "Tests of Reinforced Concrete Continuous Deep Beams," ACI Structural Journal, *Proceedings*, Vol. 94, No. 1, Jan-Feb. 1997, pp 3-11.
16. Ashour, A. F., "Shear Capacity of Reinforced Concrete Deep Beams," *Journal of Structural Engineering*, ASCE, Vol. 126, No. 9, Sep. 2000, pp. 1045-1052.
17. Yang, K. H., Chung, H. S., and Ashour, A., "Influence of Shear Reinforcement on Reinforced Concrete Continuous Deep Beams," ACI Structural Journal, *Proceedings*, Vol. 104, No. 4, July-August 2007, pp 420-429.
18. Yang, K. H., and Ashour, A. F., "Load Capacity of Reinforced Concrete Continuous Deep Beams," *Journal of Structural Engineering*, ASCE, Vol. 134, No. 6, June 1, 2008, pp. 919-929.
19. Bresler, B., and Pister, K. S., "Strength of Concrete under Combined Stresses", *ACI Journal*, Vol. 55, No. 3, 1958, pp. 321-345.
20. Bresler, B., and Scordelis, A. C., "Shear Strength of Reinforced Concrete Beams", *ACI Journal*, Proceedings, Vol. 60, No. 1, Jan. 1963, pp. 51-74.
21. Bresler, B., MacGregor, J. G., "Review of Concrete Beams Failing in Shear", Journal of the Structural Division, *Proceedings* of the American Society of Civil Engineers, Vol. 93, No. ST 1, Feb 1967, pp. 343-372.
22. Birrcher, D.; Tuchscherer, R.; Huizinga, M.; Bayrak, O.; Wood, S.; and Jirsa, J., " Strength and Serviceability Design of Reinforced Concrete Deep Beams," Report No. FHWA/TX-09/0-5253-1, Center for Transportation Research, University of Texas at Austin, Austin, TX, 2009.
23. Cervenka, V., and Pukl, R., "Computer Models for Concrete Structures," Structural Engineering International 2, 1992, pp. 103-107.

24. Cervenka, V., "Computer Simulation of Failure of Concrete Structures for Practice," Cervenka Consulting, Prague, Czech Republic, 2000.
25. Collins, M. P., and Mitchell, D., "A Rational Approach to Shear Design - The 1984 Canadian Code Provisions," ACI Journal, Vol. 83, No. 6, Nov-Dec. 1986, pp. 925-933.
26. Cook, W. D., and Mitchell, D., "Studies of Disturbed Regions near Discontinuities in Reinforced Concrete Members," *ACI Structural Journal*, Vol. 85, No. 2, March-April 1988, pp. 206-216.
27. Crist, R. A., "Shear Behavior of Deep, Reinforced Concrete Beams", *Proceedings*, RILEM Symposium on the Effects of Repeated Loading of Materials and Structures (Mexico City, 1966), Instituto do Ingeniera, Mexico, D. F., 1967, V. 4, 31 pp.
28. Crist, R. A., *Static and Dynamic Shear Behavior of Uniformly Loaded Reinforced Concrete Deep Beams*, Ph.D. Thesis, University of New Mexico, Albuquerque, New Mexico, 1971, 268 pp.
29. CSA Standard,, *CSA-A23.3-04 Design of Concrete Structures*, Canadian Standards Association, Mississauga, Ontario, 2004.
30. Kani, G. N. J., "The Riddle of Shear Failure and Its Solution," ACI Journal, *Proceedings*, Vol. 61, No. 4, April 1964, pp. 441-467.
31. Kani, G. N. J., "Basic Facts Concerning Shear Failure," ACI Journal, *Proceedings*, Vol. 63, No. 6, June 1966, pp. 675-692.
32. Kani, G. N. J., "How Safe Are Our Large Reinforced Concrete Beams?," ACI Journal, *Proceedings*, Vol. 64, No. 3, March 1967, pp. 128-142.
33. Kong, F. K., Reinforced Concrete Deep Beams, Blackie and Son Ltd., 1990, 288 pp.
34. Kong, F. K., Robin, P. J., and Cole, D. F., "Web Reinforcement Effects on Deep Beams," ACI Journal, *Proceedings*, Vol. 67, No. 6, Dec. 1970, pp. 1010-1017.

35. Kotsovos, M. D., "Behavior of Reinforced Concrete Beams with a Shear Span to Depth Ratio Between 1.0 and 2.5," ACI Journal, *Proceedings*, Vol. 81, No. 3, May-June 1984, pp. 279-286.
36. Marti, P., "Basic Tools of Reinforced Concrete Beam Design," ACI Journal, *Proceedings* V. 82, No. 1 Jan-Feb. 1985, pp. 46-56.
37. Marti, P., "Truss Models in Detailing," Concrete International Design and Construction, Vol. 7, No. 12, December 1985, pp. 66-73.
38. Matamoros, A. B., and Wong, K. H., " Design of Simply Supported Deep Beams Using Strut-and-Tie Models," *ACI Structural Journal*, Vol. 100, No. 6, Nov-Dec. 2003, pp. 429-437.
39. Mau, S. T., and Hsu, T. T. C., "Shear Strength Prediction for Deep Beams with Web Reinforcement", ACI Structural Journal, *Proceedings* Vo. 84, No. 6, November-December 1987, pp. 513-523.
40. Mau, S. T., and Hsu, T. T. C., "Formula for the Shear Strength of Deep Beams", ACI Structural Journal, *Proceedings* Vo. 86, No. 5, September-October 1989, pp. 516-523.
41. Mihaylov, B. I., Bentz, E. C., and Collins, M. P., "Two-Parameter Kinematic Theory for Shear Behavior of Deep Beams," ACI Structural Journal, *Proceedings* Vo. 110, No. 3, May-June 2013, pp. 447-456.
42. de Paiva, H. A. Rawdon, and Siess, C. P., Strength and Behavior of Deep Beams in Shear, Journal of the Structural Division, *Proceedings* of the American Society of Civil Engineers, Vol. 91, No. ST5, Otc 1965, pp. 19-41.
43. Park, R., and Paulay, T., *Reinforced Concrete Structures*, A Wiley-Interscience Publication, Wiley, New York, 1975, 769 pp.
44. Park, J. W., and Kuchma, D., "Strut-and-Tie Model Analysis for Strength Prediction of Deep Beams," *ACI Structural Journal*, Vol. 104, No.6, Nov-Dec. 2007, pp 657-666.
45. Placas, A., and Regan, p. E., "Shear Failure of Reinforced Concrete Beams," ACI Jounral, *Proceedings*, Vol.68, Oct. 1971, pp. 763-773.

46. Rogowsky, D. M., MacGregor, J. G., and Ong, S. Y., "Tests of Reinforced Concrete Deep Beams," ACI Journal, *Proceedings*, V. 83, No. 4, July-Aug. 1986, pp. 614-623.
47. Rogowsky, D. M., and MacGregor, J. G., "Design of Deep Reinforced Concrete Continuous Beams," *Concrete International*, V. 8, No. 8, Aug. 1986, pp. 46-58.
48. Rogowsky, D. M., and MacGregor, J. G., " Shears Strength of Deep Reinforced Concrete Continuous Beams," Structural Engineering Report No. 110, Department of Civil Engineering, University of Alberta, Edmonton, Nov. 1983, 178 pp.
49. MacGregor, J. G., "Derivation of Strut-and-Tie Models for the 2002 ACI Code," ACI Publication, SP-208, Examples for the Design of Structural Concrete with Strut-and-Tie Models, American Concrete Institute, Farmington Hills, MI, 2002, pp. 7-40.
50. Russo, G.; Venir, R; and Pauletta, M., "Reinforced Concrete Deep Beams-Shear Strength Model and Design Formula," *ACI Structural Journal*, Vol. 102, No. 3, May-June 2005, pp. 429-437.
51. Schlaich, J., Schaefer, K., and Jennewein, M., "Towards a Consistent Design of Reinforced Concrete Strutctures," Journal of the Prestressed Concrete Institute, Vol. 99, No. ST6, June 1973, pp. 1091-1187.
52. Smith, K. N., and Vantsiotis, A. S., "Shear Strength of Deep Beams," ACI Journal, *Proceedings*, Vo. 79, No. 3, May-June 1982, pp. 201-213.
53. Smith, K. N., and Vantsiotis, A. S., "Deep Beam Test Results Compared with Present Building Code Models," ACI Journal, *Proceedings*, Vol. 79, No. 4, July-August 1982, pp. 280-287.
54. Tang, C. Y., and Tan, K. H., "Interactive Mechanical Model for Shear Strength of Deep Beams," *Journal of Structural Engineering*, ASCE, Vol. 130, No. 10, 2004, pp. 1534-1544.

55. Vecchio, F. J., and Collins, M. P., "Modified Compression Field Theory for Reinforced Concrete Elements Subjected to Shear," *ACI Structural Journal*, Vol. 83, No. 2, March-April 1986, pp. 219-231.
56. Bentz, E. C., Vecchio, F. J., and Collins, M. P., "Simplified Modified Compression Field Theory for Calculating Shear strength of Reinforced Concrete Elements," *ACI Structural Journal*, Vol. 103, No. 4, July-August 2006, pp. 614-624.
57. Zsutty, T. C., " Shear Strength Prediction for Separate Categories of Simple Beam Tests," ACI Journal, *Proceedings*, Vol. 68, No. 2 February 1971, pp. 138-143.
58. Wight, J. K., and Parra-Montesinos, G. J., "Strut-and-Tie Model for Deep Beam Design Using ACI Appendix A of the 2002 ACI Building Code," *Concrete International*, American Concrete Institute, May 2003, pp. 63-70.
59. Wight, J. K., and MacGregor, J. G., Reinforced Concrete: Mechanics and Design, 5th ed. Prentice-Hall, Inc., Upper Saddle River, 2009, 1112 pp.

VITA

Phu Trong Nguyen was born in Ha Noi, Viet Nam, in 1978, the son of Tam Xuan Nguyen and Tuat Thi Nguyen. He attended Yen Hoa high school, Cau Giay, Ha Noi. In 1996, he entered The National University of Civil Engineering in Ha Noi. He received his Bachelor of Engineering in Institute of Construction for Offshore Engineering in 2001. In September, 2001, he began study European Master in Computational Mechanics of Continua in University of Liege, Belgium. He received Master of Science in Computational Mechanics of Continua in 2003. From 2010 to 2013, he pursued Doctoral degree of Structural Engineering in The University of Texas at Austin, Texas. Upon receiving his Doctor of Philosophy in Engineering, he will continue to teaching and researching in The National University of Civil Engineering, Ha Noi, Viet Nam.

Email address: phunguyen111@utexas.edu

This dissertation was typed by the author.